CHANGES IN THE STRUCTURE OF SW30HR RO MEMBRANE EXPOSED TO CHLORAMINATED SEAWATER AND SYNTHETIC SOLUTIONS

BY

TENNIE RENKENS

THESIS

Submitted in partial fulfillment of the requirements
for the degree of Master of Science in Environmental Engineering in Civil Engineering
in the Graduate College of the
University of Illinois at Urbana-Champaign, 2012

Urbana, Illinois

Adviser:

Professor Benito Mariñas

ABSTRACT

Changes in the structure of the SW30HR RO membrane exposed to seawater, phosphate buffer, and standard seawater disinfected with monochloramine (NH_2Cl) are investigated. Three types of experiments were performed: (1) exposure of RO membrane (active and support layers) to monochloramine (2, 20 and 200 mg/L as Cl_2) and target proportional levels of iodide (0.06, 0.6 and 6 mg/L) or bromide (60, 600 and 6,000 mg/L) at constant exposure CT=384 mg×h/L; (2) exposure of support layer only to monochloramine at CT values of 1,000 and 30,000 mg×h/L at a monochloramine concentration of 200 mg/L as Cl_2; (3) exposure of RO membrane (active and support layers) to monochloramine at CT values of 1,000, 5,000 and 30,000 mg×h/L at a monochloramine concentration of 200 mg/L as Cl_2 in the presence of only 6 mg/L of iodide, only 6,000 mg/L of bromide, and both 6 mg/L of iodide and 6,000 mg/L of bromide. Results revealed that monochloramine may be reacting with the polysulfone support of RO membranes. RBS analyses have revealed that the RO membrane support might undergo damage. Recent work involves determining the effect of active layer-bound halogens on carboxylic group accessibility. Cesium (Cs^+), silver (Ag^+), and barium (Ba^{2+}) were used as ion probes to quantify the changes associated with membranes exposed to three different batch reactor conditions (1) seawater with 2 ppm NH_2Cl; (2) phosphate buffer with 2 ppm NH_2Cl and 65 mg/L KBr as Br^-; (3) standard seawater with 2 ppm NH_2Cl and 65 mg/L KBr as Br^-. Preliminary results indicate a shift in the pKa values of active layer carboxylic groups in batch reactors containing NH_2Cl in comparison to control reactors.

TABLE OF CONTENTS

CHAPTER 1. INTRODUCTION……1

CHAPTER 2. MATERIALS AND METHODS……..…9

CHAPTER 3. RESULTS AND DISCUSSION……..16

CHAPTER 4. CONCLUSIONS…….49

REFERENCES……51

APPENDIX…….54

CHAPTER 1. INTRODUCTION

Reverse osmosis and nanofiltration (RO/NF) membranes provide a physical barrier against pathogens and contaminants, and thus they provide a versatile water treatment technology. However, in practice RO/NF membranes do not perform to their full potential due to pervasive operational problems such as concentration polarization, and associated membrane scaling and fouling. Scaling and fouling can be caused by inorganics, organic matter, and microorganisms. Biofouling is described as the attachment and growth of microorganisms on the membrane surface. To inhibit biofouling, a disinfectant such as chlorine or chloramine, must be applied to the RO unit feed stream. The criteria for choosing a disinfectant is based on the desire to effectively disinfect the feed stream, and minimize disinfection byproducts without damaging the RO membrane. Compared to chloramine, the application of chlorine is more likely to generate harmful disinfection byproducts (DBPs) and damage the membrane (Tanaka, 1994). Chloramine provides the necessary disinfection power without producing regulated DBPs (Applegate, Erkenbrecher Jr, & Winters, 1989).

The attack on the polyamide (PA) portion of the membrane by chlorine has been previously studied (Avlonitis, Hanbury, & Hodgkiess, 1992; Cran, Bigger, & Gray, 2011; Dasilva, Tessaro, & Wada, 2006; Gabelich, Frankin, Gerringer, Ishida, & Suffet, 2005; Kang et al., 2007; Kawaguchi & Tamura, 1984; Koo, Lee, Jung, Hong, & Yoon, 2008.; Y. Kwon & Leckie, 2006; Y.-N. Kwon & Leckie, 2006; Shemer & Semiat, 2011; Soice, Greenberg, Krantz, & Norman, 2004; Soice et al., 2002). There are two potential chlorination mechanisms suggested in these works: (1) direct aromatic substitution; and (2) formation of an N-Cl bond on the secondary amide nitrogen followed by the Orton rearrangement to ultimately produce the chloro-substituted aromatic ring. Mechanism 1 has only been observed under high levels of chlorination

that are unlikely to be used in RO membrane plants; however, Mechanism 2 is generally accepted as the pathway in which the PA membrane active layer is chlorinated. Although mechanism 2 is a process involving two stages, these two stages are kinetically distinct. The formation of the N-Cl bond (stage 1) has been found to be reversible whereas the Orton rearrangement (stage 2) is irreversible (Kawaguchi & Tamura, 1984). Furthermore, stages 1 and 2 are also physically distinct. The formation of the N-Cl bond is described as the transformation of the crystalline regions of the polymer into amorphous regions and the Orton rearrangement as the oxidant attacking the more susceptible amorphous regions (Avlonitis et al., 1992). These mechanisms on their own damage the membrane active layer, however, in the presence of catalysts such as metal ions they become even more harmful (Causserand & Rouaix, 2008; Murphy, 1991; Tessaro, Dasilva, & Wada, 2005).

The effect that monochloramine (NH_2Cl) has on the PA portion of the membrane has also been studied (Cran et al., 2011; Gabelich, 2002; Gabelich et al., 2005; Shemer & Semiat, 2011). The oxidative/biocidal properties of typical chlorinated oxidants such as hypochlorous acid [$H^{+1}(O^{2-}Cl^{1+})^{-}$], hypochlorite [$(O^{2-}Cl^{1+})^{-}$], and monochloramine [$NH_2^{1-}\ Cl^{1+}$] is due to the +1 valence state of the chlorine atom (Cl) (White, 1992). In the absence of a catalyst, NH_2Cl is thought to chlorinate the PA membrane, to a lesser degree, through the same mechanism of N-Cl formation followed by the Orton rearrangement. However, when metal ions are present, in natural waters or as residual coagulants, the NH_2Cl attack is via the amidogen radical ($\bullet NH_2$). From reactions conducted in the presence of membranes and NH_2Cl + Fe(II), it was hypothesized that $\bullet NH_2$, formed during the reaction between NH_2Cl and Fe(II), lowers the activation energy of the chlorination reaction thereby allowing NH_2Cl to directly attack the PA.

(Gabelich et al., 2005). Oxidation of the membrane via NH_2Cl is not the only potential problem during preventative biofouling treatments.

RO plants are often prevalent in coastal areas with little access to fresh water. As mentioned before, NH_2Cl can be added to the feed stream of these RO units to prevent biofouling of the membrane by microorganisms. Potential interactions between NH_2Cl and constituents found in this feed stream present another set of challenges. Specifically, bromide and iodide found in these waters react with the primary oxidant, NH_2Cl, to form secondary oxidizing agents bromochloramine (NHBrCl) and hypoiodous acid (HOI), respectively. Interestingly, NHBrCl and HOI share a common characteristic with NH_2Cl and HOCl of a halogen with a +1 valence state.

A common technique to measure changes in the bonding of the PA membrane is Fourier Transform Infrared Spectroscopy (FTIR). A basic goal of spectroscopy is to determine the amount of light that is emitted at each wavelength. A simple way to measure a spectrum is with a monochromator. A monochromator blocks all wavelengths of light except one wavelength determined by the user. This single wavelength passes through a detector and the intensity of the signal indicates the amount of light emitted at that wavelength. By varying the monochromator settings, the entire spectrum can be collected.

FTIR obtains the same information as a monochromator but in a different way. FTIR measures the total beam intensity contributed by many different wavelengths of light reaching the detector at the same time. In the instrumental set-up, there are multiple possible mirror configurations that interfere with some wavelengths and not with others. These mirrors, located between the light source and the detector, are moved between data points so that different sets of wavelength are collected. So, multiple data points are obtained as the beam is varied to contain a

different combination of wavelengths. Then, a computer combines the data points and works backwards to determine the intensity of light at each wavelength. The name "Fourier transform" refers to the algorithm required to turn the raw light intensity data for each mirror position into light intensity at each wavelength (Smith, 2011).

PA exhibits four notable characteristic peaks at 1663, 1609, 1541, and 1444 cm^{-1}. Out of those four peaks, the peaks at 1663 and 1541 cm^{-1} are the Amide I and Amide II peaks, respectively. The amide I peak is predominantly due to the C=O stretching of the secondary amide group and the amide II peak is mainly due to the N-H bending of the amide group (Skrovanek, Howe, & Painter, 1985). The amide I and amide II peaks both shift in frequency, and change in intensity after exposure of PA to chlorine. In the absence of chlorine, the amide I peak is at a lower frequency because of hydrogen bonding between C=O and N-H functionalities of the amide which decrease the double bond character of the C=O group. If chlorine disrupts those hydrogen bonds, the peak shifts to a higher frequency, as is observed experimentally with an increase in CT (ppm x hr). The replacement of the H with a Cl during the formation of N-Cl in mechanism 2 is in agreement with this finding. In the absence of chlorine, the N-H bending associated with the amide II peak is restricted due to hydrogen bonding interactions with C=O or other N-H groups. But as the CT increases, the amide II peak decreases in intensity because of the formation of N-Cl groups which disrupt the hydrogen bonds (Kwon & Leckie, 2006a,b; Socrates, 1994). FTIR data has also been collected for membranes exposed to NH_2Cl. Cran et al. (2011) performed experiments that exposed PA membranes to 4 hr x 100 ppm NH_2Cl. Similar to Kwon and Leckie (2006a,b), a decrease in the absorbance of the amide II peak was observed indicating membrane oxidation. This peak decreased even more with the addition of Al^{3+}, Fe^{2+}, Cut^{2+}, and $Al^{3+} + Fe^{2+}$, suggesting these metals have a catalytic effect on the reaction between

NH_2Cl and the membrane active layer. Similarly, Gabelich et al. (2005) exposed PA membranes to 300 hours x 2.5 ppm NH_2Cl. Their FTIR results showed that there was no change in the absorbance values of the amide I and amide II peaks suggesting that membrane oxidation did not occur for membranes exposed to NH_2Cl, NH_2Cl + Fe(II), or NH_2Cl + Fe(III). A quick comparison of these two studies highlights the effect that the concentration of NH_2Cl may have on PA membrane oxidation. It is common for studies to use high NH_2Cl concentrations in order to achieve appropriate RO plant CT values, however, these values may not accurately reflect the phenomena occurring at more realistic NH_2Cl concentrations.

Rutherford backscattering spectroscopy is another technique to measure changes in membrane structure. RBS is a surface science technique that can be used to determine the elemental distribution of the active layer as well as the top portion (~2 μm) of the support layer, the thickness and roughness of the active layer, and the partitioning of probes of heavy elements at the aqueous/active layer interface. RBS has a helium ion source, an accelerator which energizes the helium ions and directs them toward the membrane sample, and a detector to measure the energy of backscattered ions. The helium ions are accelerated towards the sample, interact with atoms in the sample, and are backscattered towards the detector with a certain energy spectrum. The kinetic energy of the helium ion varies depending on the mass and depth of the target atom within the sample. So, helium ions experience a loss in kinetic energy when they penetrate and exit the sample. What this energy loss does is to introduce a depth scale in the RBS spectrum. An ion that is scattered at a certain depth experiences an additional energy loss on the way in and out of the sample. Thus it ends up with a kinetic energy lower than that of an ion which experiences a similar backscattering event near the sample surface.

In comparison to other surface science techniques such as X-ray photoelectron spectroscopy (XPS) RBS provides elemental composition as a function of depth beyond upper 5 nm surface. Unlike RBS XPS could not represent the full depth profile of membrane active layers (Bartels, 1989). RBS was also confirmed to be a suitable technique to characterize a variety of commercial RO/NF membranes. Assay protocols were developed to ensure the RBS helium ion fluence thresholds wouldn't compromise the integrity of membrane elemental composition and thickness (Mi et al., 2006, 2007).

RO/NF membrane active layers are formed by interfacial polymerization process which results in a fully aromatic polyamide with various degrees of cross-linking. As shown in Fig. 1, the non-cross-linked portions of the PA result in the formation of carboxylic functional groups (FGs).

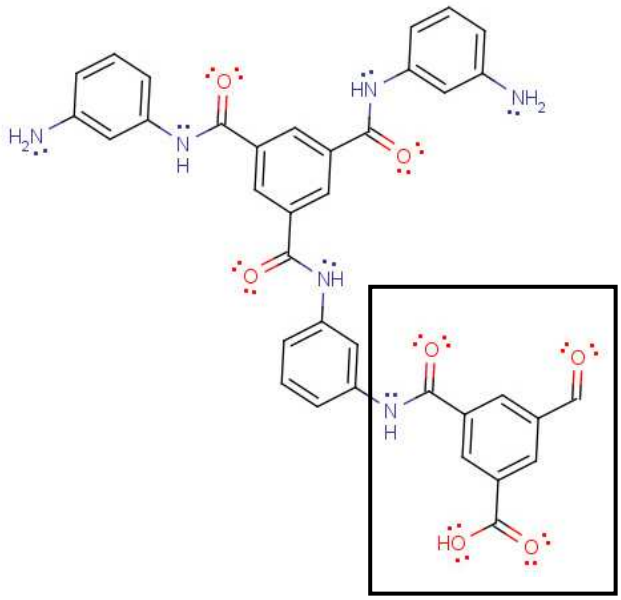

Figure 1. Structure of fully aromatic polyamide of RO membrane active layer with a box highlighting a carboxylic group resulting from incomplete cross-linking.

The functional groups present in a membrane influence the interactions between the membrane and solute and moreover affect membrane performance. Also, because the formation of FGs is due to incomplete polymerization, the concentration of FGs has a large impact on the pore size distribution (PSD) of the membrane (Freger, 2003; Petersen, 1993). The PSD of thin films of cross-linked aromatic polyamide RO membranes are composed of two types of pores: network pores with radii of about 2.1-2.4 Å; and aggregate pores with radii of 3.5-4.5 Å (Kim, 2005). A technique was developed to measure the concentration of functional groups through the use of ion probes (Coronell et al., 2008). The amine and carboxylic functional groups present in the aromatic polyamide RO membranes have pH dependent charges. When these groups are charged, counterion probe that associate with the charge can then be quantified using RBS. The probes therefore are a tool to quantify the functional groups in the active layer of the membrane. Silver ion has been used to quantify the carboxylic groups because the radius of Ag^{+} is 0.81-1.42 Å range (Shannon, 1976). This range is below the lowest radius of the smaller network pores (2.1-2.4 Å) in the PA active layer, so Ag^{+} ions should be able to access all carboxylic groups in the active layer. Also, the 1+ valence state of Ag means that one Ag will neutralize one deprotonated carboxylic group. Therefore, the concentration of Ag detected in the active layer should be equal to the concentration of carboxylic groups in the active layer. Other ion probes such as barium (Ba^{2+}) and cesium (Cs^{+}) can also be used to obtain information about chemical properties of the membrane such as pore accessibility.

Because membranes are a physical barrier, they can experience fouling by microorganisms and organic matter, and degradation inflicted by oxidizing agents and associated byproducts. Therefore, having an understanding of what mechanisms are occurring at a

molecular level in the membrane surface and throughout the active layer depth should be a powerful tool.

This research focused on elucidating the chemistry involved in RO/NF membrane active layer degradation during various chemical treatment approaches designed to prevent biofouling. Batch experiments with SW30HR membranes and subsequent analyses with RBS, ion probes, and FTIR were performed to determine the effect of secondary oxidizing agents, formed from the reaction between monochloramine, iodide, and bromide, on membrane structure. From this work, we hoped to gain valuable insight concerning the strengths and weaknesses of membranes in order to aid current membrane technology and create a new generation of more robust membranes.

CHAPTER 2. MATERIALS AND METHODS

2.1 Membranes

Batch experiments were performed with coupons of the SW30HR (Dow FilmTec Co., USA) thin film composite RO membrane. The active layer of this membrane is made of fully aromatic polyamide prepared by interfacial polymerization on top of an asymmetric polysulfone support. Upon completion of the batch experiments, pieces (2.5×5.0 cm^2) of the tested membranes as well as untested samples were cut for analyses by Rutherford Backscattering spectrometry as described in a subsequent section. Polysulfone membrane coupons (Sepro, 4115 Avenida de la Plata, Oceanside, CA 92056) were used in experiments to represent the polysulfone support layer present in the SW30HR membrane. Membranes were immersed in MilliQ water (Millipore system with resistivity of the water of 18.2 MΩ.cm) for at least 24 hours prior to use.

2.2 Experimental Approach

2.2.1 Batch experiments

Batch reactors contained phosphate buffer solutions (pH=8.3 or pH=7.9, 15 mM), standard seawater (pH=8.3 or pH=7.9), or real seawater (pH=7.9). The buffer solutions and standard seawater were spiked with 65 mg KBr/L (as Br^-) and 60 µg KI/L (as I^-) to represent the typical concentrations found in RO membrane plant conditions. Membrane coupons were inserteded in amber-colored glass bottles (to slow down the disinfectant decay) containing monochloramine (NH_2Cl)) and spiked or not spiked with KI and/or KBr, and placed on a shaker table rotating at 120 rpm. The membranes removed from the batch reactor daily immediately re-immersed in solutions made fresh. The purpose of the approach was to expose the membranes to

a more stable composition of chloraminated standard seawater, buffer, or real seawater. Following a certain exposure period, the membranes were rinsed three consecutive times in a 1 to 1000 dilution of their respective reactor solution, each time for 10 minutes, and then air-dried prior to RBS analysis. Membranes samples for additional ion probe experiments were stored in their respective 1 to 1000 dilution reactor solution until analysis time.

2.3 Reagent preparation and characterization

2.3.1 Phosphate buffer

Phosphate buffer solutions with a total phosphate concentration of 0.015 M were prepared using sodium phosphate dibasic heptahydrate and sodium phosphate monobasic monohydrate (Fischer Scientific, 99.0% purity) dissolved in MilliQ water (Millipore system with resistivity of the water of 18.2 MΩ.cm). The pH was adjusted using concentrated NaOH and HCl.

2.3.2 Standard seawater

Standard seawater was prepared according to *Methods of Seawater Analysis* (Grasshoffiklaus & Manfred, 1999) using ammonium chloride, magnesium chloride hexahydrate, sodium bicarbonate, and calcium chloride dehydrate with purity of 99.0% or greater purchased from Fischer Scientific. Sodium chloride, boric acid, and potassium chloride with purity of 99.0 % or greater were purchased from EMD. Sodium sulfate, potassium iodide (KI), and potassium bromide (KBr) also with purity of 99.0 % or greater were purchased from Sigma Aldrich. The KI and KBr used for spiking the batch reactors were FT-IR grade (99.99% trace metals basis).

Standard seawater chemicals were all dissolved in MilliQ water (Millipore system with resistivity of the water of 18.2 MΩ.cm).

2.3.3 Monochloramine

Monochloramine was prepared with MilliQ water (Millipore system with resistivity of the water of 18.2 MΩ.cm) using ammonium chloride (NH_4Cl) and sodium hypochlorite (NaOCl) stock solutions. The stock NaOCl concentration was determined to be 0.78 M using a UV spectroscopy (maximum absorbance measurement at 291 nm and molar absorptivity= 350 cm^{-1}). Dilute NH_4Cl and NaOCl solutions were prepared in phosphate buffer (pH=8.3) at a N:Cl ratio of 1.1:1. The stock solution of monochloramine was prepared by slowly pipetting the NaOCl solution into the NH_4Cl solution under high magnetic stirring over a time period of 40 to 80 minutes. The concentration of monochloramine was determined using a UV spectroscopy (maximum absorbance measurement at 243 nm and molar absorptivity=433 cm^{-1}).

2.3.4 ICP-MS analyses

The potential presence of metal impurities in phosphate buffer, standard seawater, and real seawater were assessed by performing a first round of qualitative ICP-MS analyses at the University of Illinois Champaign-Urbana. Copper, manganese, molybdenum, nickel and vanadium were found to be present at part-per-billion (ppb) levels in standard seawater, while just molybdenum and vanadium were observed in real seawater and only molybdenum was found in phosphate buffer. Additional ICP-MS analyses were performed specifically looking for iron, copper, aluminum, and manganese. Aluminum and manganese were detected in sub-1 ppm

concentrations in both standard seawater and real seawater. Iron is often difficult to detect in ICP-MS partly due to the necessity to dilute the high salt concentration in the samples.

2.3.5 Total organic carbon (TOC) analyses

The TOC concentrations of the real seawater and standard seawater measured with a Shimadzu TOC-VCPH analyzer (Shimadzu Scientific Instruments, Columbia, MD) were found to be 1.7 mg/L and 0.44 mg/L, respectively.

2.4 Membrane analyses

2.4.1 Ion probe solutions

All chemicals used were A.C.S. grade with 99%+ purity. Cesium chloride (CsCl), Silver nitrate ($AgNO_3$), and barium nitrate ($Ba(NO_3)_2$) from Sigma-Aldrich were used as sources of Cs^+, Ag^+, and Ba^{2+}. The concentrations of cesium ($1x10^{-6}$-$1x10^{-3}$ M), silver ($1x10^{-6}$-$2x10^{-4}$ M), and barium ($1x10^{-6}$-$2x10^{-4}$ M) in solution were always below their solubility limit at the pH tested. All ion-probe solutions were prepared with nanopure water. The pH of cesium, silver, and barium solutions was adjusted to the desired value by addition of HNO_3 or NaOH. Silver solutions were prepared and used under dark conditions to prevent photodegradation.

2.4.2 Sample preparation for ion probing with Ag^+

Membrane coupons were soaked three times, each time for 10 min, in a $2x10^{-4}$ M or $2x10^{-5}$ M solution of $AgNO_3$ at the target pH to saturate accessible $R–COO^-$ groups with Ag^+. Then, to reduce excess Ag^+ not associated to $R–COO^-$ groups the samples underwent three consecutive immersions, each lasting 10 min, in a 10^{-6} M solution of $AgNO_3$ at the same pH used

in the saturation step. Throughout each 10 min interval, the pH was monitored continuously and the pH was recorded at 3 , 6 , and 10 min. The average and standard deviation of the recorded pH values throughout the entire saturation and subsequent reduction steps were calculated. Lastly, the samples were air-dried at room temperature for ≥24 h. Prepared samples were analyzed by RBS (see below).

2.4.3 Sample preparation for ion probing with Cs^+

Membrane coupons were soaked three times, each time for 10 min, in a $1x10^{-3}$ M solution of CsCl at the pH of interest to saturate accessible R–COO^- groups with Cs^+. Then, to reduce excess Cs^+ not associated to R–COO^- groups the samples underwent three consecutive immersions, each lasting 10 min, in a 10^{-6} M solution of CsCl at the same pH used in the saturation step. Throughout each 10 min interval, the pH was monitored continuously and the pH was recorded at 3, 6, and 10 min. The average and standard deviation of the recorded pH values throughout the entire saturation and subsequent reduction steps were calculated. Lastly, the samples were air-dried at room temperature for ≥24 h. Prepared samples were analyzed by RBS (see below).

2.4.4 Sample preparation for Ag^+/Ba^{2+} ion exchange

Ion exchange experiments were performed to study the displacement of Ag^+ by Ba^{2+} from the R–COO^- groups in the active layer of the SW30HR membrane. Membrane coupons were soaked three times, each time for 10 min, in a $2x10^{-4}$ M or $2x10^{-5}$ M solution of $AgNO_3$ at the pH of interest to saturate accessible R–COO^- groups with Ag^+. Then, to reduce excess Ag^+ not associated to R–COO^- groups the samples underwent three consecutive immersions, each lasting

10 min, in a 10^{-6} M solution of $AgNO_3$ at the same pH used in the saturation step. Throughout each 10 min interval, the pH was monitored continuously and the pH was recorded at 3, 6, and 10 min. Then, the same membrane coupons were transferred and soaked three times, each time for 10 min, in a $2x10^{-4}$ M solution of $Ba(NO_3)_2$ at the pH of interest. Then, to reduce excess Ba^{2+} not associated to R– COO^- groups the samples underwent three consecutive immersions, each lasting 10 min, in a 10^{-6} M solution of $Ba(NO_3)_2$ at the same pH used in the saturation step. Throughout each 10 min interval, the pH was monitored continuously and the pH was recorded at 3, 6, and 10 min. The average and standard deviation of the recorded pH values throughout the entire saturation and subsequent reduction steps of both $AgNO_3$ and $Ba(NO_3)_2$ solutions were calculated. Lastly, the coupons were air-dried and analyzed by RBS (see below).

2.4.5 Rutherford backscattering spectrometry (RBS)

Rutherford backscattering spectrometry (RBS) was used to quantify Cs^+, Ag^+, Ba^{2+}, Br, and I in the active layer of treated membrane samples. Membrane coupons were attached to the sample stage using a double-sided thermally conductive adhesive tape (T410 material, Marian, Chicago, IL). Then, a circular, 3-mm, 2-MeV He^+ beam generated with a Van de Graaff accelerator (High Voltage Engineering Corp., Burlington, MA) was scanned back and forth over the surface of the membrane sample until the desired number of counts was reached. The incident, exit, and scattering angles of the He^+ beam were 22.5^o, 52.5^o and 150^o, respectively. A detector measured the energy and counts of backscattered ions. The software SIMNRA® (Mayer, Duggan, & Morgan, 1998) was used for data analysis to obtain the composition and atomic density (10^{15} atoms/cm^2) of the active and support layers. Using this information, the

concentration of each element of interest in the active or support layer of the sample was calculated. The spectra were normalized to the sulfur plateau at an arbitrary value of 300.

2.4.6 FTIR

FTIR spectrometry was used to measure the changes in characteristic functional groups of the polyamide membrane polymers taking place in different batch reactors. A NEXUS 670 FTIR spectrometer (Thermo Nicolet Corporation, Madison, WI) equipped with a smart golden gate accessory, DTGS-KBr detector, KBr beam-splitter and diamond crystal were used. The IR source was set at 45° incident angle. Dry membrane samples were mounted with active layer facing the crystal surface. A total of 5 "spots" were taken per sample and the spectra were averaged.

CHAPTER 3. RESULTS AND DISCUSSION

3.1 Batch experiments with SW30HR RO membrane in standard seawater

An initial set of experiments were performed to assess if experimental results obtained with high monochloramine, iodide or bromide concentrations (factor of 10 and 100 times; a factor of 1000 was not used to avoid exceedingly fast rates of monochloramine decomposition) would be representative of those obtained at concentrations representative of those encountered in practice (2 ppm monochloramine, and 60 mg/L bromide or 0.06 mg/L iodide). The experimental conditions used are listed in Table 1. As shown in the table the contact time was adjusted to achieve the same CT of monochloramine in all cases.

Table 1. Batch experimental conditions at increasing monochloramine and iodide or bromide concentrations and corresponding decreasing contact times resulting in constant exposure or CT

NH_2Cl (ppm)	KI [mg/l]	Hours	NH_2Cl CT (ppm-h)
2	0.06	192	384
20	0.6	19.2	384
200	6	1.92	384
NH_2Cl (ppm)	KBr [mg/l]	Hours	NH_2Cl CT (ppm-h)
2	60	192	384
20	600	19.2	384
200	6000	1.92	384

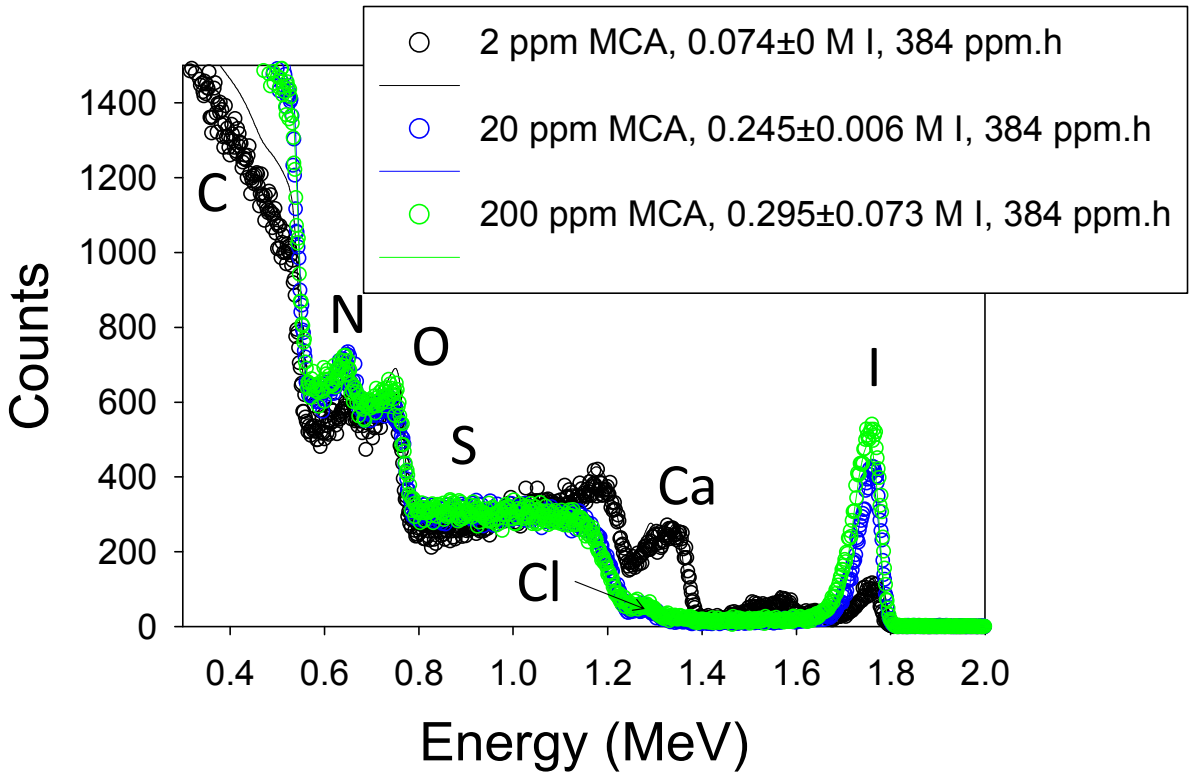

Figure 2. RBS spectra of RO membranes exposed to standard seawater with 2 ppm monochloramine and 0.06 ppm iodide (black) as well as solutions of these constituents at 10 times (blue) and 100 times (light green) higher concentrations at contact times resulting in constant exposure or CT of 384 ppm-h in all cases. The open circles are experimental data and the solid lines are simulated spectra.

Experimental results shown in Figure 2 reveal two main characteristics: (1) an iodine peak (at ~1.75 MeV) corresponding to iodination of the polyamide active layer; and (2) the presence of calcium (signal front at ~1.4 MeV) in the support. Iodination of the active layer would be consistent with the formation of secondary oxidizing agent HOI from the reaction of monochloramine and iodide. Once normalizing the spectra with respect to carbon plateau (signal front at ~0.55 MeV) it appears that iodination of the active layer by HOI although it increased

with increasing monochloramine/iodide concentrations but not nearly proportionally suggesting that much of the iodination of the active layer has been completed by a CT of 384 ppm-h. In contrast the level of calcium in the support layer increased with increasing monochloramine concentration within the range investigated. This was interpreted as the polysulfone undergoing gradual transformation, possibly with cleavage of polymer changes that resulted in the formation of charged chemical groups such as carboxylic and sulfonic groups that would be deprotonated at the pH used and retain calcium by ion exchange sorption.

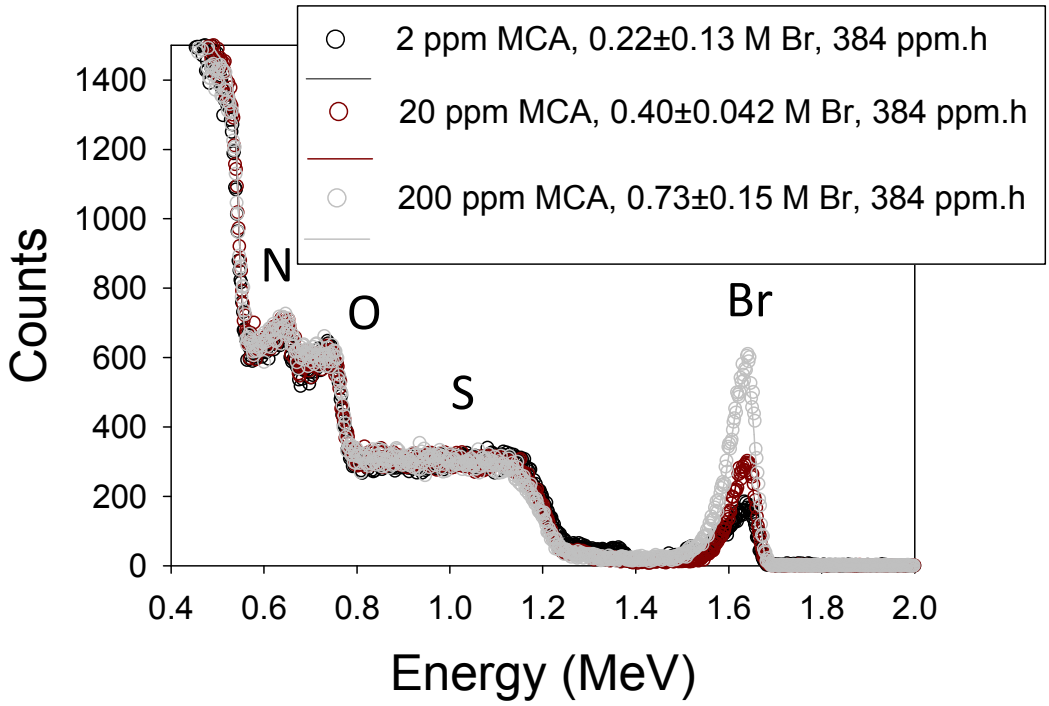

Figure 3. RBS spectra of RO membranes exposed to standard seawater with 2 ppm monochloramine and 60 ppm bromide (black) as well as solutions of these constituents at 10 times (dark red) and 100 times (light grey) higher concentrations at contact times resulting in constant exposure or CT of 384 ppm-h in all cases. The open circles are experimental data and the solid lines are simulated spectra.

RBS spectra in Figure 3 reveal the presence of a bromine peak (at ~1.65 MeV) corresponding to bromination of the polyamide active layer. Bromination of the active layer would be consistent with the formation of secondary oxidizing agents such as NHBrCl from the reaction of monochloramine and bromide. In contrast to the observation with the solutions containing iodide (Figure 3), the presence of calcium in the support layer was less pronounced compared to the experiments with iodide and only measurable at the lowest concentrations (longest exposure time) tested. A comparison of the three spectra revealed a trend in the level of bromination with increasing monochloramine/bromide concentration similar to that observed for the case of the iodide experiments. The extent of bromination increased with increasing monochloramine/bromide concentrations but not proportionally to the oxidizing agent concentration used suggesting active layer bromination might be approaching a maximum level by the CT of 384 ppm-h used. This claim is also supported by the level of bromine being similar even though somewhat higher than that of iodine in spite of the fact that the concentration of the two halogens differed by a factor of 1000. The lower rate of calcium incorporation into the support layer suggests that monochloramine might be responsible for the chemical attack of the support since in the presence of excess bromide it would quickly disappear to form bromochloramine and other secondary bromine-containing oxidizing agents. That was not the case in the solution with iodide since in that case monochloramine was in excess and only a small portion would react to form HOI.

The observation in the experiments at variable monochloramine, iodide and bromide concentrations is that the highest level of support damage and corresponding calcium uptake occurred at the lowest concentrations but the longest exposure time investigated was somewhat unexpected. This indicated that exposure time might play a more important role than oxidizing

agent concentration. To test this possibility, additional experiments were performed at constant monochloramine and iodide or bromide ion concentrations with increasing contact times up to 150 h, and corresponding increasing exposure or CT. The experimental conditions used are listed in Table 2.

Table 2. Batch experimental conditions at constant monochloramine and iodide or bromide concentrations and corresponding increasing contact times resulting in increasing exposure or CT

NH_2Cl (ppm)	KI [mg/l]	Hours	NH_2Cl CT (ppm-h)
200	6	5	1000
200	6	25	5000
200	6	150	30000
NH_2Cl (ppm)	KBr [mg/l]	Hours	NH_2Cl CT (ppm-h)
200	6000	5	1000
200	6000	25	5000
200	6000	150	30000

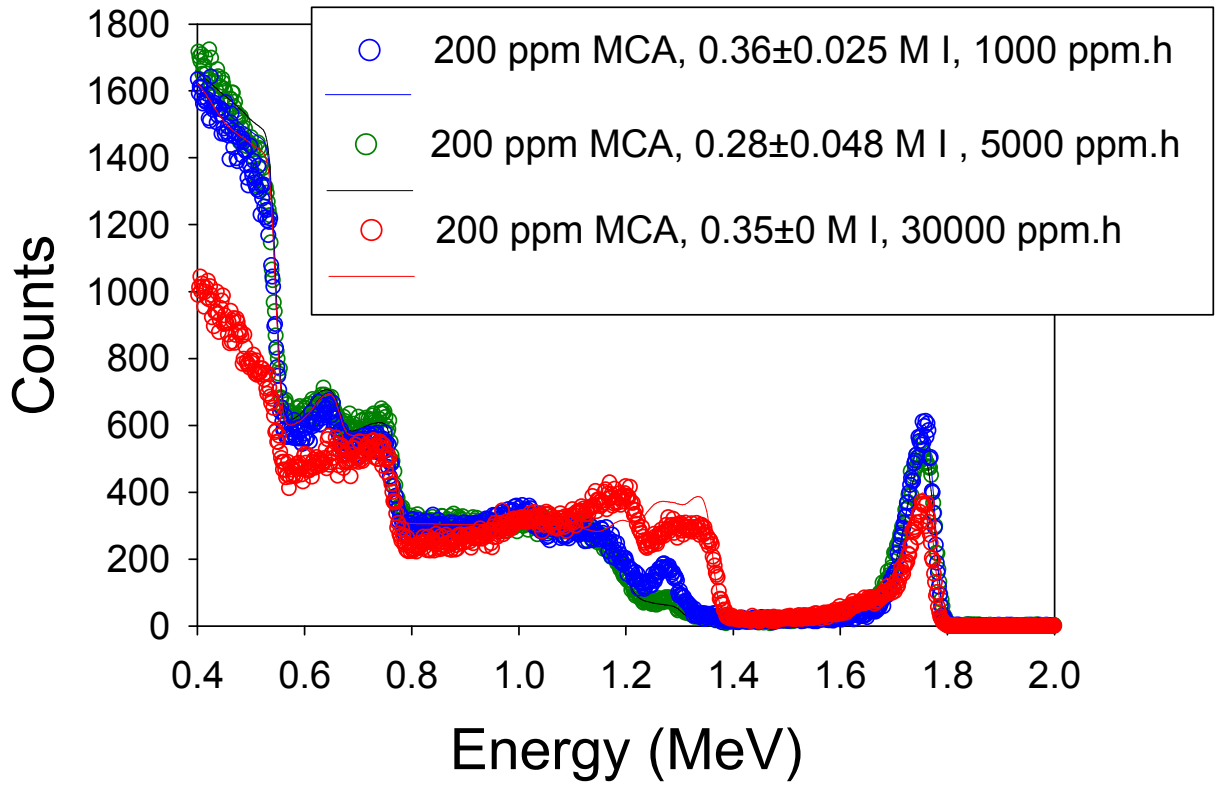

Figure 4. RBS spectra of RO membranes exposed to standard seawater with 200 ppm monochloramine and 6 ppm iodide at various contact times resulting in exposures or CT of 1000 ppm-h (blue), 5000 ppm-h (green), and 30000 ppm-h (red). The open circles are experimental data and the solid lines are simulated spectra.

Results obtained for the experiments performed with 200 ppm of monochloramine and 6 ppm of iodide are shown in Figure 4. Similar to the results shown in Figure 2, the two main observations were an iodine peak (at ~1.75 MeV) corresponding to iodination of the polyamide active layer, and the presence of calcium (signal front at ~1.4 MeV) and magnesium (peak at ~1 MeV on top of the sulfur plateau) in the support. Once normalizing the spectra with respect to carbon plateau (signal front at ~0.55 MeV) it appears that iodination of the active layer by HOI

occurred rapidly and was approximately complete at the CT of 1000 ppm-h. The level of calcium in the support layer increased with increasing CT within the range investigated. But perhaps the most interesting observation is the level of support damage and associated calcium uptake was similar to that shown in Figure 2 when using only 2 ppm monochloramine but comparable contact time (150 h at 200 ppm, and 192 h at 2ppm). This observation suggest that the transformation of the support layer requires the presence of monochloramine but it is controlled by some other constituents present in the solution, perhaps a metal acting as catalyst, at lower levels and thus limiting the rate of the reaction.

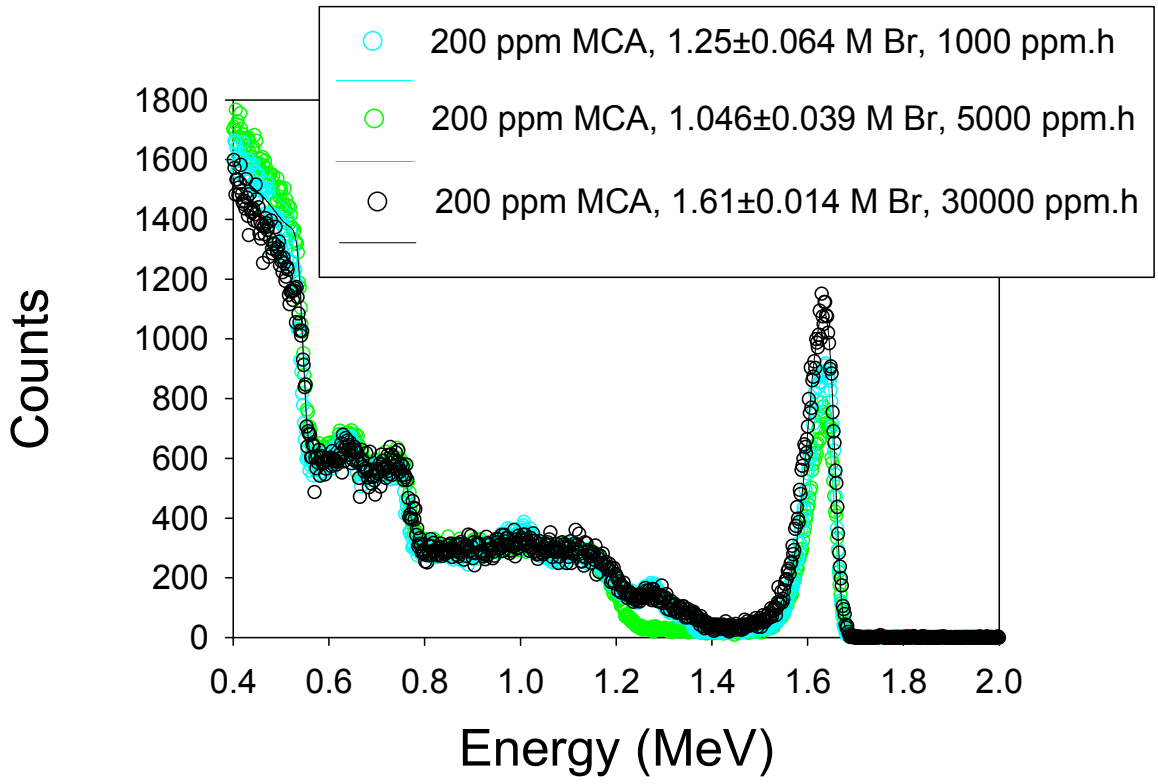

Figure 5. RBS spectra of RO membranes exposed to standard seawater with 200 ppm monochloramine and 6000 ppm bromide at various contact times resulting in exposures or CT of 1000 ppm-h (cyanide), 5000 ppm-h (light green), and =30000 ppm-h (black). The open circles are experimental data and the solid lines are simulated data.

Results obtained for the experiments performed with 200 ppm of monochloramine and 6000 ppm of bromide are shown in Figure 5. Similar to the results in Figure 3, the main observation was a bromine peak (at ~1.65 MeV) corresponding to bromination of the polyamide active layer by a secondary oxidizing agents such as NHBrCl produced from the reaction of monochloramine and bromide. In contrast to the observation with the solutions containing iodide (Figures 2 and 4) and in agreement with the observation in Figure 3, the presence of calcium (signal front at ~1.4 MeV) and magnesium (peak at ~1 MeV on top of the sulfur plateau) in the support were much less pronounced. Also consistent with the discussion for the spectra in Figure 3, a comparison of the three spectra in Figure 5 did not reveal a trend in the level of bromination with increasing CT suggesting similarly to the case of the iodide experiments that bromination of the active layer occurred rapidly and was also approximately complete at a CT of 1000 ppm-h.

Experiments discussed in this section were performed with only one of the two halides, iodide or bromide present in solution. The competition between secondary disinfectants to react with the RO membrane in the more realistic case of both iodide and bromide being present was investigated by performing the experiments shown in Table 3.

Table 3. Batch experimental conditions at constant monochloramine, iodide and bromide concentrations and corresponding increasing contact times resulting in increasing exposure or CT

NH_2Cl (ppm)	KI [mg/l]	KBr [mg/l]	Hours	NH_2Cl CT (ppm-h)
200	6	6000	5	1000
200	6	6000	25	5000
200	6	6000	150	30000

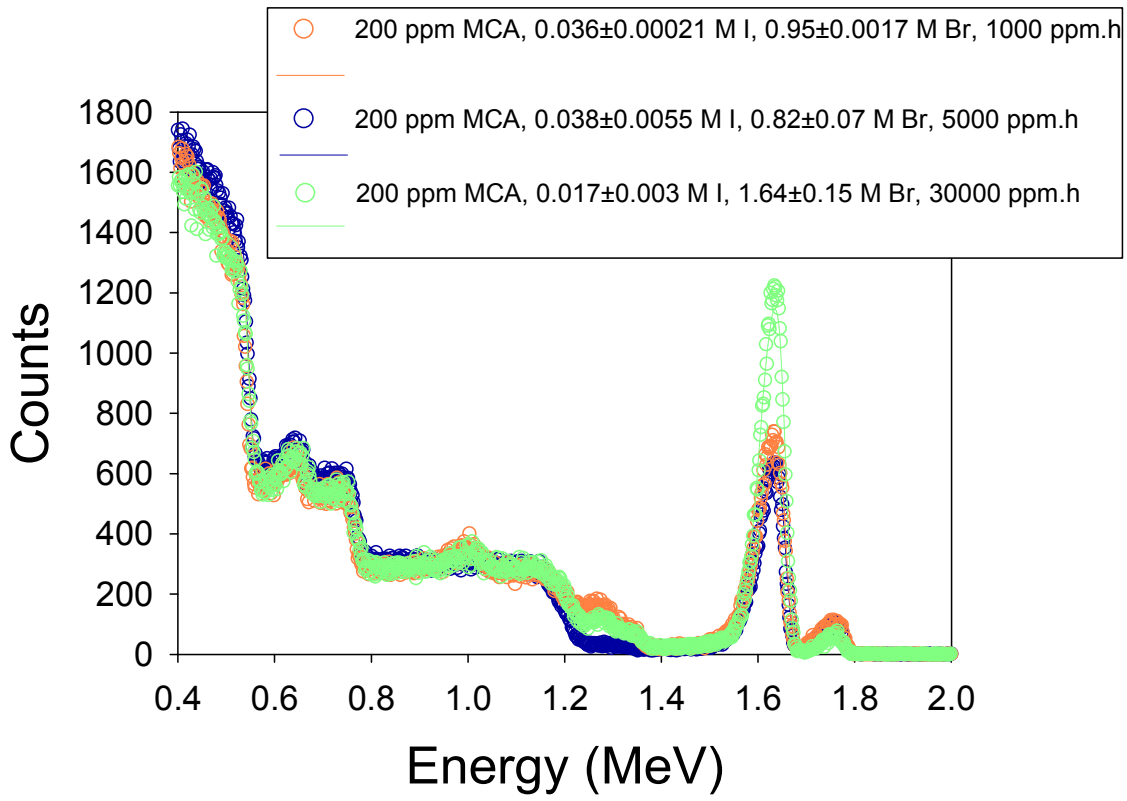

Figure 6. RBS spectra of RO membranes exposed to standard seawater with 200 ppm monochloramine, 6 ppm iodide and 6000 ppm bromide at various contact times resulting in exposures or CT of 1000 ppm-h (orange), 5000 ppm-h (blue), and =30000 ppm-h (light green). The open circles are experimental data and the solid lines are simulated data.

Results obtained for the experiments performed with 200 ppm of monochloramine, 6 ppm of iodide and 6000 ppm of bromide are shown in Figure 6. The results are similar to those shown in Figure 6 except for the appearance of an iodine peak. Bromination was predominant although only by a factor of ~20-100, smaller than the factor of 1000 corresponding to the difference in the initial concentration of the two halides in solution. The presence of bromide in excess with respect to that of monochloramine once again resulted in presence of calcium (signal front at ~1.4 MeV) in the support being much less pronounced than when bromide was absent.

3.2 Batch experiments with SW30HR RO membrane in phosphate buffer (pH=8.3) solutions

Experimental sets were also performed with phosphate buffer solutions instead of standard seawater but otherwise using the same conditions shown in Tables 1, 2 and 3. Resulting RBS spectra are shown in Figures 7 and 8 (conditions in Table 1), 9 and 10 (conditions in Table 2), and Figure 11 (conditions in Table 3). A comparison of Figures 7-11 to the corresponding Figures 2-6 revealed that the observations regarding halogenation of the active layer with bromine and iodine are similar in phosphate buffer and standard seawater but the damage of the support layer in the absence of bromide did not take place. This key difference suggests that a minor constituent present in standard seawater but not present in the phosphate buffer solution might be responsible for the support layer degradation and corresponding calcium uptake. The observed difference also questions if the support damage effect is associated with common constituents present in seawater or a minor constituent present as impurity in one of the reagents used to prepared standard seawater. This question motivated changes in the original experimental plan to check if the support deterioration would occur with real seawater. One additional difference apparent by comparing Figures 6 and 11 is that HOI was more effective in competing with bromine species for the halogenation of the active layer. This is likely the result of differences in the kinetic of secondary oxidizing agent formation under the lower ionic strength conditions of the phosphate buffer solution compared to the standard seawater.

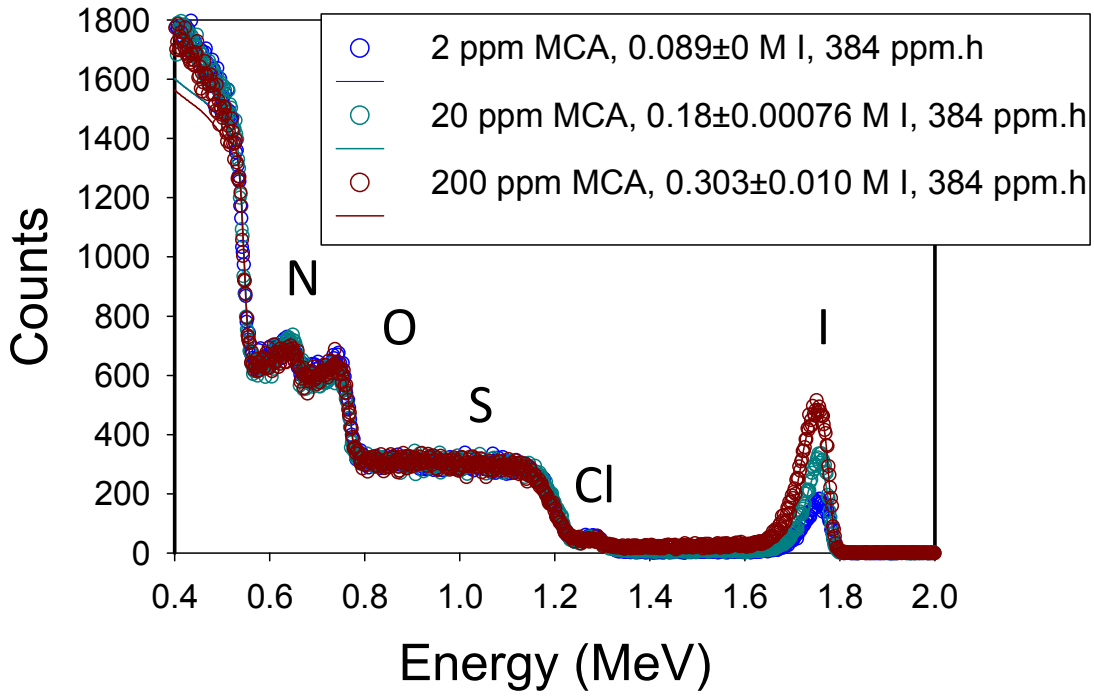

Figure 7. RBS spectra of RO membranes exposed to phosphate buffer solution with 2 ppm monochloramine and 0.06 ppm iodide (blue) as well as solutions of these constituents at 10 times (dark green) and 100 times (dark red) higher concentrations at contact times resulting in constant exposure or CT of 384 ppm-h in all cases. The open circles are experimental data and the solid lines are simulated spectra.

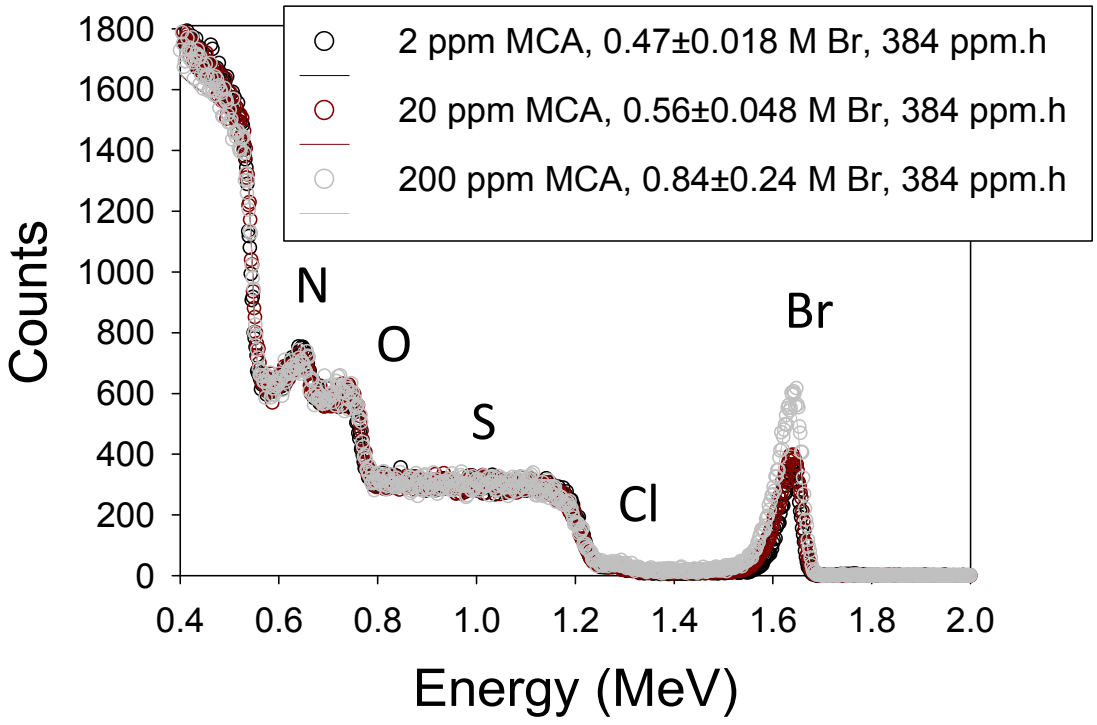

Figure 8. RBS spectra of RO membranes exposed to phosphate buffer solution with 2 ppm monochloramine and 60 ppm bromide (black) as well as solutions of these constituents at 10 times (dark red) and 100 times (light grey) higher concentrations at contact times resulting in constant exposure or CT of 384 ppm-h in all cases. The open circles are experimental data and the solid lines are simulated spectra.

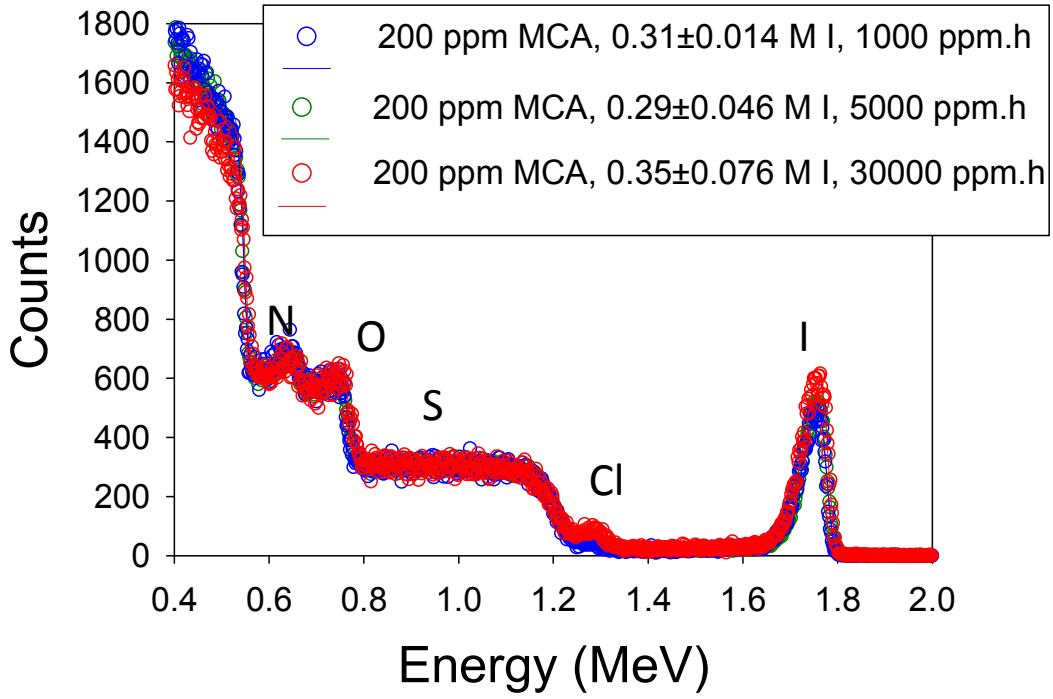

Figure 9. RBS spectra of RO membranes exposed to phosphate buffer solution with 200 ppm monochloramine and 6 ppm iodide at various contact times resulting in exposures or CT of 1000 ppm-h (blue), 5000 ppm-h (green), and 30000 ppm-h (red). The open circles are experimental data and the solid lines are simulated spectra.

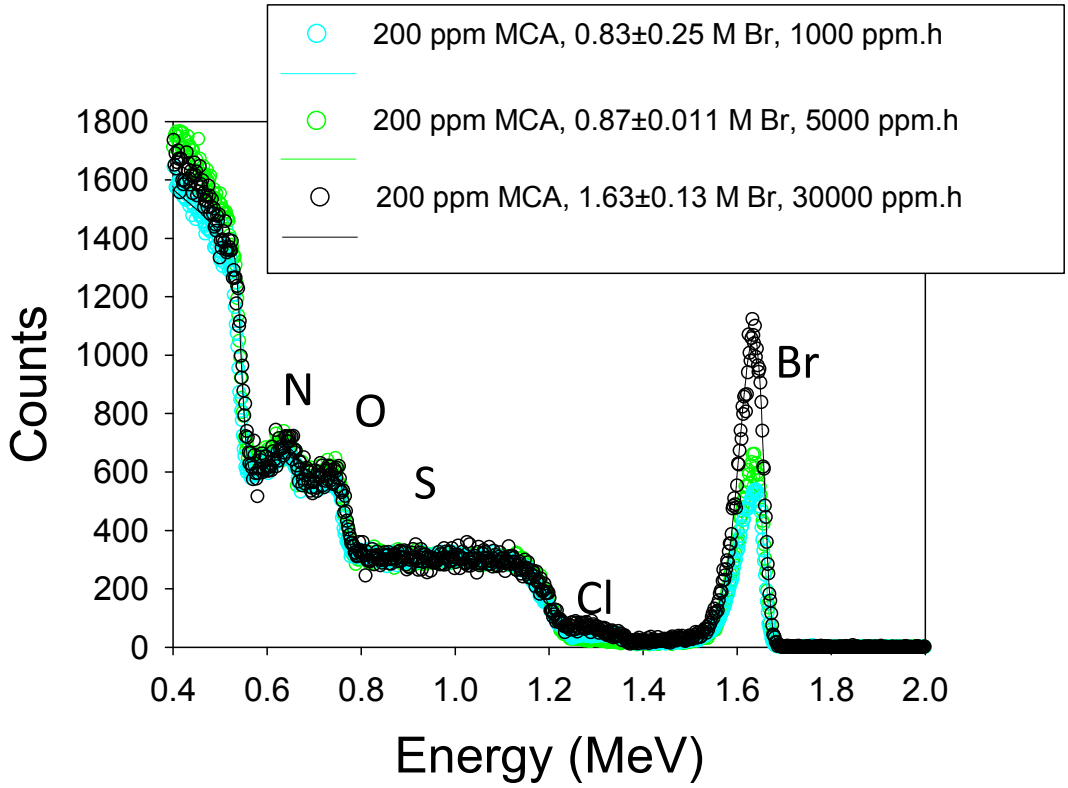

Figure 10. RBS spectra of RO membranes exposed to phosphate buffer solution with 200 ppm monochloramine and 6000 ppm bromide at various contact times resulting in exposures or CT of 1000 ppm-h (cyanide), 5000 ppm-h (light green), and =30000 ppm-h (black). The open circles are experimental data and the solid lines are simulated data.

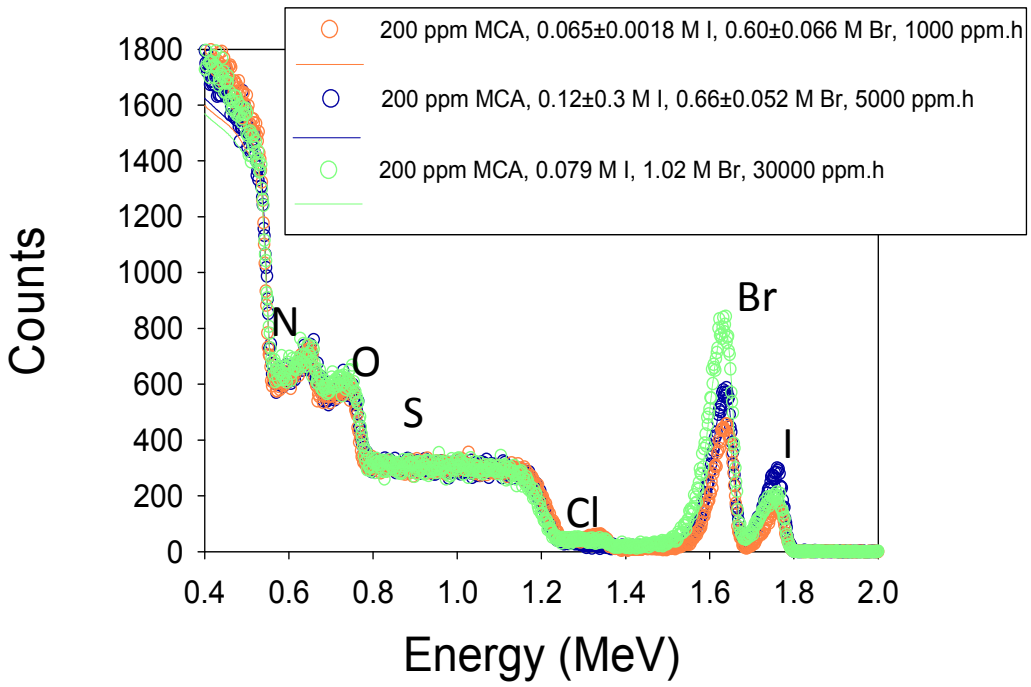

Figure 11. RBS spectra of RO membranes exposed to phosphate buffer solution with 200 ppm monochloramine, 6 ppm iodide and 6000 ppm bromide at various contact times resulting in exposures or CT of 1000 ppm-h (orange), 5000 ppm-h (blue), and =30000 ppm-h (light green). The open circles are experimental data and the solid lines are simulated data.

3.3 Batch experiments with Sepro polysulfone membranes in standard seawater and phosphate buffer

Tests were performed to check if monochloramine would react with polysulfone support in the absence of the PA active layer. Experiments were performed with standard seawater and phosphate buffer solution, using monochloramine concentration of 200 ppm and contact time of 150 hours corresponding to a exposure or CT = 30000 ppm-h. The experiments were performed without addition of iodide or bromide. Experimental results are shown in Figure 12. The spectra are consistent with those observed with the SW30HR RO membrane. Monochloramine exposure in standard seawater resulted in deterioration of the polysulfone and corresponding uptake of

calcium, while no polysulfone damage or calcium uptake took place with the phosphate buffer solution.

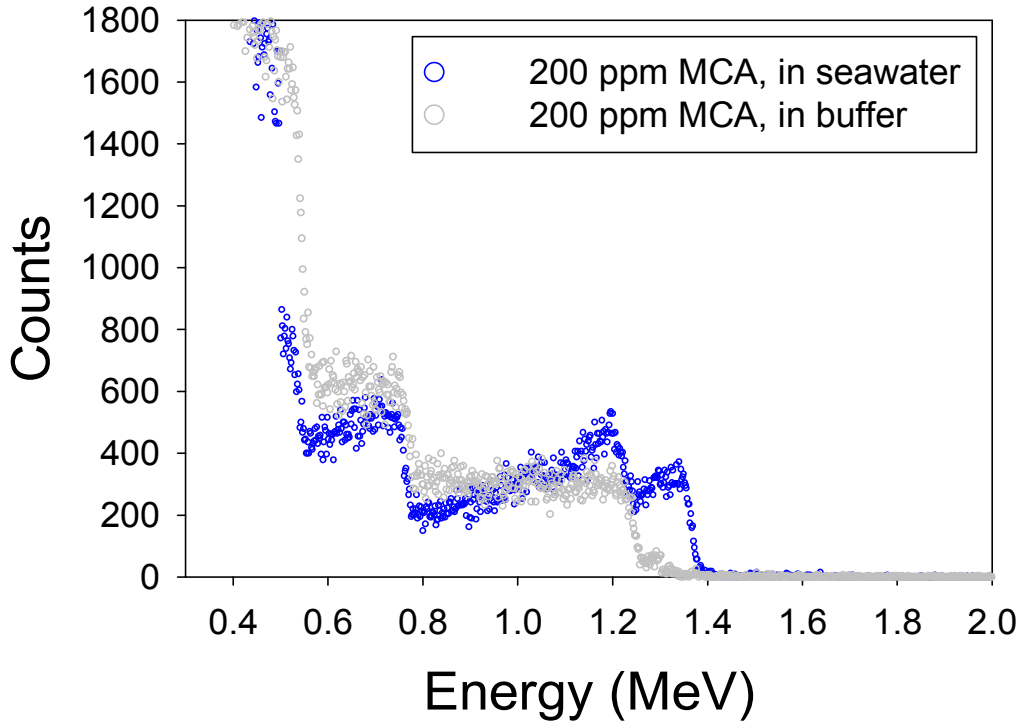

Figure 12. RBS spectra of polysulfone membrane exposed to 200 ppm of monochloramine in standard seawater (blue) and phosphate buffer solution (grey) in both cases at a contact time of 150 hours resulting in and exposure or CT of 30000 ppm-h.

3.4 Batch experiments with real seawater

The experiments outlined in Sections 3.1-3.3 illustrate that there is a phenomenon occurring in the batch reactors containing standard seawater which is not occurring in the batch reactors containing phosphate buffer. Based on these results we hypothesized that the polysulfone support component of the RO membrane is being broken down by monochloramine

(or its byproducts) and the divalent cations calcium and to a lesser extent magnesium participate in ion exchange with the resulting deprotonated carboxylic and/or sulfonic groups in the support. Although standard seawater has been used in previous studies to replicate real seawater conditions, we felt the use of real seawater was necessary to ensure that the phenomenon we observed was not an artifact of the chemical constituents used to make the standard seawater. Because the observation with standard seawater revealed that contact time was the key parameter while monochloramine concentration did not play a role, the more realistic concentration of 2 ppm was used for monochloramine. The experimental batch reactors contained 2 ppm NH_2Cl in real seawater (at a natural pH=7.9). The control batch reactors contained real seawater and the same volume of phosphate buffer that was added to the experimental batch reactors as NH_2Cl. This was done to ensure that the concentration of seawater constituents was equal in both the control and experimental reactors. Sepro brand polysulfone membranes were tested. After 21 days, the batch experiments were terminated and the resulting membrane coupons were analyzed. The RBS results in Figure 13 show no evidence of the polysulfone membrane degradation observed in the previous experiments conducted in standard seawater. The control and experimental membrane spectra were indistinguishable. It was concluded that the observed phenomena may require a longer exposure time than 21 days so these experiments were restarted and continued by another student. Those results will not be reported herein.

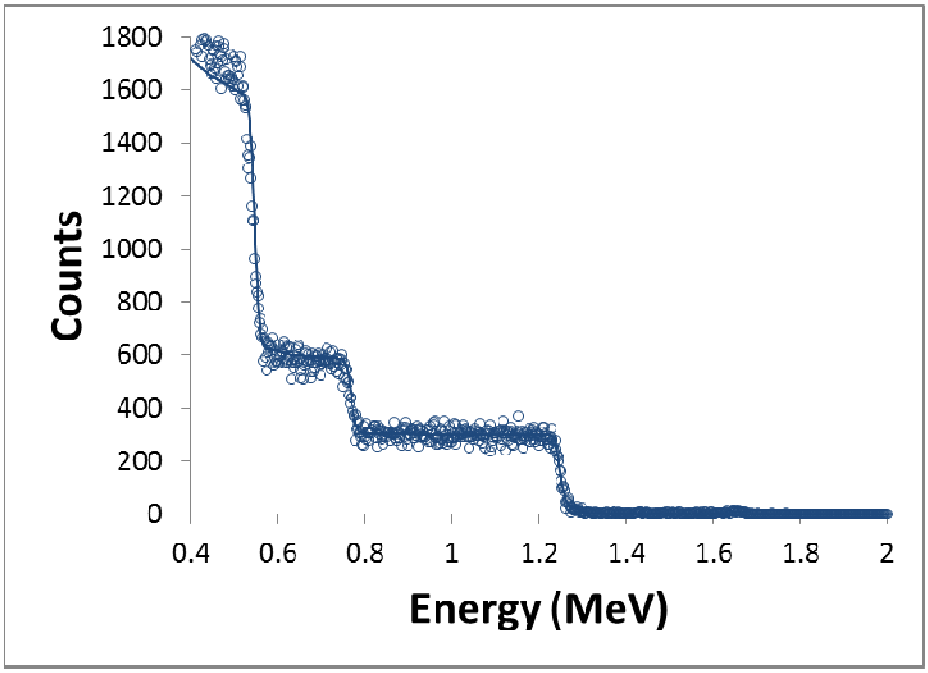

Figure 13. RBS spectra of a polysulfone membrane sample exposed to ~1000 ppm h NH_2Cl at pH=7.9. Carbon from 0.4-0.55 MeV, oxygen plateau from ~0.6-0.75 MeV, sulfur plateau from ~0.75-1.25 MeV. The open circles are experimental data and the solid line is simulated data.

3.5 Ion probing an untreated SW30HR RO membrane with cesium chloride (CsCl)

Untreated SW30HR RO membrane coupons were soaked in CsCl solutions according to the procedure discussed in Section 2.4.5. The pK_a values for $R\text{-}COO^-$ groups in the polyamide active layer are reported to be 5.23 and 8.97 (Coronell et al., 2008). Therefore, a saturation pH of 10.3 was used in order to maximize the concentration of deprotonated carboxylic sites potentially available to Cs^+. The resulting RBS spectrum is shown in Figure 14. Based on modeling within SIMNRA, if cesium was present in the active layer, it would appear around ~1.75 MeV. The spectrum shows no evidence that cesium is present in the active layer at a detectable concentration. The unhydrated radius of Cs^+ is in the range of 1.86-2.1 Å (Kielland, 1937;

Volkov, Paula, & Deamer, 1997). The two reported pore sizes for prepared membranes with fully aromatic PA are 2.1-2.4 Å and 3.5-4.5 Å (Kim, 2005). There may be interconnectivity between the different pore sizes so it is possible that the Cs^+ was not able to access carboxylic groups because the larger pores may be accessible only through the smaller pores. Another possibility is that the pore sizes of the SW30HR RO membrane are smaller than those reported by Kim et al.

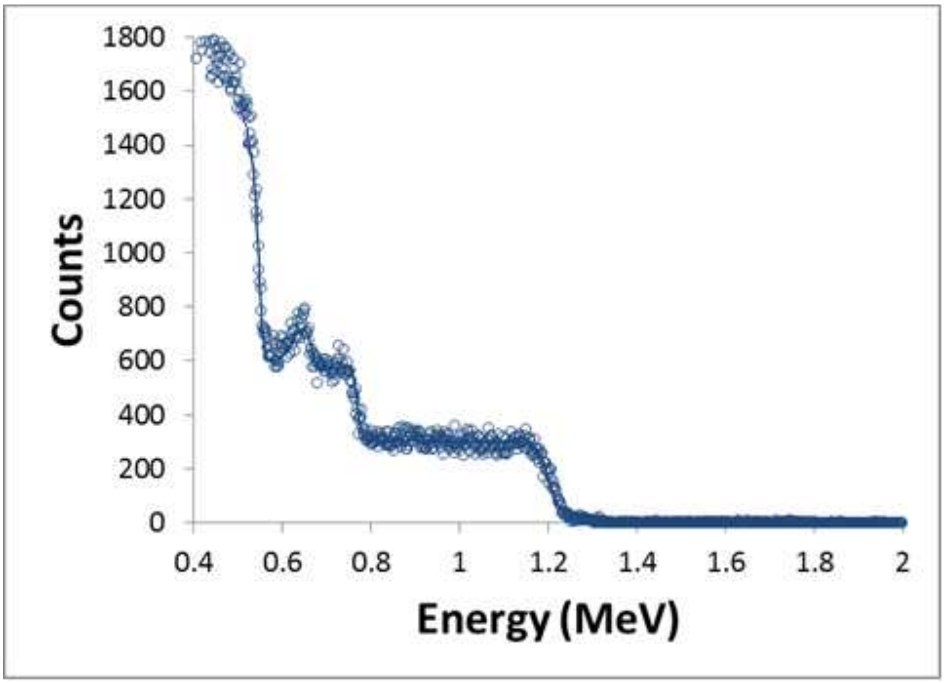

Figure 14. Untreated SW30HR RO membrane immersed in CsCl ion probe solutions at pH~10.3. The open circles are experimental data and the solid line is the simulated spectrum.

3.6 Ion probing an untreated SW30HR RO membrane with silver nitrate ($AgNO_3$)

Untreated SW30HR RO membrane coupons were soaked in $AgNO_3$ solutions according to the procedure discussed in Section 2.4.4. A range of experimental pH values were used to achieve various levels of deprotonation for the $R\text{-}COO^-$ groups in the polyamide active layer consistent with the pK_a values of 5.23 and 8.97 reported for the FT30 membranes (Coronell et

al., 2008). The resulting RBS spectra are shown in Figure 15. The silver peaks are centered at ~1.70 MeV and increase in counts as the pH of the $AgNO_3$ solutions increases. This is consistent with the carboxylic groups becoming deprotonated as the pH increases thereby allowing the Ag^+ to neutralize the -1 charge.

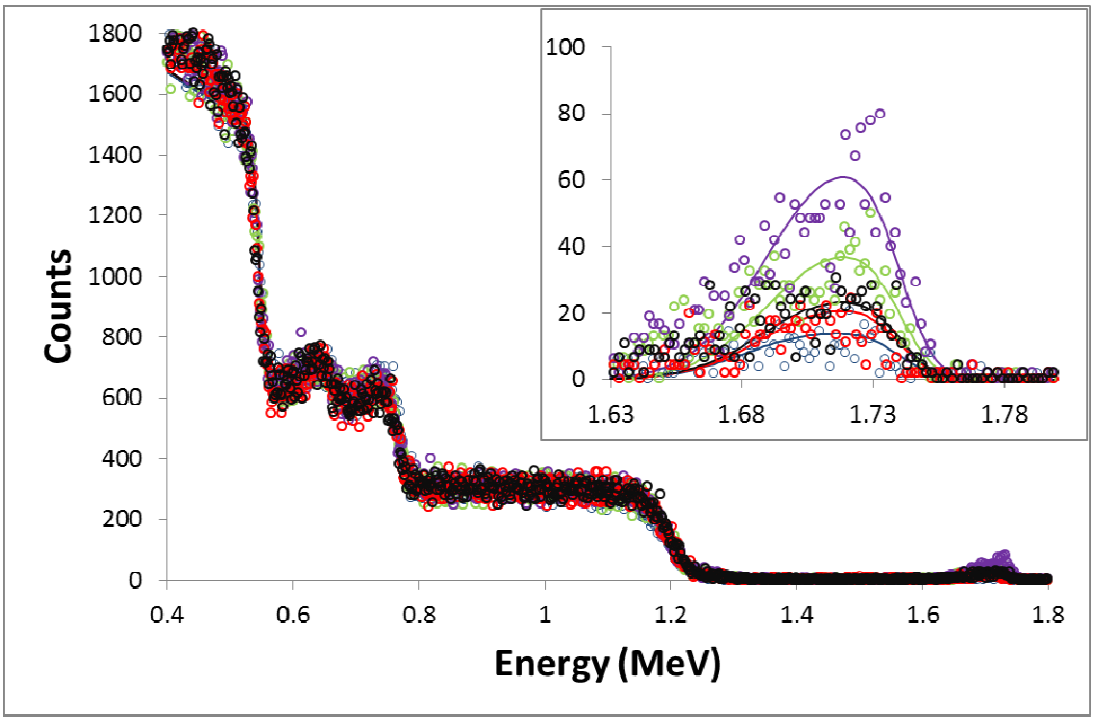

Figure 15. Untreated SW30HR RO membrane probed with silver at pH 5.87 (blue), pH 7.05 (red), pH 7.85 (black), pH 8.89 (green), and pH 9.63 (purple). The open circles are experimental data and the solid lines are simulated spectra.

The silver concentrations obtained for untreated SW30HR RO membrane are plotted as a function of pH in Figure 16. Also shown in the figure are lines corresponding to fitting the silver concentrations as a function of pH using Equation 1 (Orlando Coronell et al., 2008).

(1)

Where $R–COO^-$ is the concentration of deprotonated carboxylic groups, $C_{T,R\text{-}COOH}$ is the total concentration of carboxylic groups (protonated and deprotonated) in the active layer, $K_{a,i}$ is the ith acid dissociation constant of the carboxylic groups (i=1 or 2), and $[H^+]$ is the proton concentration corresponding to the pH of the ion probe solution. The $[R–COO^-]$ obtained from RBS analyses are plotted against the corresponding $[H^+]$ values in Figure 16. The line plot also shown in the figure was obtained by using $C_{T,R\text{-}COOH}$, $pK_{a,1}$, $pK_{a,2}$, and as fitting parameters..

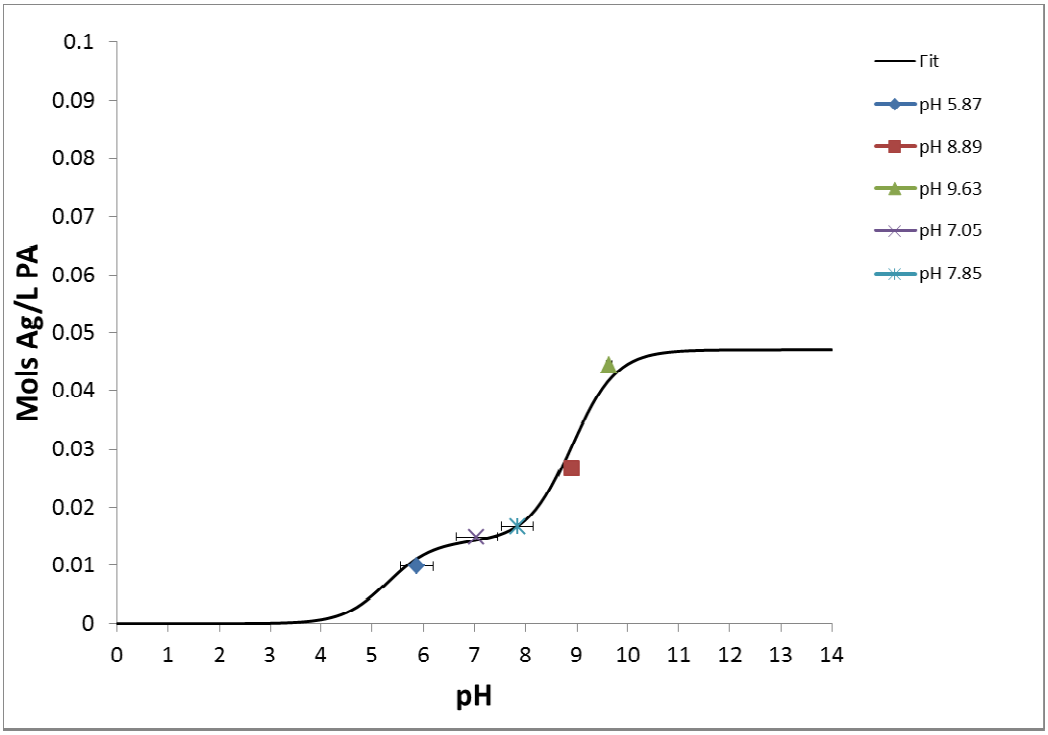

Figure 16. Untreated SW30HR RO membrane probed with silver at pH 5.87 (diamond), pH 7.05 (X), pH 7.85 (star), pH 8.89 (square), and pH 9.63 (triangle). The solid line represents the fit of Equation 1 to the experimental data.

The fitting parameters were $C_{T,R\text{-}COOH}$=0.047 M, = 0.3, =0.7, pK_{a1}=5.3, and pK_{a2}=8.89. A comparison to the fitting parameters obtained by Coronell et al. for the FT30

membrane revealed similarity with , = 0.19, =0.81, pK_{a1}=5.23, and pK_{a2}=8.97 (Coronell et al., 2008). In contrast, the total concentration of carboxylic groups is markedly different to the value $C_{T,R\text{-}COOH}$=0.432 M (Coronell et al., 2008) reported for the SW30HR RO membrane. Such observation would be consistent with the SW30HR sample used in this study having smaller pore sizes than the older FT30 membrane sample. This would also explain the observations for the experiment using cesium as ion probe (Section 3.5).

3.7 Ion exchange with an untreated SW30HR RO membrane with silver and barium

Untreated SW30HR RO membrane coupons were soaked in $AgNO_3$ and $Ba(NO_3)_2$ solutions according to the procedure discussed in Section 2.4.6. The ion probe solutions had the same pH as the solutions in Section 3.6. The barium data is shown in Figure 17 and is plotted on the same scale as Figure 16 in order to compare.

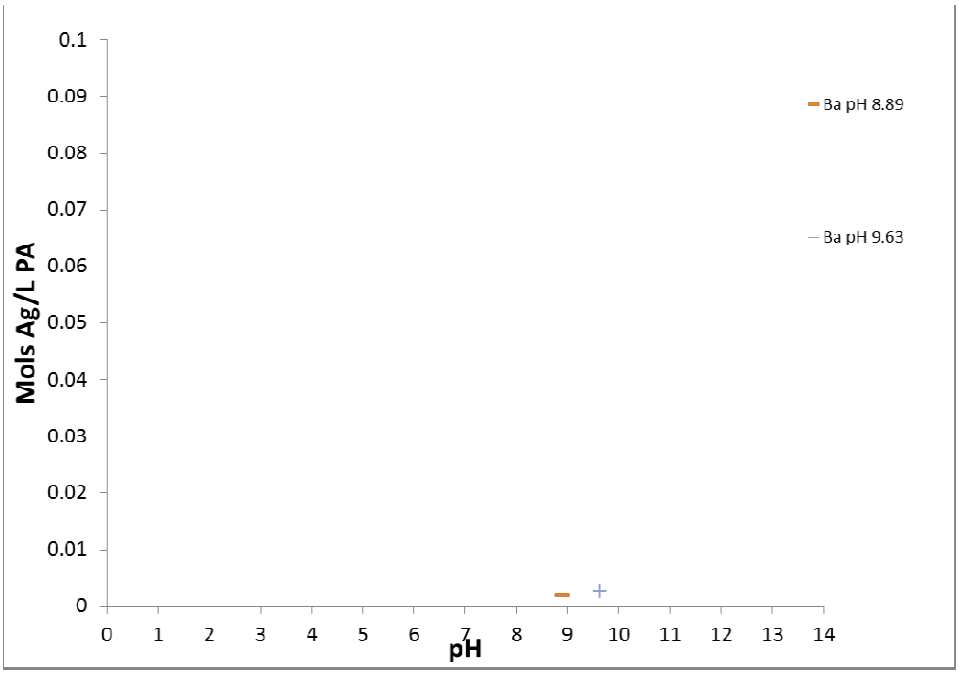

Figure 17. Untreated SW30HR RO membrane probed with barium pH 8.89 (dash symbol), and pH 9.63 (plus symbol).

The barium concentrations at pH 5.87, 7.05, and 7.85 were not detected in the active layer by RBS. It has already been determined that Ag^{+}, which has $R_{unhydrated}$=0.81-1.42 Å, was detected at a concentration of one tenth of that found in FT30 membranes so it is not surprising that Ba^{2+} with a larger radius, $R_{unhyrated,\ Ba}{}^{2+}$=2.1 Å (Kielland, 1937), could not access the apparently smaller pores of the SW30HR membrane. Based on this finding, the SW30HR RO membranes treated in phosphate buffer, standard seawater, and real seawater were not probed with solutions of $Ba(NO_3)_2$ because the barium would not be detectable throughout a majority (pH 5 through pH 8) of the carboxylic group titration curve.

3.8 Ion probing SW30HR RO membranes treated with phosphate buffer

Batch experiments containing phosphate buffer were conducted in order to perform ion probe experiments and FTIR analyses on the treated membranes. Our hope was to utilize silver and barium probes to determine the effect of these batch conditions on carboxylic group accessibility and to use FTIR to asses any changes in the characteristic functional groups of the membrane. The experimental batch reactors contained phosphate buffer (15 mM, pH =7.9), 2 ppm NH_2Cl , and 65 mg/L KBr as Br^{-}. The control batch reactors contained phosphate buffer (15 mM, pH =7.9) and 65 mg/L KBr as Br^{-}. KI was not added to the batch reactors in these experiments because the iodine and barium peaks overlap in the RBS energy spectrum making it difficult to accurately quantify the ion probe concentration. The membranes were transferred to batch reactors with fresh solutions every 24 hours for 20 days. The resulting RBS spectrum of the membrane samples prior to ion probe experiments is shown in Figure 18. There is a bromine peak centered around 1.6 MeV due to bromination of the active layer. The bromine concentration

in the experimental spectrum was calculated to be 0.837 M Br. Using the polymer repeating unit for the fully aromatic polyamide, $C_{36}H_{24}N_6O_6$, the bromination level observed would correspond to approximately 61 percent of the polyamide having one bromine addition or $C_{36}H_{23}N_6O_6Br$ and the rest remaining in its original form $C_{36}H_{24}N_6O_6$.

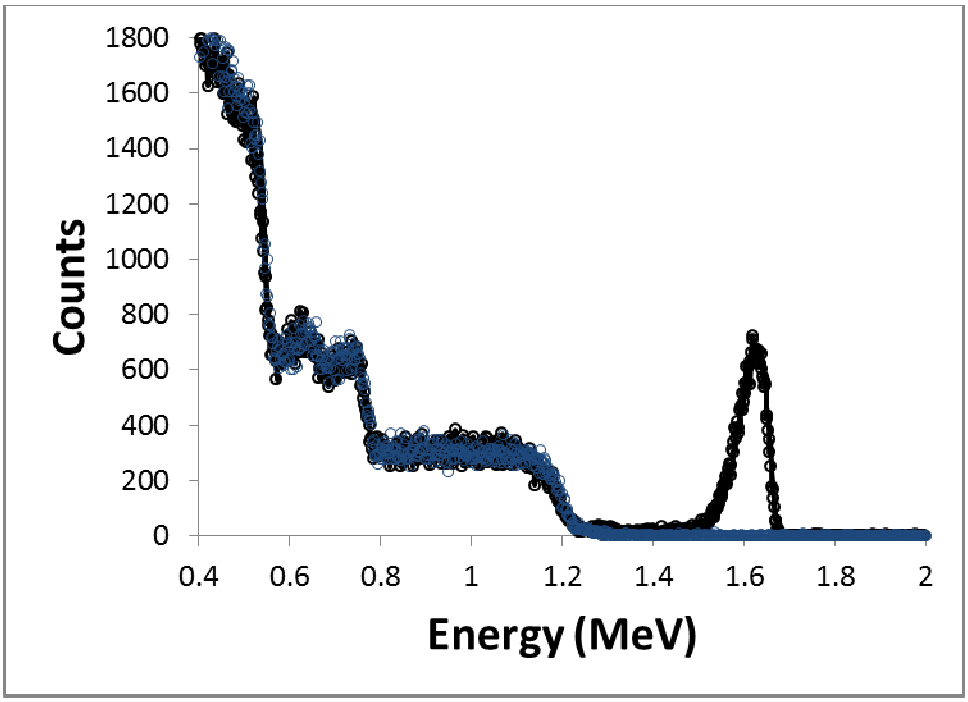

Figure 18. SW30HR RO membrane exposed to 960 ppm h NH_2Cl in phosphate buffer at pH=7.9 with 65 mg/L KBr as Br^-. The open circles are experimental data and the solid line is simulated data. The blue spectrum is the control and the black spectrum is the experimental reactor.

The results of the silver ion probe experiments are shown in Figure 19.

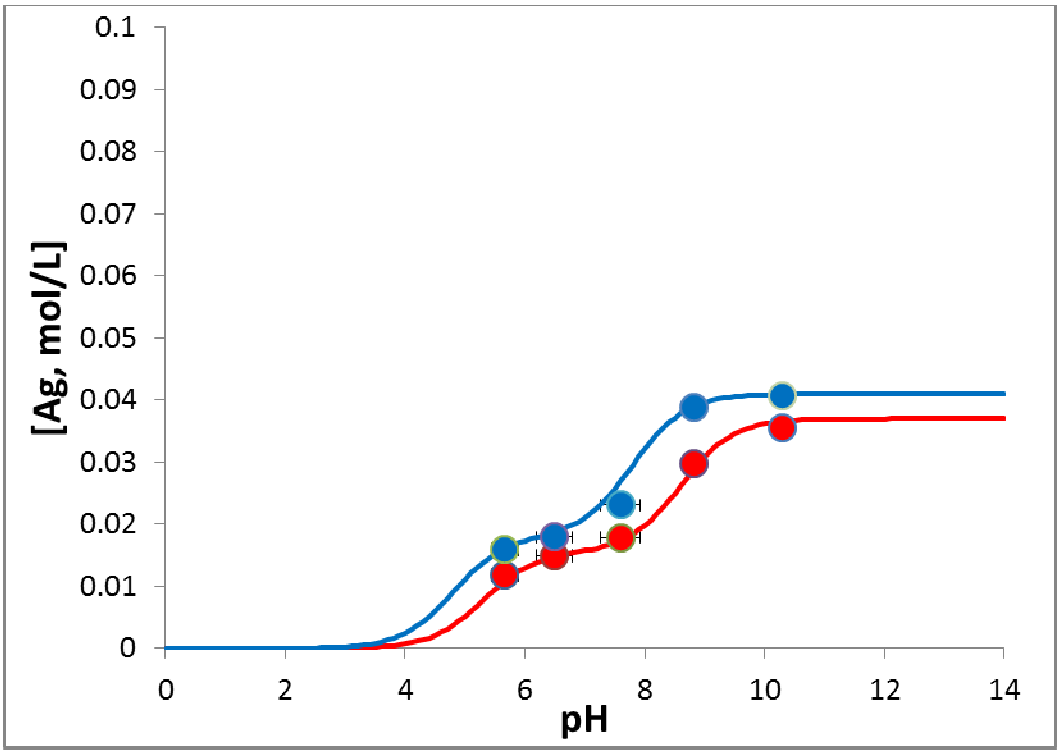

Figure 19. SW30HR RO membrane exposed to 960 ppm h NH_2Cl in phosphate buffer at pH=7.9 with 65 mg/L KBr as Br^- then probed with silver at various pHs. The red circles are the control data (without NH_2Cl) and the blue circles are the experimental data (with NH_2Cl). The solid red and blue lines are fit to the data, using Equation 1, to the control and experimental data, respectively.

The fitting parameters for the control (red line) were $C_{T,R\text{-}COOH}$=0.037 M, = 0.42, =0.58, pK_{a1}=5.3, and pK_{a2}=8.6. The fitting parameters for the experimental (blue line) were $C_{T,R\text{-}COOH}$=0.041 M, = 0.44, =0.56, pK_{a1}=4.8, and pK_{a2}=7.8. The pK_a values of the NH_2Cl data are lower than the pK_a values of the control data. This would be consistent with the carboxylic groups being more accessible to neutralization by silver. This suggests less cross-linking of the polyamide, a higher dielectric constant inside the pores, and therefore lower pK_a

values. The bromination of the active layer may result in this increase in accessible carboxylic groups.

3.9 Ion probing SW30HR RO membranes treated with standard seawater

Batch experiments containing standard seawater were conducted in order to perform ion probe experiments and FTIR analyses on the treated membranes. Our hope was to utilize silver and barium probes to determine the effect of these batch conditions on carboxylic group accessibility and to use FTIR to assess any changes in the characteristic functional groups of the membrane. The experimental batch reactors contained standard seawater prepared according to Grassholf et al. 1999 (pH =7.9), 2 ppm NH_2Cl , and 65 mg/L KBr as Br^-. The control batch reactors contained standard seawater (pH =7.9) and 65 mg/L KBr as Br^-. KI was not added to the batch reactors in these experiments because the iodine and barium peaks overlap in the RBS energy spectrum making it difficult to accurately quantify the ion probe concentration. The membranes were transferred to batch reactors with fresh solutions every 24 hours for 20 days. The resulting RBS spectrum of the membrane samples prior to ion probe experiments is shown in Figure 20. There is a bromine peak centered around 1.6 MeV due to bromination of the active layer from NHBrCl. The bromine concentration in the experimental spectrum was calculated to be 0.997 M Br. Using the polymer repeating unit for the fully aromatic polyamide, $C_{36}H_{24}N_6O_6$, the bromination level observed would correspond to approximately 72 percent of the polyamide having one bromine addition or $C_{36}H_{23}N_6O_6Br$ and the rest remaining in its original form $C_{36}H_{24}N_6O_6$.

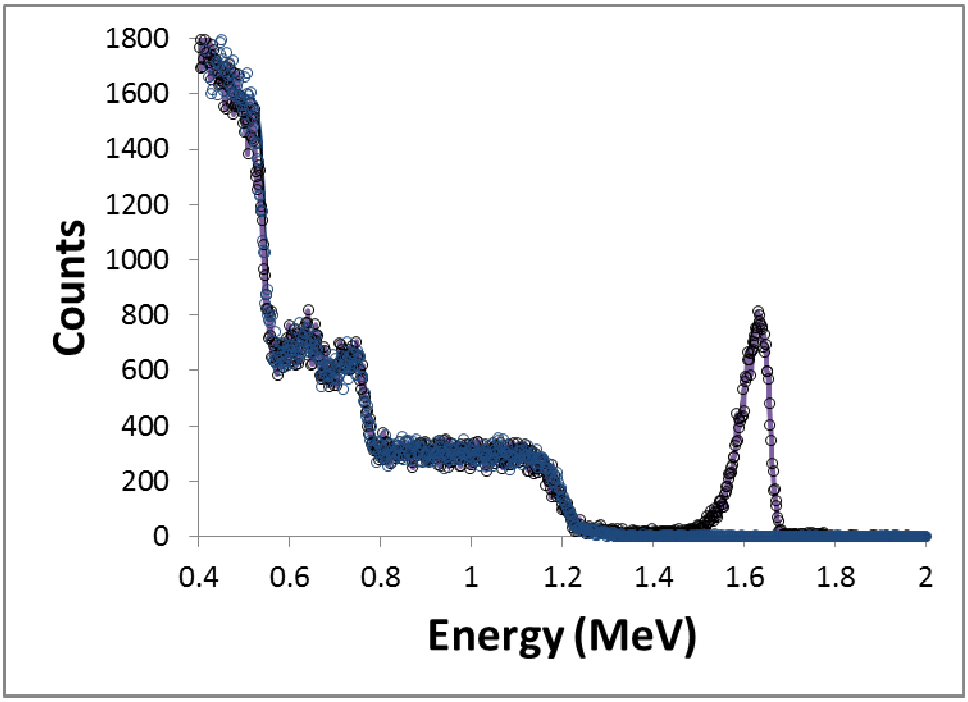

Figure 20. SW30HR RO membrane exposed to 960 ppm h NH_2Cl in standard seawater at pH=7.9 with 65 mg/L KBr as Br^-. The open circles are experimental data and the solid line is simulated data. The blue spectrum is the control and the black spectrum is the experimental reactor.

The results of the silver ion probe experiments are shown in Figure 21.

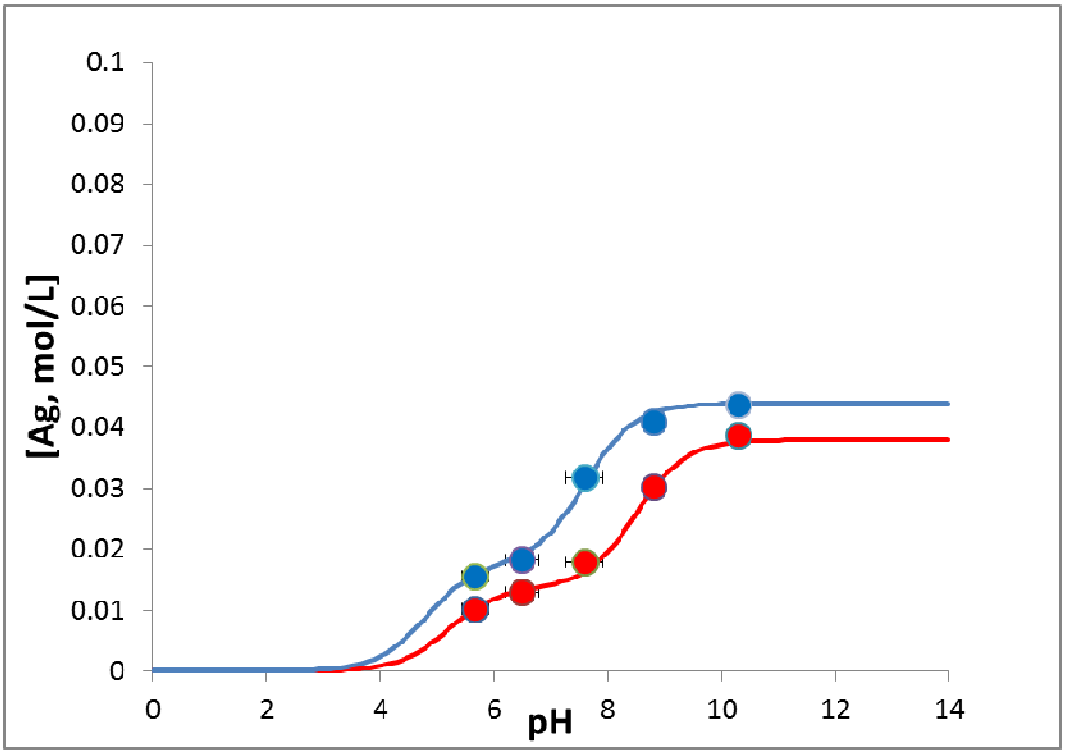

Figure 21. SW30HR RO membrane exposed to 960 ppm h NH_2Cl in standard seawater at pH=7.9 with 65 mg/L KBr as Br^- then probed with silver at various pHs. The red circles are the control data (without NH_2Cl) and the blue circles are the experimental data (with NH_2Cl). The solid red and blue lines are fit to the data, using Equation 1, to the control and experimental data, respectively.

The fitting parameters for the control (red line) were $C_{T,\text{R-COOH}}$=0.038 M, = 0.36, =0.64, pK_{a1}=5.2, and pK_{a2}=8.5. The fitting parameters for the experimental (blue line) were $C_{T,\text{R-COOH}}$=0.044 M, = 0.40, =0.60, pKa1=4.8, and pKa2=7.6. Similar to the observation with phosphate buffer, the pK_a values of the NH_2Cl data are lower than the pK_a values of the control data. Again, this would be consistent with the carboxylic groups being more accessible to neutralization by silver, and suggests less cross-linking of the polyamide, and a higher dielectric

constant. The bromination of the active layer may result in this increase in accessible carboxylic groups.

3.10 Ion probing SW30HR RO membranes treated with real seawater

Batch experiments containing real seawater were conducted in order to perform ion probe experiments and FTIR analyses on the treated membranes. The experimental batch reactors contained real seawater (pH =7.9) and 2 ppm NH_2Cl. The control batch reactors contained standard seawater (pH =7.9). The membranes were transferred to fresh batch reactor solution every 24 hours for 20 days. The resulting RBS spectrum of the membrane samples prior to ion probe experiments is shown in Figure 22. There is a bromine peak centered around 1.6 MeV due to bromination of the active layer from NHBrCl or some other active bromine species. The bromine concentration in the experimental spectrum was calculated to be 0.69 M. The iodine peak is barely visible but is centered near 1.75 MeV due to iodination of the active layer from HOI. The iodine concentration in the experimental spectrum was calculated to be 2.01×10^{-5} M. Using the polymer repeating unit for the fully aromatic polyamide, $C_{36}H_{24}N_6O_6$, the bromination level observed would correspond to approximately 51 percent of the polyamide having one bromine addition or $C_{36}H_{23}N_6O_6Br$, 0.7 percent of the polyamide having one iodine addition or $C_{36}H_{23}N_6O_6I$, and the rest remaining in its original form $C_{36}H_{24}N_6O_6$.

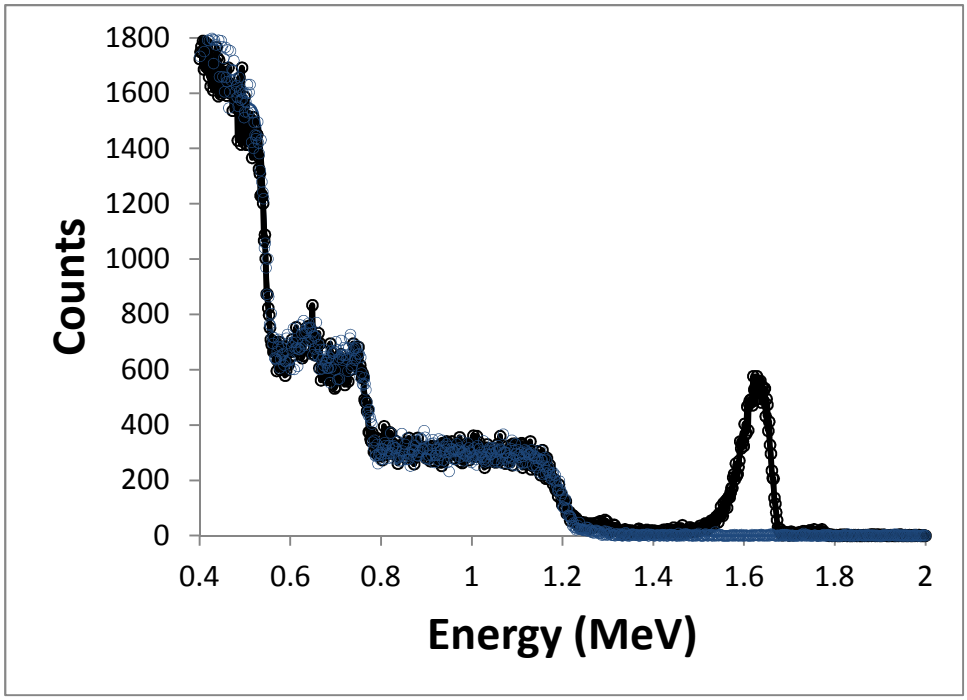

Figure 22. SW30HR RO membrane exposed to 960 ppm h NH_2Cl in real seawater at pH=7.9. The open circles are experimental data and the solid line is simulated data. The blue spectrum is the control and the black spectrum is the experimental reactor.

The results of the silver ion probe experiments are shown in Figure 23.

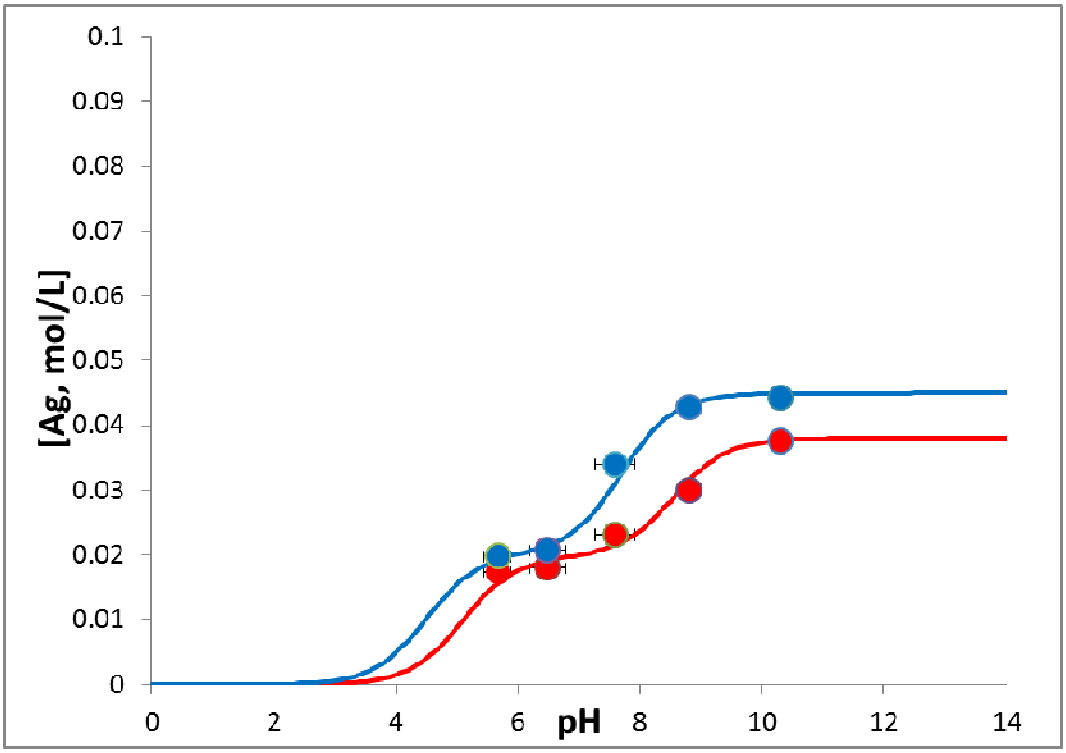

Figure 23. SW30HR RO membrane exposed to 960 ppm h NH_2Cl in real seawater at pH=7.9 then probed with silver at various pHs. The red circles are the control data (without NH_2Cl) and the blue circles are the experimental data (with NH_2Cl). The solid red and blue lines are fit to the data, using Equation 1, to the control and experimental data, respectively.

The fitting parameters for the control (red line) were $C_{T,\text{R-COOH}}$=0.038 M, = 0.52, =0.48, pK_{a1}=5.1, and pK_{a2}=8.55. The fitting parameters for the experimental (blue line) were $C_{T,\text{R-COOH}}$=0.045 M, = 0.45, =0.55, pK_{a1}=4.5, and pK_{a2}=7.7. Again, the pK_a values of the NH_2Cl data are lower than the pK_a values of the control data. Real seawater and standard seawater may have a greater effect than phosphate buffer due to trace metal ions catalyzing the reactions between both NH_2Cl and bromide (to form secondary oxidizing agent NHBrCl) and NHBrCl and the polyamide active layer. The second reaction effect is more probable as a similar

concentration of bromine was detected in membranes treated in reactors with phosphate buffer and real seawater.

Although it appears the bromine concentration in the active layer has not reached its maximum, the monobromination observed under each batch reactor condition is consistent with bromine being an electron withdrawing group which deactivates the ring from further bromination (Soice et al., 2002).

3.11 FTIR analysis of SW30HR RO membranes in phosphate buffer, standard seawater, and real seawater

FTIR analyses were performed according to the method outlined in Section 2.4.6. The data of five replicates from each sample were averaged. The results are shown in Figure 24.

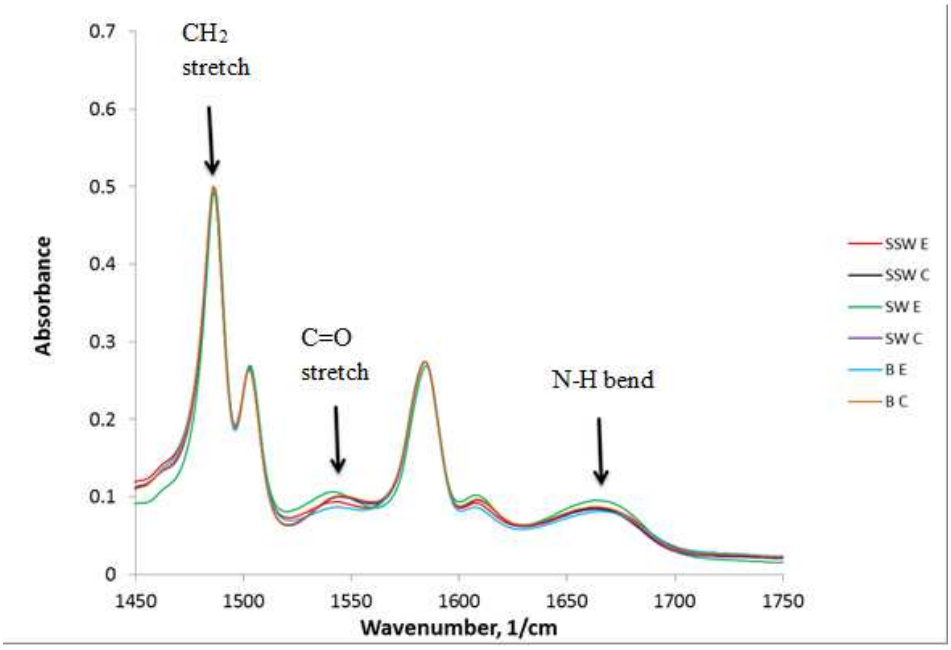

Figure 24. FTIR spectrum of SW30HR RO membranes exposed to seawater, standard seawater, or phosphate buffer, 2 ppm NH_2Cl, and 65 mg/L KBr as Br^- (reactors with real seawater did not contain added KBr).

The spectra were normalized to the CH_2 stretch of polysulfone at 1486 cm^{-1} because this peak is assumed to not change under our batch reactor conditions. The C=O stretch of the secondary amide group (Amide I peak) around 1663 cm^{-1} was not significantly different among the samples. The N-H bend of the amide group (Amide II peak) around 1541 cm^{-1} also did not vary significantly. These results are consistent with those found by Gabelich who exposed his membranes to a similar NH_2Cl concentration and did not observe any changes in the Amide II peak. These results do not mean that the membrane is not being damaged. The detection limit of this method may not be low enough to detect the damages occurring in the membrane. However, we can infer that these reaction conditions do not result in the same degree of chlorination/oxidation of the active layer as other studies have shown. Realistically, this is due to the lower NH_2Cl concentration employed in the batch reactors not the total exposure time. Evidence for this argument is confirmed by studies done by Cran et al vs Gabelich et al in which Cran saw noticeable differences in the characteristic amide peaks and Gabelich did not. These studies used similar CTs (ppm x h) but a 10 fold difference in NH_2Cl concentration (Cran et al., 2011; Gabelich et al., 2005). The FTIR results also suggest that the concentration of secondary oxidizing agents did not noticeably change the characteristic polyamide peaks in the active layer.

CHAPTER 4. CONCLUSIONS

This research focused on elucidating the chemistry involved in RO/NF membrane active layer degradation during monochloramine treatment designed to prevent biofouling. The objectives of this work were to conduct batch experiments with SW30HR membranes and perform analyses of the resulting membrane samples by RBS, aided with heavy ion probes, and FTIR to determine the effect of monochloramine and secondary oxidizing agents formed from the reaction between monochloramine, iodide, and bromide on membrane structure.

Initial batch experiments conducted in standard seawater using higher NH_2Cl, bromide, and iodide concentrations revealed the occurrence of both bromination and iodination of the active layer. However, the concentration of bromine and iodine detected in the active layer was not proportional to the concentrations introduced in to the reactors. A calcium peak was also observed with synthetic seawater in the absence of bromide after ~190 h of exposure to ~2 mg/L of NH_2Cl. This was hypothesized to be a transformation of the polysulfone support resulting in an increased concentration of carboxylic or sulfonic groups and that retained calcium by ion exchange sorption. In the presence of bromine, the calcium peak was not as pronounced. The effect of contact time was tested and calcium concentration increased with increased CT at ~200 mg/L of NH_2Cl. The calcium uptake was similar to previous experiments using 2 ppm NH_2Cl but at comparable contact time. We concluded that NH_2Cl is needed for this effect to be observed but may be controlled by other constituents like metal catalysts witch limit the reaction. Experiments with initially both bromide and iodide revealed that bromination predominates and the calcium peak was again less pronounced than when bromide is present. Equivalent experiments conducted in phosphate buffer showed no apparent deterioration of the support. Consistent with these results, a Sepro polysulfone membrane intended to represent the support

layer exposed to NH_2Cl in standard seawater and phosphate buffer changed in the standard seawater but not in the phosphate buffer. These experiments changed the course of the work to determine if the changes observed with the support would occur in the presence of real seawater. Experiments conducted with Sepro membranes, 2 ppm NH_2Cl, and real seawater for 21 days did not reveal the occurrence of membrane support damage.

The next set of experiments involved the use of ion probes. Untreated SW30HR RO membranes were probed with solutions of CsCl, $AgNO_3$, and $Ba(NO_3)_2$ at various pH levels. Cesium was not detected in the active layer and barium was detected at only the highest pH values. This is indicative that these ions could not access the pores of the membrane containing the carboxylic groups. The silver probe could be detected at all of the tested pH values. However, the total concentration of carboxylic groups in the active layer of the SW30HR RO membrane tested in this project was found to be approximately 15 percent of that previously reported for the FT30 membrane.

Membrane samples treated in phosphate buffer, standard seawater, and real seawater were probed with silver at the same pH values. Experimental results revealed that treatment with chloramine resulted in an increase in the total concentration of carboxylic groups and decrease in both pK_a values for all three types of water tested. This would be consistent with the carboxylic groups becoming more accessible to neutralization by silver.

FTIR data of the same treated membranes used in the silver probe experiments did not show the occurrence of measurable changes in polyamide functional group characteristics.

REFERENCES

Applegate, L. E., Erkenbrecher Jr, C. W., & Winters, H. (1989). New chloroamine process to control aftergrowth and biofouling in permasepR B-10 RO surface seawater plants. *Desalination*, *74*, 51–67. Elsevier. Retrieved from http://www.sciencedirect.com/science/article/pii/0011916489850428

Avlonitis, S., Hanbury, W. T., & Hodgkiess, T. (1992). Chlorine degradation of aromatic polyamides. *Desalination*, *85*(3), 321-334. doi:10.1016/0011-9164(92)80014-Z

Bartels, C. (1989). A surface science investigation of composite membranes. *Journal of Membrane Science*, *45*, 225-245.

Causserand, C., & Rouaix, S. (2008). Ageing of polysulfone membranes in contact with bleach solution: role of radical oxidation and of some dissolved metal ions. *Chem. Eng. Process*, *47*, 48-56.

Coronell, Orlando, Mariñas, B. J., Zhang, X., & Cahill, D. G. (2008). Quantification of functional groups and modeling of their ionization behavior in the active layer of FT30 reverse osmosis membrane. *Environmental science & technology*, *42*(14), 5260-6. Retrieved from http://www.ncbi.nlm.nih.gov/pubmed/18754378

Cran, M. J., Bigger, S. W., & Gray, S. R. (2011). Degradation of polyamide reverse osmosis membranes in the presence of chloramine. *Desalination*, *283*, 58-63. Elsevier B.V. doi:10.1016/j.desal.2011.04.050

Dasilva, M., Tessaro, I., & Wada, K. (2006). Investigation of oxidative degradation of polyamide reverse osmosis membranes by monochloramine solutions. *Journal of Membrane Science*, *282*(1-2), 375-382. doi:10.1016/j.memsci.2006.05.043

Freger, V. (2003). Nanoscale heterogeneity of polyamide membranes formed by interfacial polymerization. *Langmuir*, *19*, 4791-4797.

Gabelich, C. (2002). Effects of aluminum sulfate and ferric chloride coagulant residuals on polyamide membrane performance. *Desalination*, *150*, 15-30.

Gabelich, C., Frankin, J., Gerringer, F., Ishida, K., & Suffet, I. (2005). Enhanced oxidation of polyamide membranes using monochloramine and ferrous iron. *Journal of Membrane Science*, *258*(1-2), 64-70. doi:10.1016/j.memsci.2005.02.034

Grasshoffiklaus, K., & Manfred, K. (1999). General remarks to the tables. *Analysis*.

Kang, G.-D., Gao, C.-J., Chen, W.-D., Jie, X.-M., Cao, Y.-M., & Yuan, Q. (2007). Study on hypochlorite degradation of aromatic polyamide reverse osmosis membrane. *Journal of Membrane Science*, *300*(1-2), 165-171. doi:10.1016/j.memsci.2007.05.025

Kawaguchi, T., & Tamura, H. (1984). Chlorine-resistant membrane for reverse osmosis. I. Correlation between chemical structures and chlorine resistance of polyamides. *Journal of Applied Polymer Science*, *29*(11), 3359-3367. doi:10.1002/app.1984.070291113

Kielland, J. (1937). Individual activity coefficients of ions in aqueous solutions. *Journal of American Chemical Society*, *59*, 1675-1678.

Kim, S. H. O. (2005). Positron Annihilation Spectroscopic Evidence to Demonstrate the Flux-Enhancement Mechanism in Membrane. *Environmental Science & Technology*, *39*(6), 1764-1770.

Koo, J.-young, Lee, J. H., Jung, Y. D., Hong, S. P., & Yoon, S. R. (n.d.). Chlorine Resistant Membrane and The Mechanism of Membrane Degradation by Chlorine. *Environment*, 2958-2969.

Kwon, Y., & Leckie, J. (2006a). Hypochlorite degradation of crosslinked polyamide membranesII. Changes in hydrogen bonding behavior and performance. *Journal of Membrane Science*, *282*(1-2), 456-464. doi:10.1016/j.memsci.2006.06.004

Kwon, Y.-N., & Leckie, J. O. (2006b). Hypochlorite degradation of crosslinked polyamide membranes. *Journal of Membrane Science*, *283*(1-2), 21-26. doi:10.1016/j.memsci.2006.06.008

Mayer, M., Duggan, J., & Morgan, I. (1998). Proceedings of the 15th International Conference on the Application of Accelerators in Research and Industry, Denton, TX. *SIMNRA, a simulation program for the analysis of NRA, RBS and ERDA* (p. 541).

Mi, B., Cahill, D. G., & Mariñas, B. J. (2007). Physico-chemical integrity of nanofiltration/reverse osmosis membranes during characterization by Rutherford backscattering spectrometry. *Journal of Membrane Science*, *291*(1-2), 77-85. doi:10.1016/j.memsci.2006.12.052

Mi, B., Coronell, O., Marinas, B., Watanabe, F., Cahill, D., & Petrov, I. (2006). Physico-chemical characterization of NF/RO membrane active layers by Rutherford backscattering spectrometry☆. *Journal of Membrane Science*, *282*(1-2), 71-81. doi:10.1016/j.memsci.2006.05.015

Murphy, A. (1991). Deterioration of cellulose acetate by transition metal salts in aqueous chlorine. *Desalination*, *85*, 45-52.

Petersen, R. (1993). Composite reverse osmosis and nanofiltration membranes. *Journal of Membrane Science*, *83*, 81-150.

Shannon, R. (1976). Revised effective ionic radii and systematic studies of interatomic distances in halides and chalcogenides. *Acta Crystallography*, *A32*, 751-767.

Shemer, H., & Semiat, R. (2011). Impact of halogen based disinfectants in seawater on polyamide RO membranes. *Desalination*, *273*(1), 179-183. doi:10.1016/j.desal.2010.05.056

Skrovanek, D., Howe, S., & Painter, P. (1985). Hydrogenbonding in polymers—infrared temperature studies of an amorphous polyamide. *Macromolecules*, *18*.

Smith, B. (2011). *Fundamentals of Fourier Transform Infrared Spectroscopy, Second Ed*. CRC Press.

Socrates, G. (1994). *Infrared Characteristic Group Frequencies*. Wiley/Interscience.

Soice, N. P., Greenberg, A. R., Krantz, W. B., & Norman, A. D. (2004). Studies of oxidative degradation in polyamide RO membrane barrier layers using pendant drop mechanical analysis. *Journal of Membrane Science*, *243*(1-2), 345-355. doi:10.1016/j.memsci.2004.06.039

Soice, N. P., Maladono, A. C., Takigawa, D. Y., Norman, A. D., Krantz, W. B., & Greenberg, A. R. (2002). Oxidative Degradation of Polyamide Reverse Osmosis Membranes : Studies of Molecular Model Compounds and Selected Membranes. *Polymer*.

Tanaka, S. (1994). New disinfection method in RO seawater desalination systems. *Desalination*.

Tessaro, I., Dasilva, J., & Wada, K. (2005). Investigation of some aspects related to the degradation of polyamide membranes: aqueous chlorine oxidation catalyzed by aluminum and sodium laurel sulfate oxidation during cleaning. *Desalination*, *181*, 275-282.

Volkov, A., Paula, S., & Deamer, D. (1997). Two mechanisms of permeation of small neutral molecules and hydrated ions across phospholipid bilayers. *Bioelectrochemistry and Bioenergetics*, *42*, 153-160.

White, G. . (1992). *The Handbook of Chlorination and Alternative Disinfectants, 3rd edition*. New York: Van Nostrand Reinhold.

APPENDIX

Figure	RBS files
2	0061-0069
3	0070-0078
4	0099, 0107, 0108, 0132, 0133, 0152, 0153
5	0117, 0118, 0119, 0138, 0156, 0157
6	0103, 0111, 0144, 0145, 0160, 0161
7	0079-0096
8	0088-0096
9	0120, 0121, 0122, 0154, 0155, 0134, 0135
10	0102, 0105, 0106, 0158, 0159, 0140, 0141
11	0104, 0115, 0116, 0162, 0163, 0146, 147
12	0136, 0137, 0142, 0143
13	0204
14	0255
15	0328-0349
17	0334, 0335, 0330, 0331
18	0383, 0397
20	0382, 0396
22	0361, 0398

RBS files

Figure 2:

0061

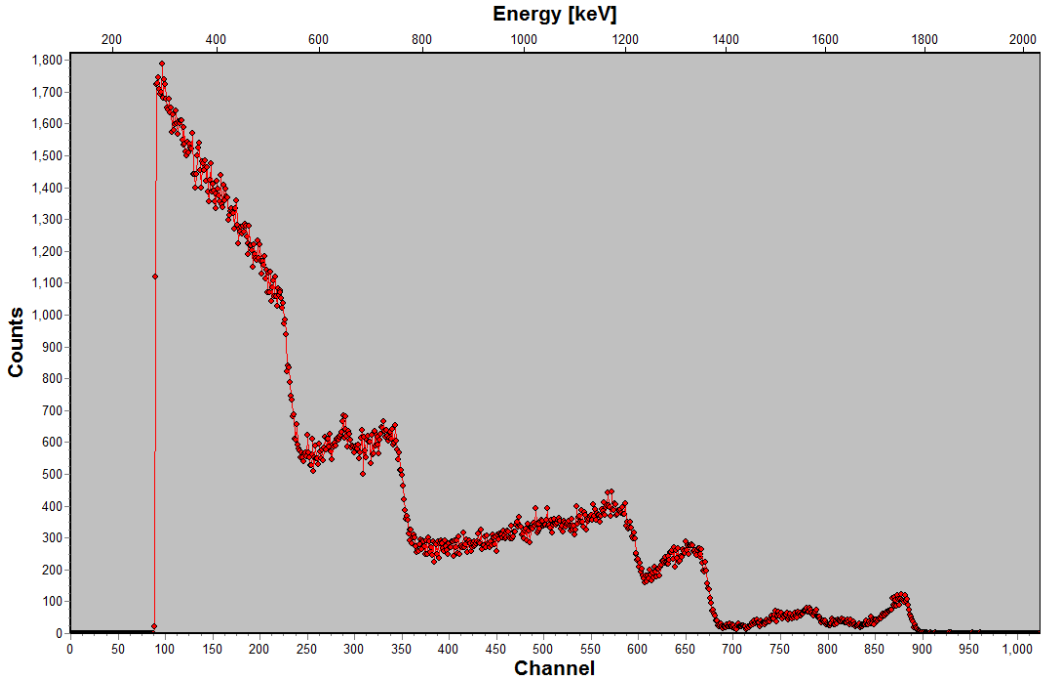

0062

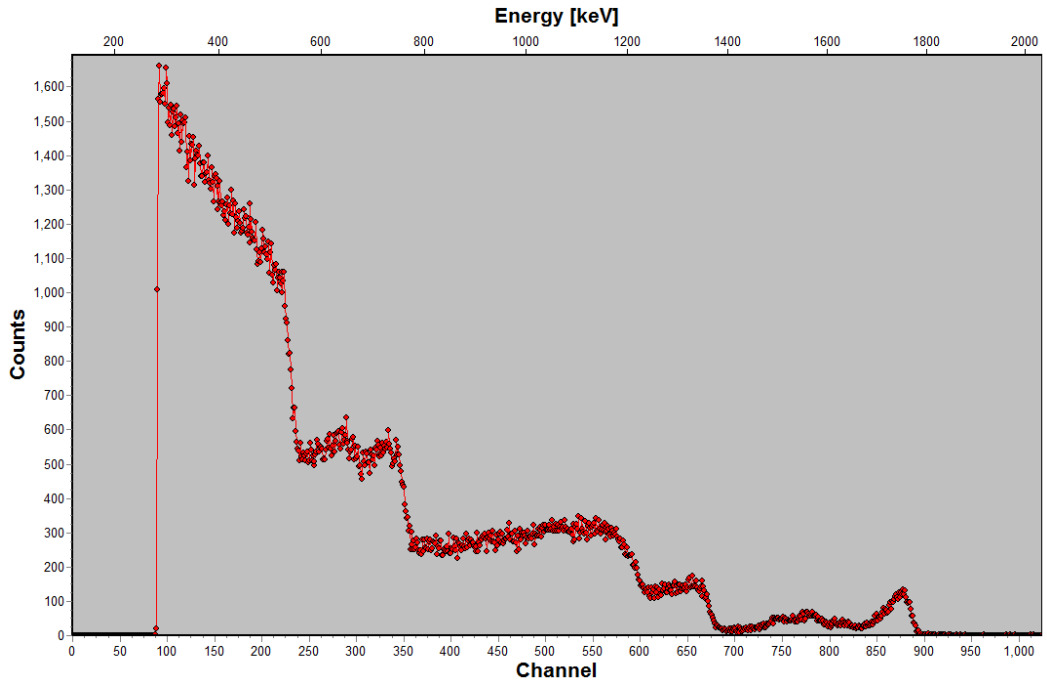
Energy [keV]
200 400 600 800 1000 1200 1400 1600 1800 2000
Counts
0 100 200 300 400 500 600 700 800 900 1,000 1,100 1,200 1,300 1,400 1,500 1,600
0 50 100 150 200 250 300 350 400 450 500 550 600 650 700 750 800 850 900 950 1,000
Channel

0063

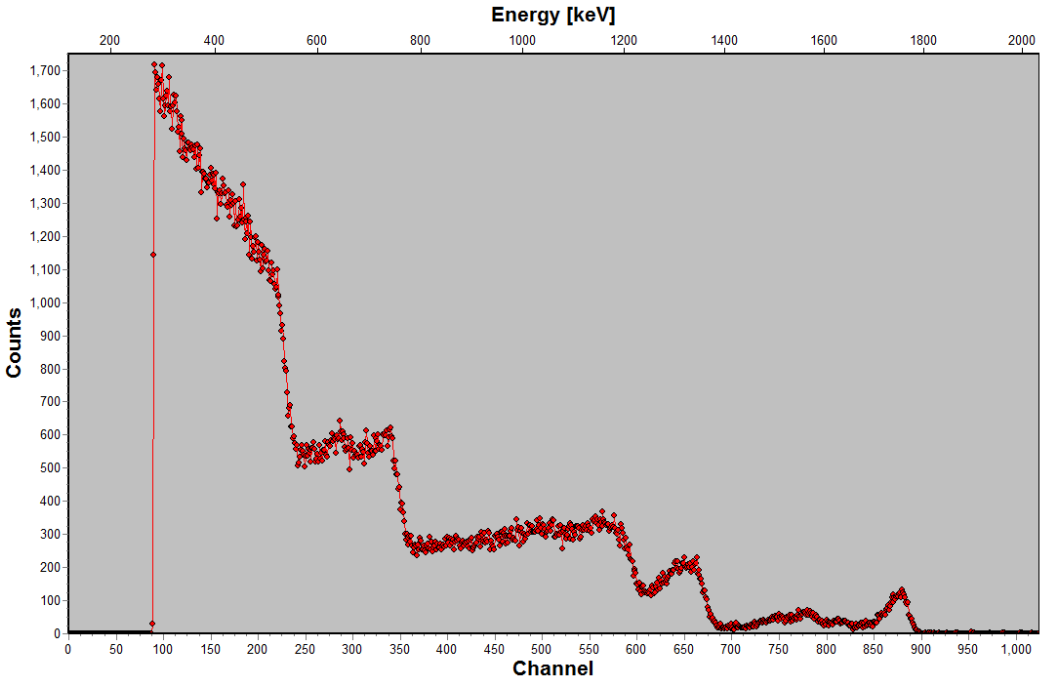
Energy [keV]
200 400 600 800 1000 1200 1400 1600 1800 2000
Counts
0 100 200 300 400 500 600 700 800 900 1,000 1,100 1,200 1,300 1,400 1,500 1,600 1,700
0 50 100 150 200 250 300 350 400 450 500 550 600 650 700 750 800 850 900 950 1,000
Channel

0064

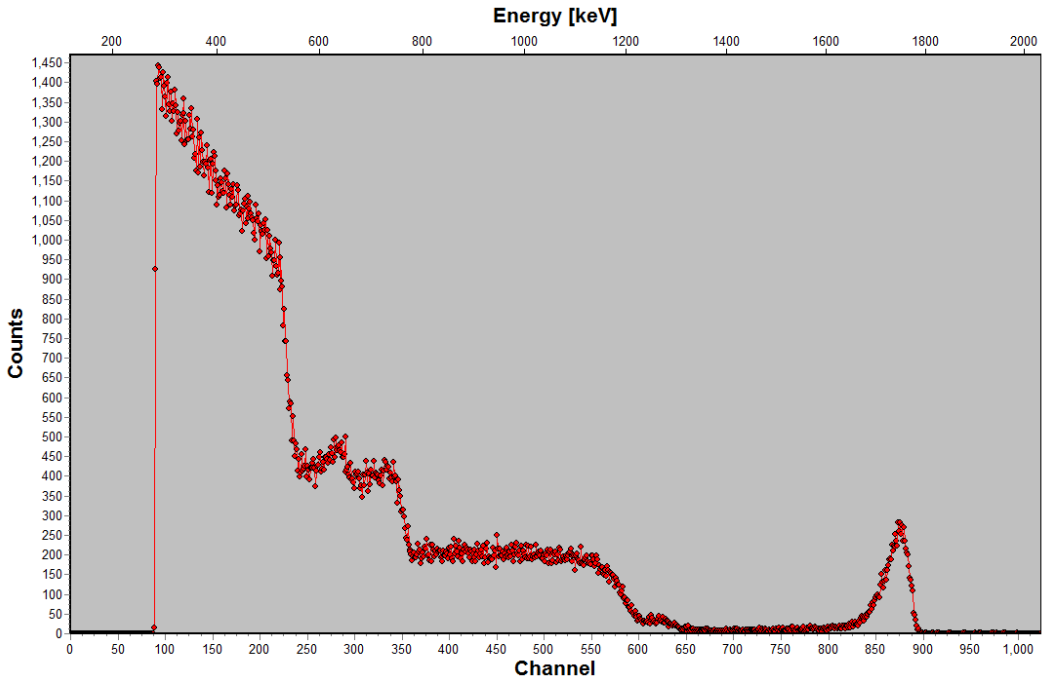

0065

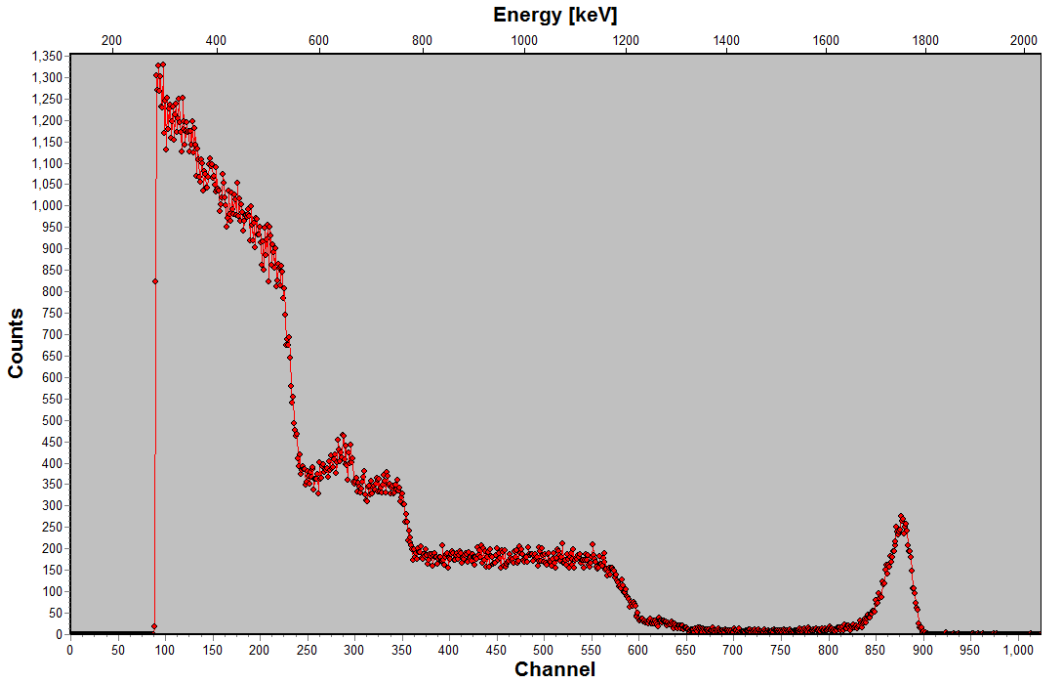

0066

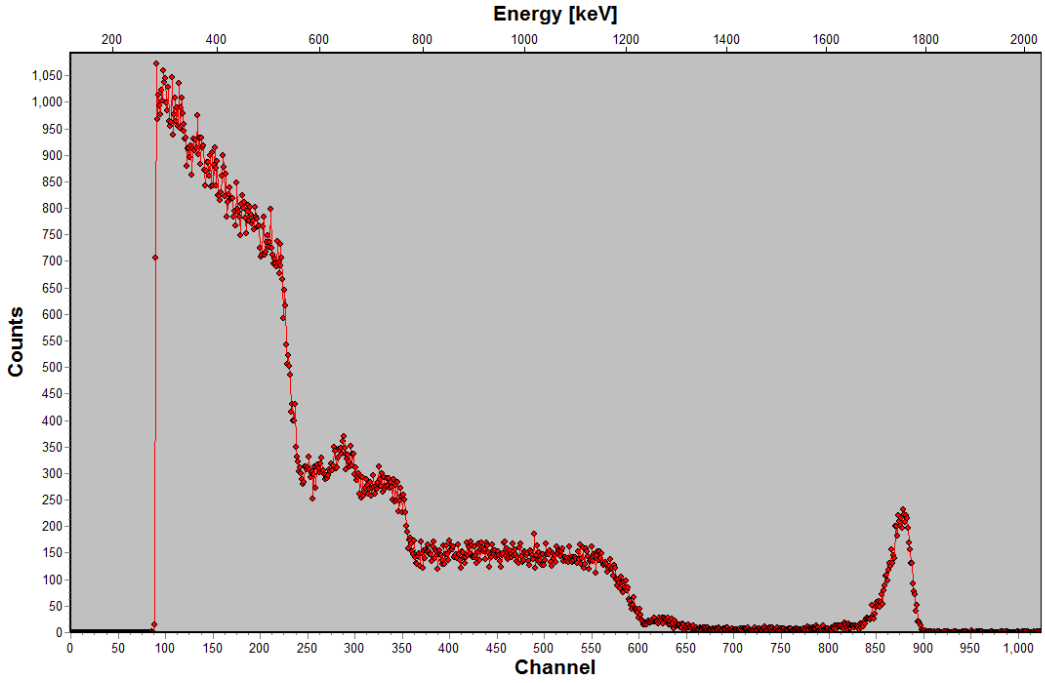

0067

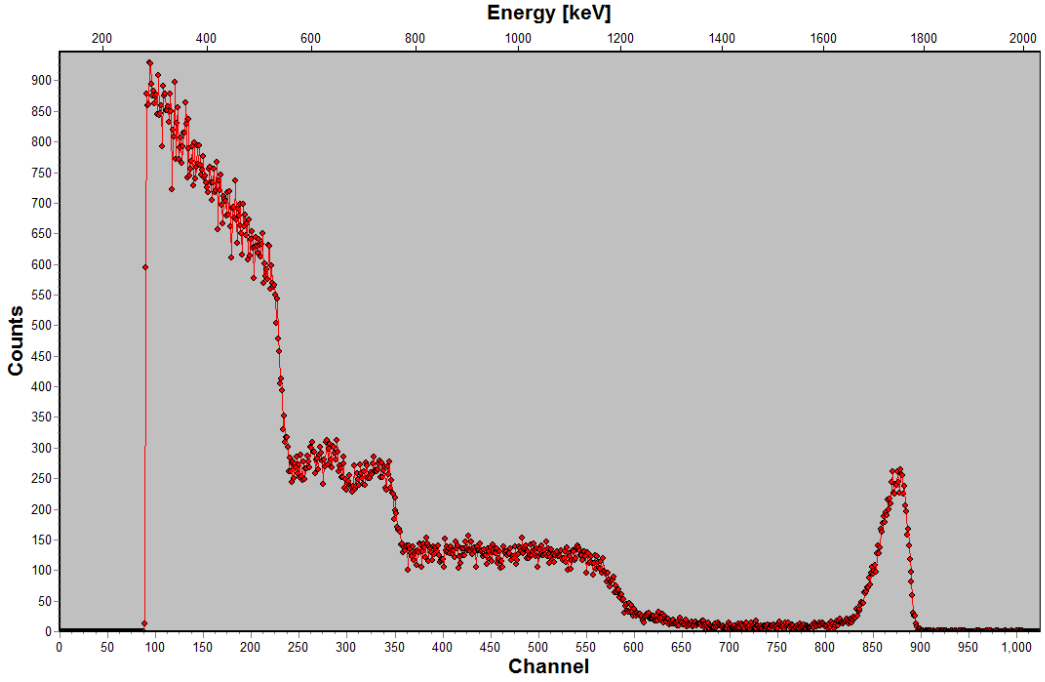

0068

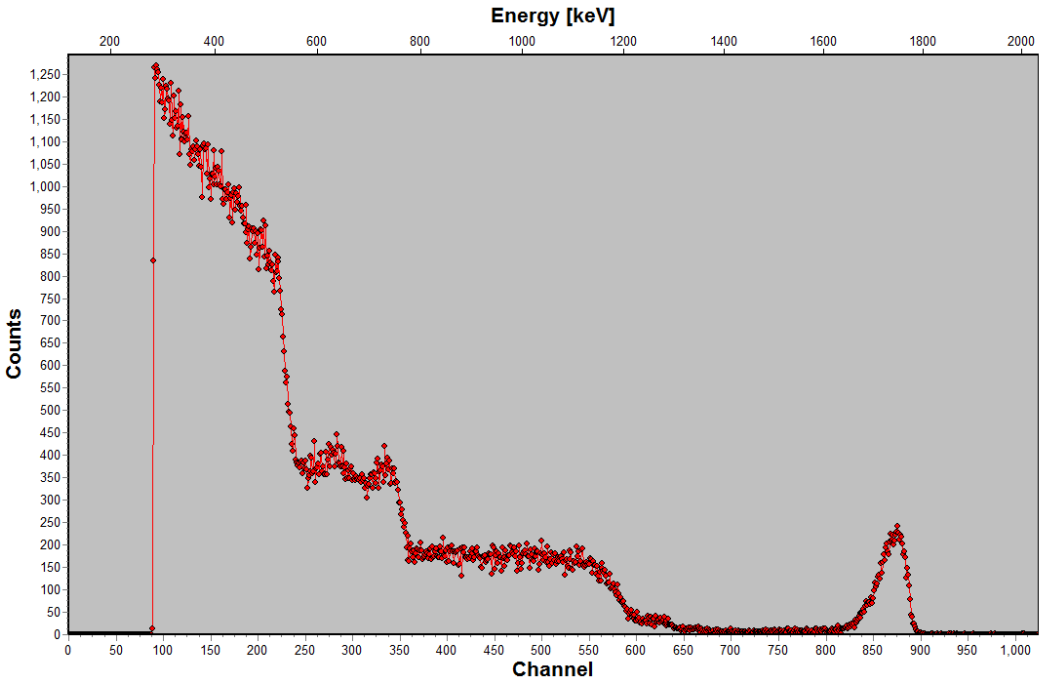

0069

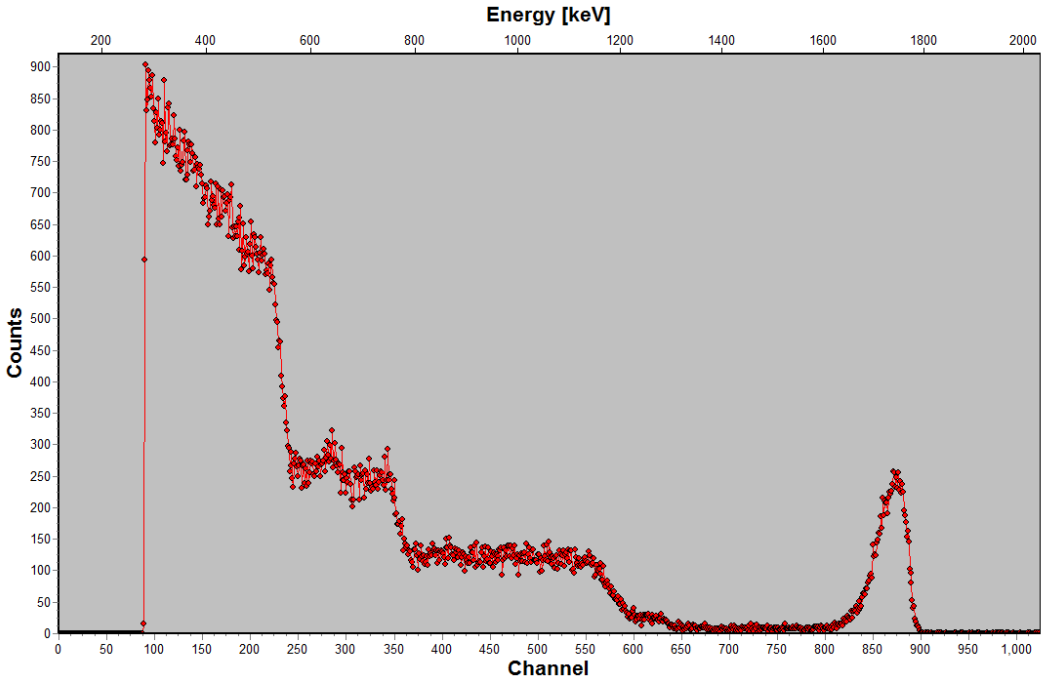

Figure 3:

0070

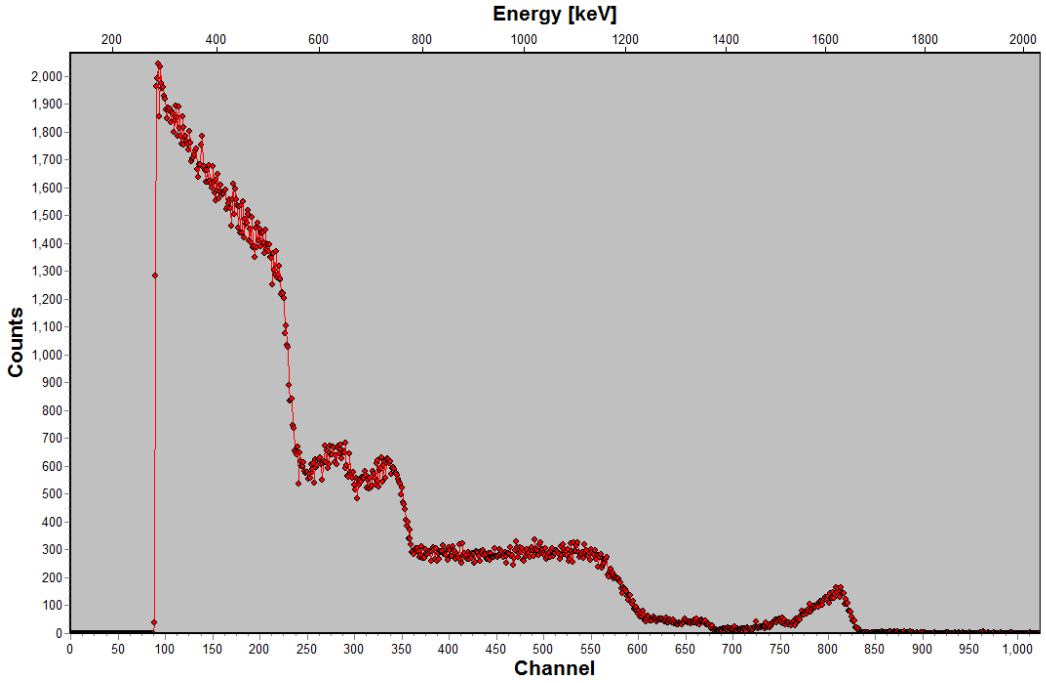

0071

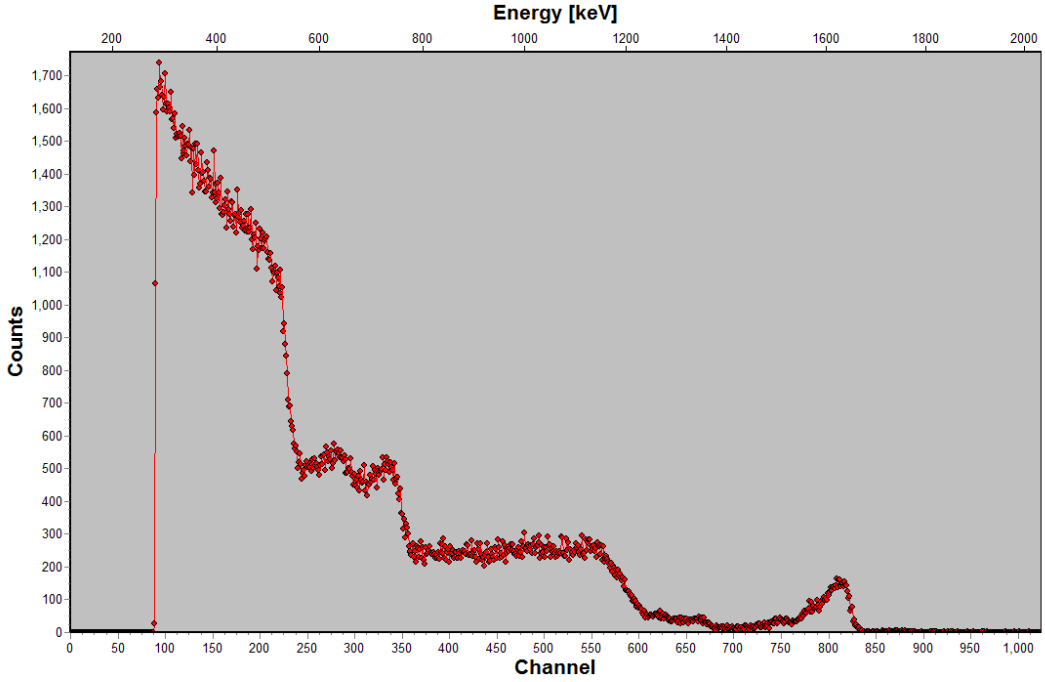

0072

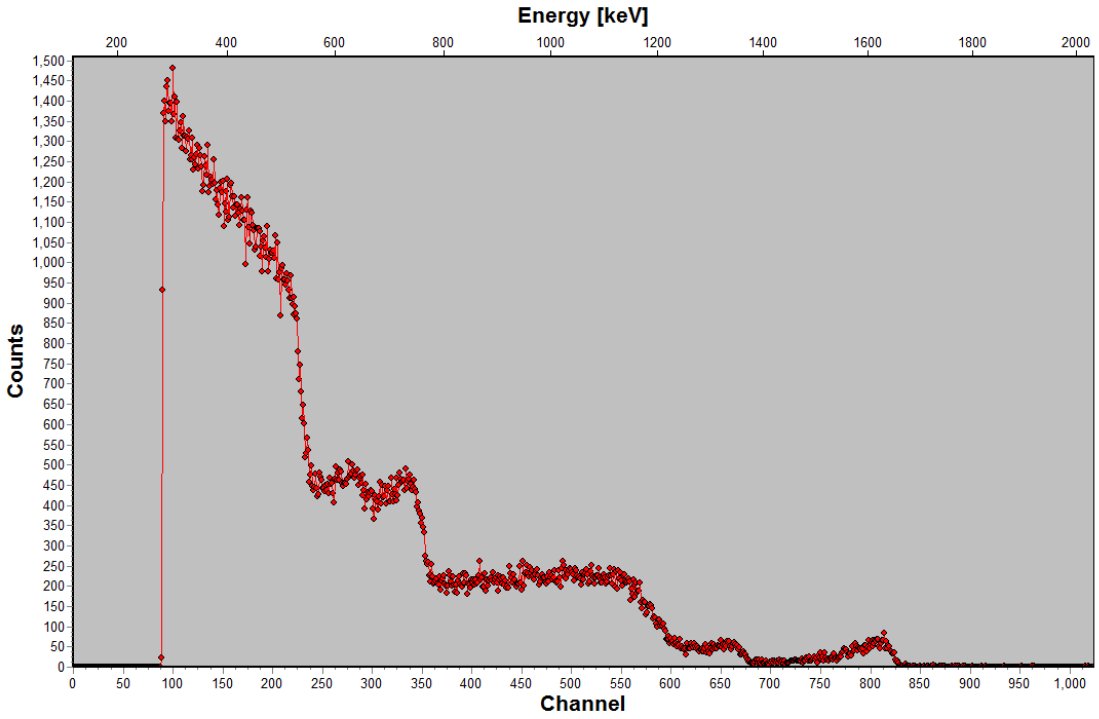

0073

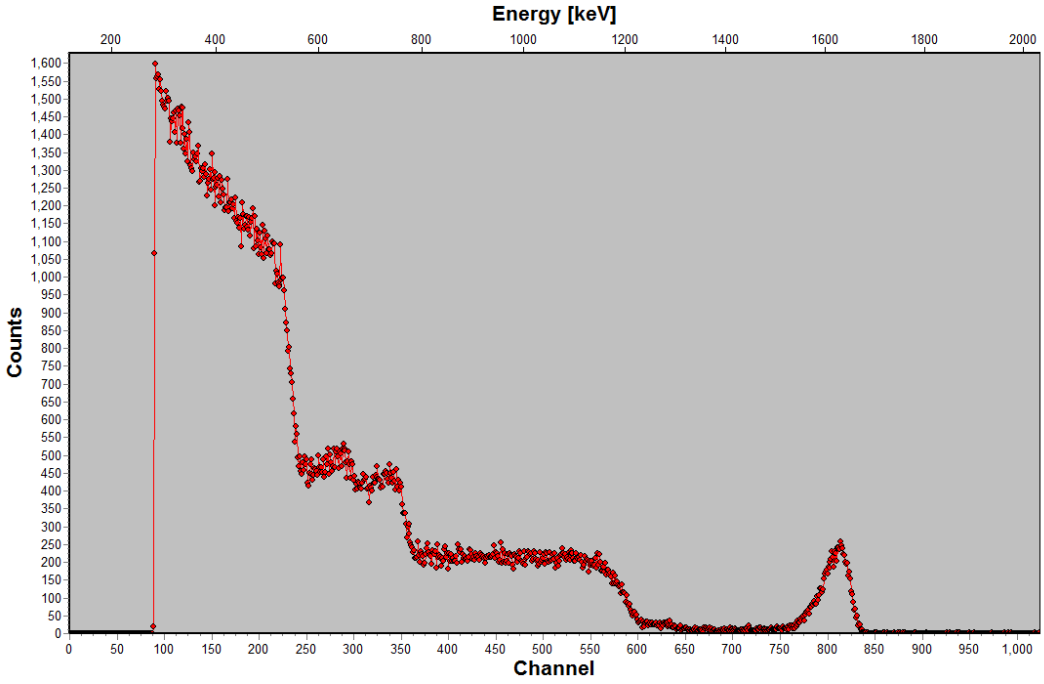

0074

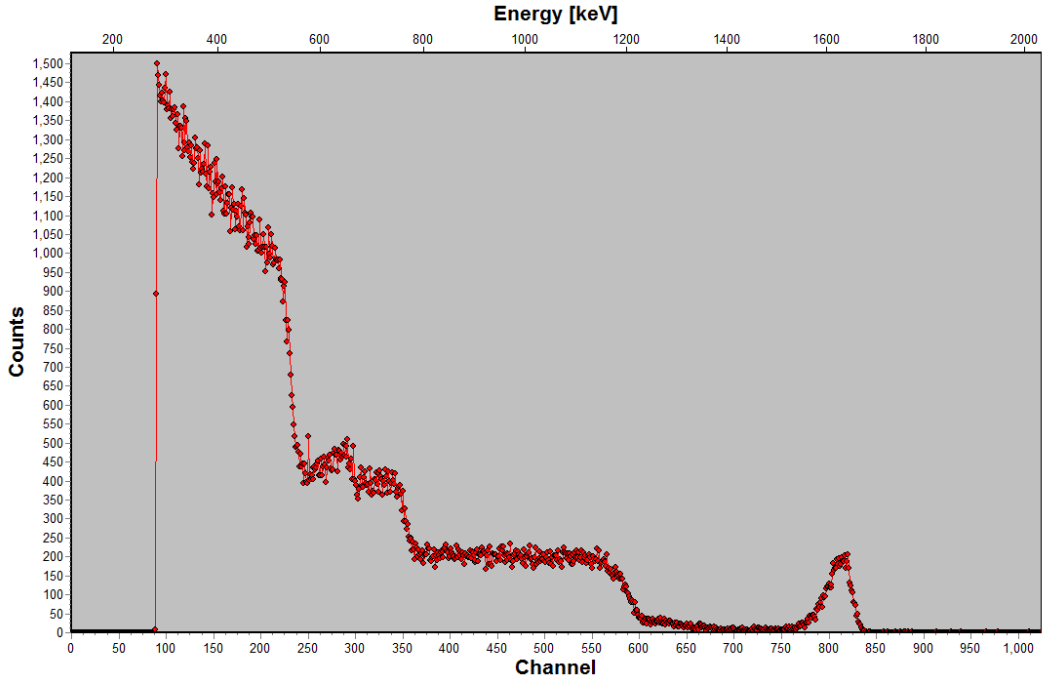

0075

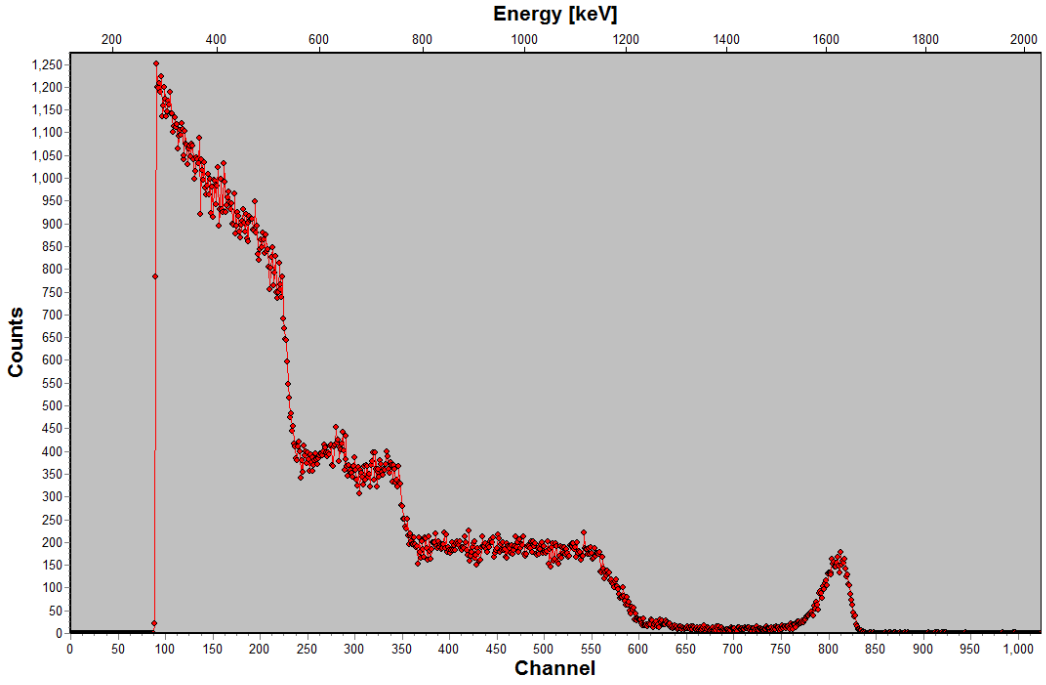

0076

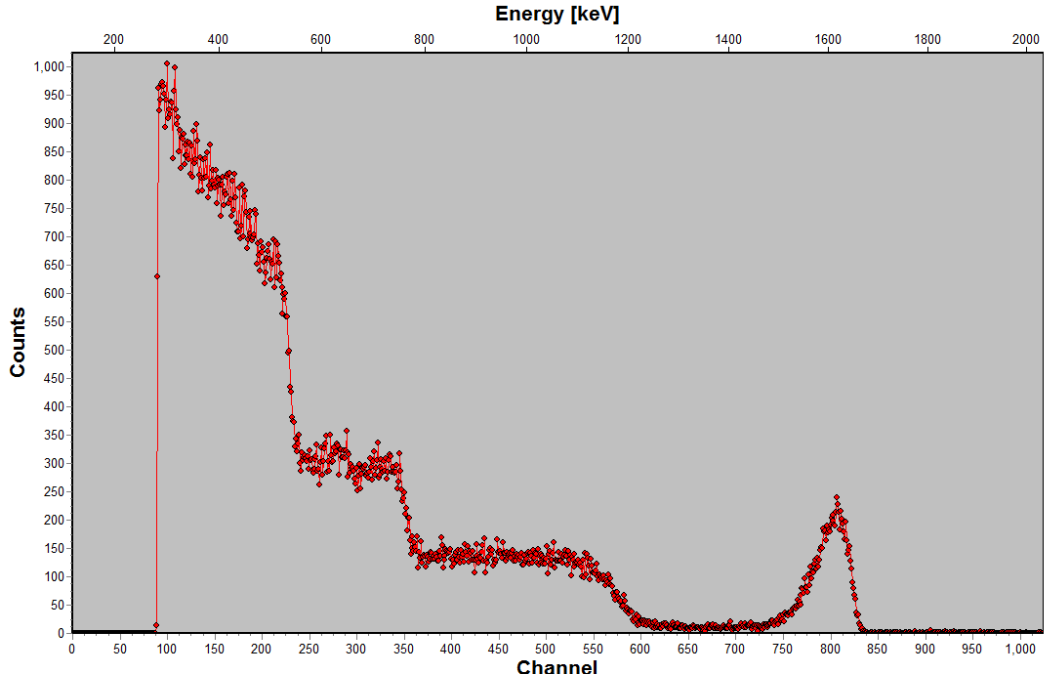

0077

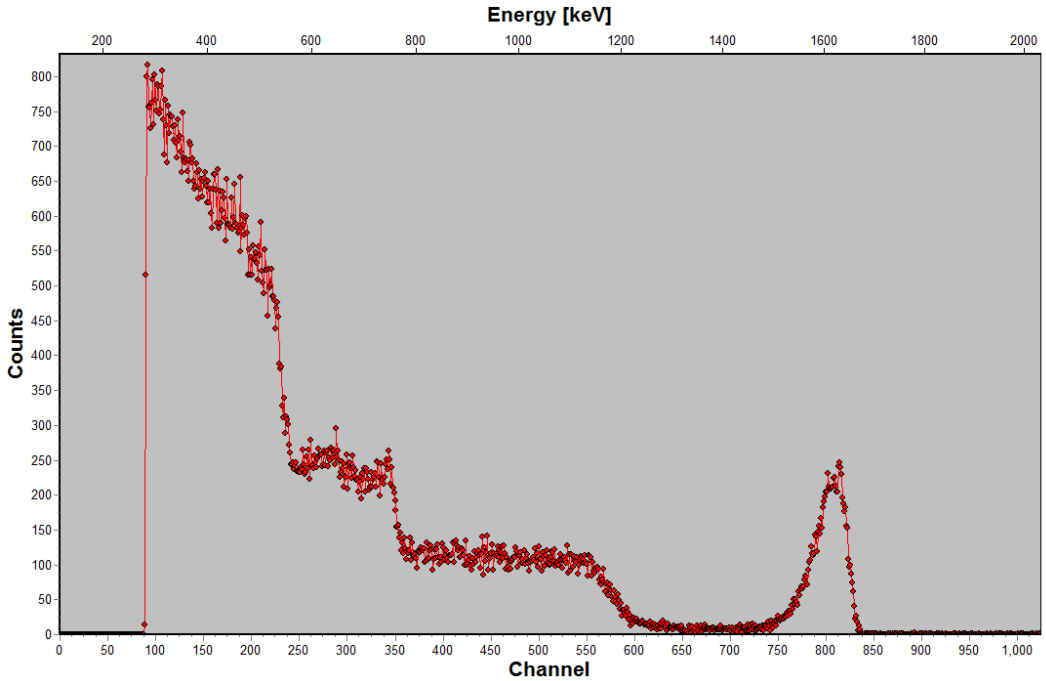

0078

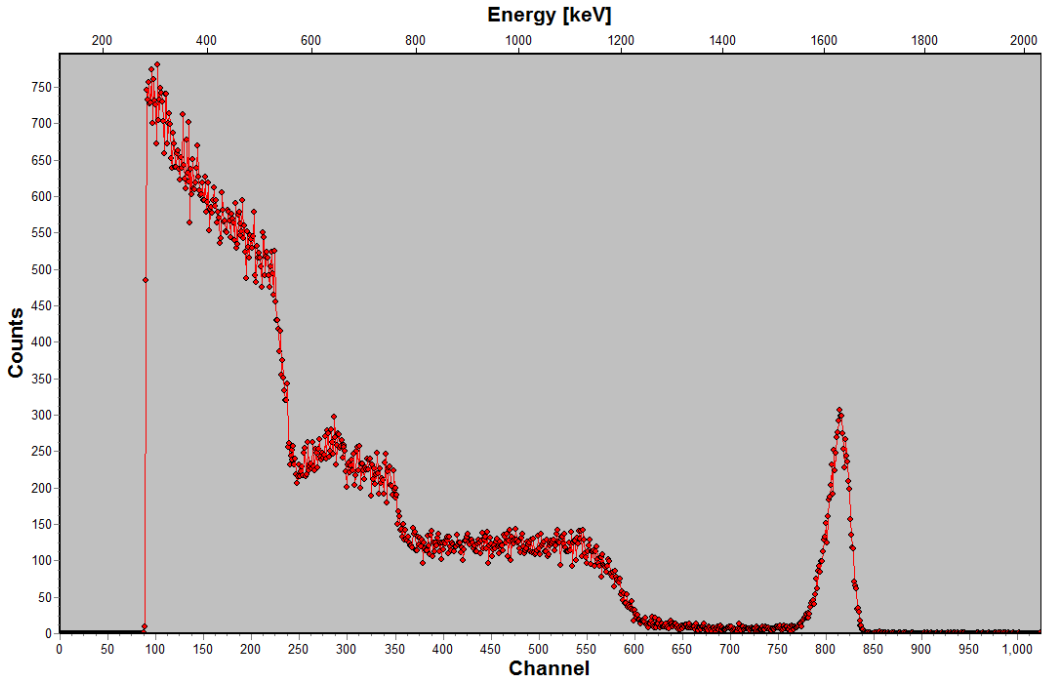

Figure 4:

0099

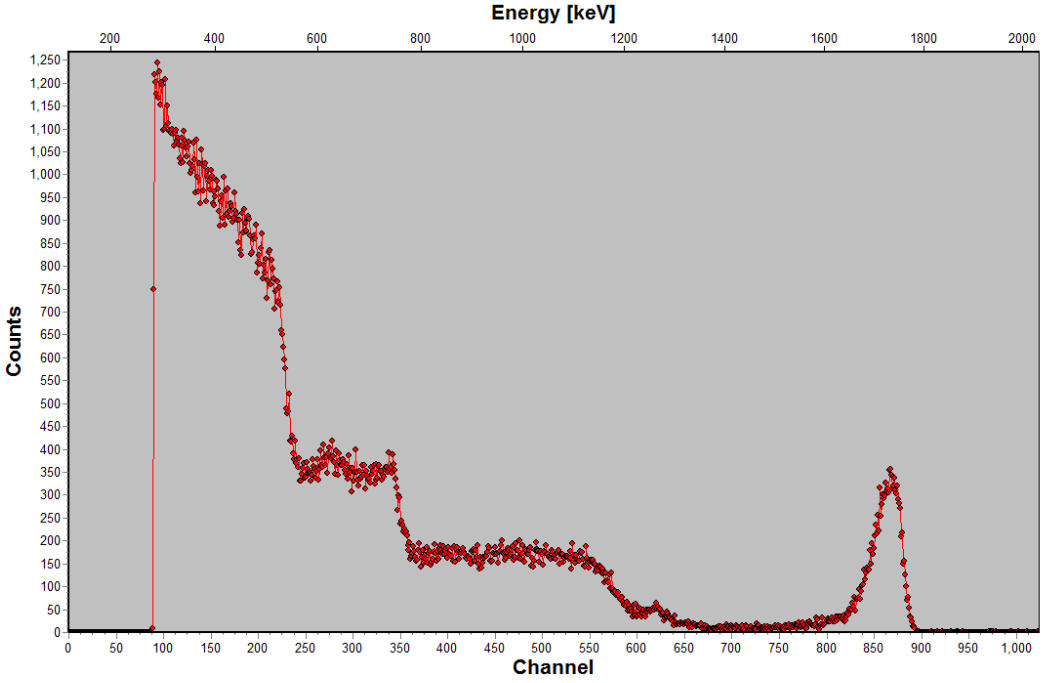

0107

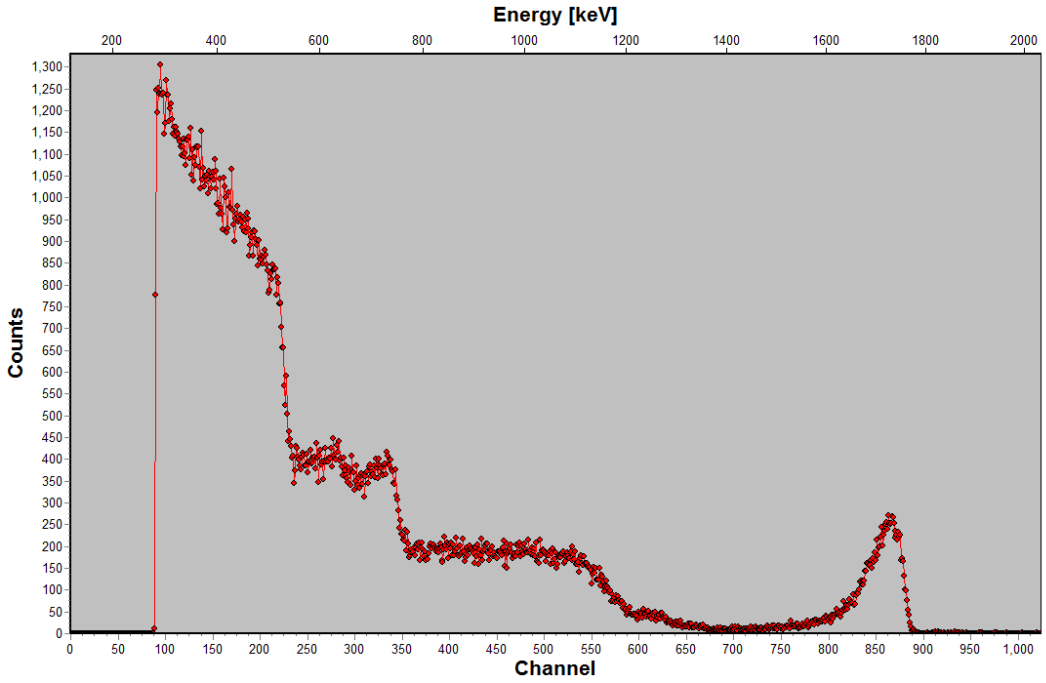

0108

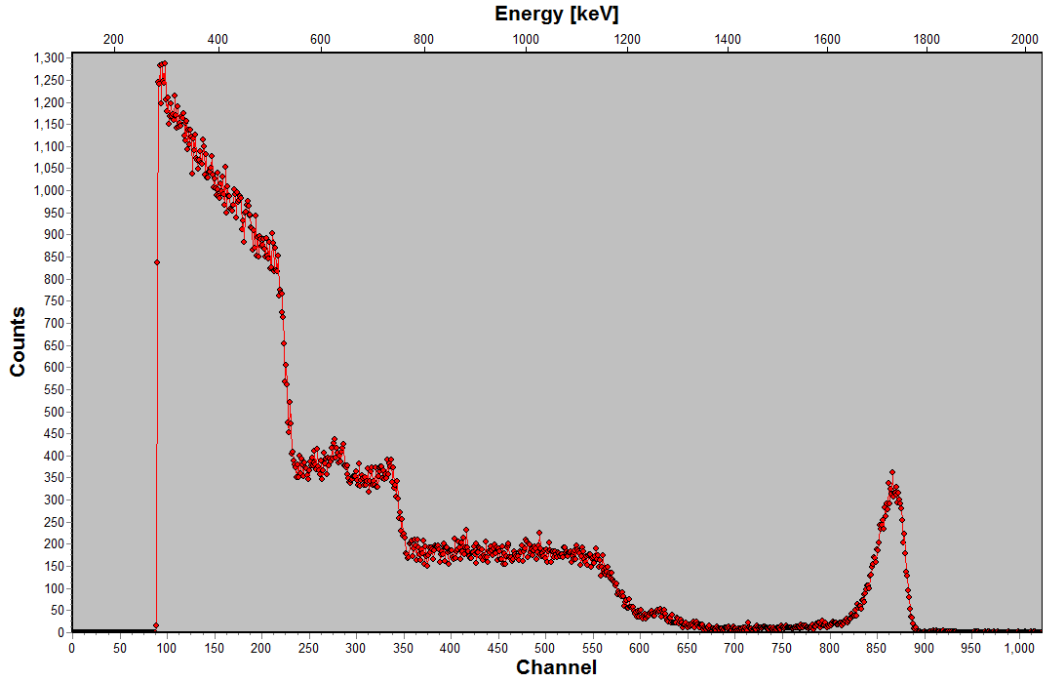

0132

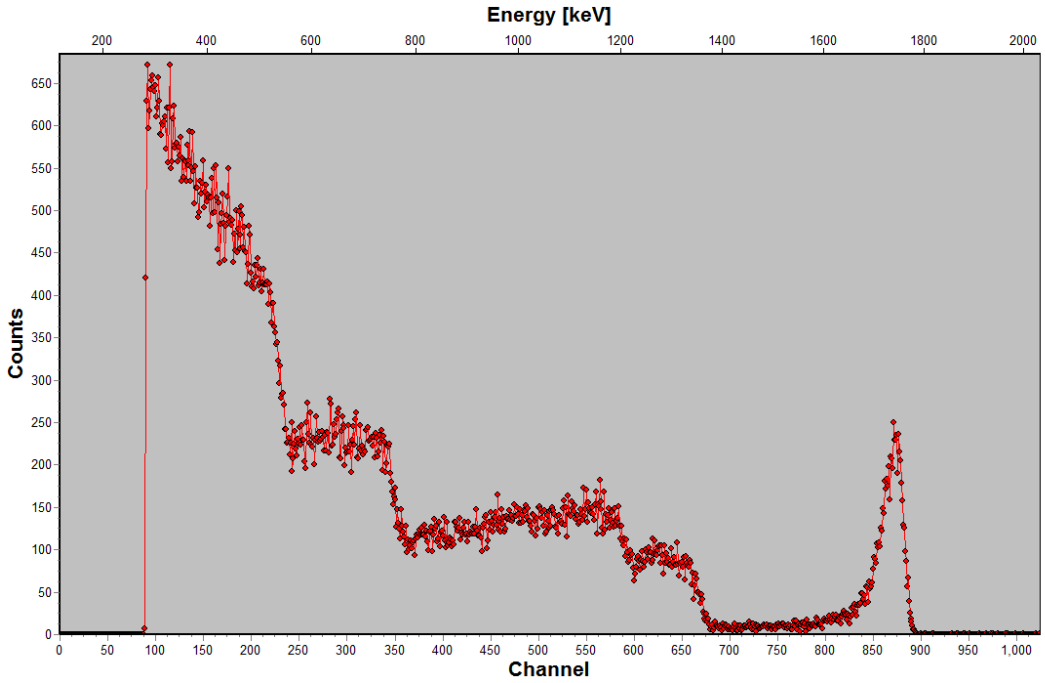
Energy [keV]
200 400 600 800 1000 1200 1400 1600 1800 2000
Counts
0 50 100 150 200 250 300 350 400 450 500 550 600 650
Channel
0 50 100 150 200 250 300 350 400 450 500 550 600 650 700 750 800 850 900 950 1,000

0133

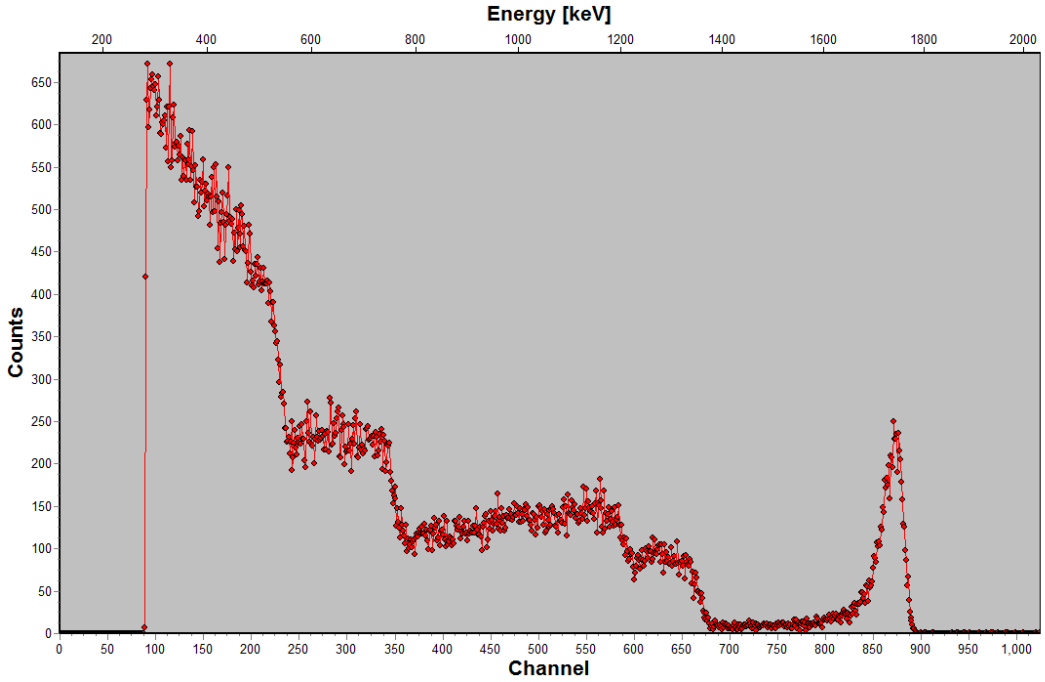
Energy [keV]
200 400 600 800 1000 1200 1400 1600 1800 2000
Counts
0 50 100 150 200 250 300 350 400 450 500 550 600 650
Channel
0 50 100 150 200 250 300 350 400 450 500 550 600 650 700 750 800 850 900 950 1,000

0152

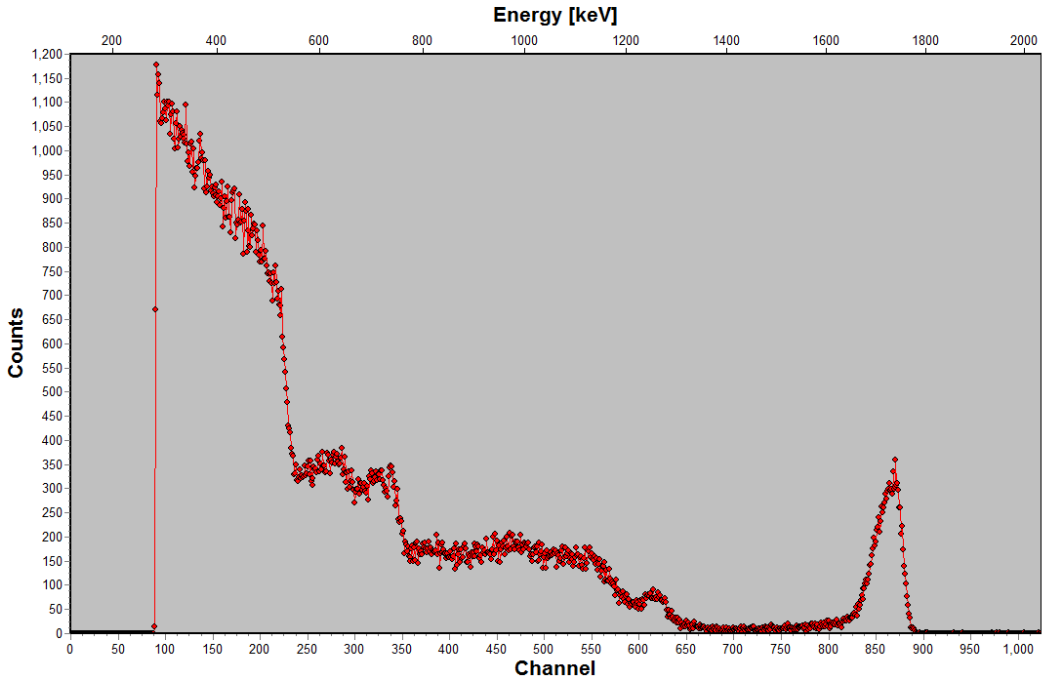

0153

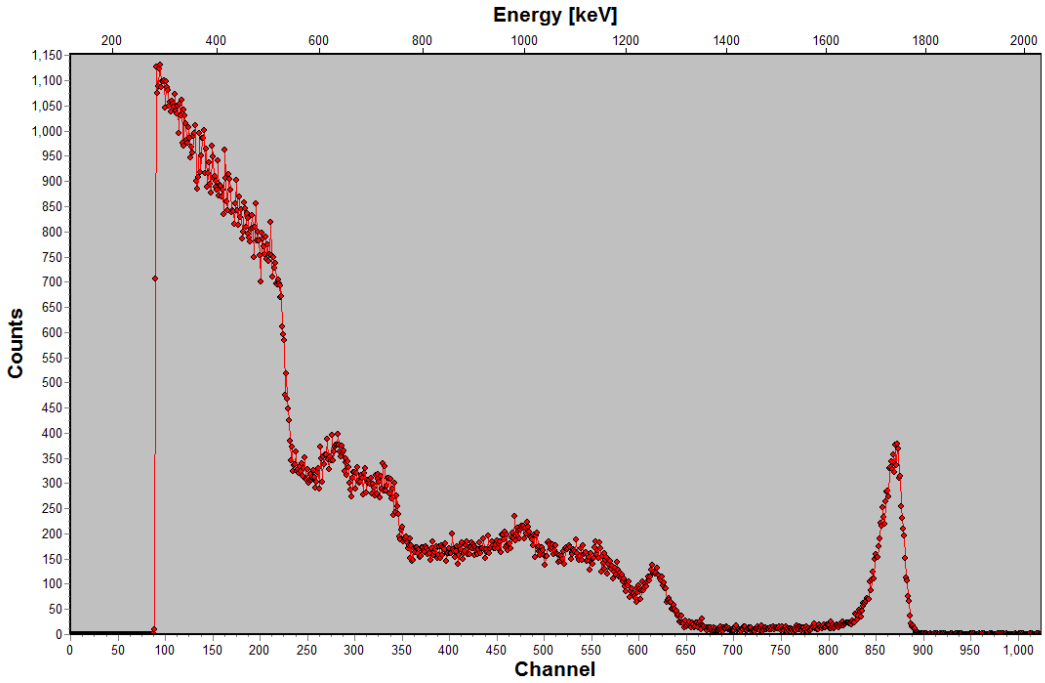

Figure 5:

0117

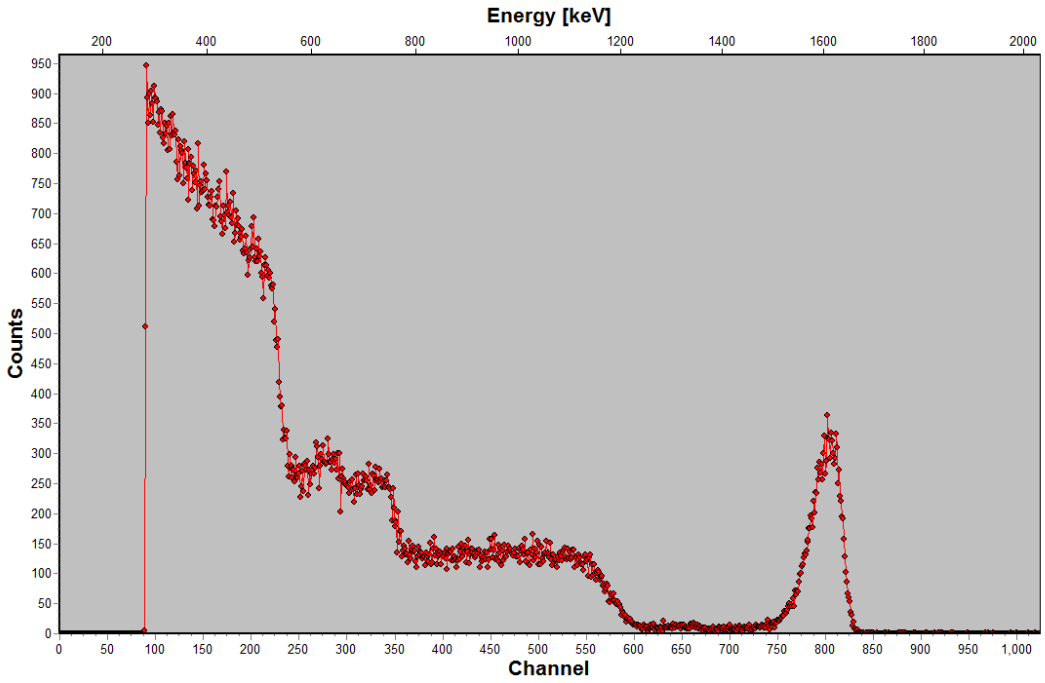

0118

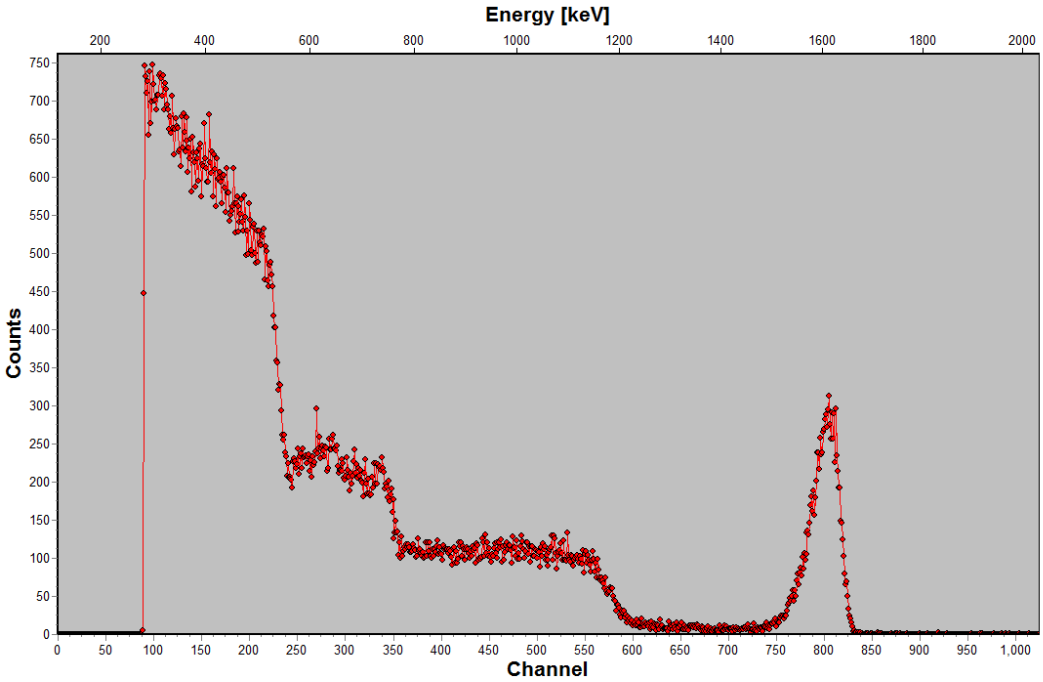

0119

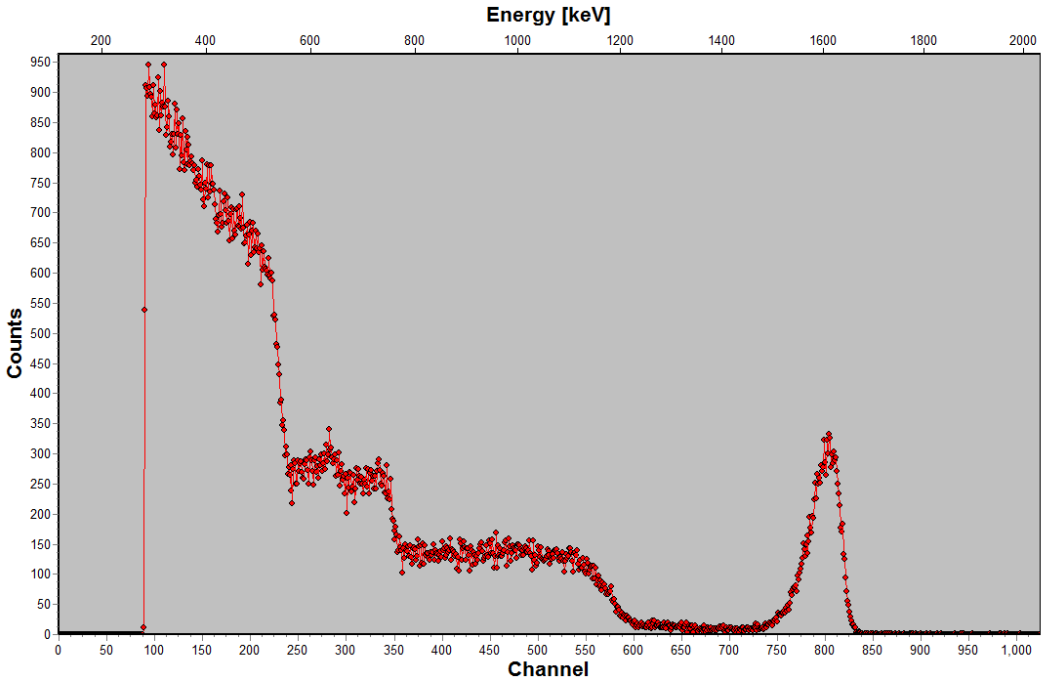

0138

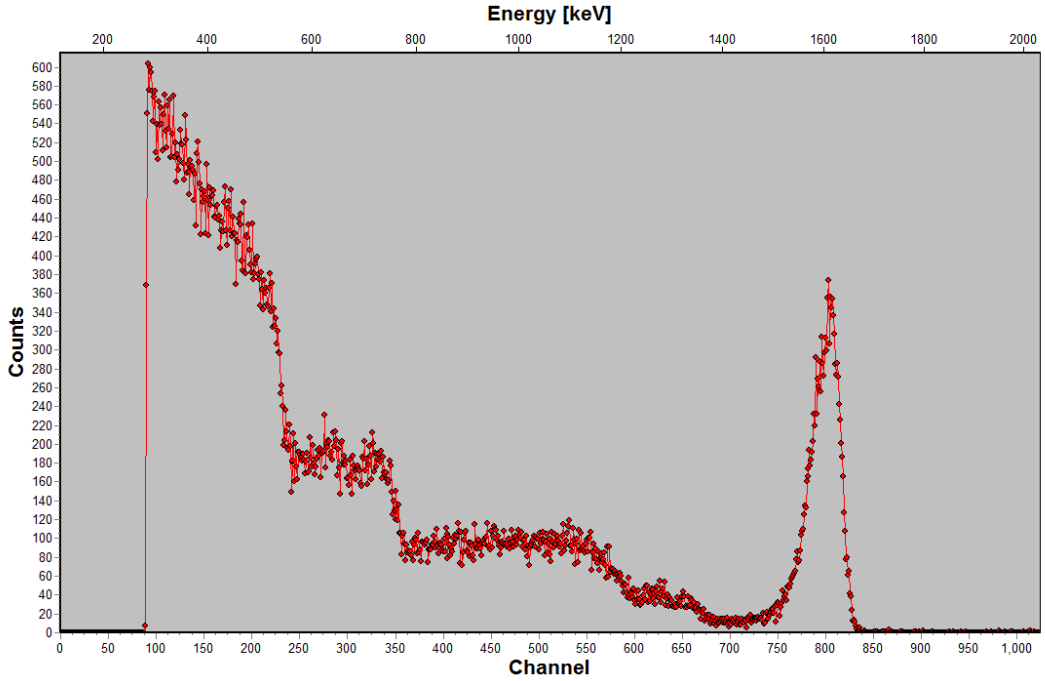

0156

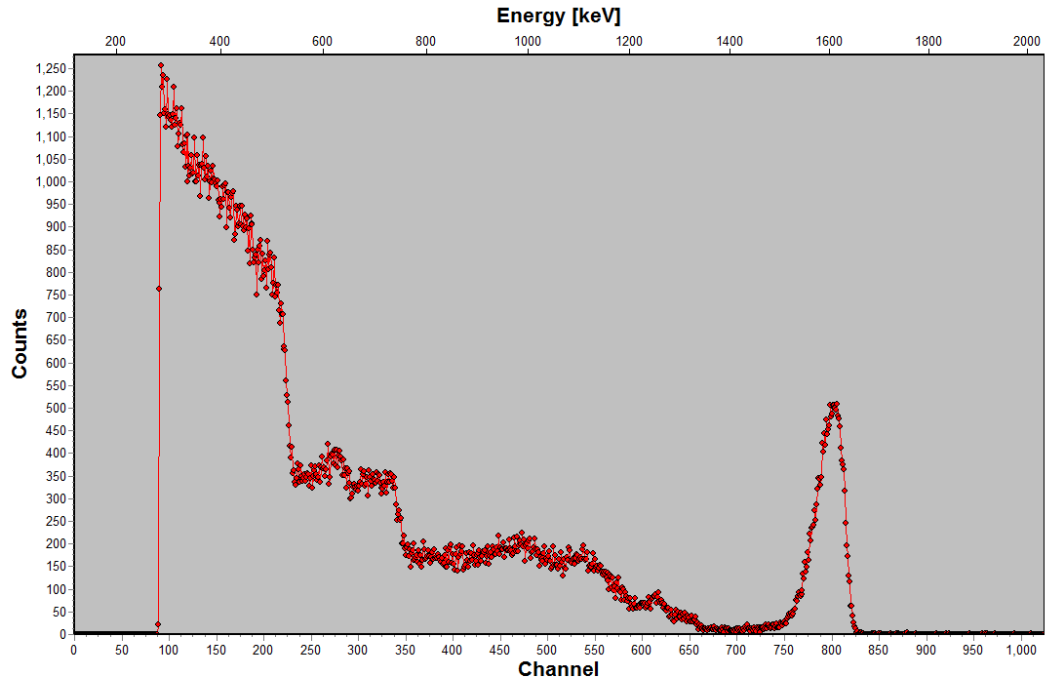

0157

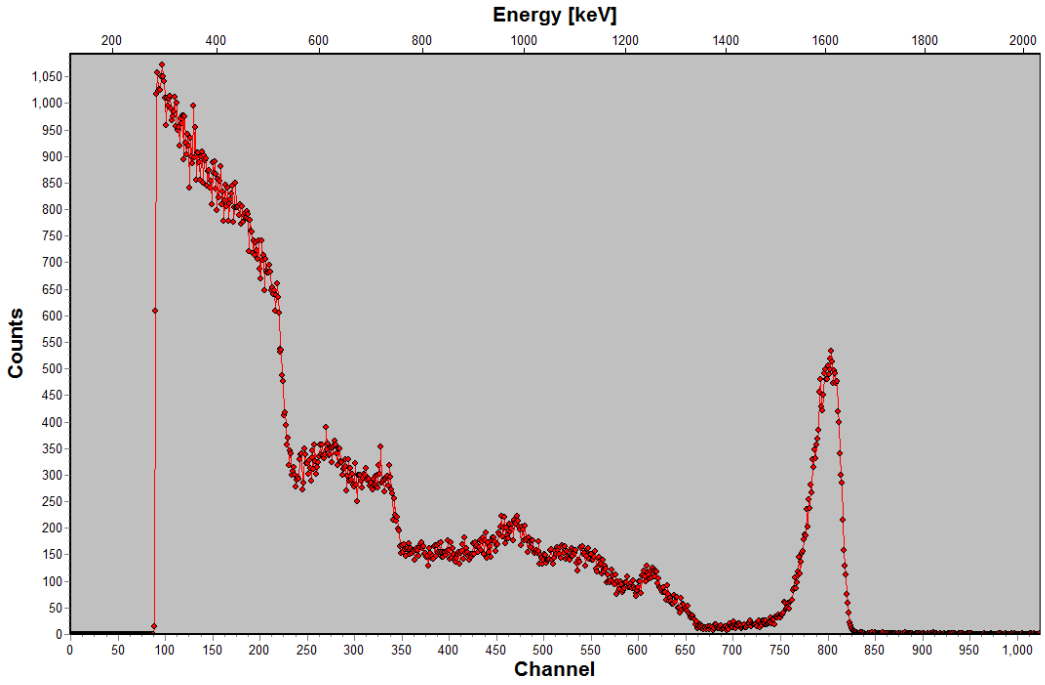

Figure 6:

0103

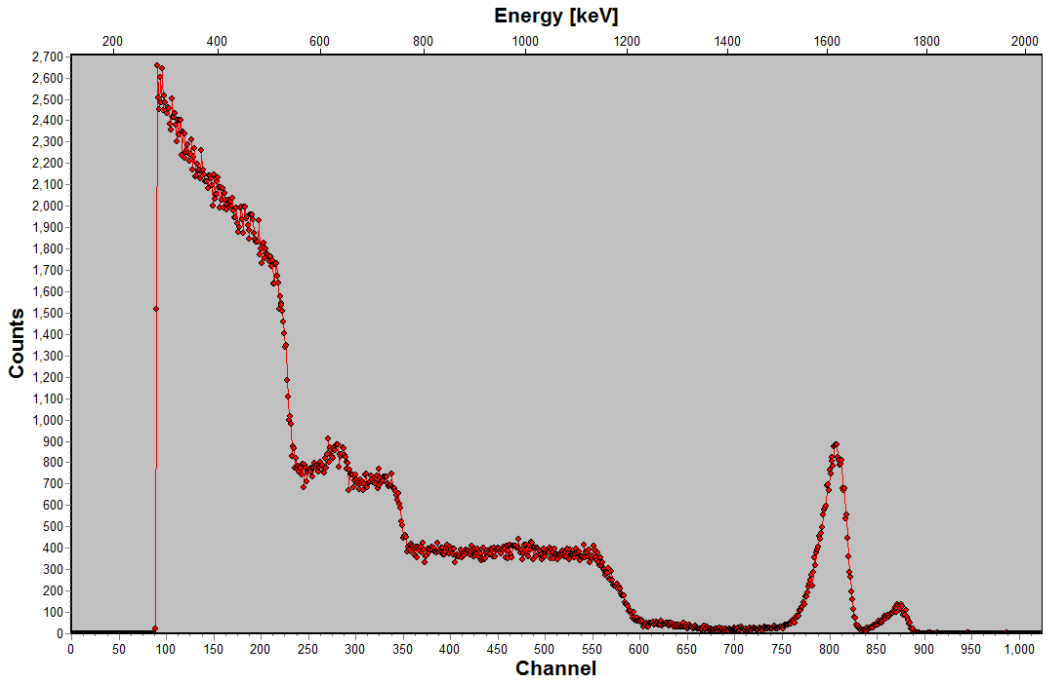

0111

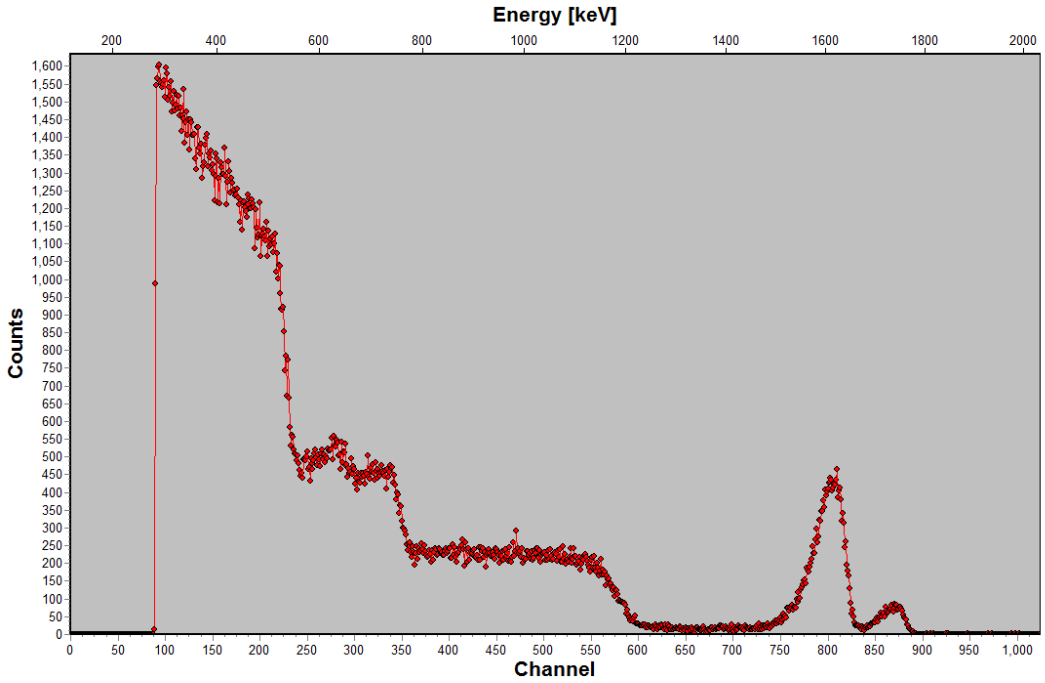

0144

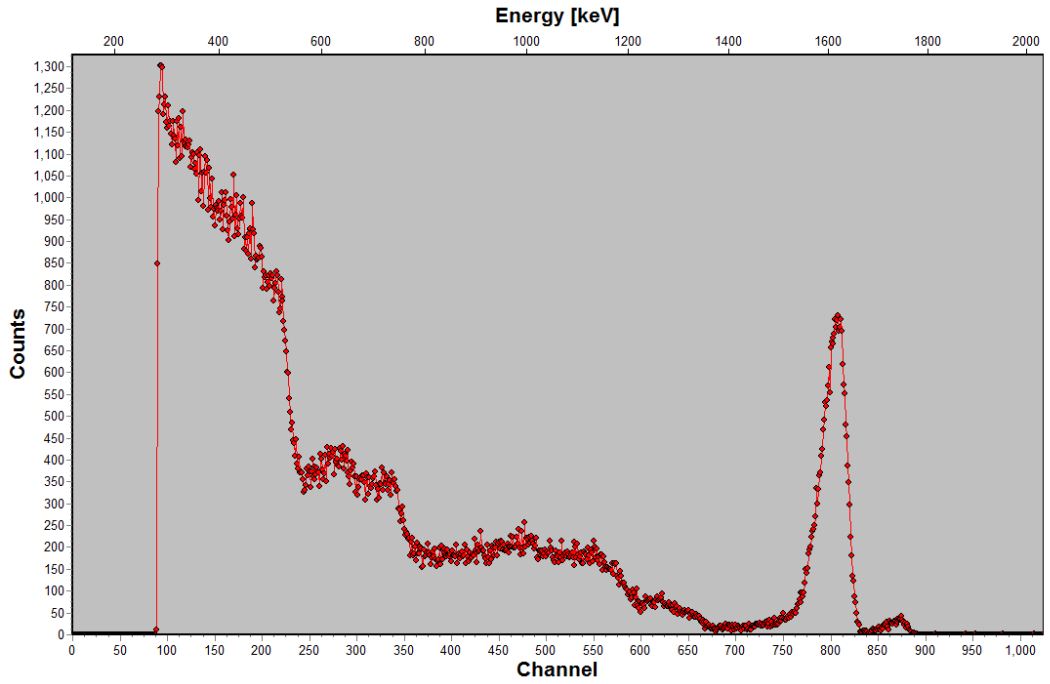

0145

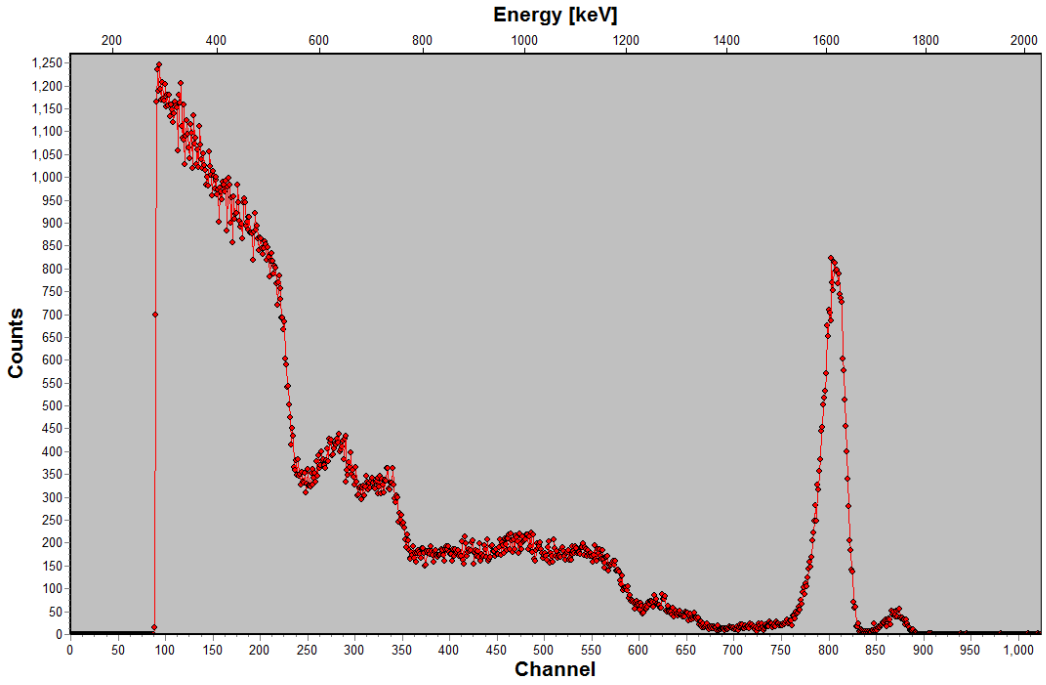

0160

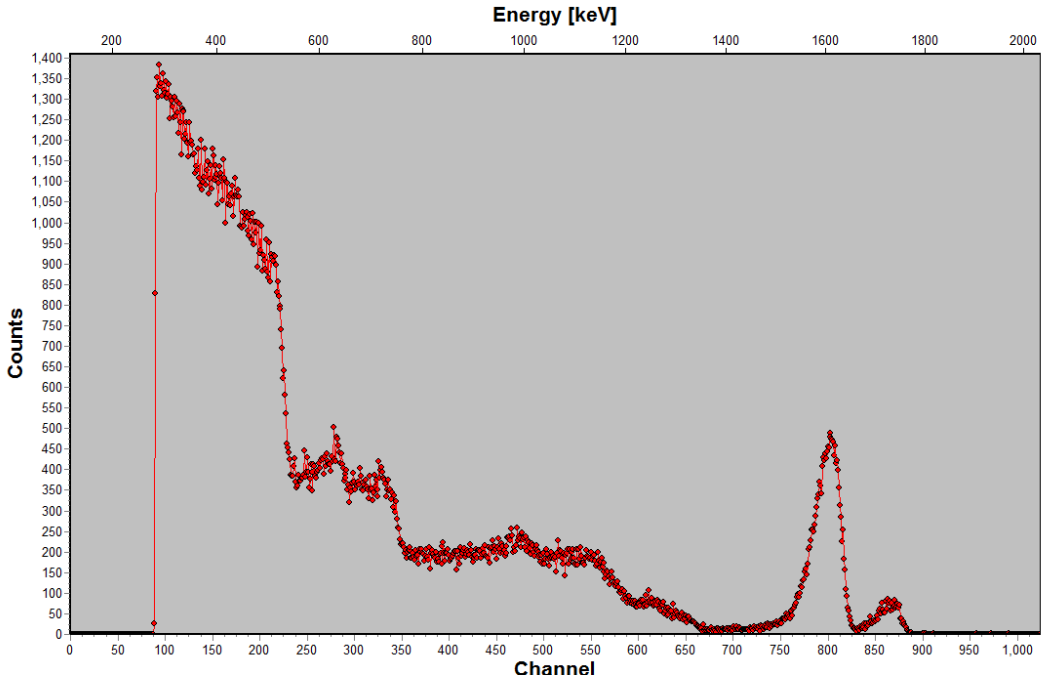

0161

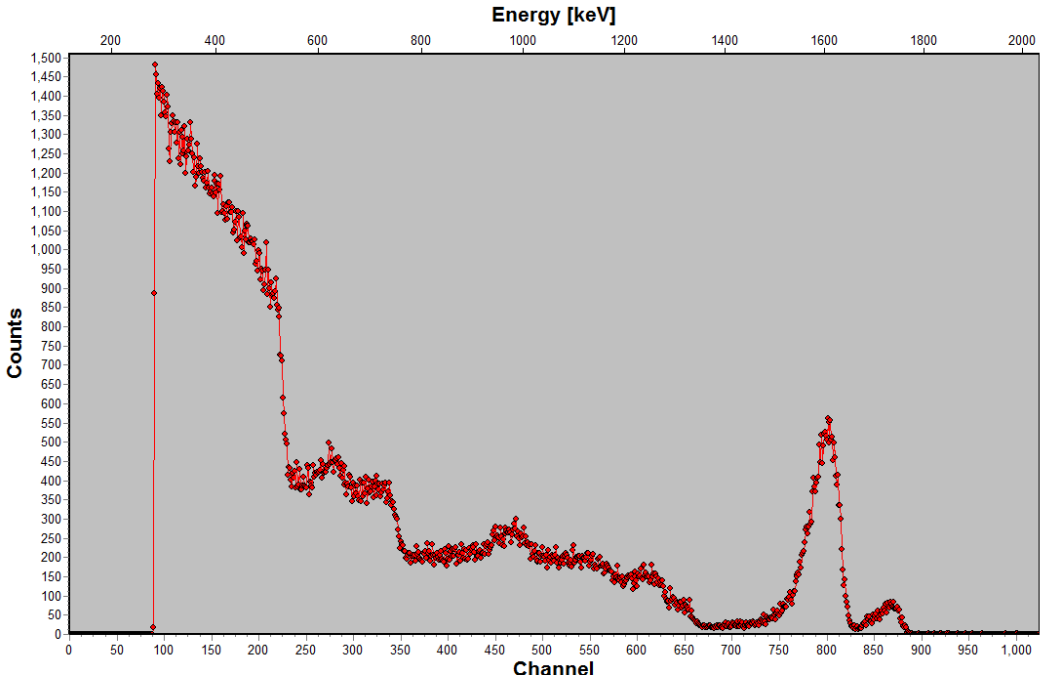

Figure 7:

0079

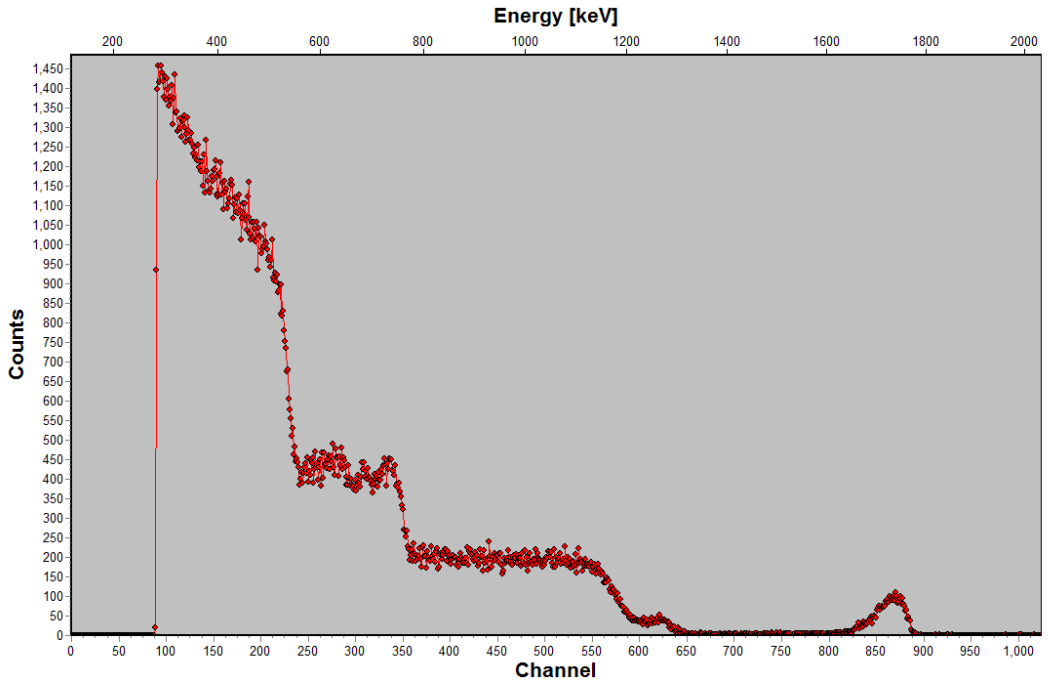

0080

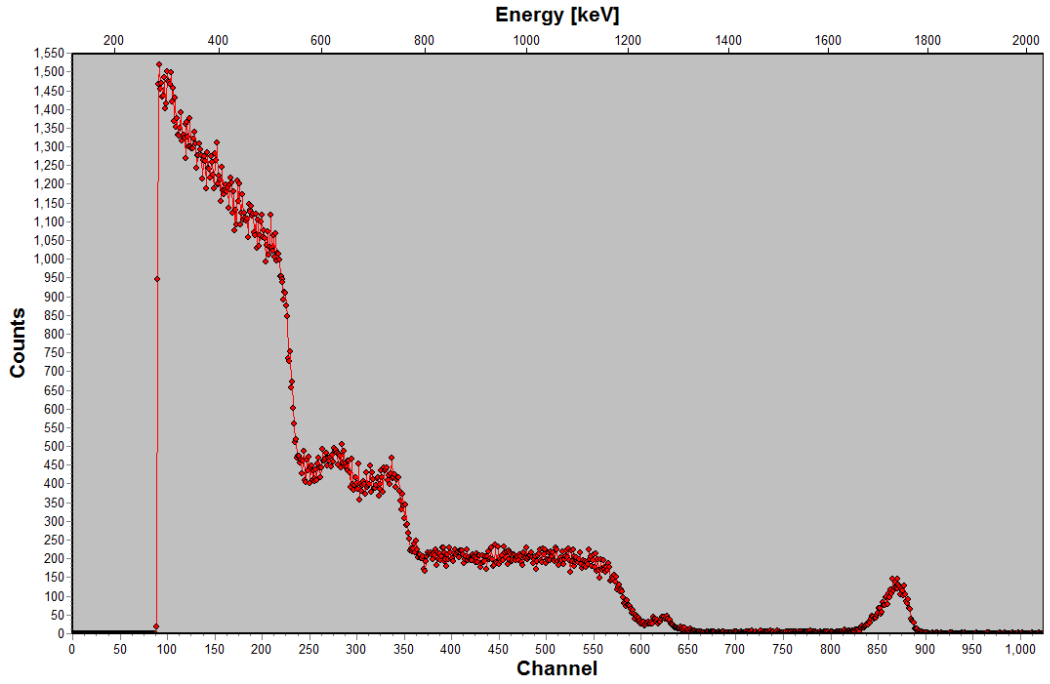

0081

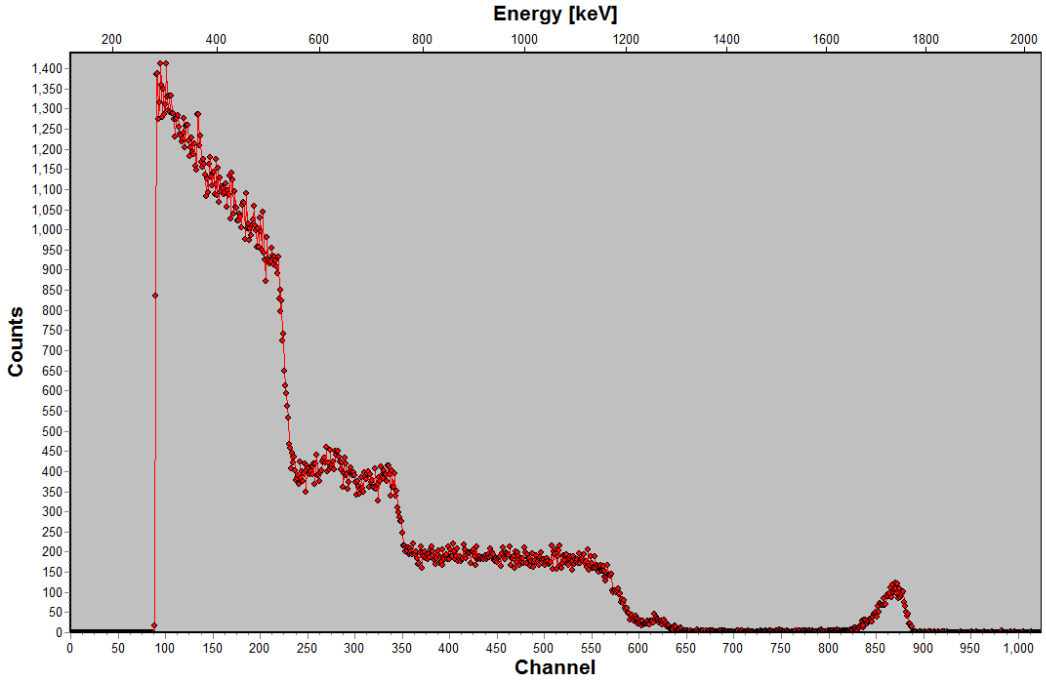

0082

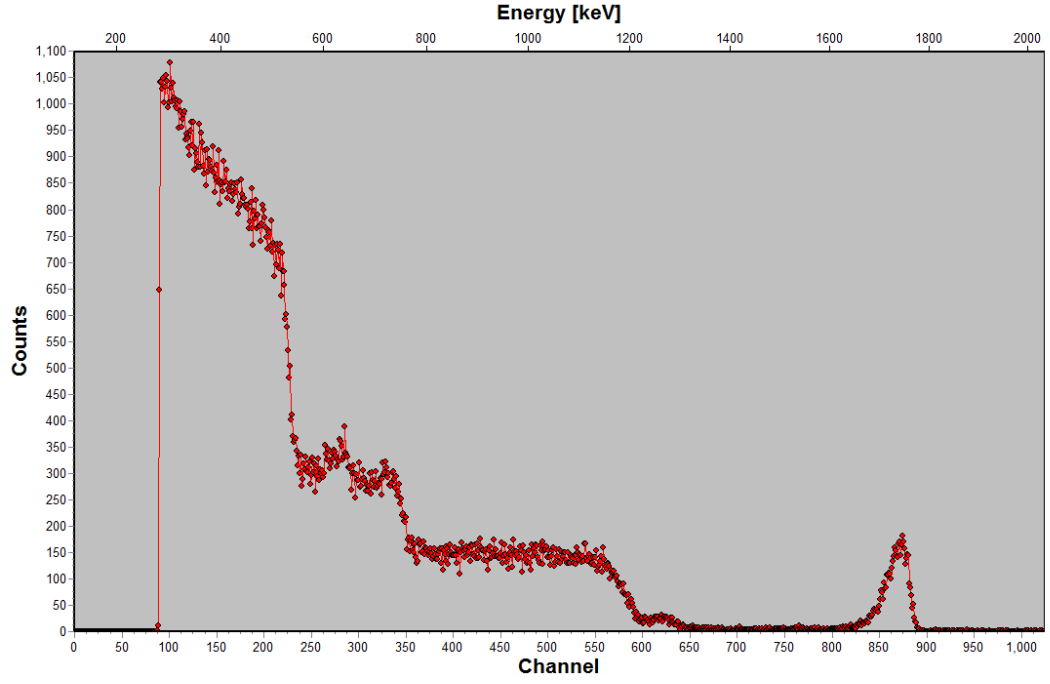

0083

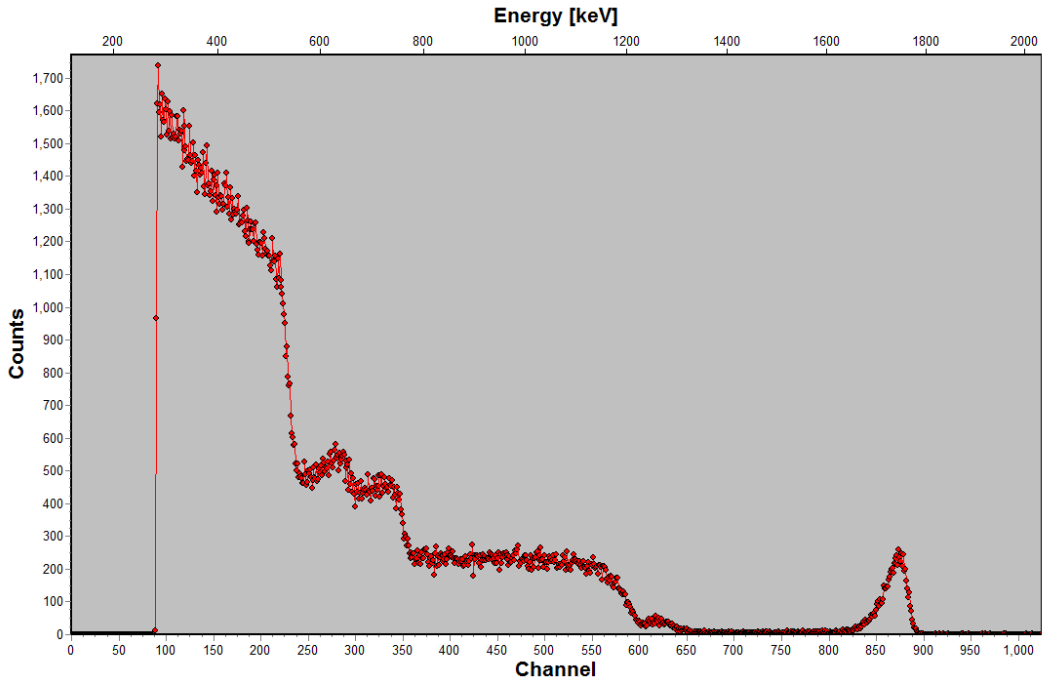

0084

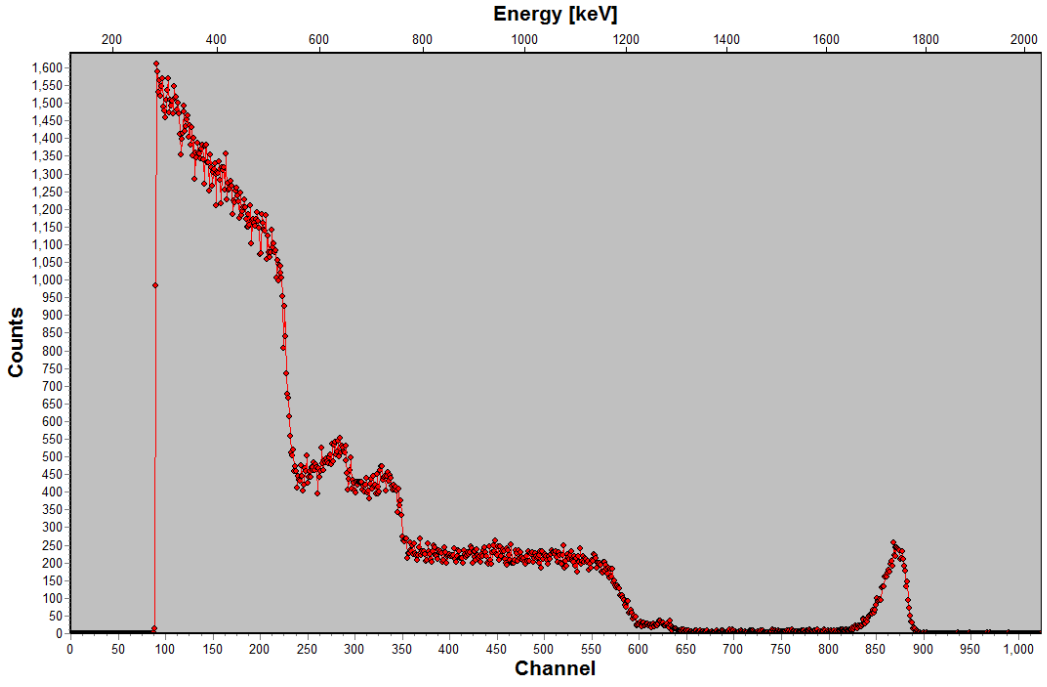

0085

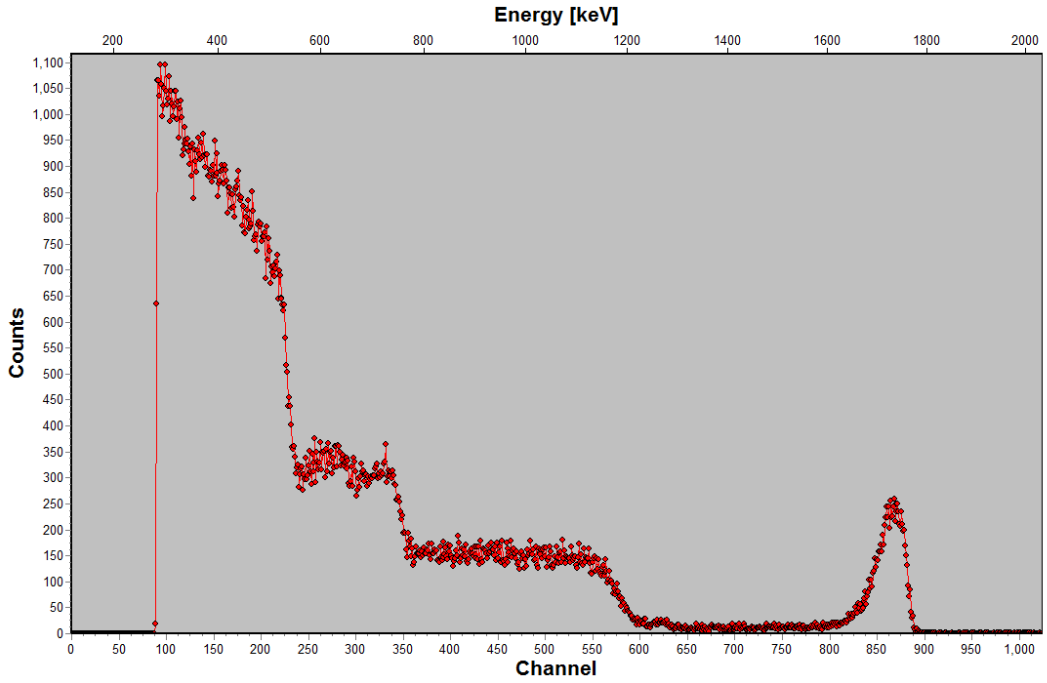
Energy [keV]
200 400 600 800 1000 1200 1400 1600 1800 2000
Counts
0 50 100 150 200 250 300 350 400 450 500 550 600 650 700 750 800 850 900 950 1,000
Channel

0086

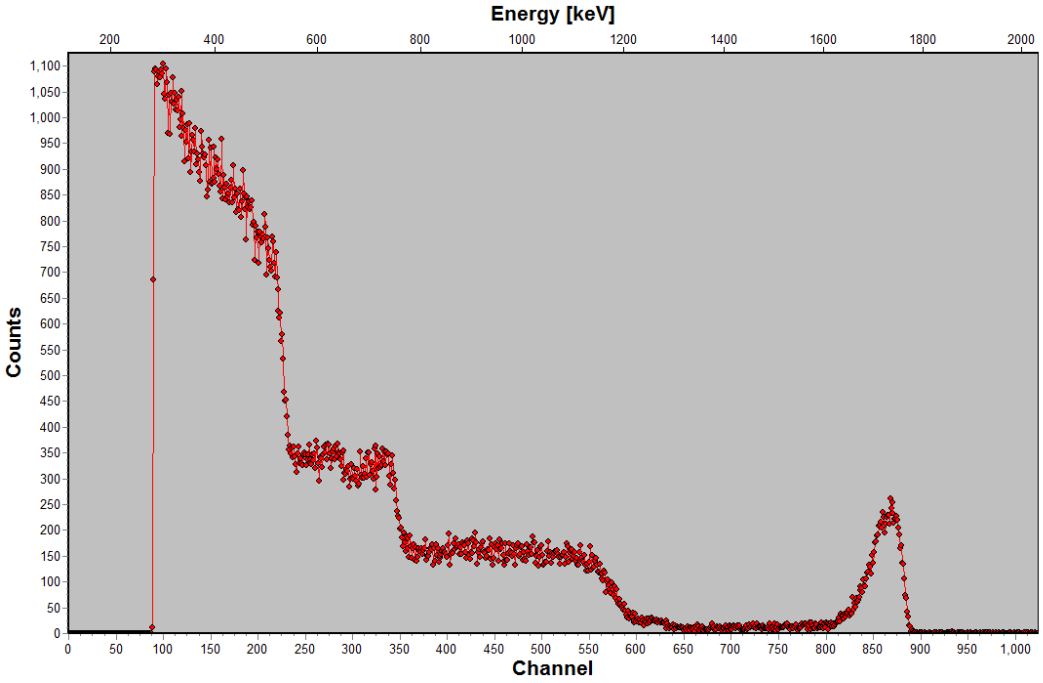
Energy [keV]
200 400 600 800 1000 1200 1400 1600 1800 2000
Counts
0 50 100 150 200 250 300 350 400 450 500 550 600 650 700 750 800 850 900 950 1,000
Channel

0087

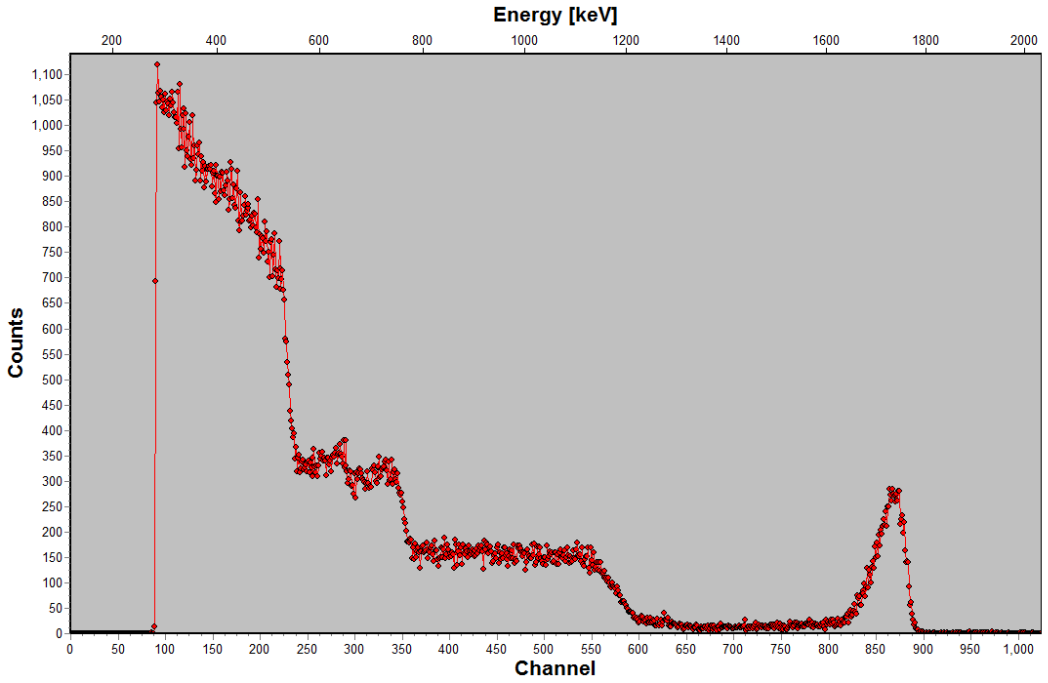

Figure 8:

0088

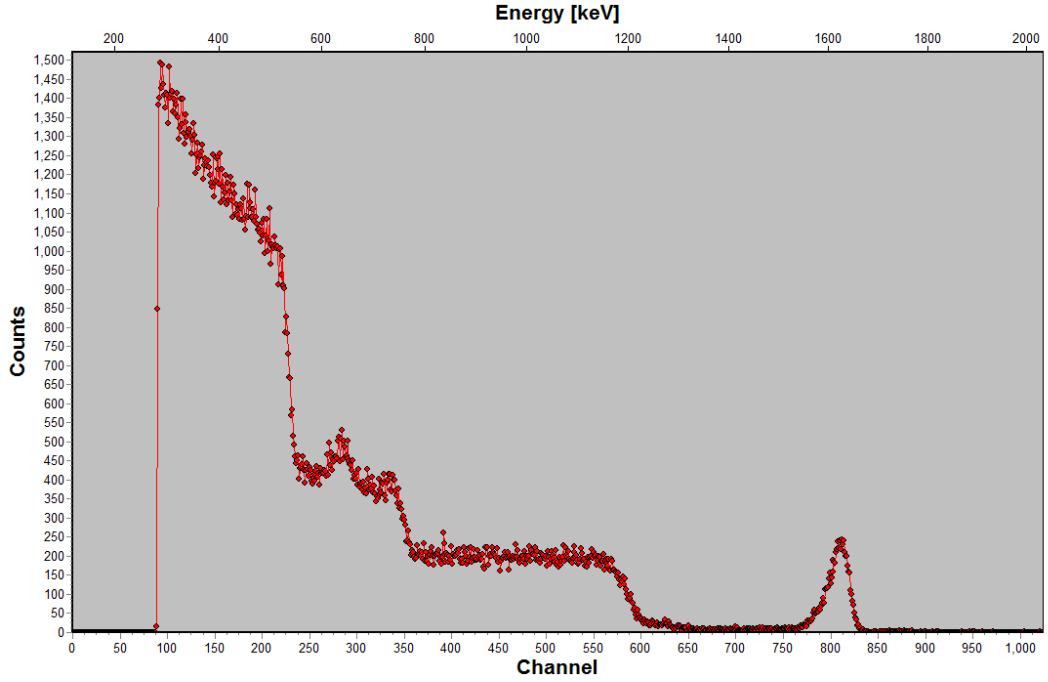

0089

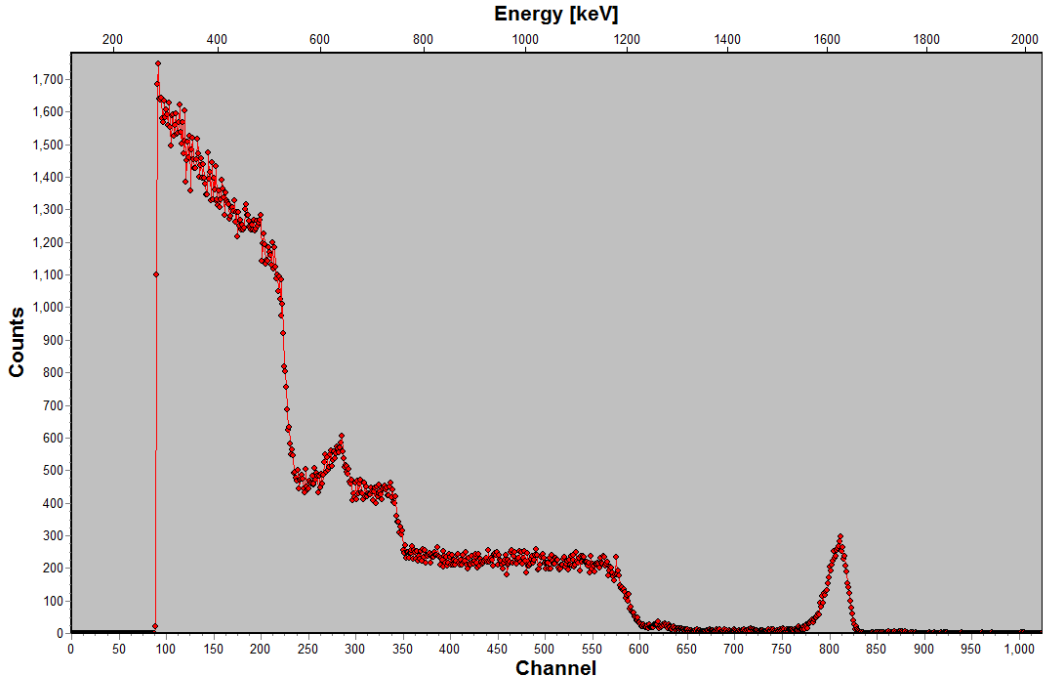

0090

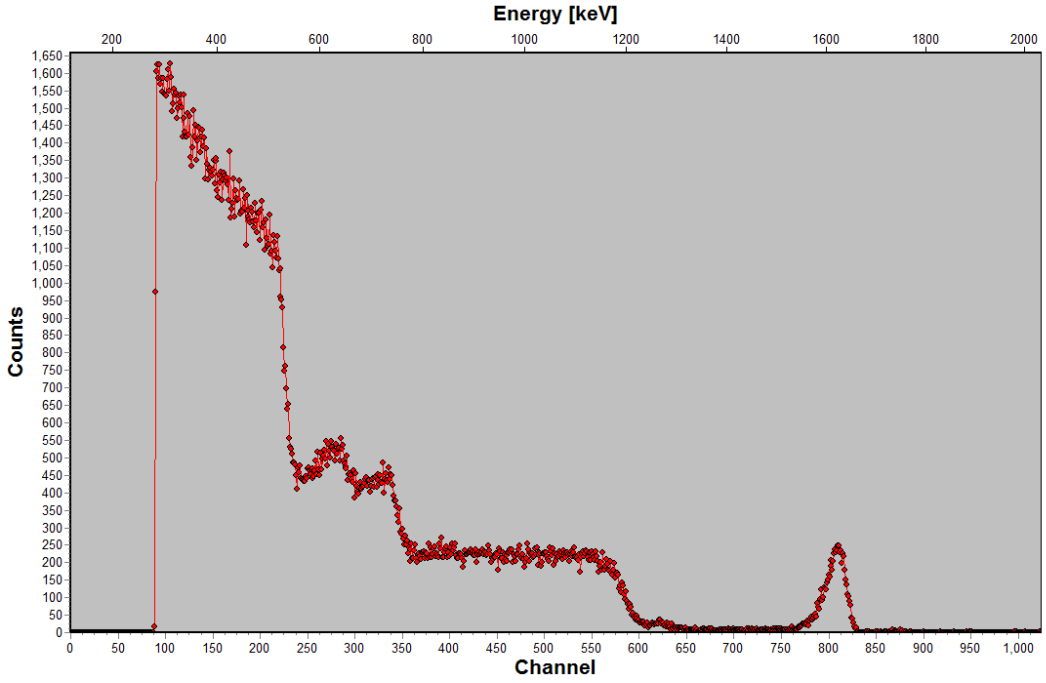

0091

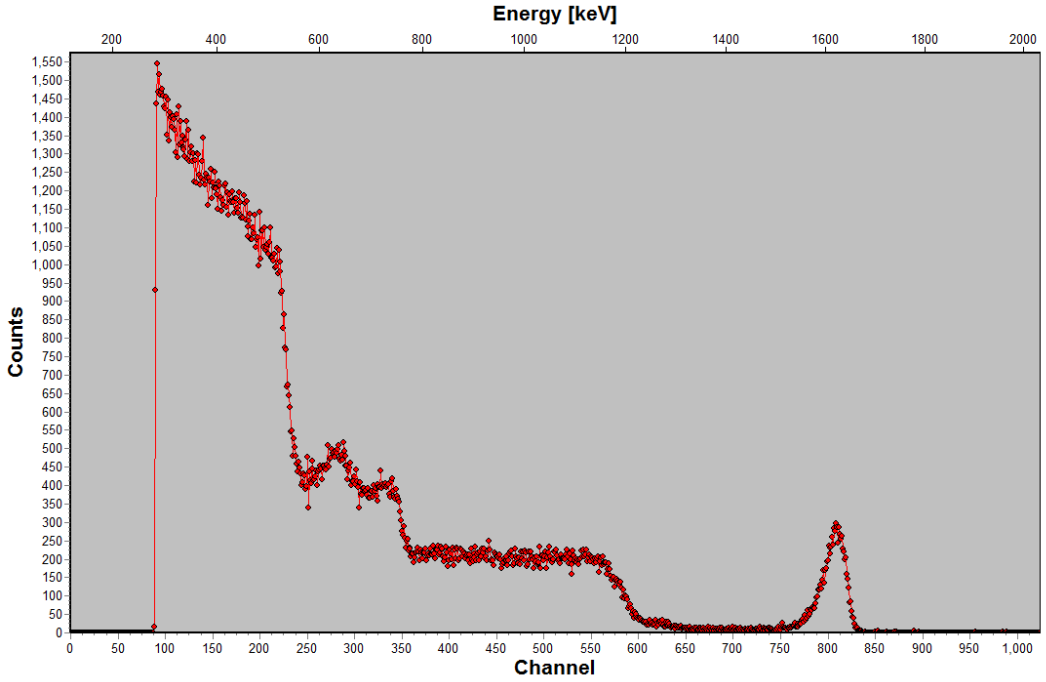

0092

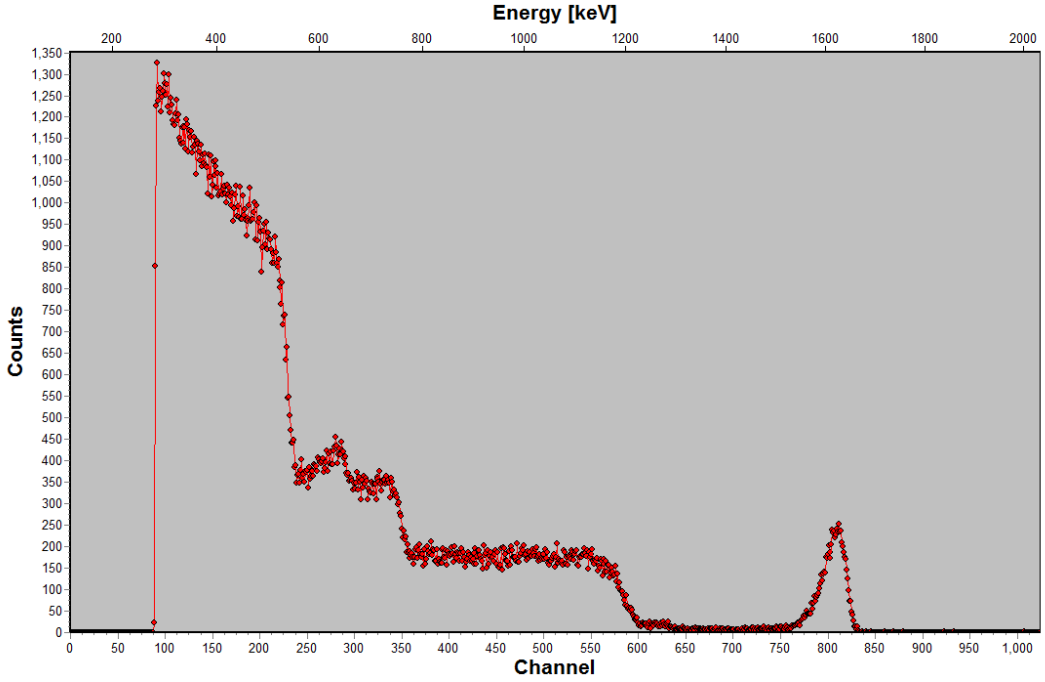

0093

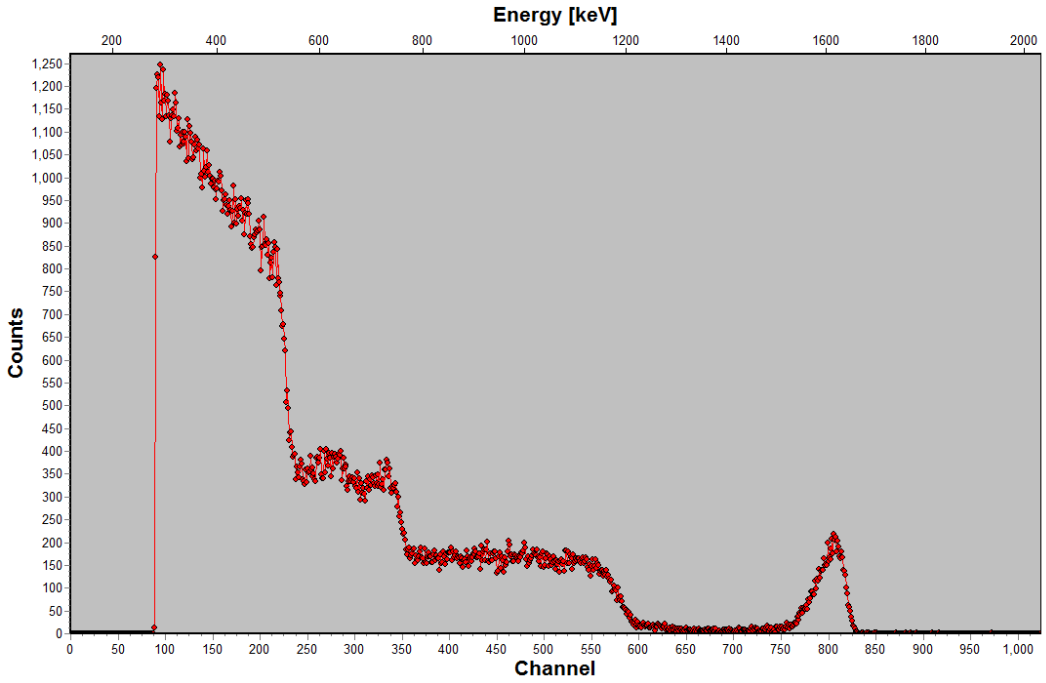

0094

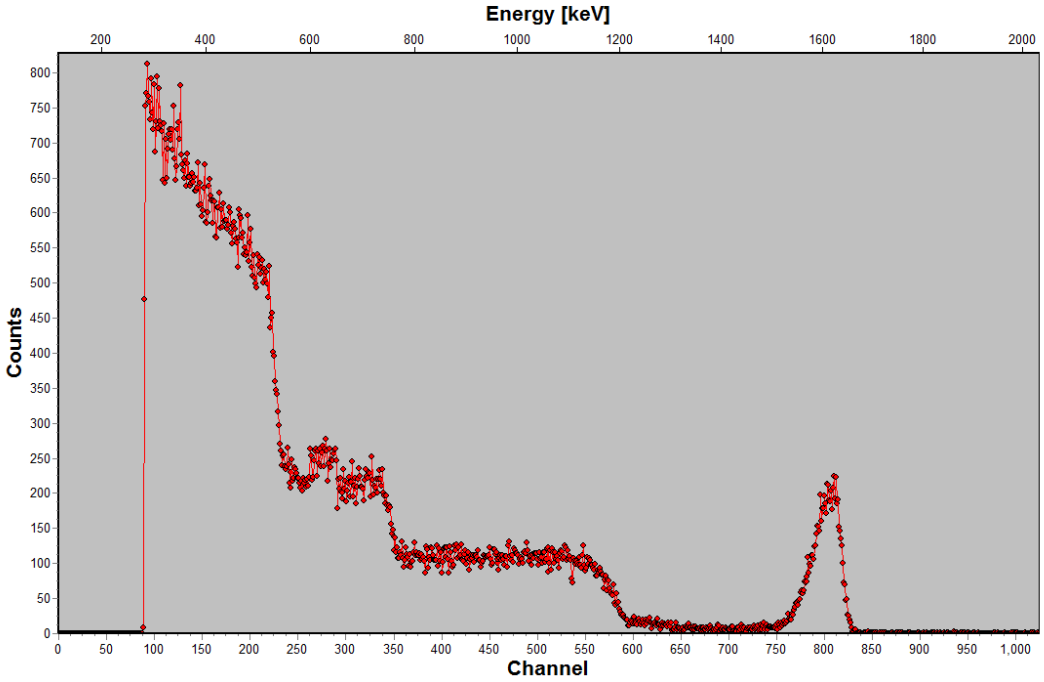

0095

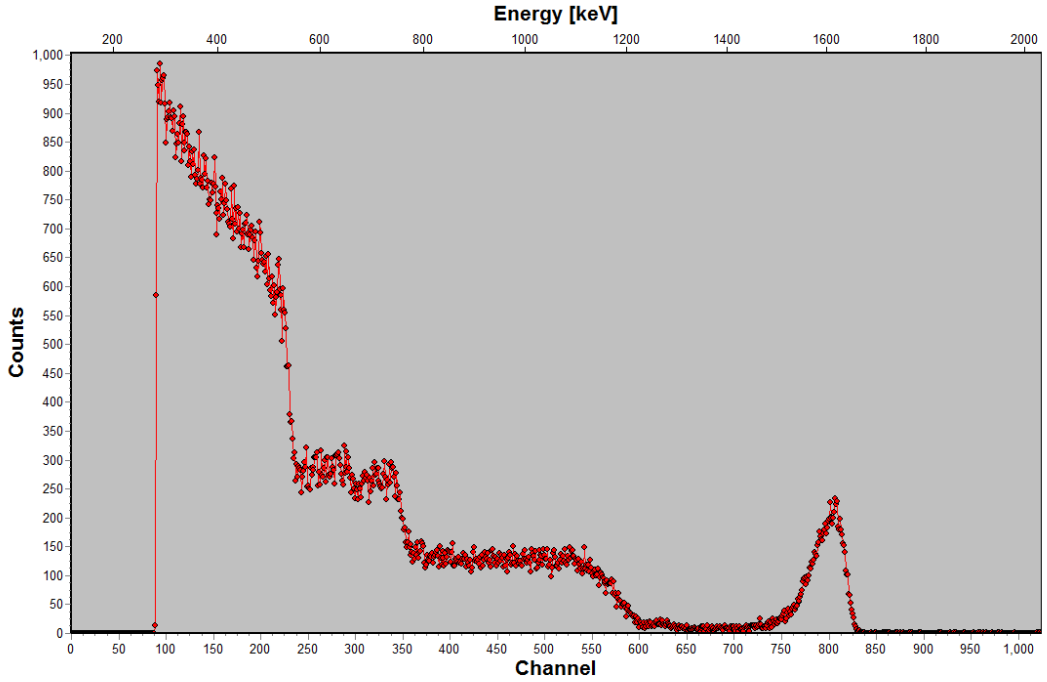

0096

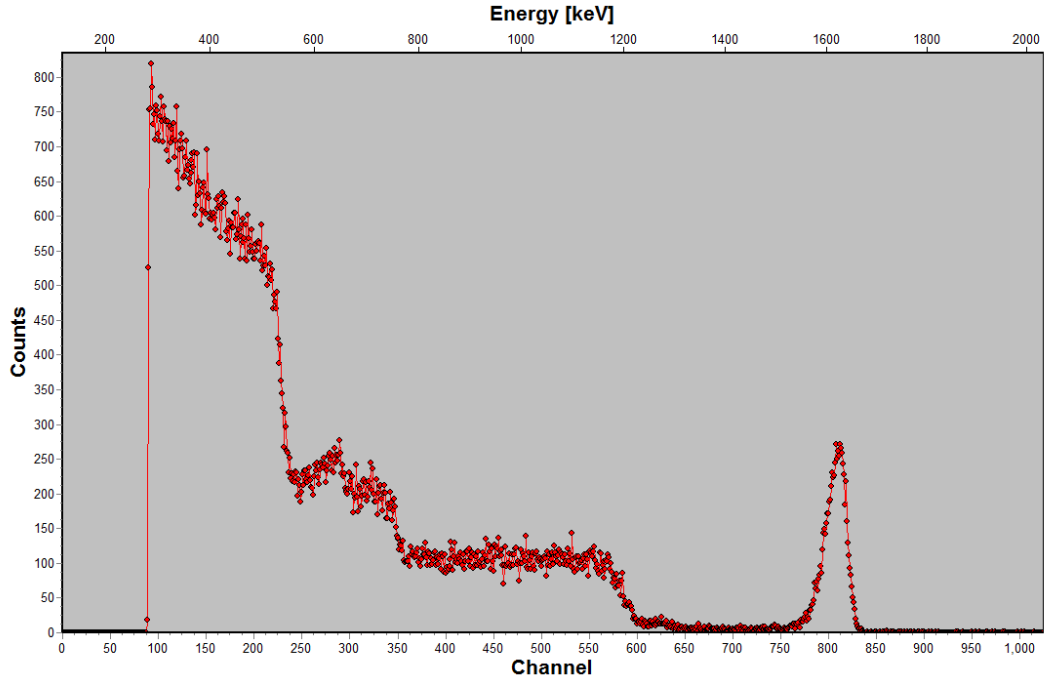

Figure 9:

0120

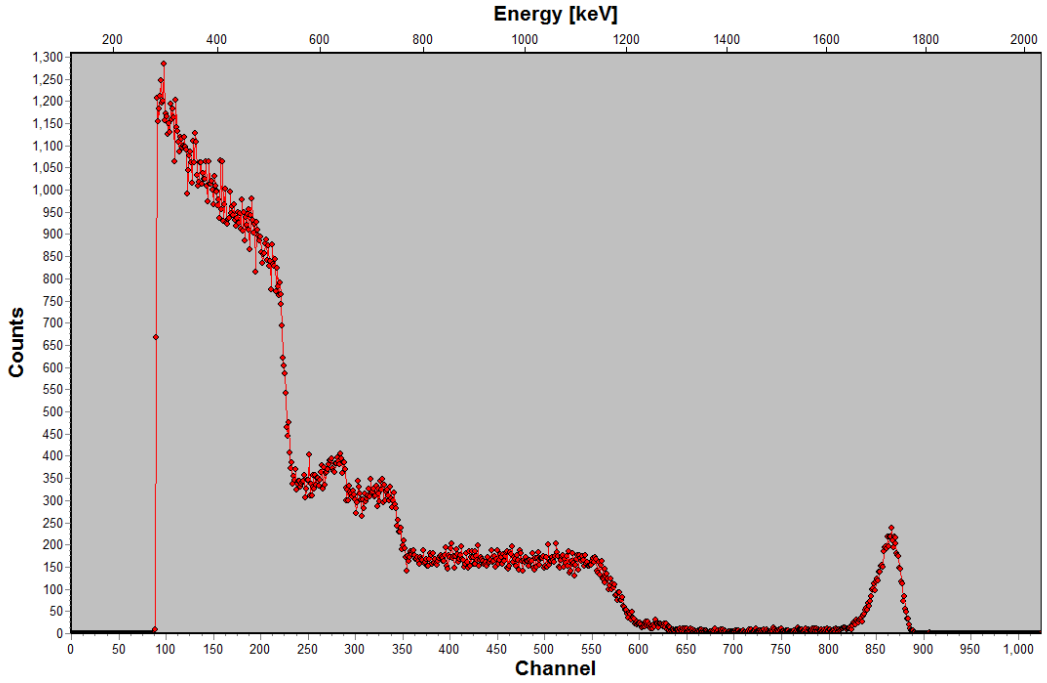

0121

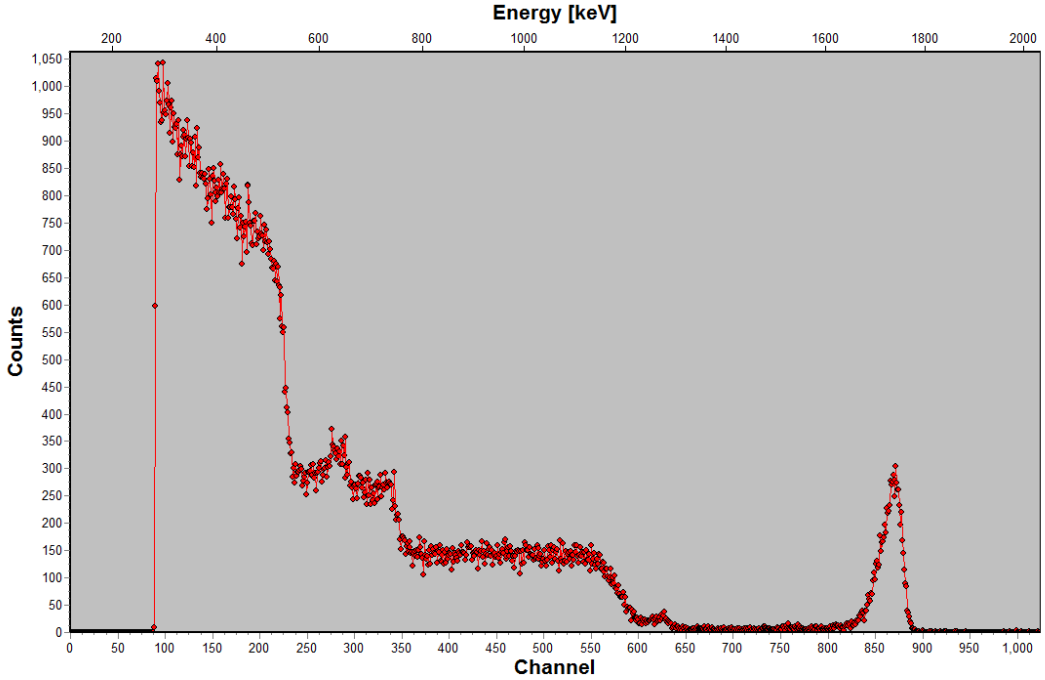

0122

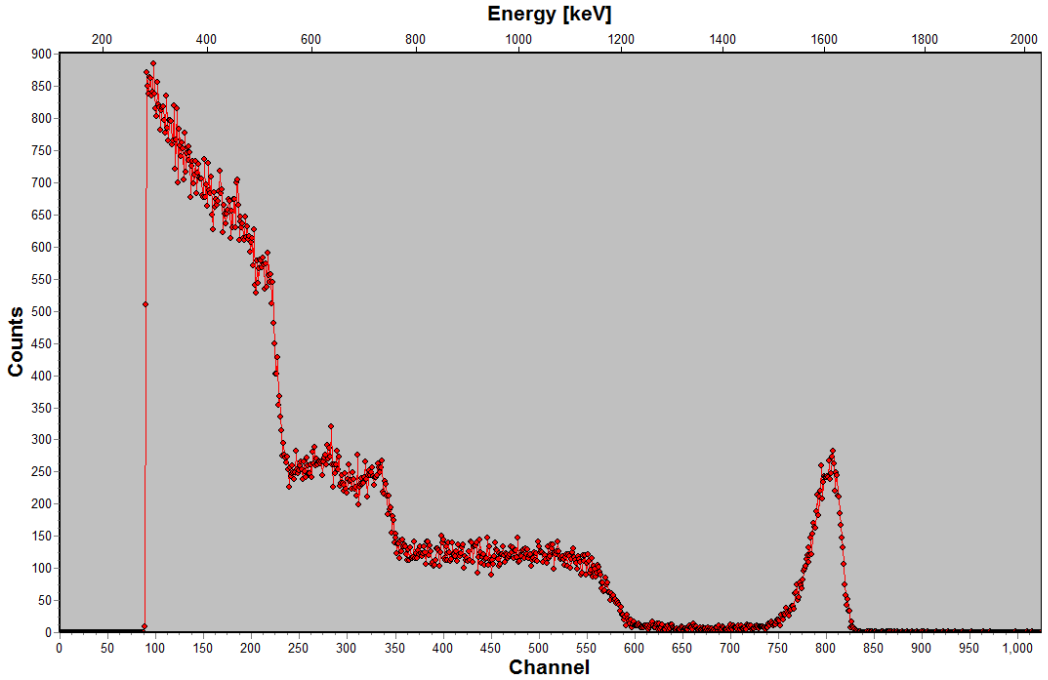

0154

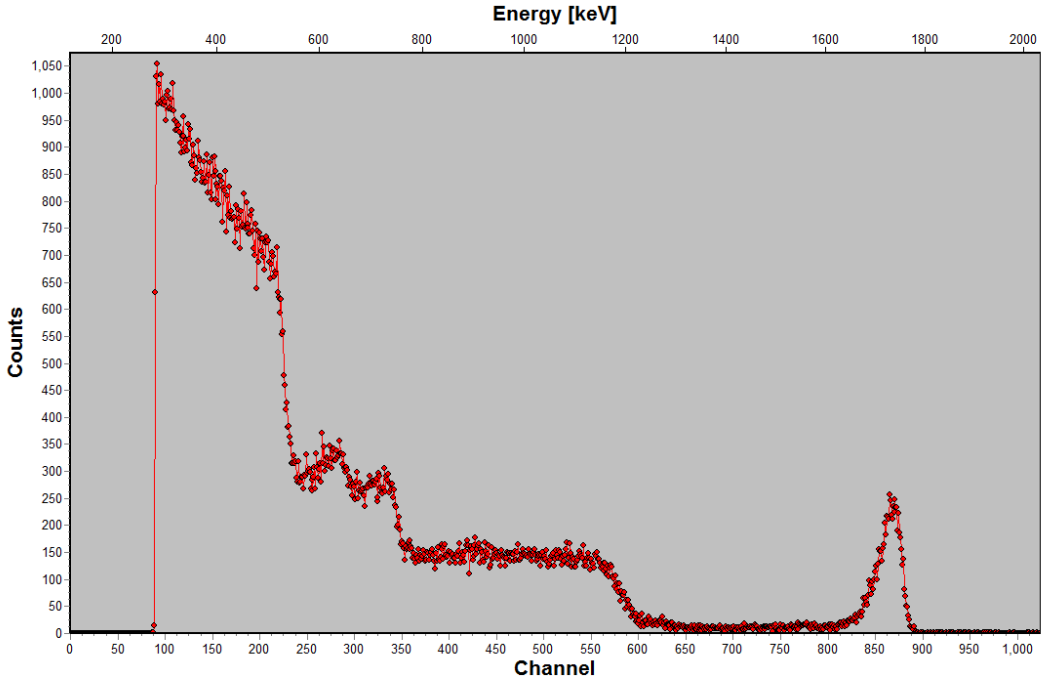

0155

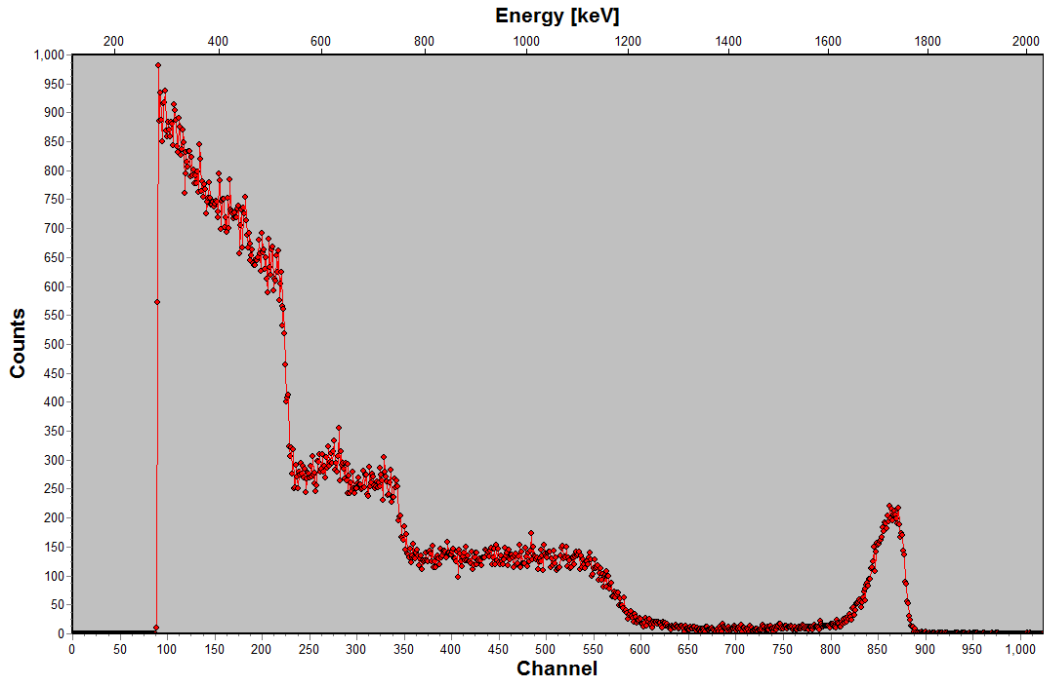

0134

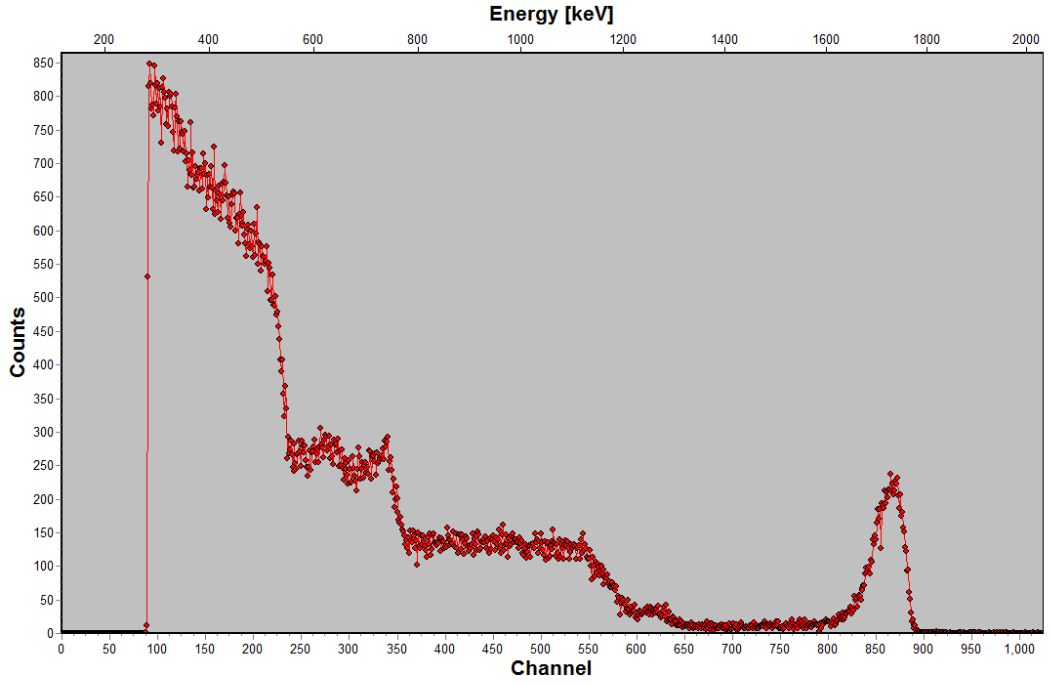

0135

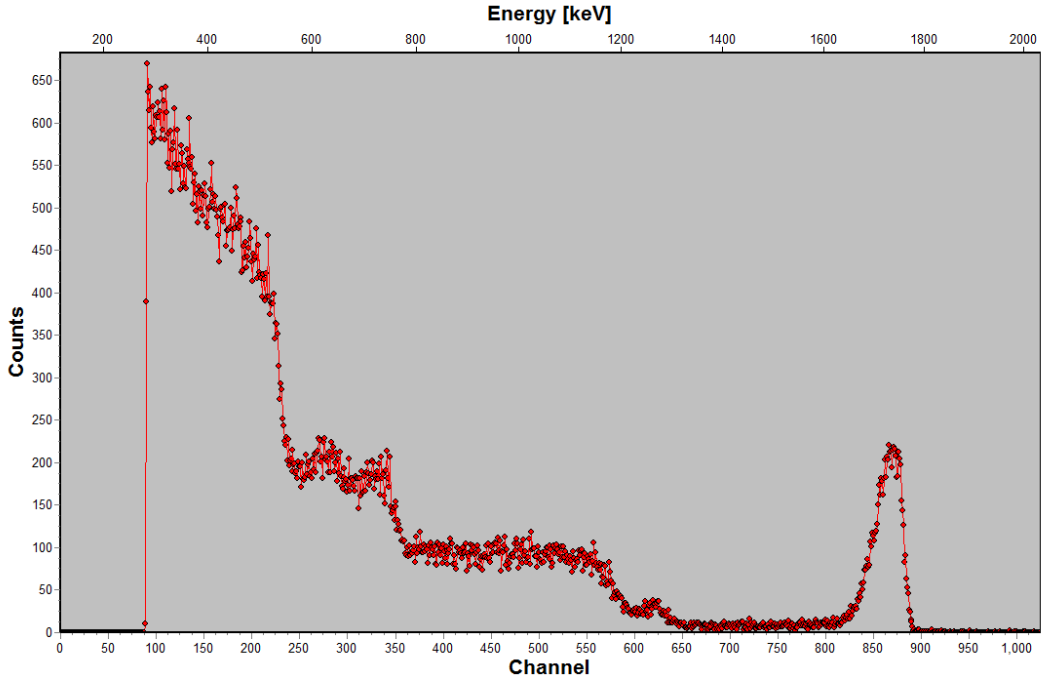

Figure 10:

0102

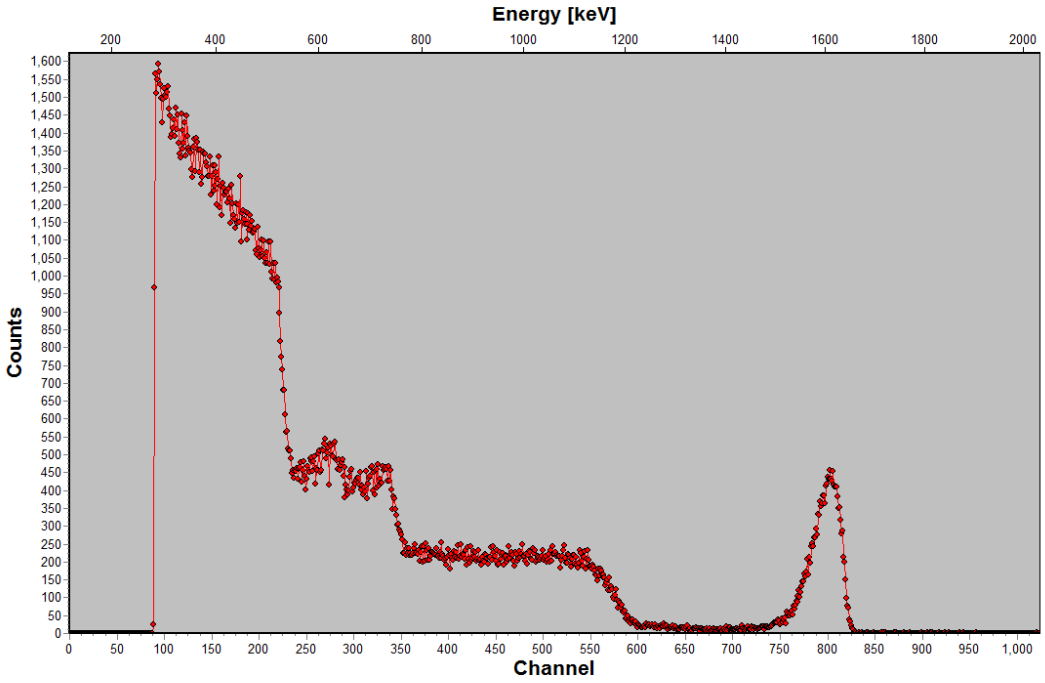

0105

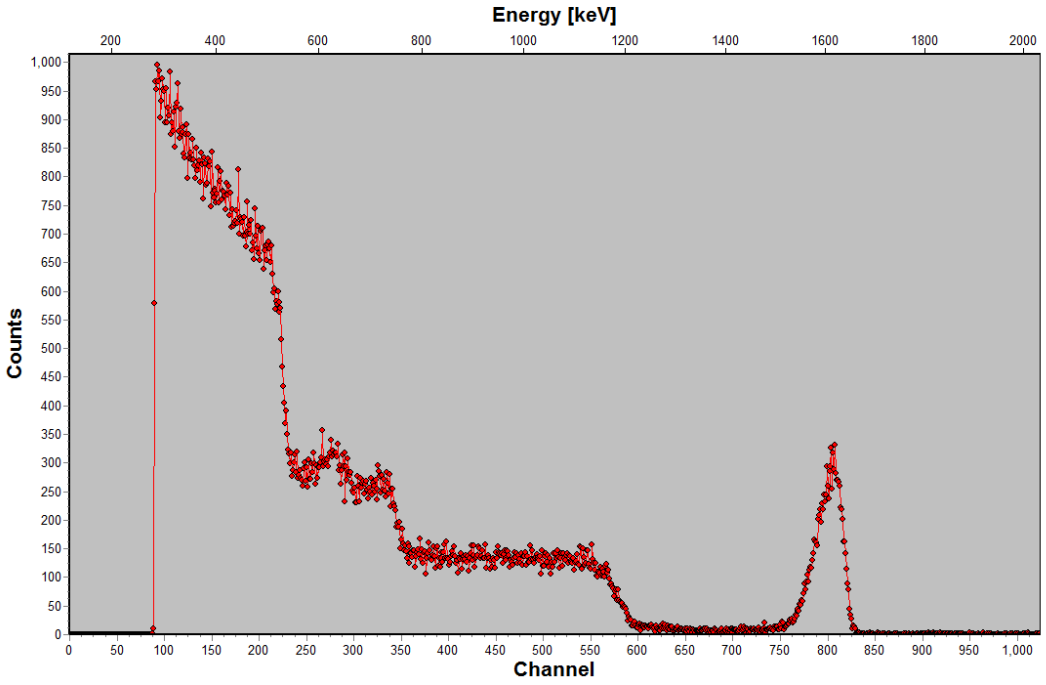

0106

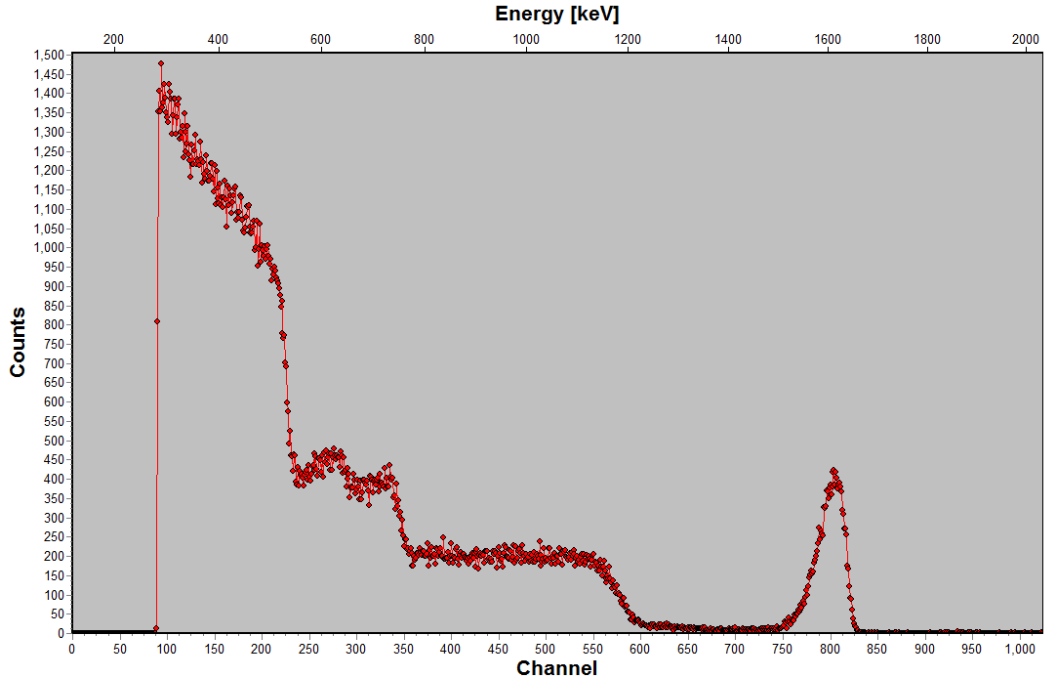

0158

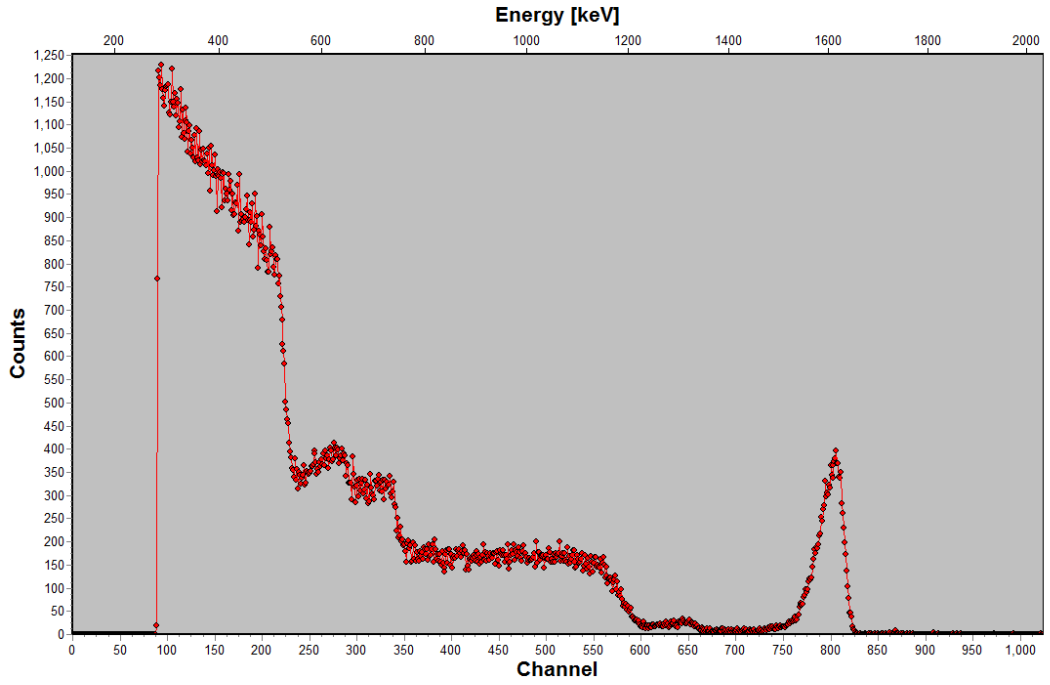

0159

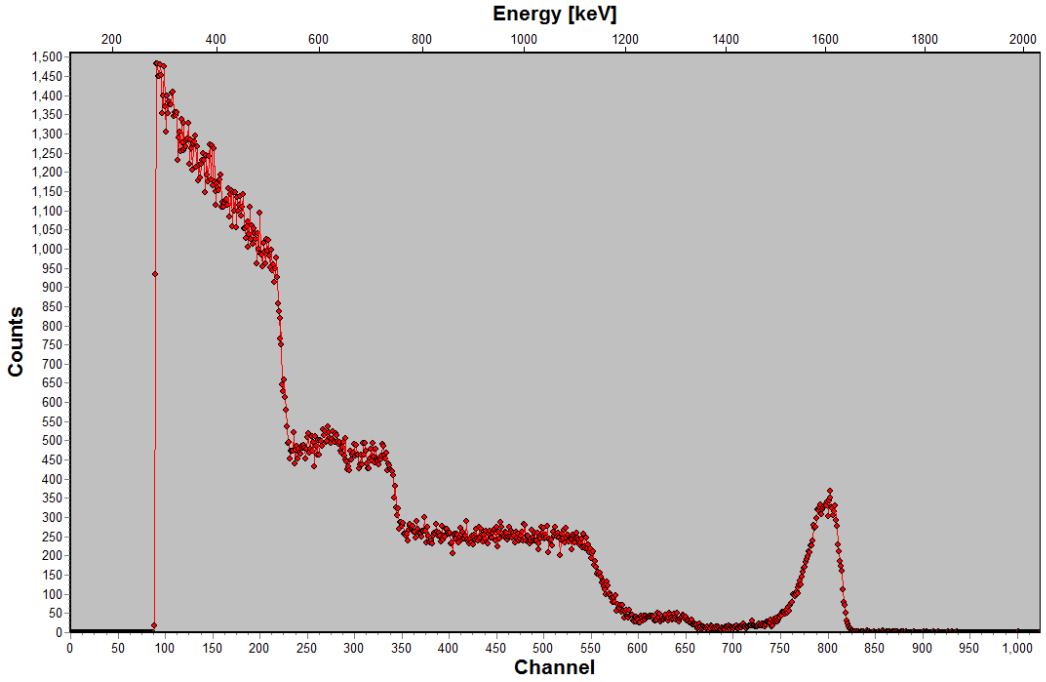

0140

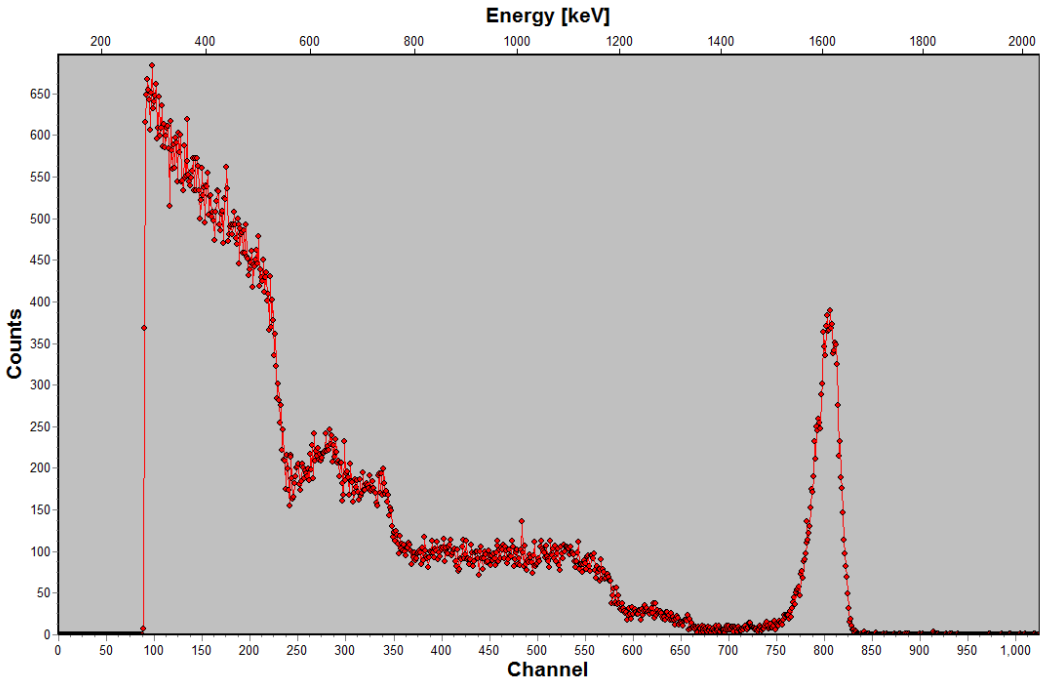

0141

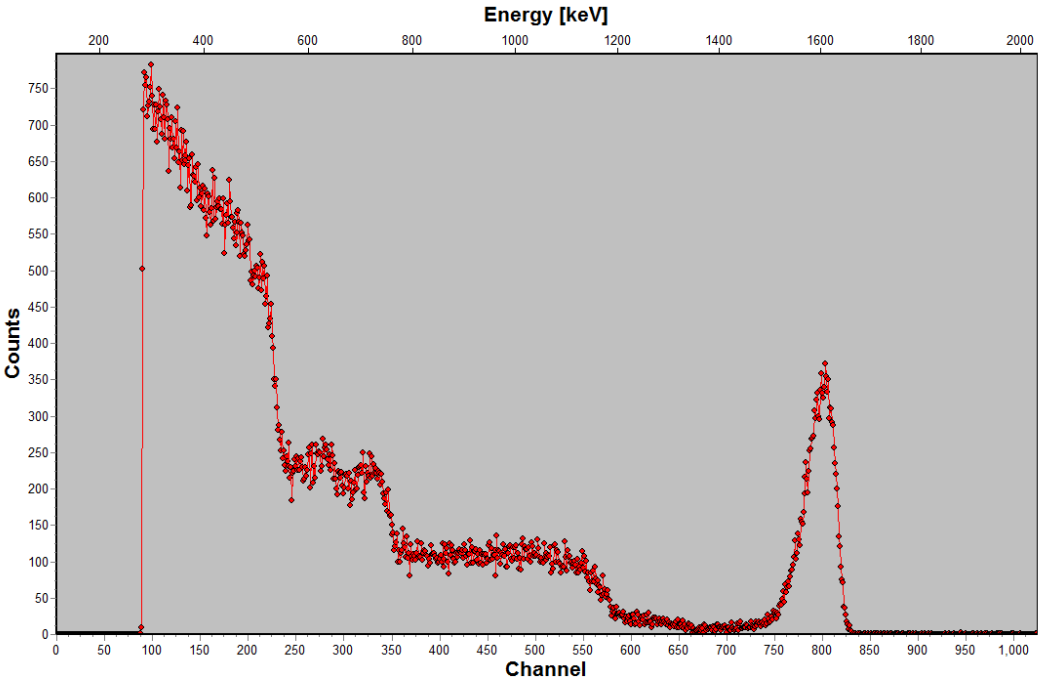

Figure 11:

0104

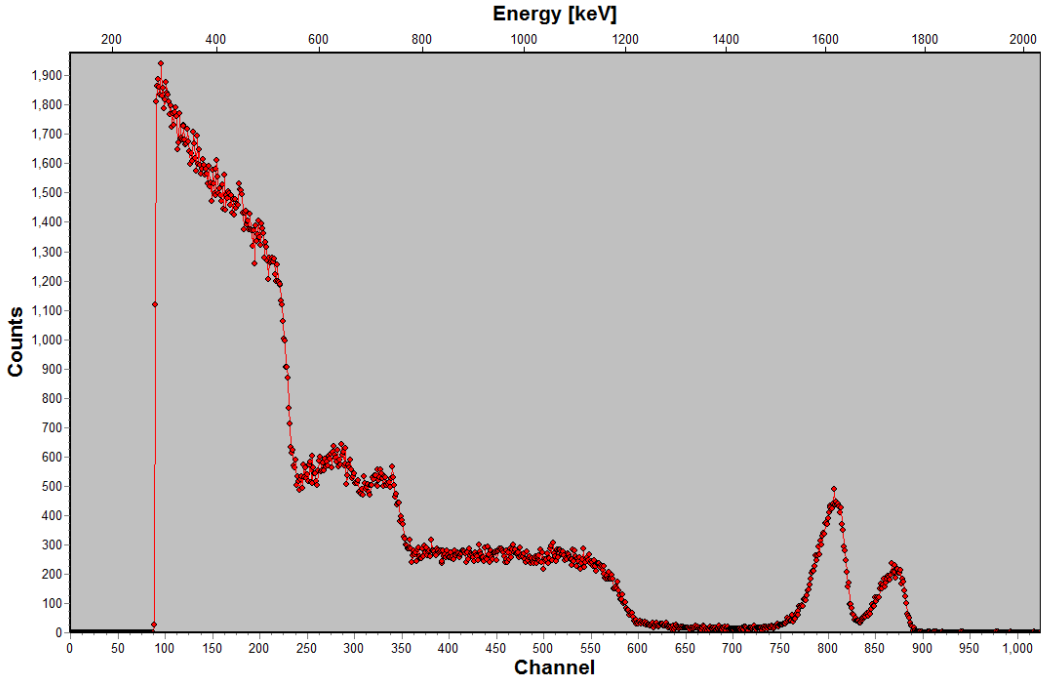

0115

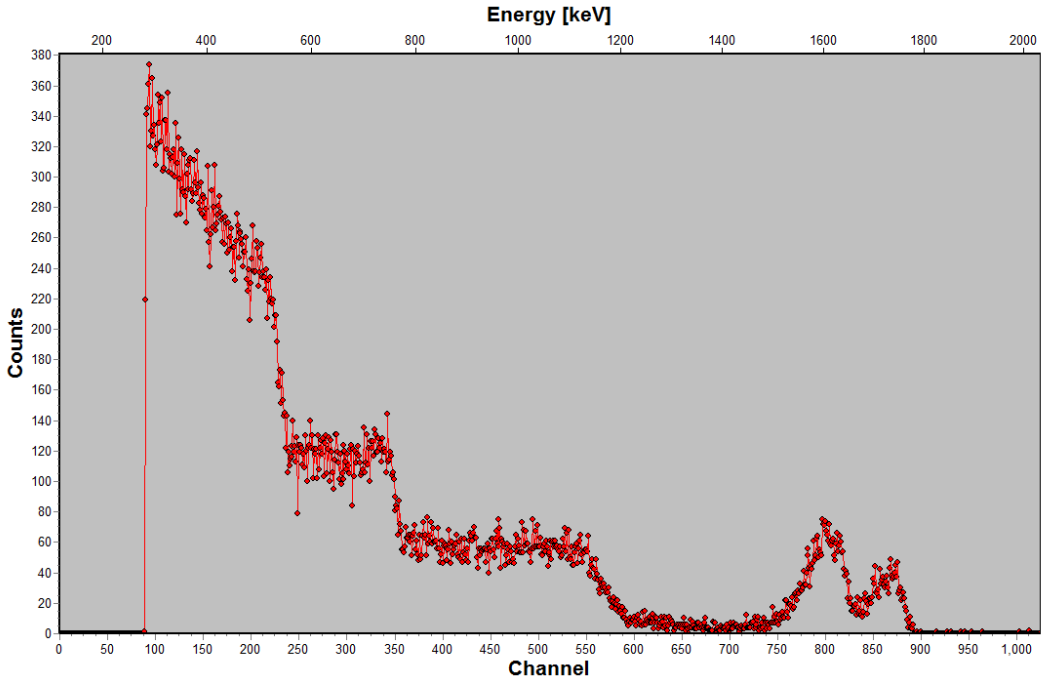

0116

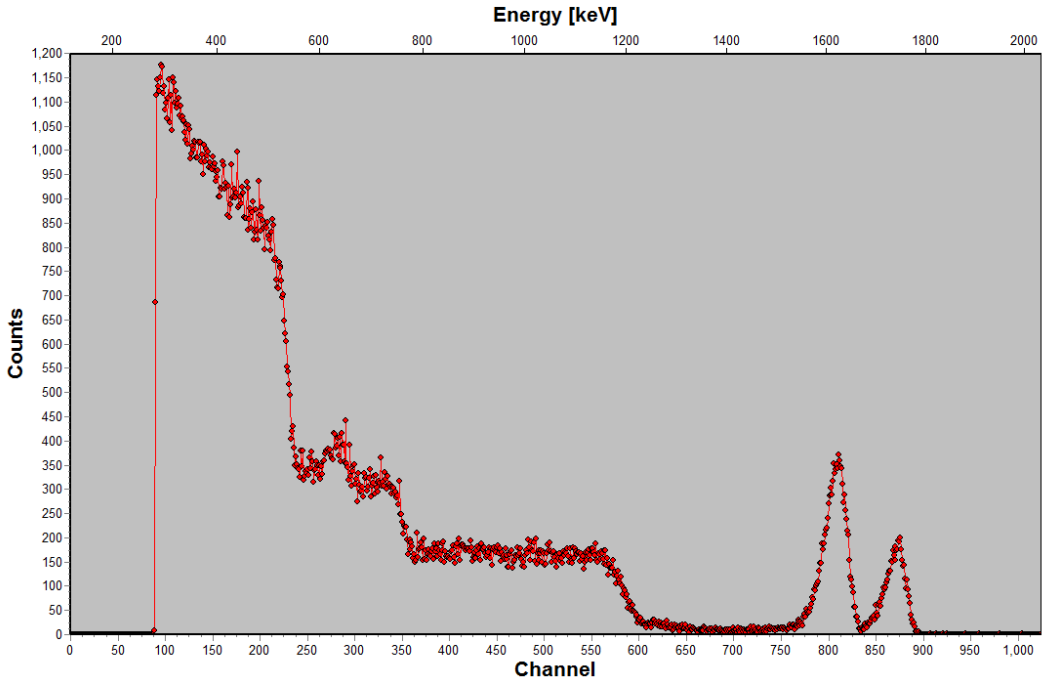

0162

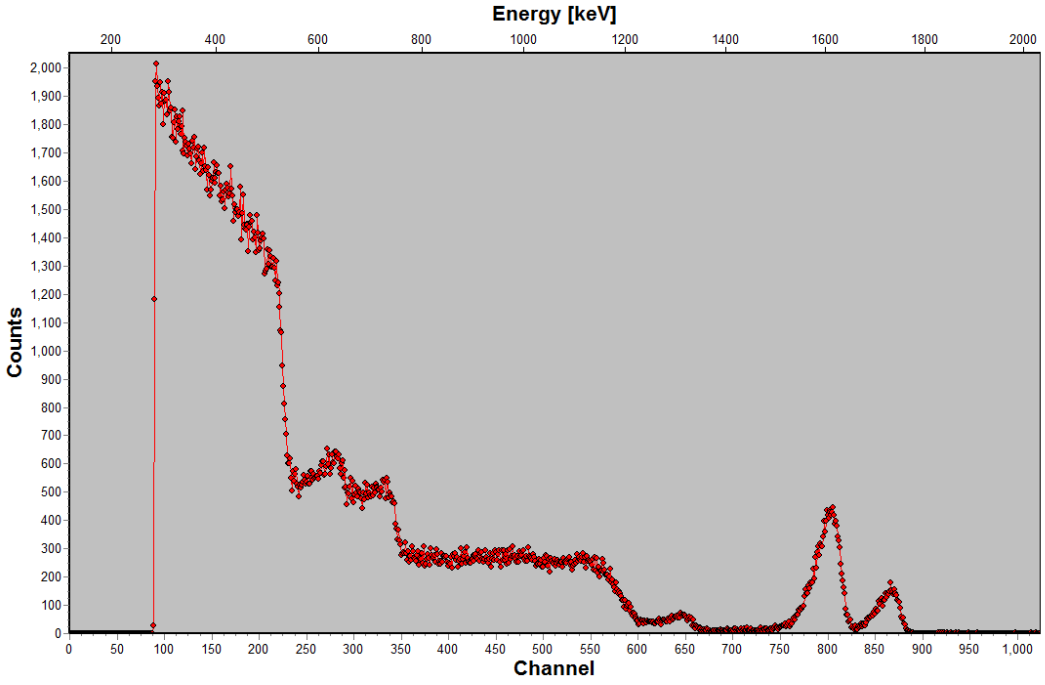

0163

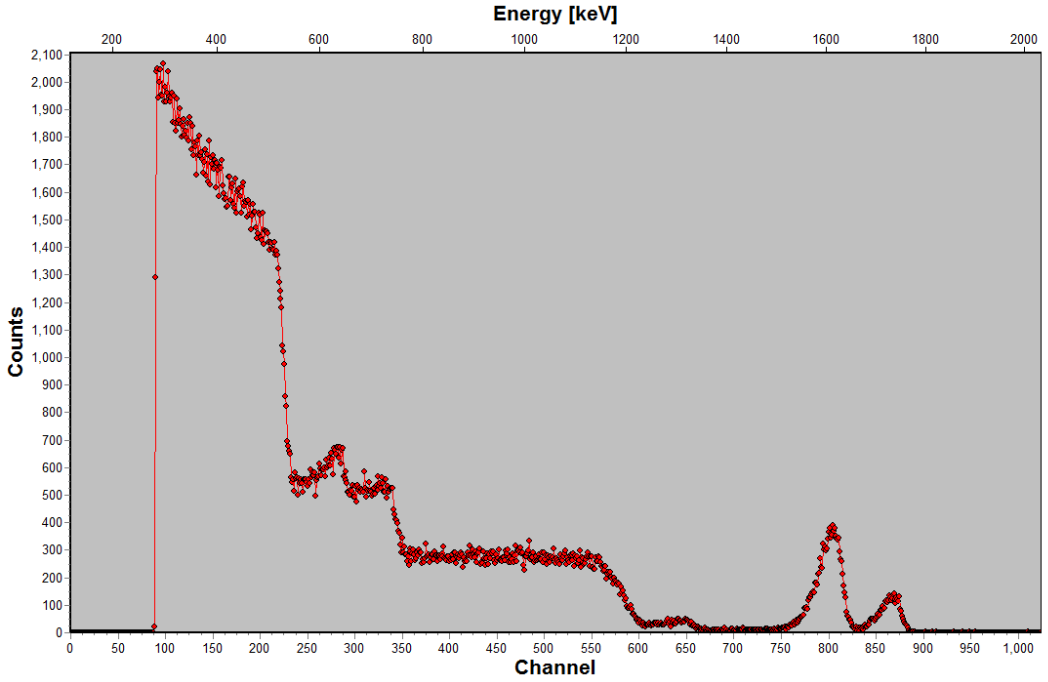

0146

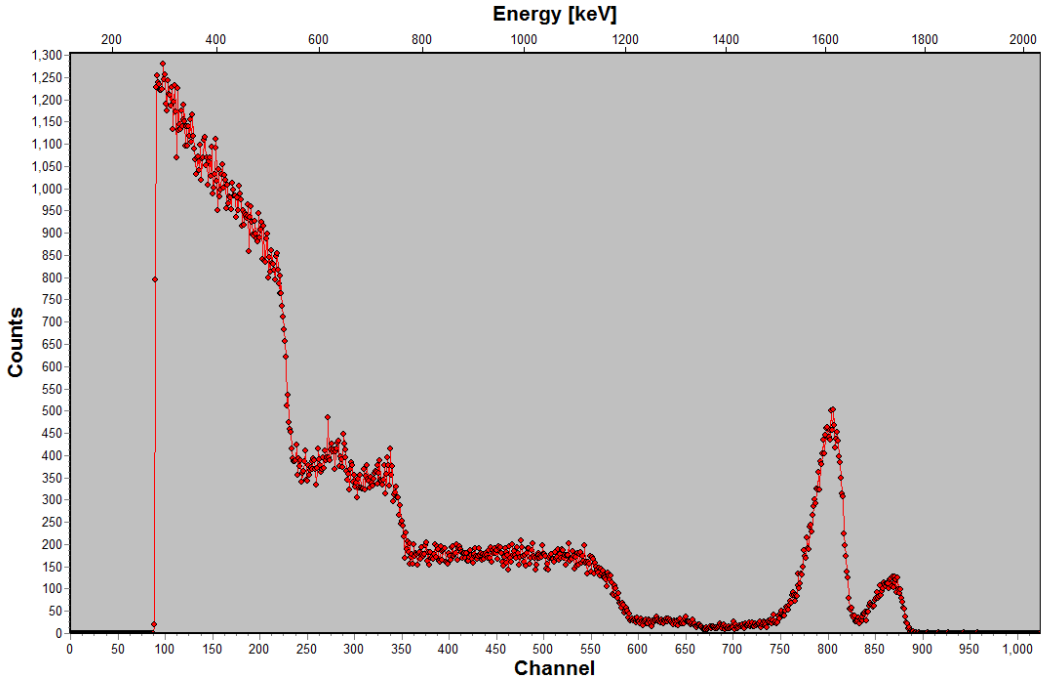

0147

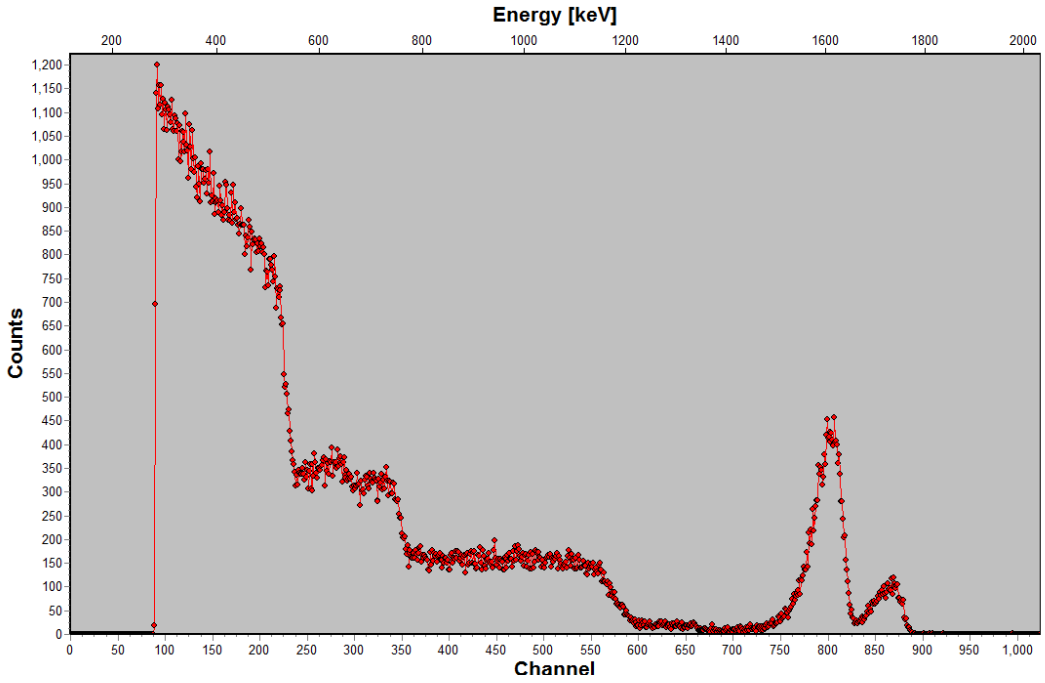

Figure 12:

0136

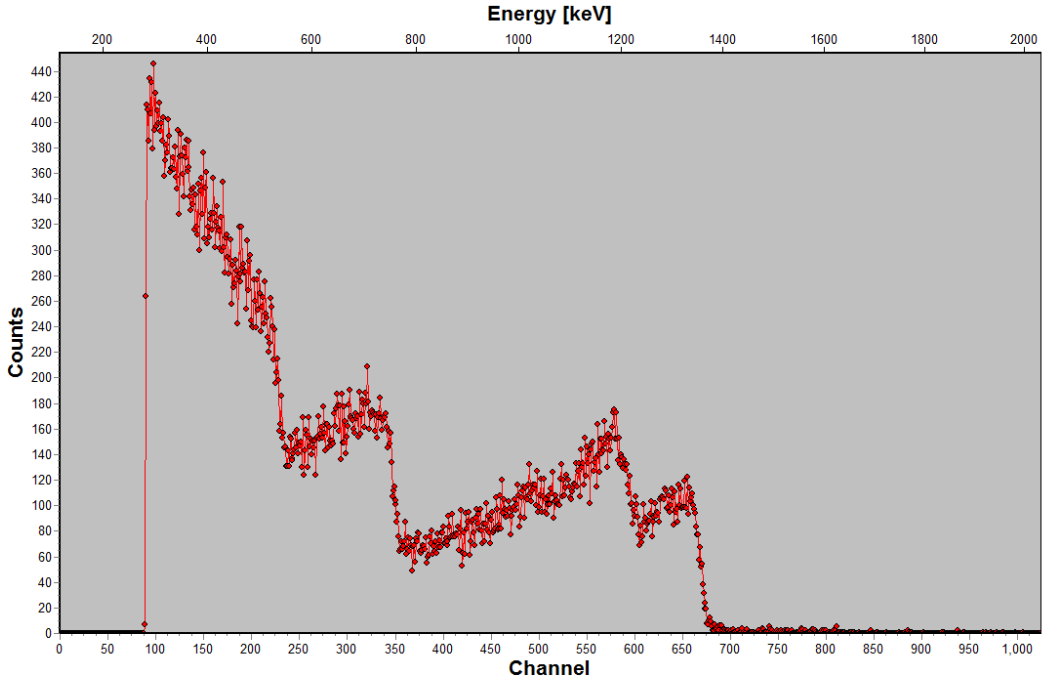

0137

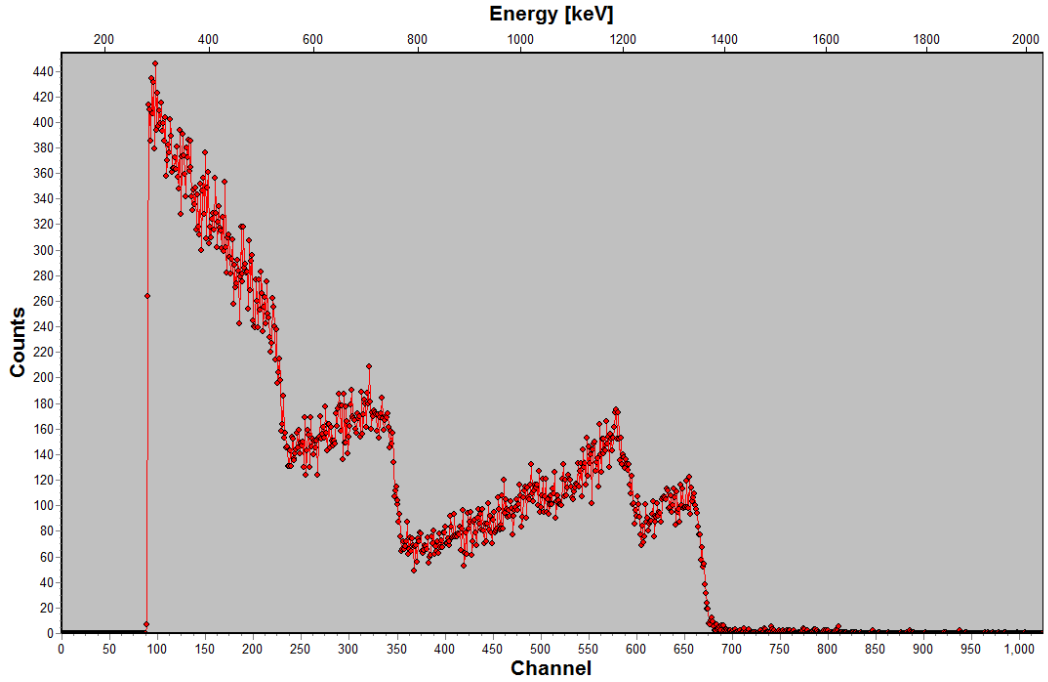

0142

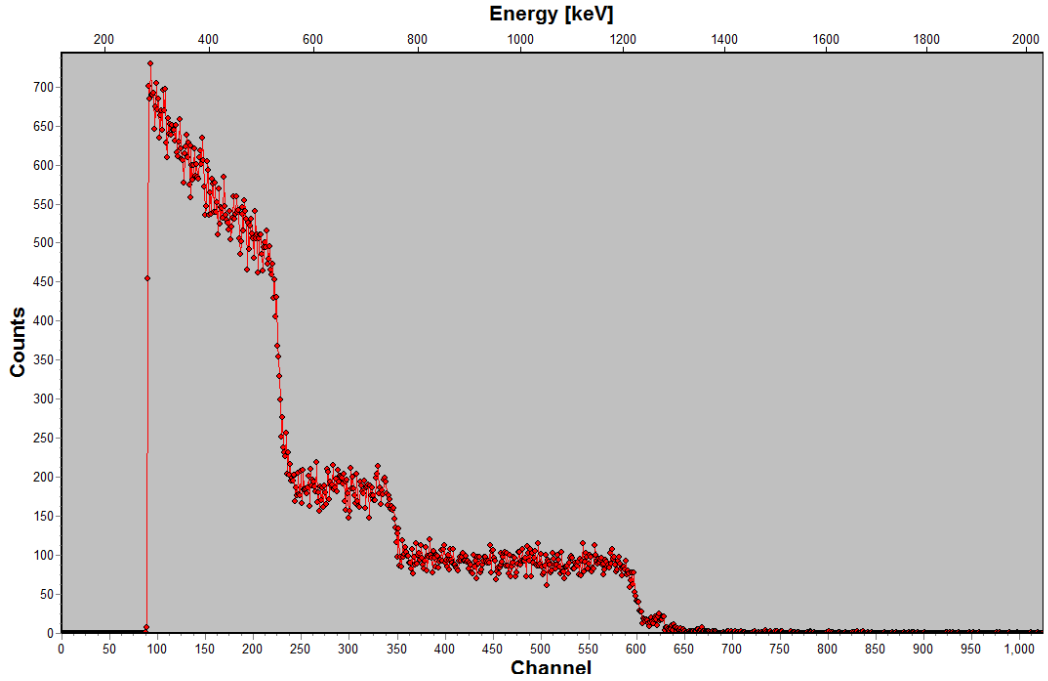

0143

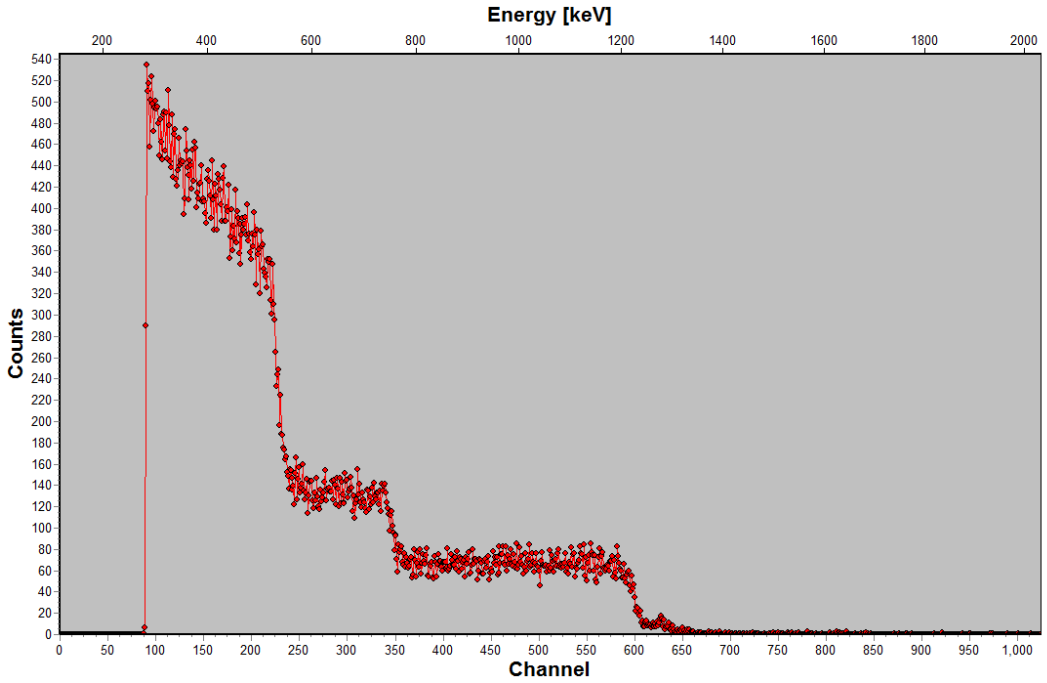

Figure 13:

0204

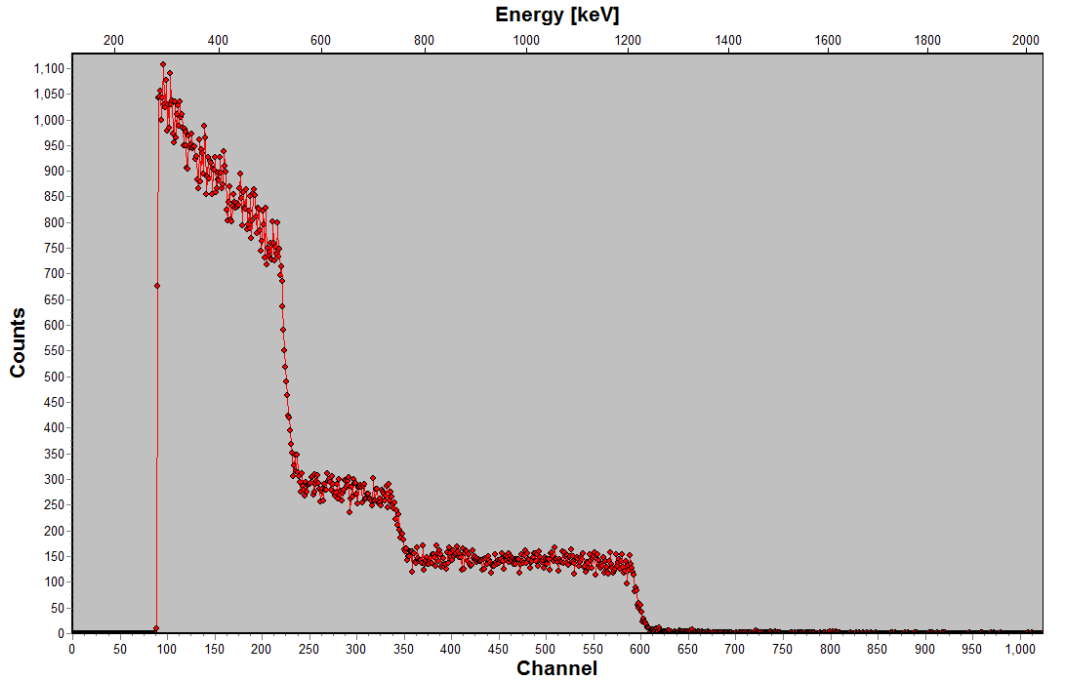

Figure 14:

0255

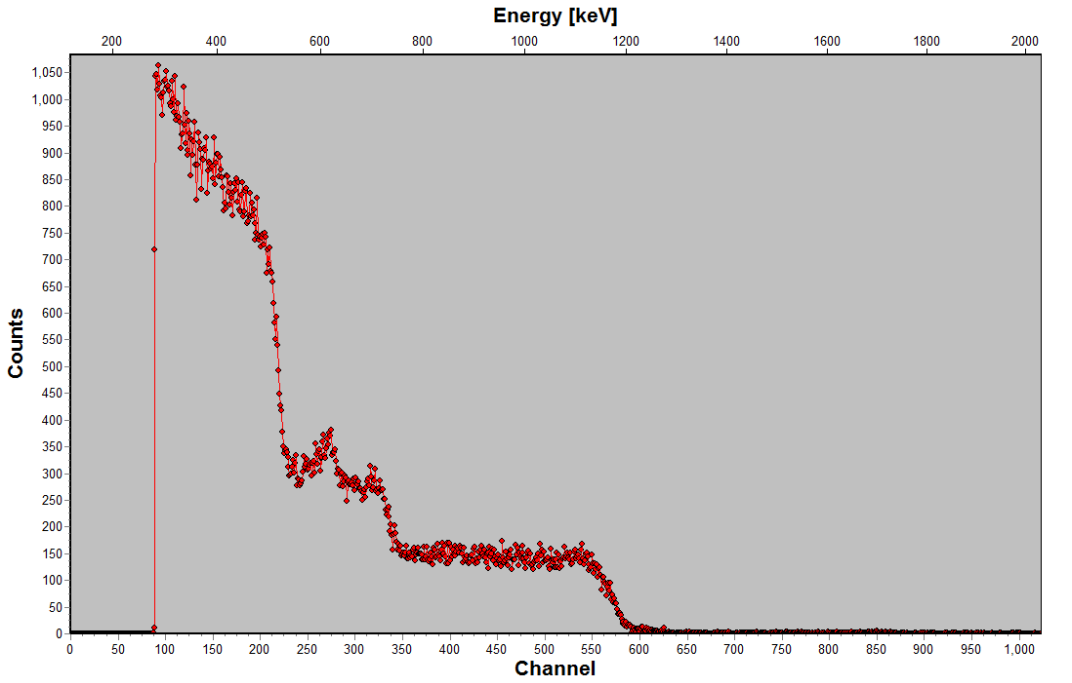

Figure 15 and 16:

0328

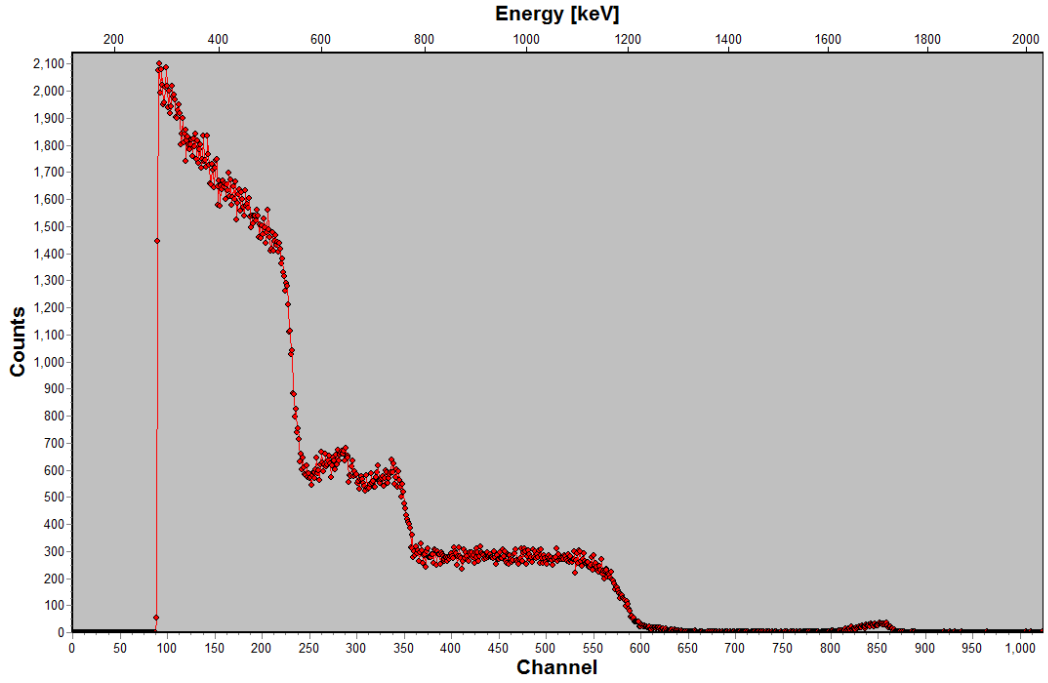

0329

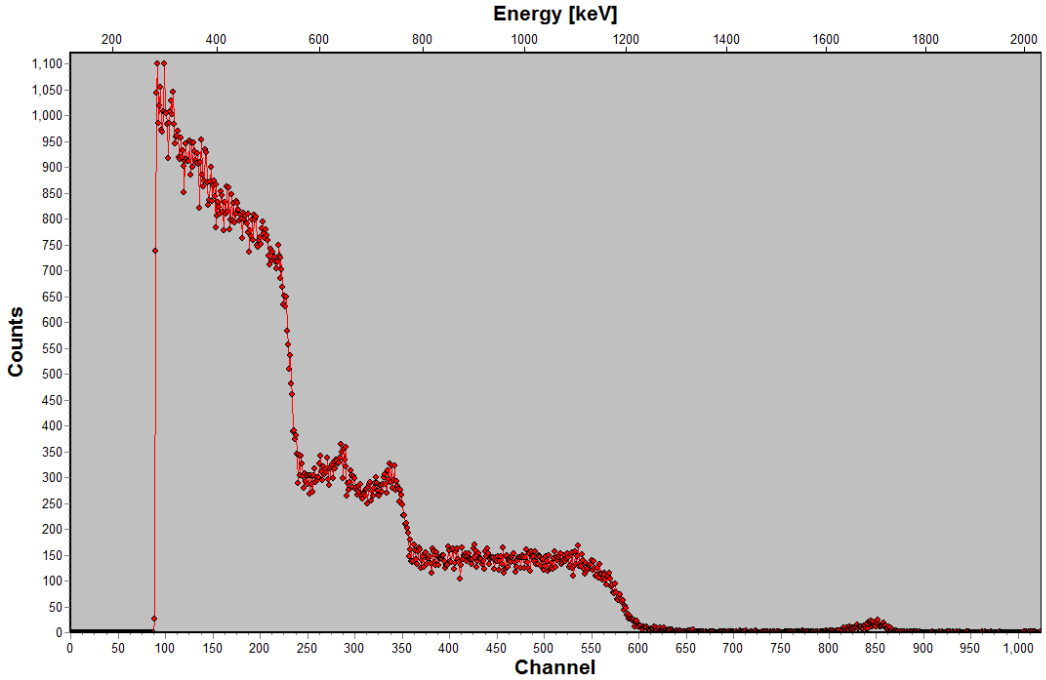

0330

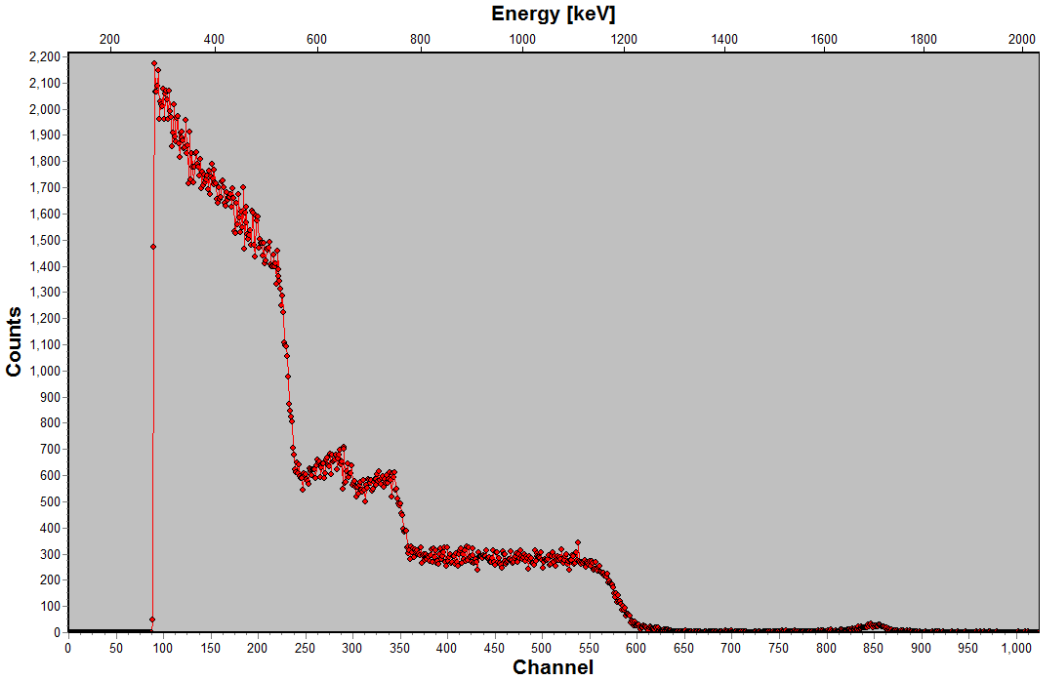

0331

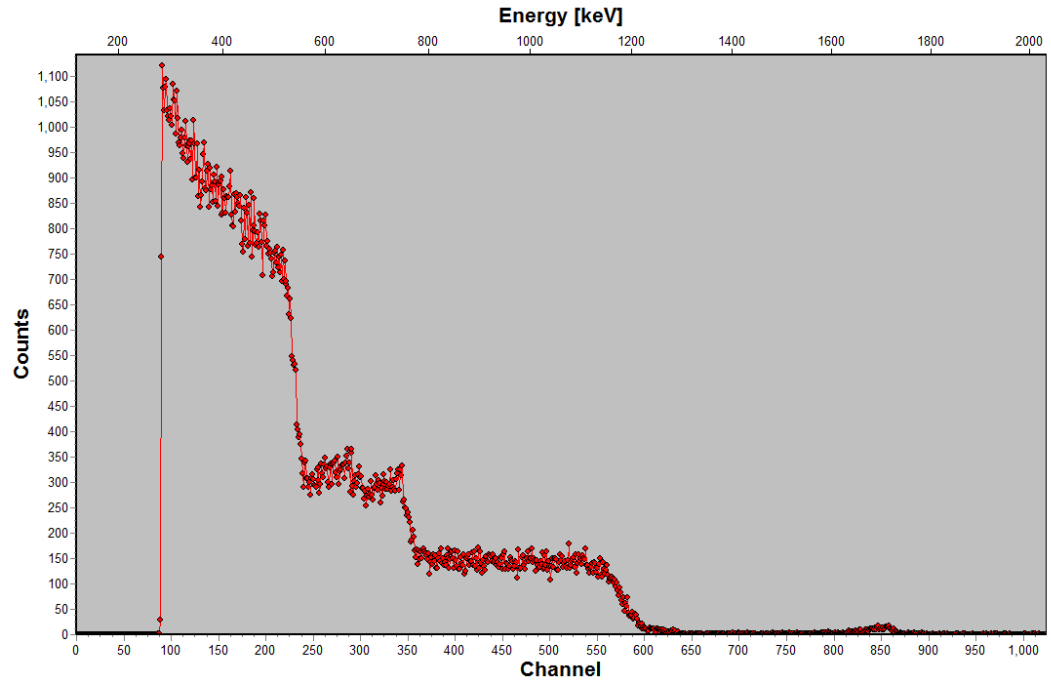

0332

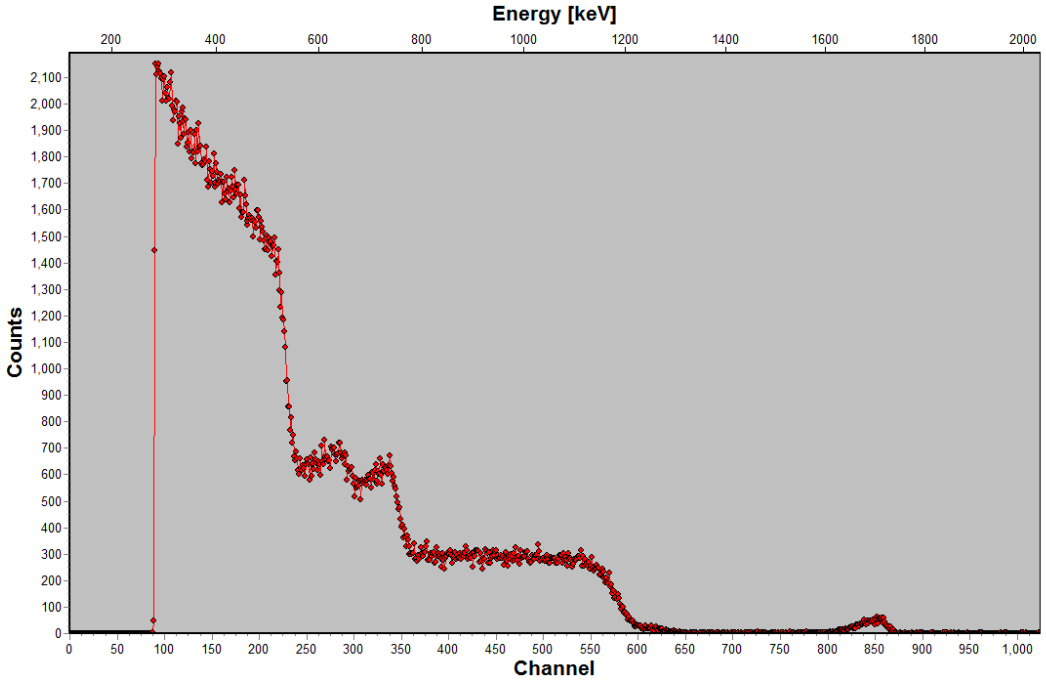

0333

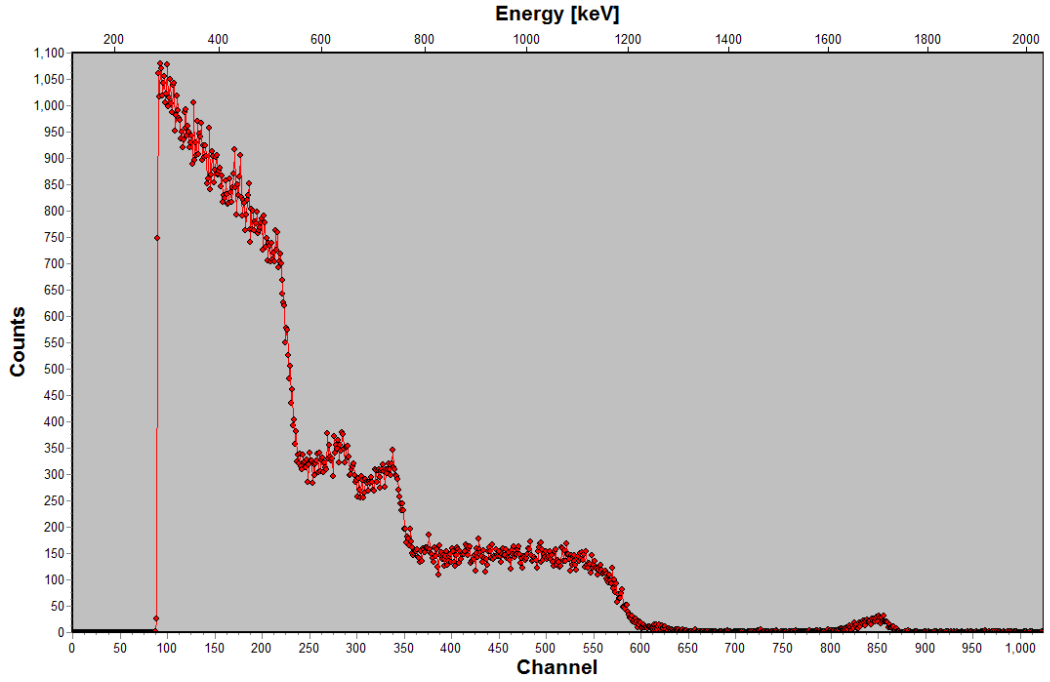

0334

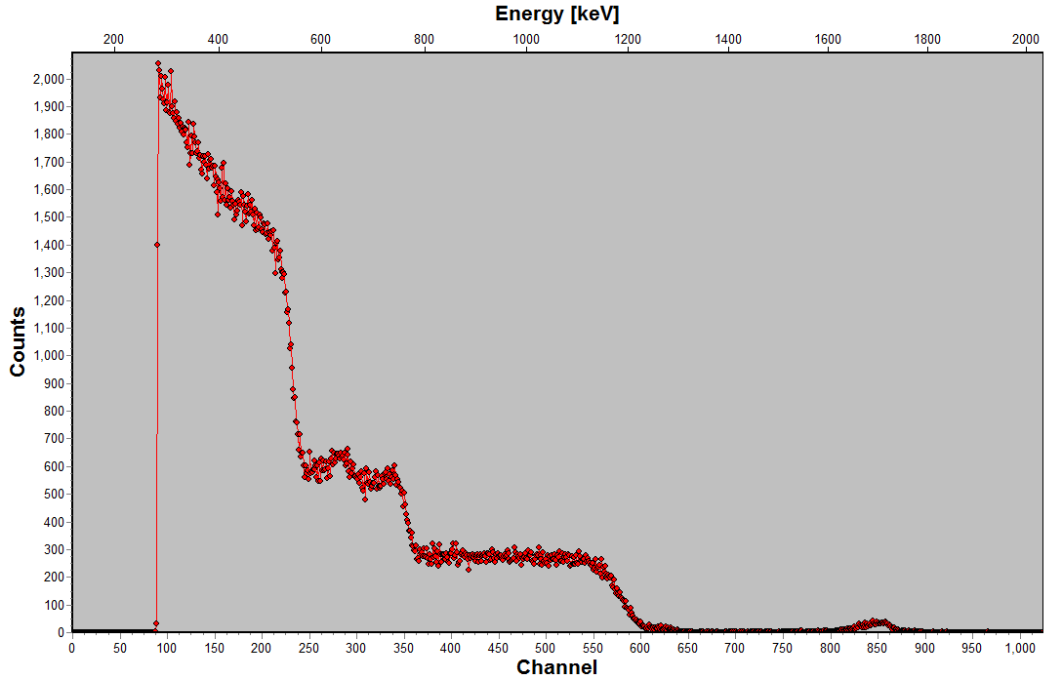

0335

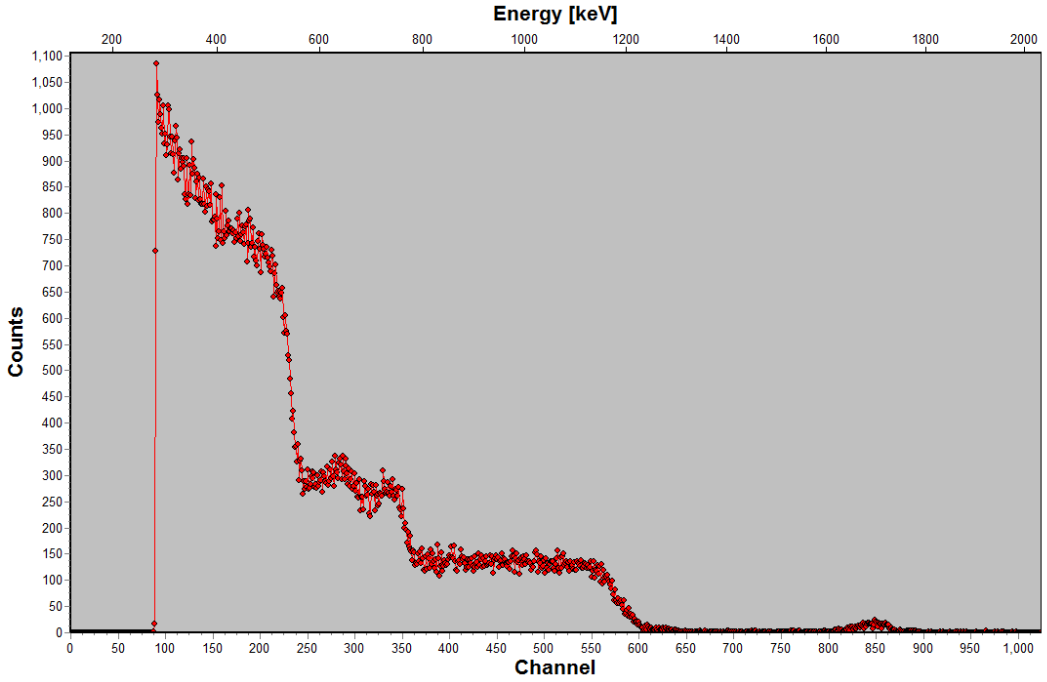

0336

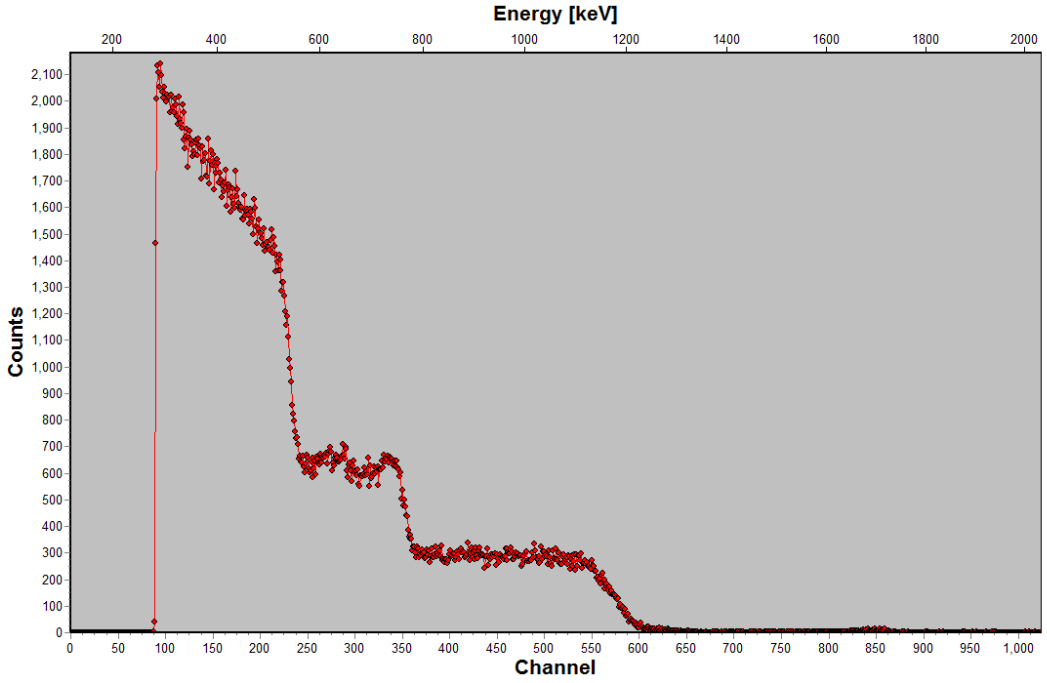

0337

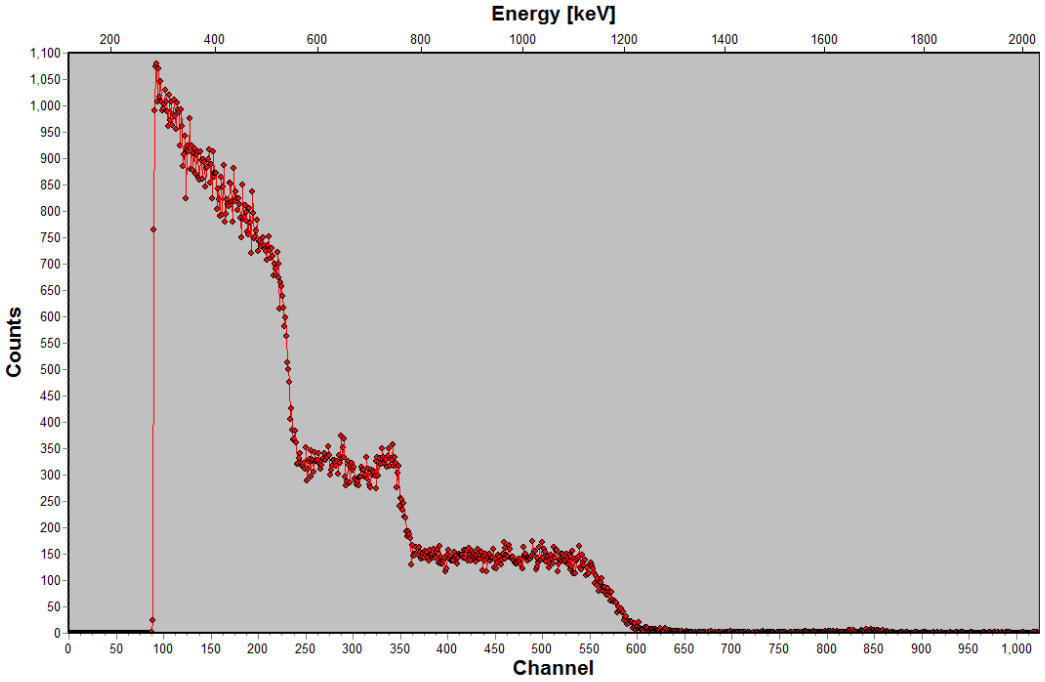

0338

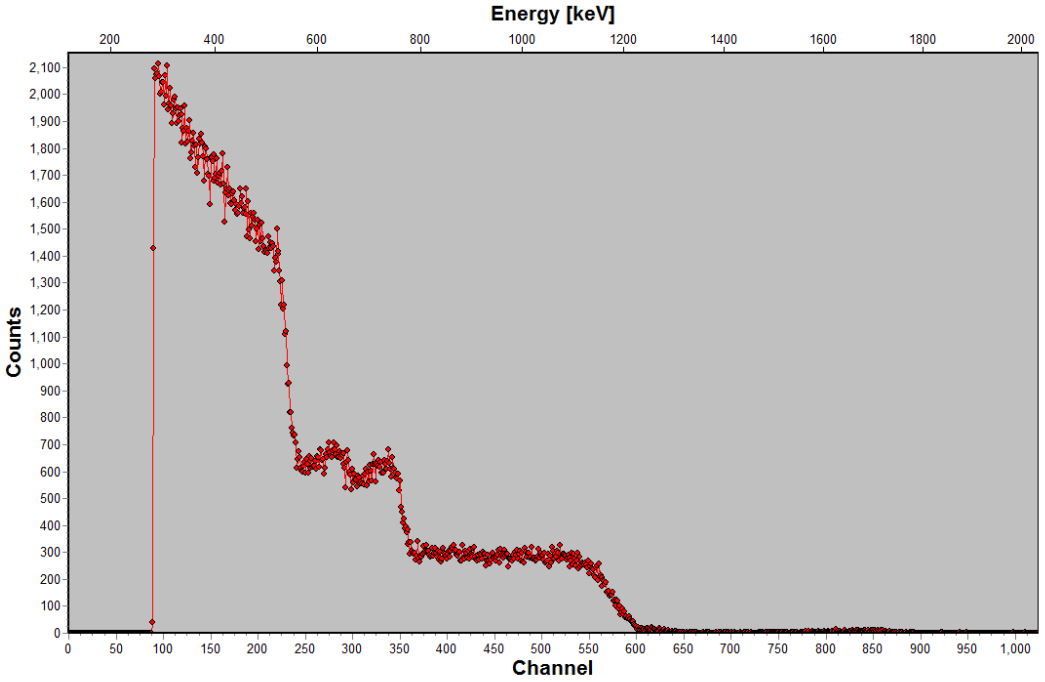

0339

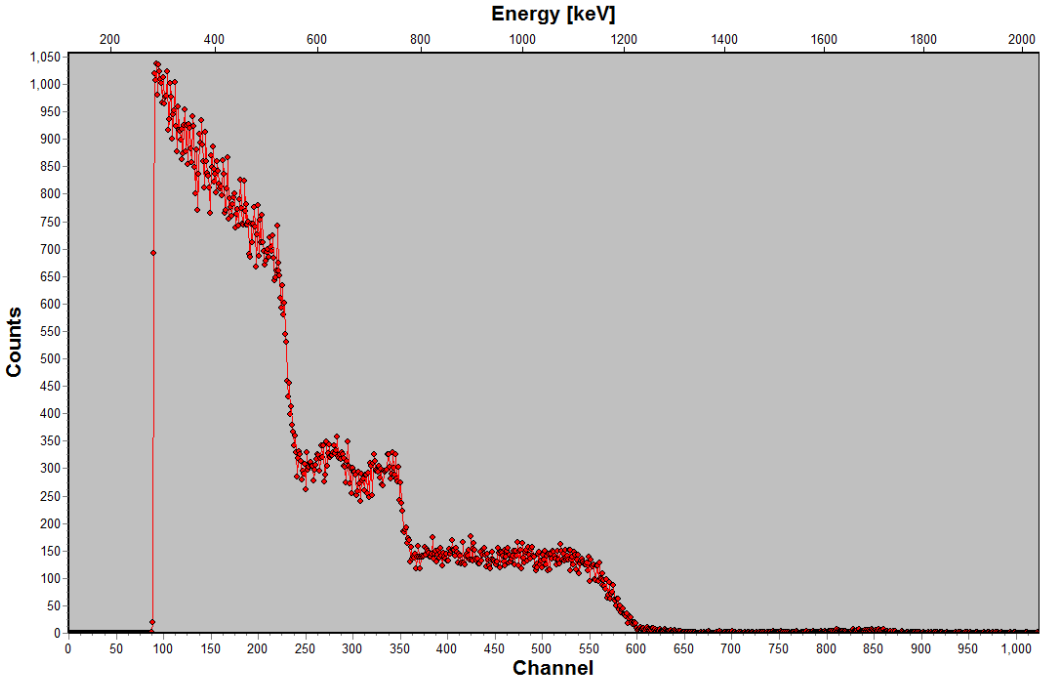

0340

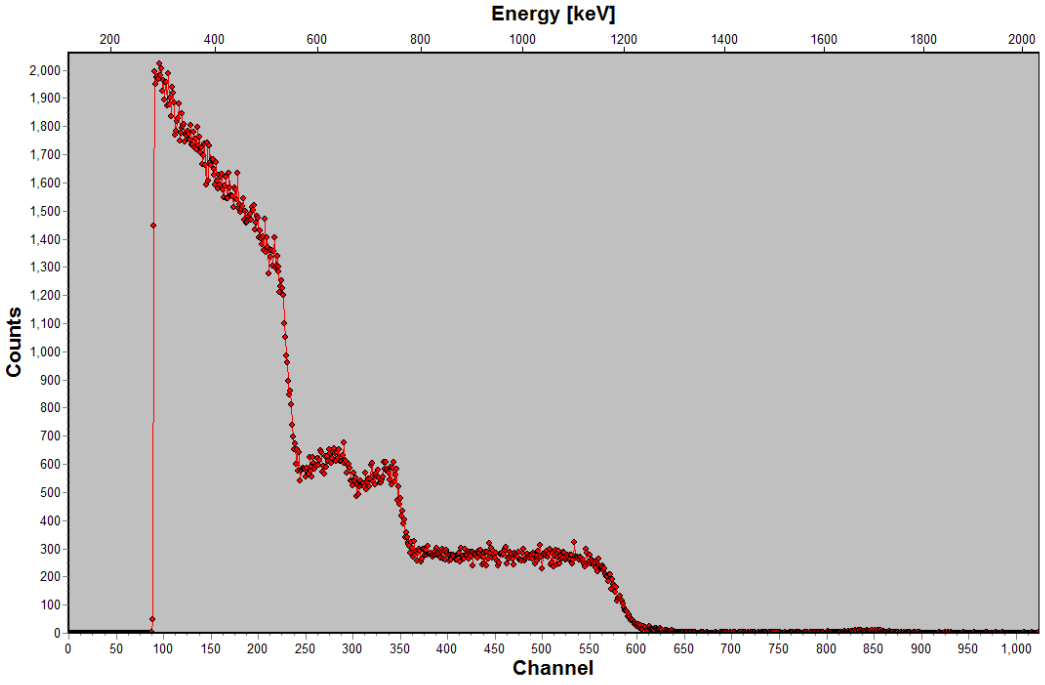

0341

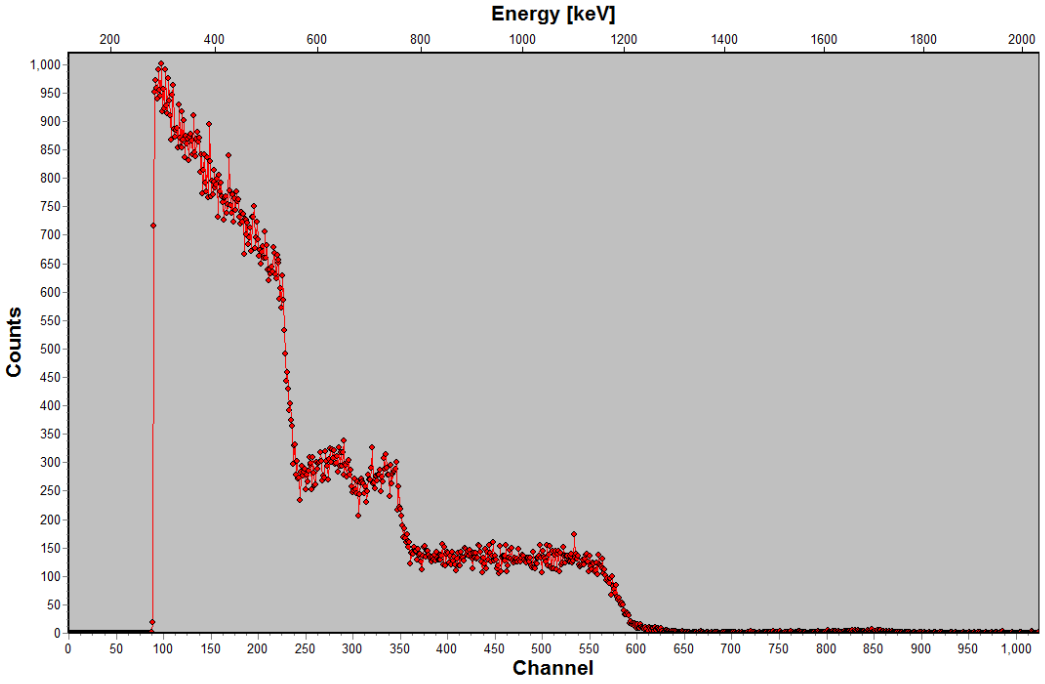

0342

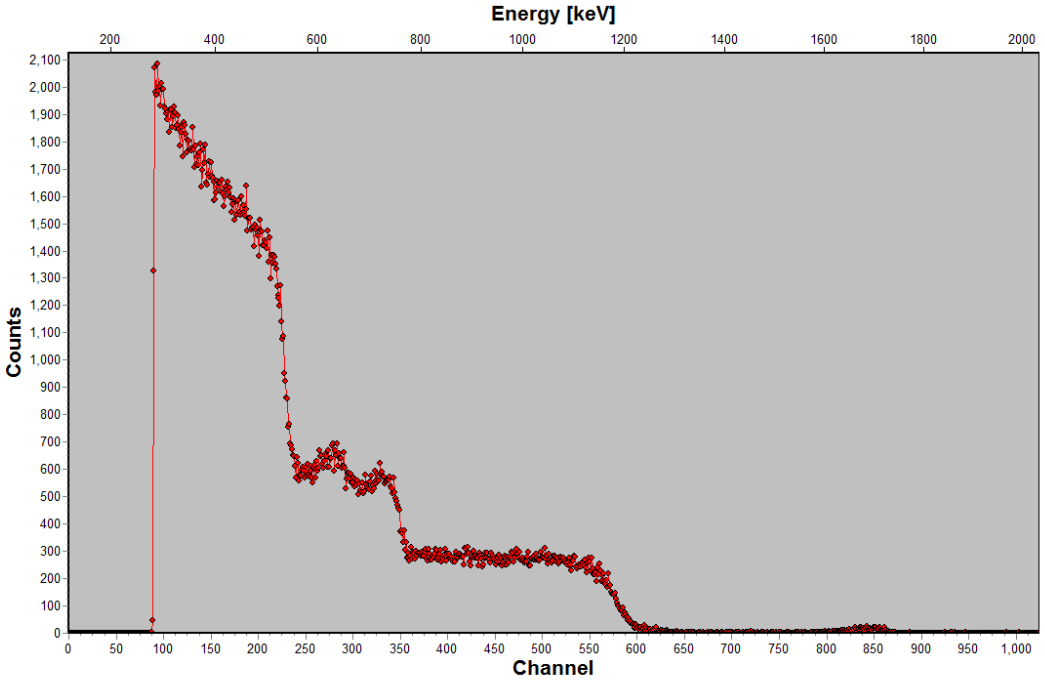

0343

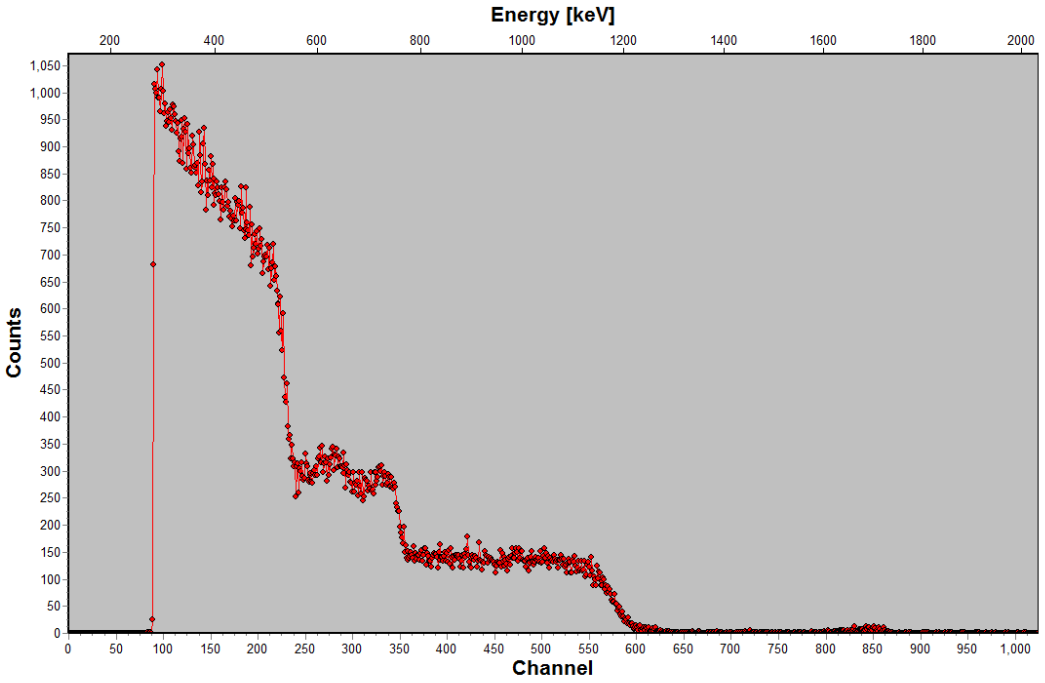

0344

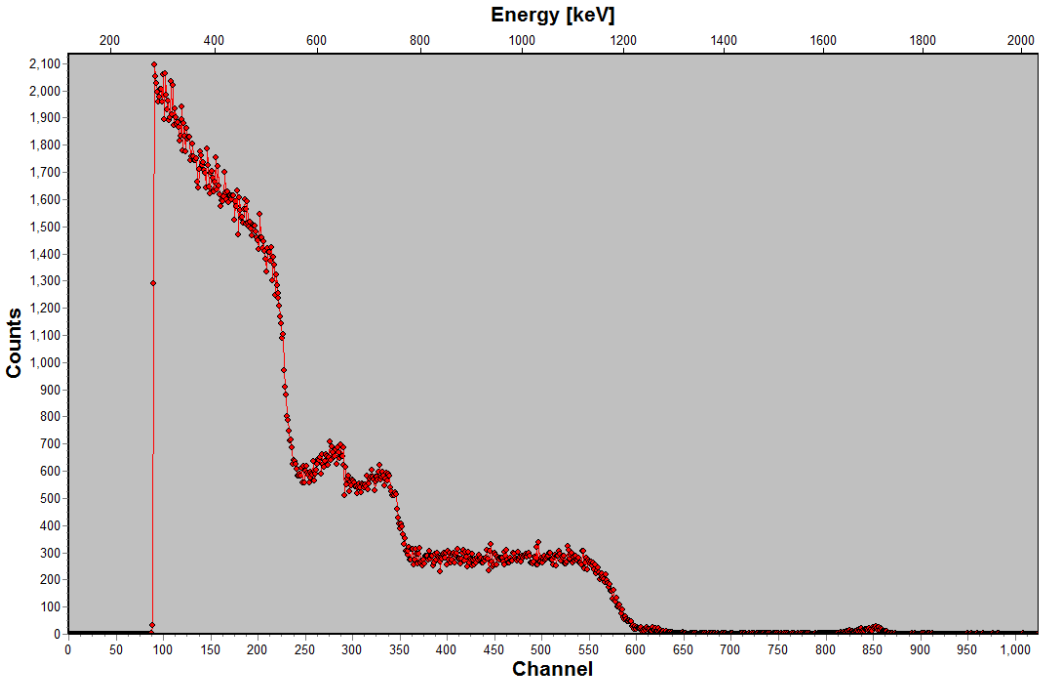

0345

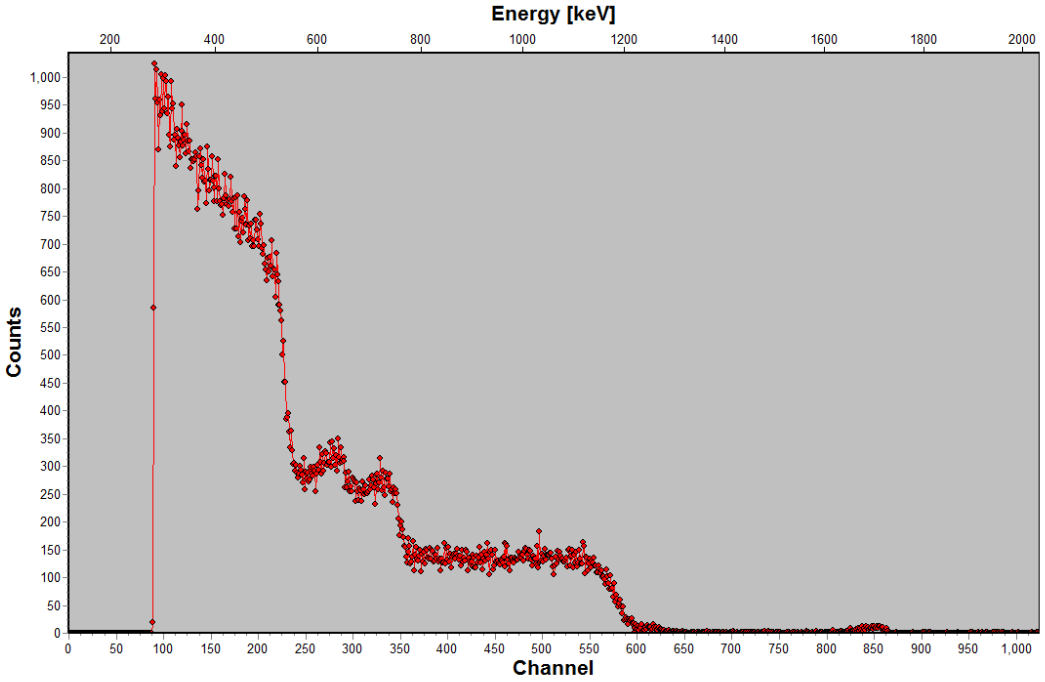

0346

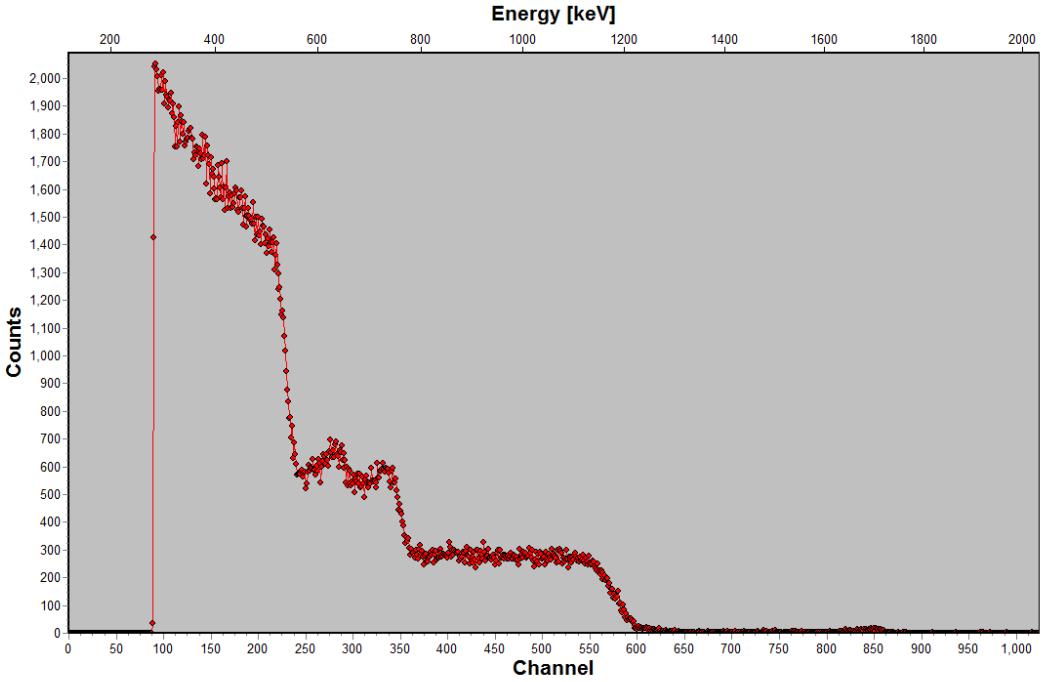

0347

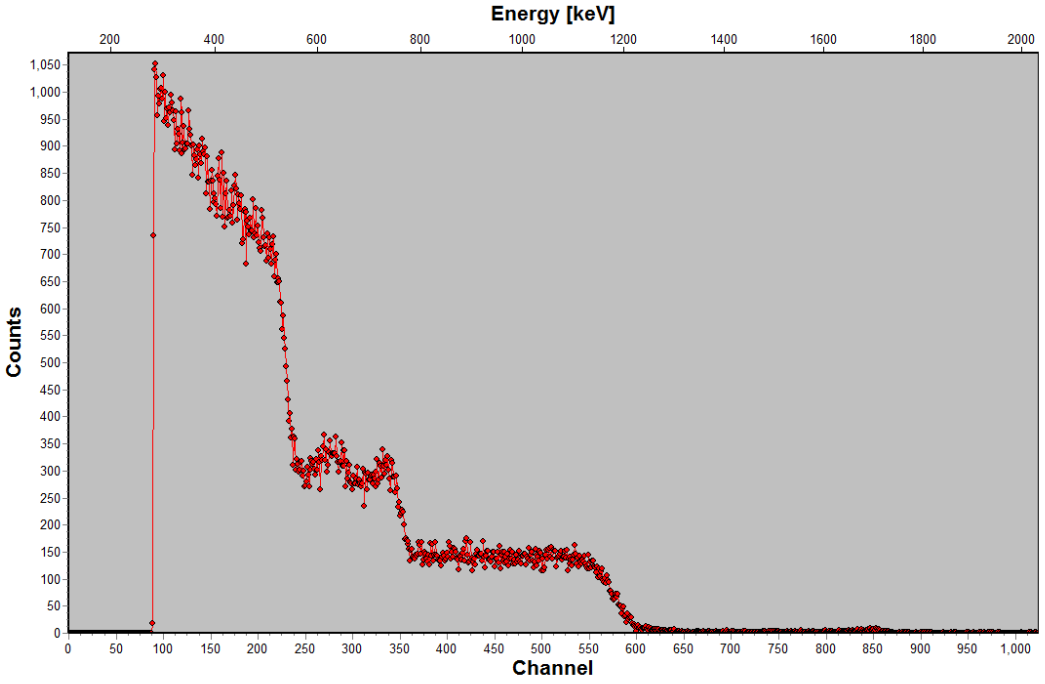

0348

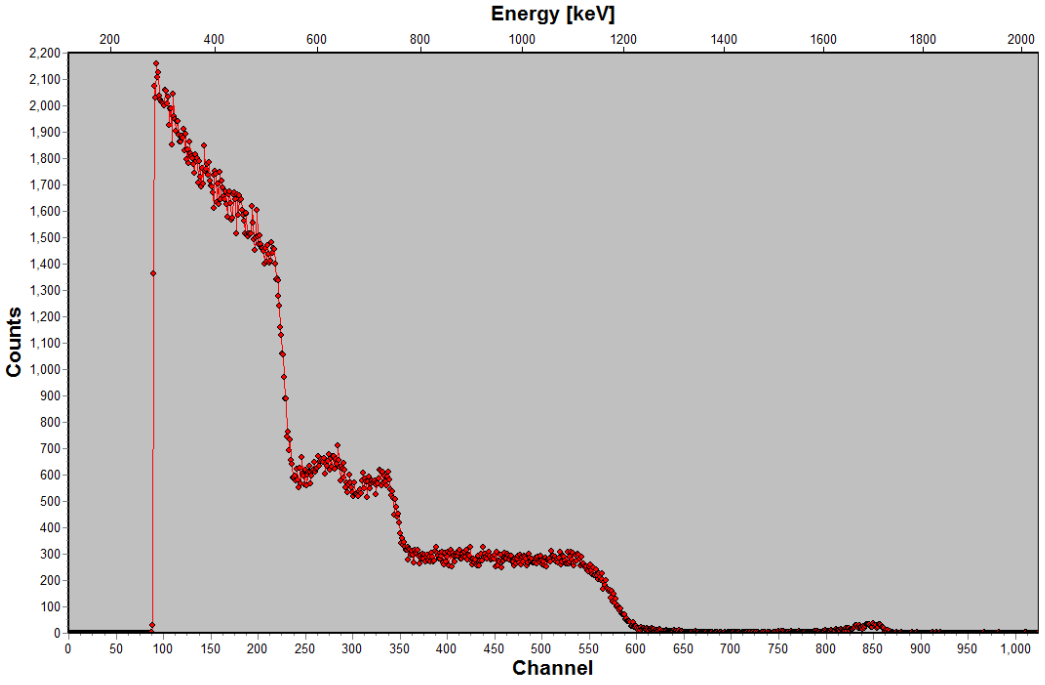

0349

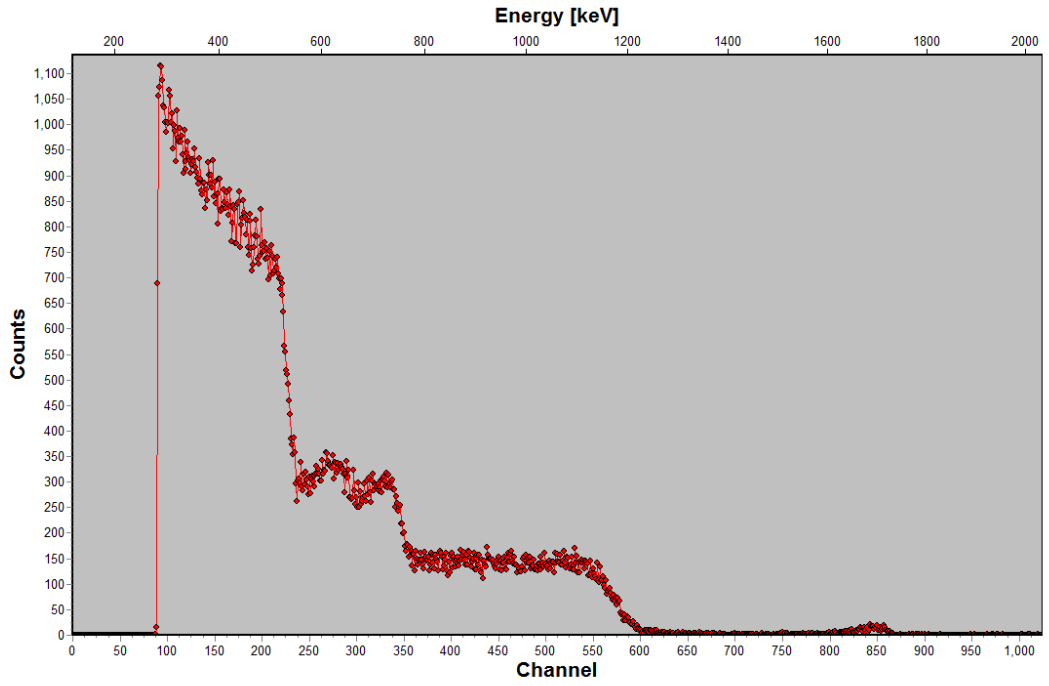

Figure 17:

0334

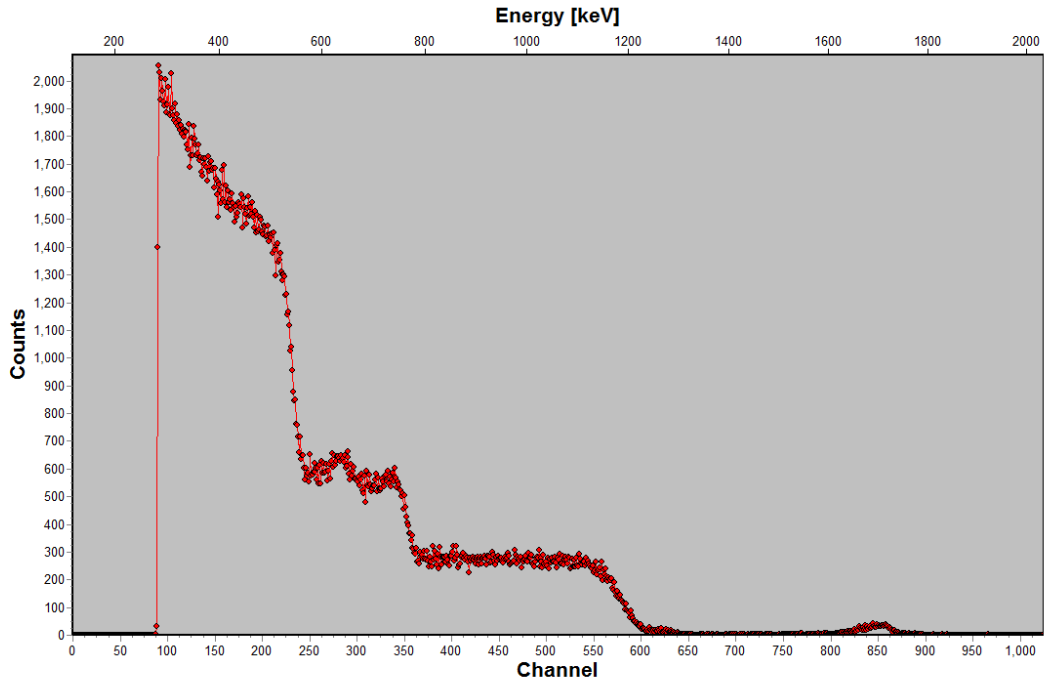

0335

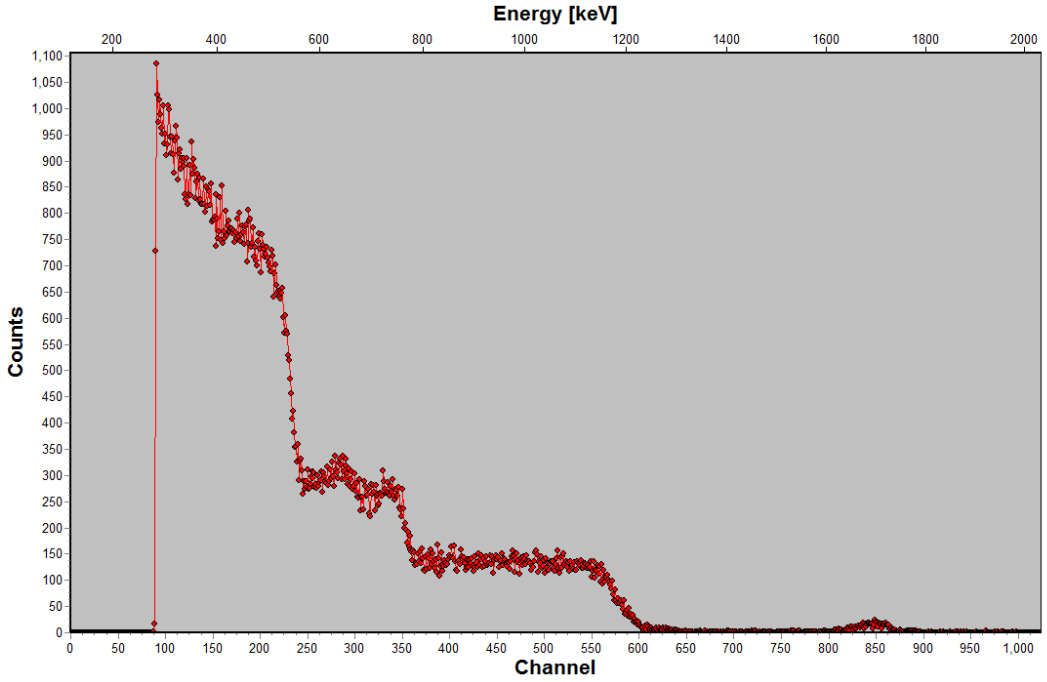

0330

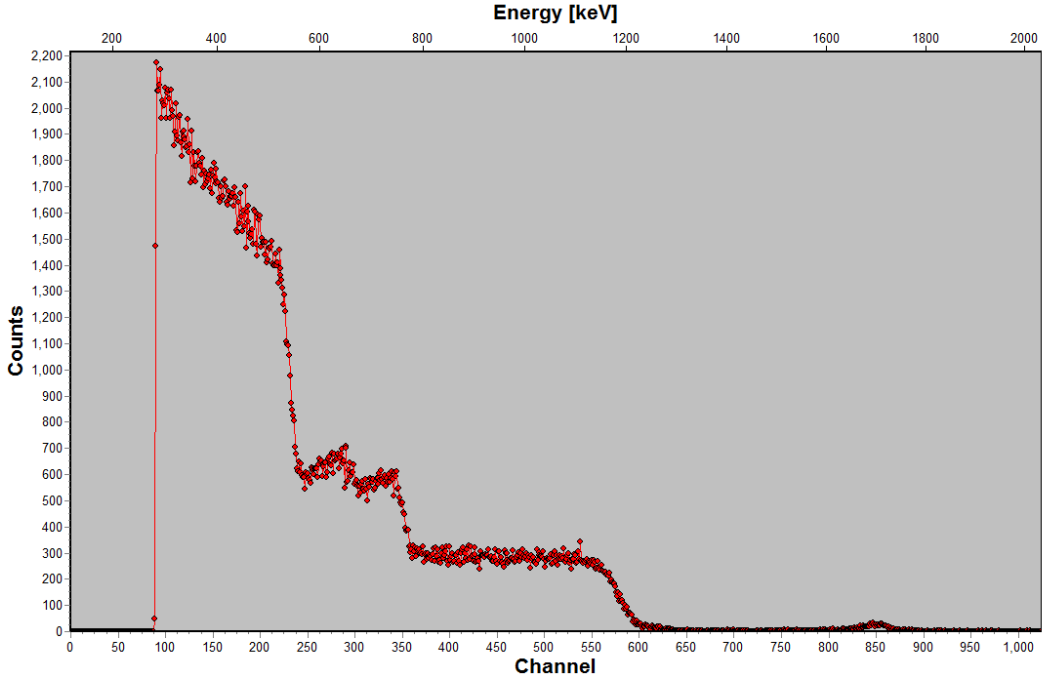

0331

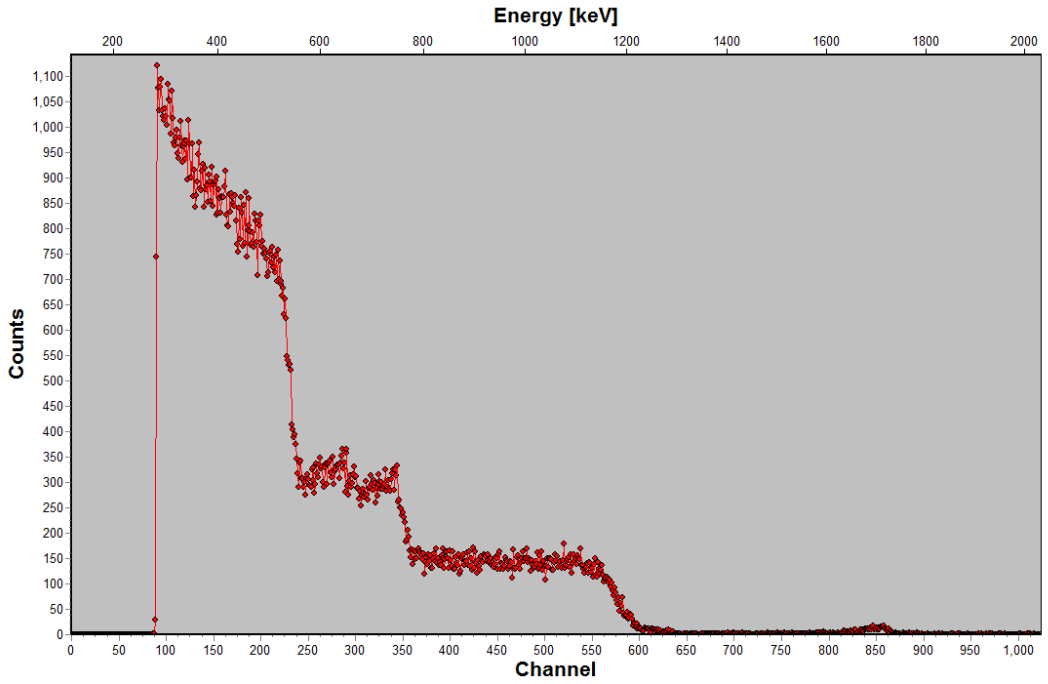

Figure 18:

0383

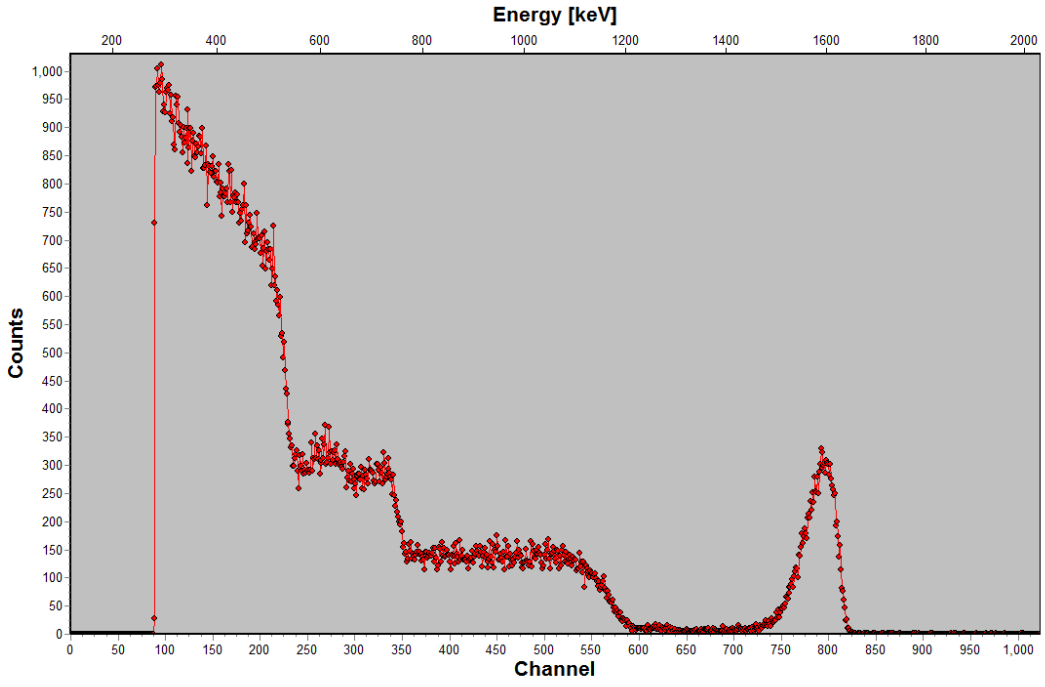

0397

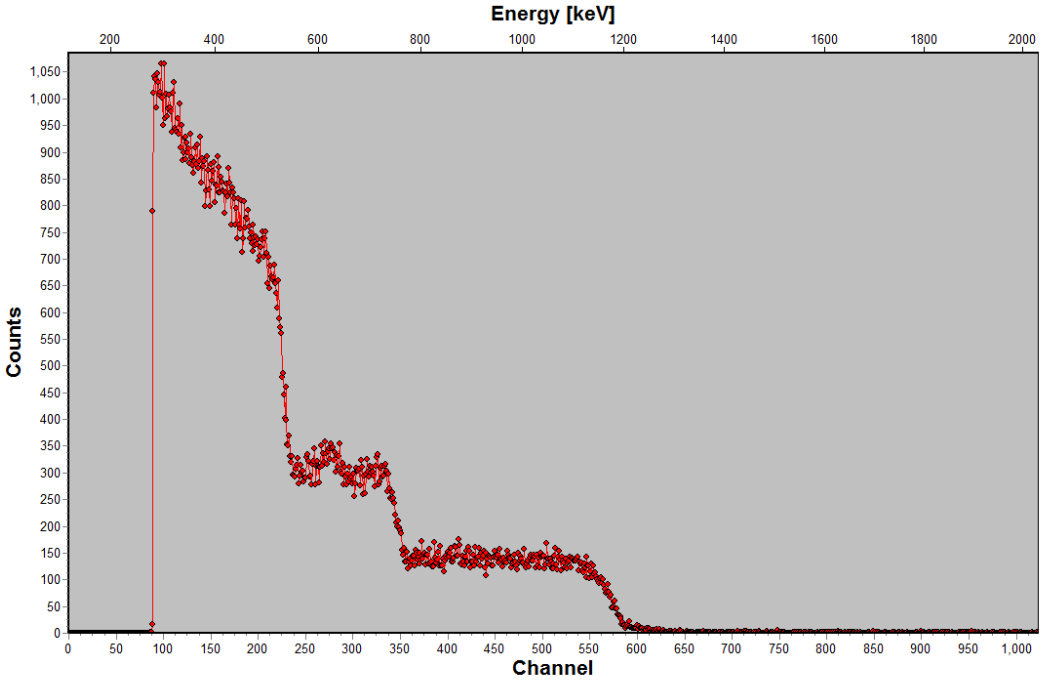

Figure 19:

0350

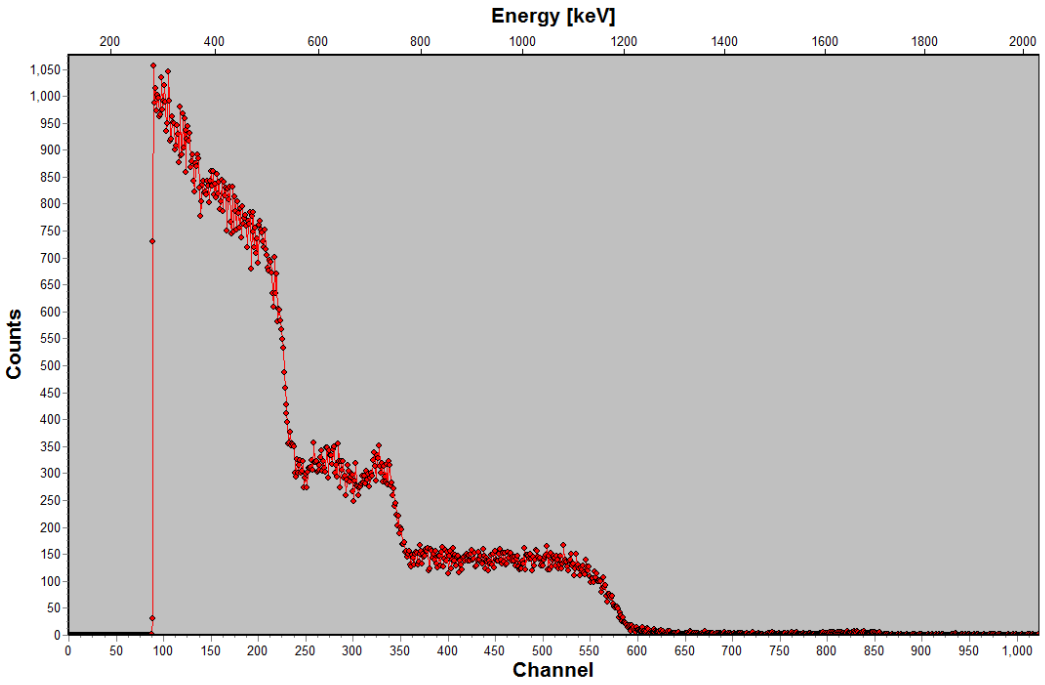

0351

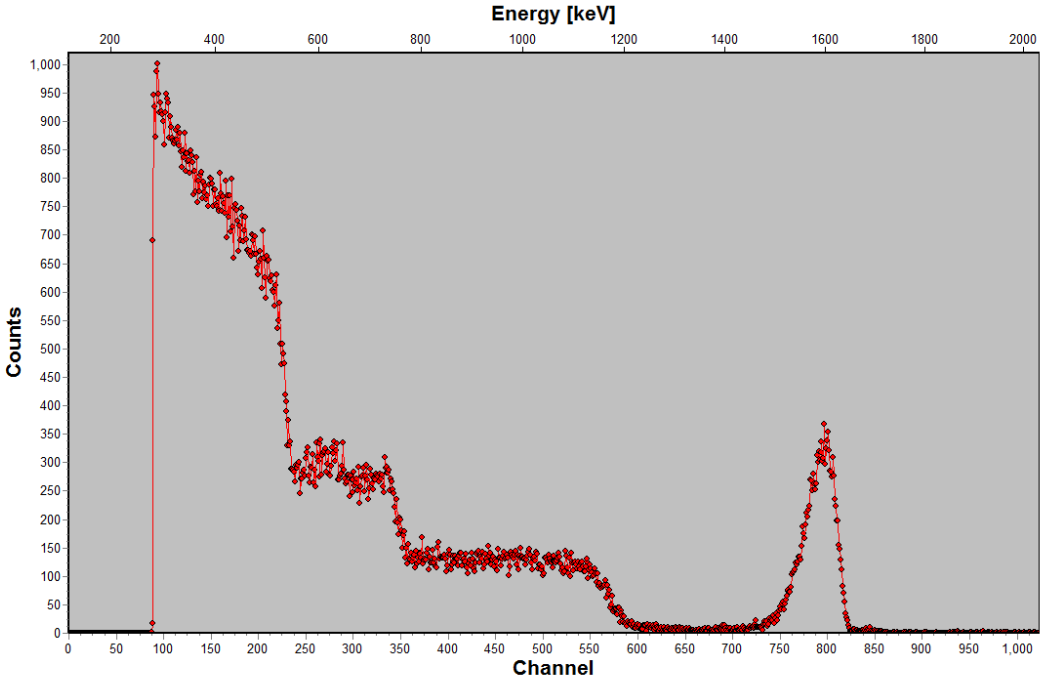

355

0355

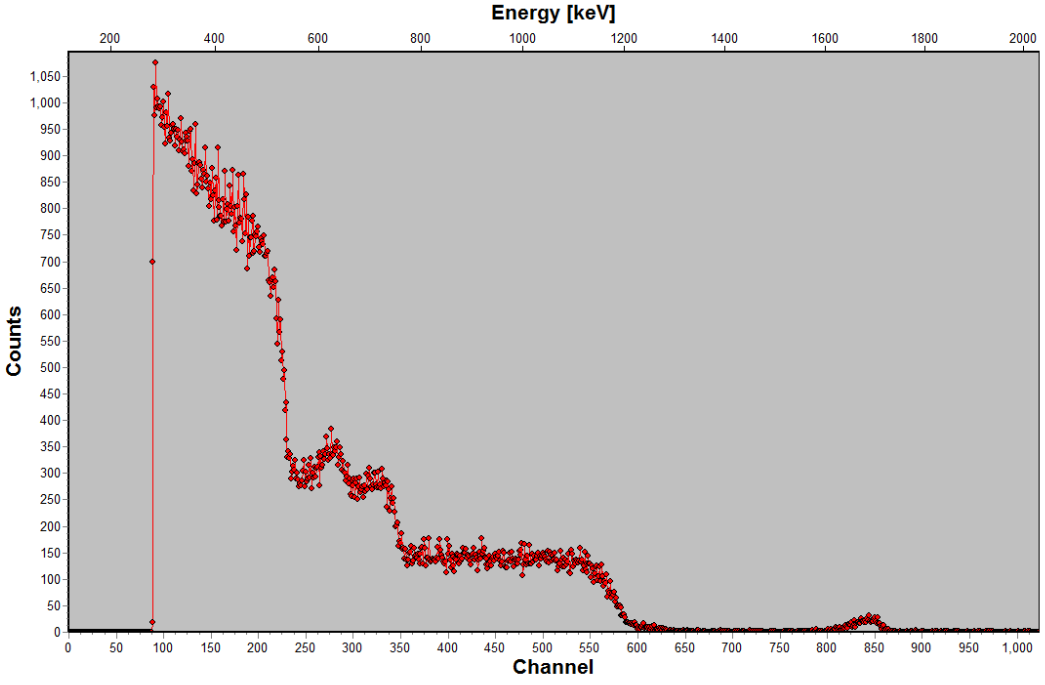

0356

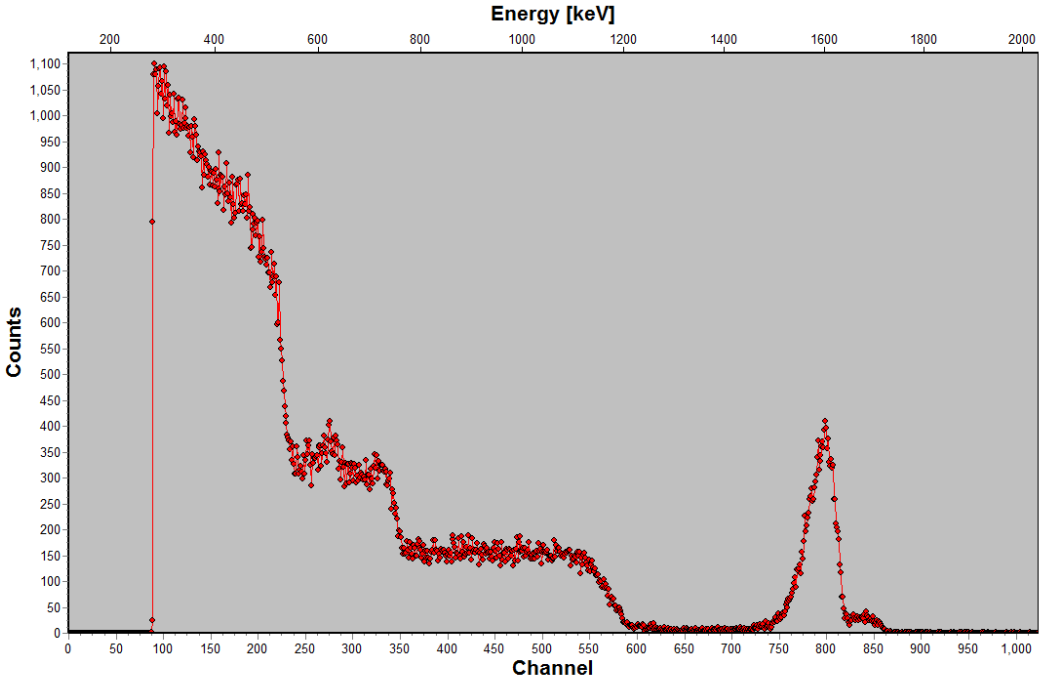

0362

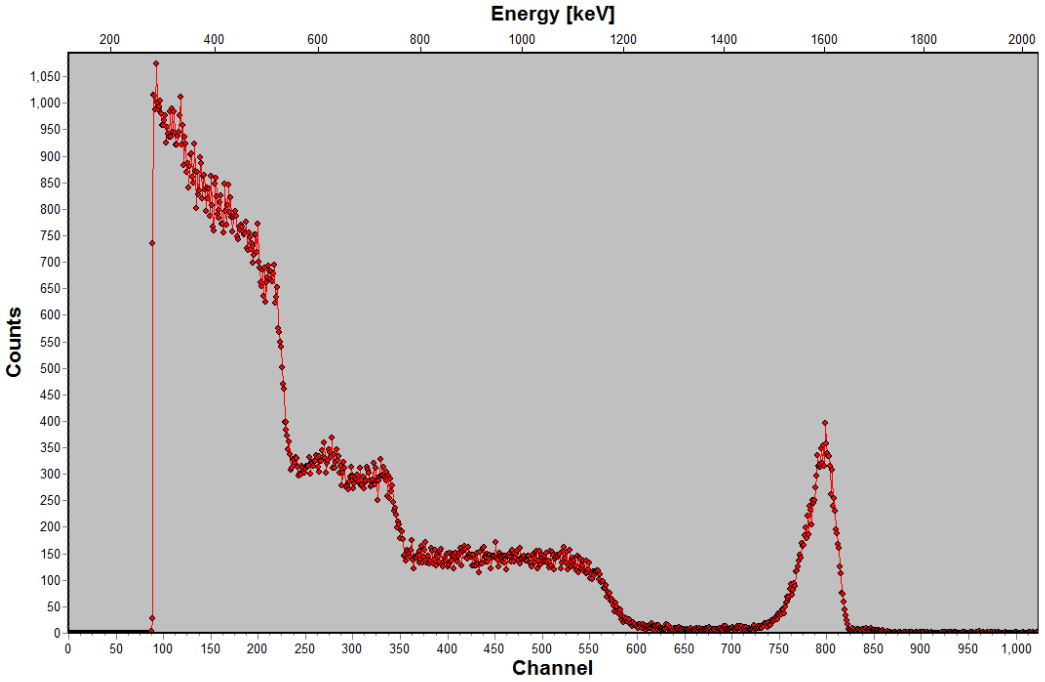

0363

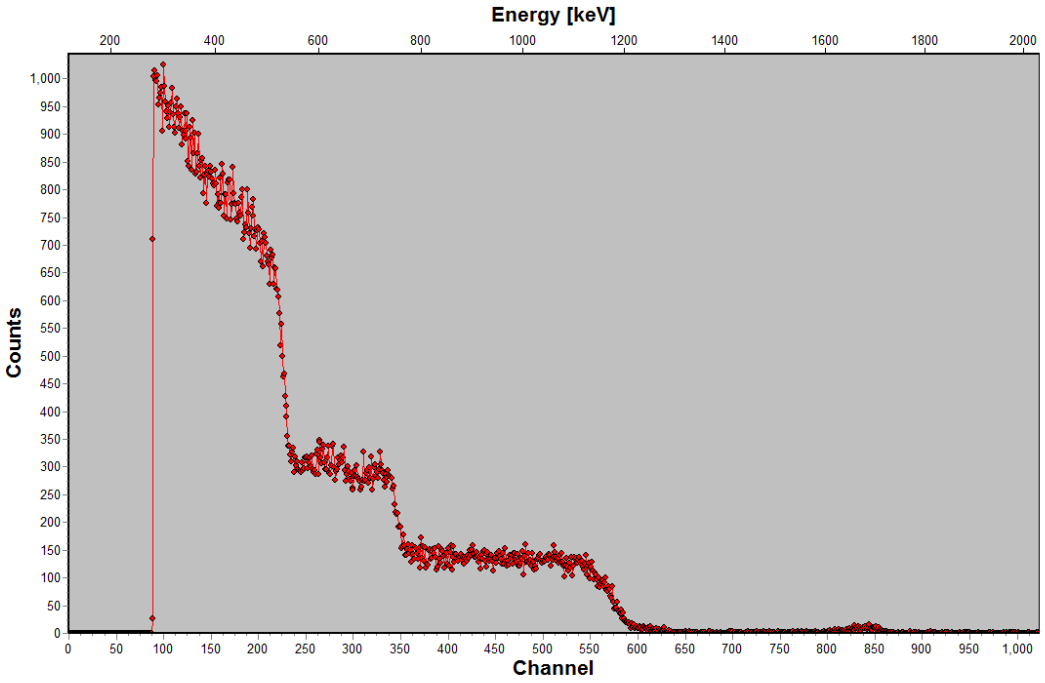

0374

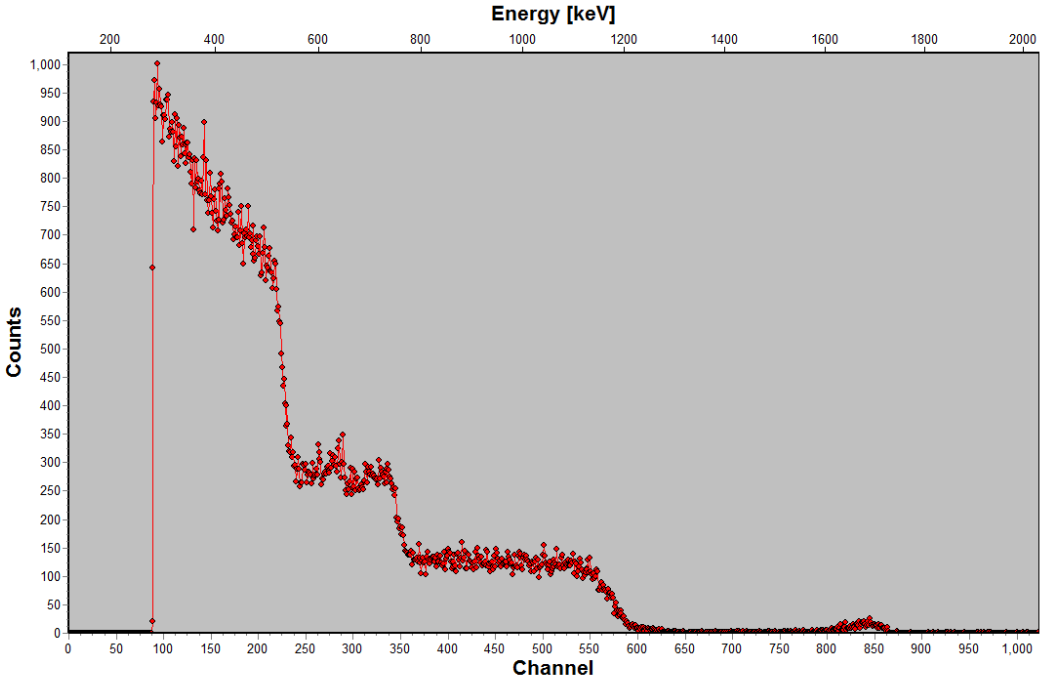

0375

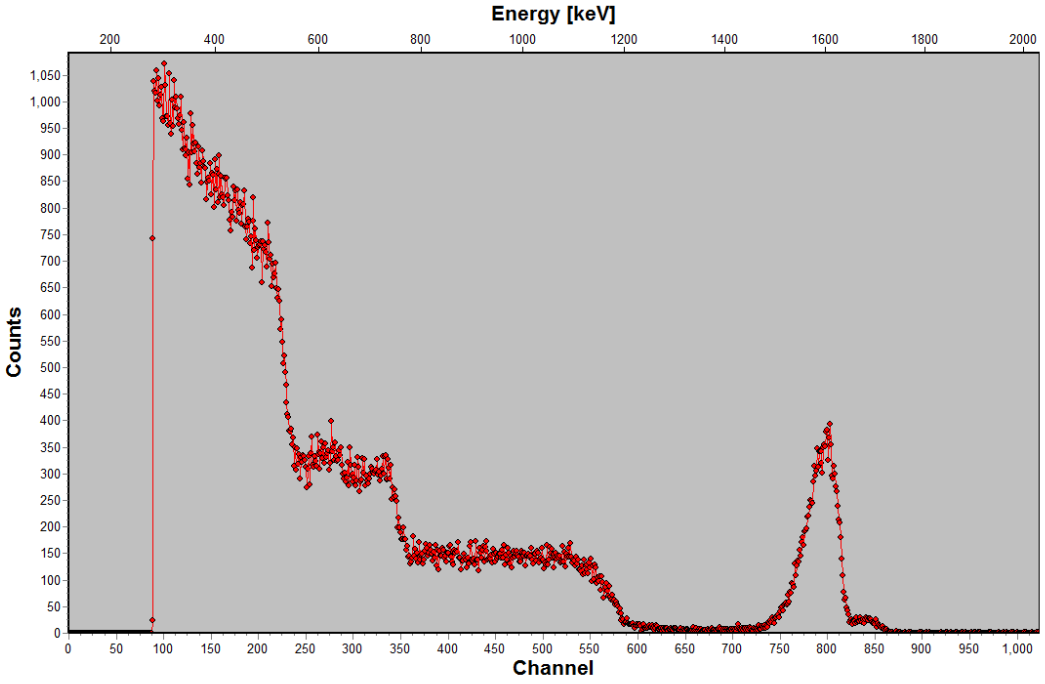

0390

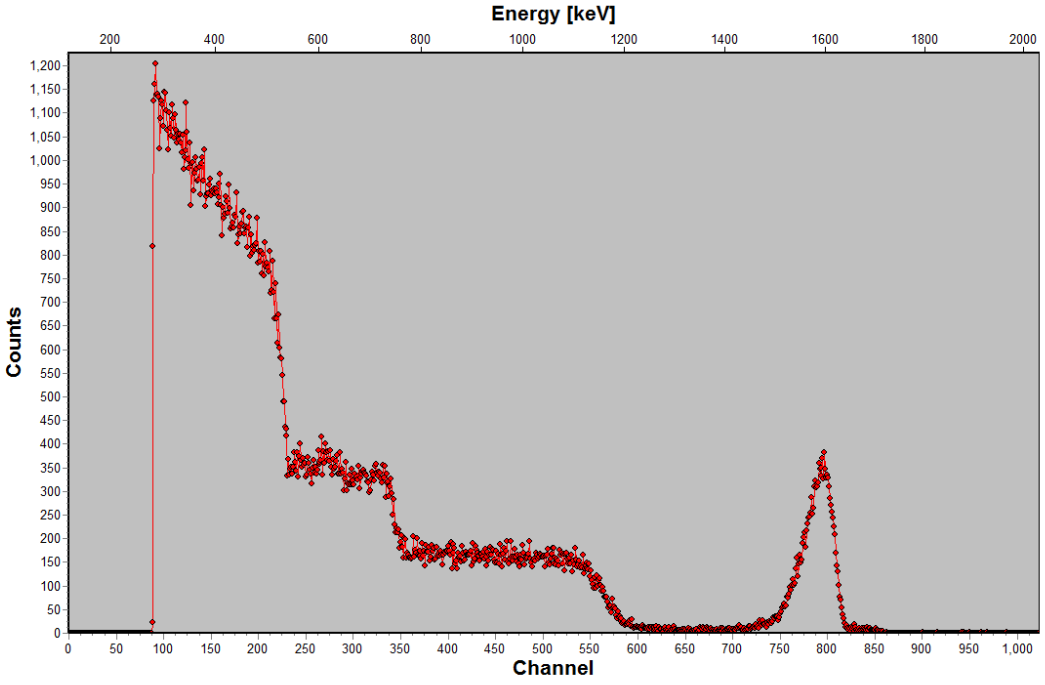

0391

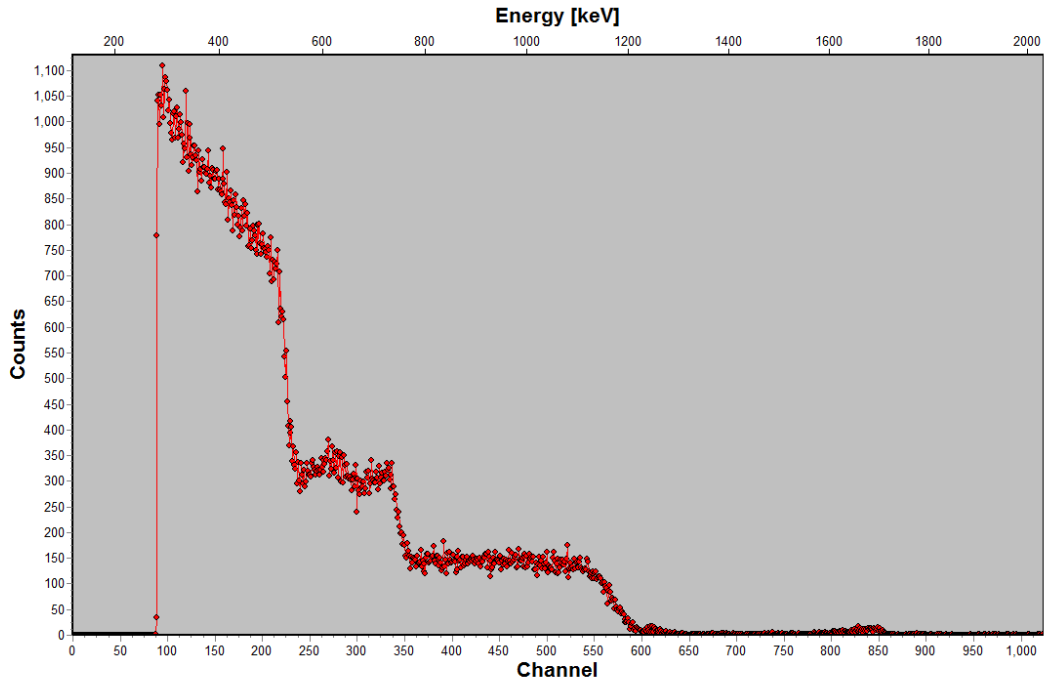

Figure 20:

0382

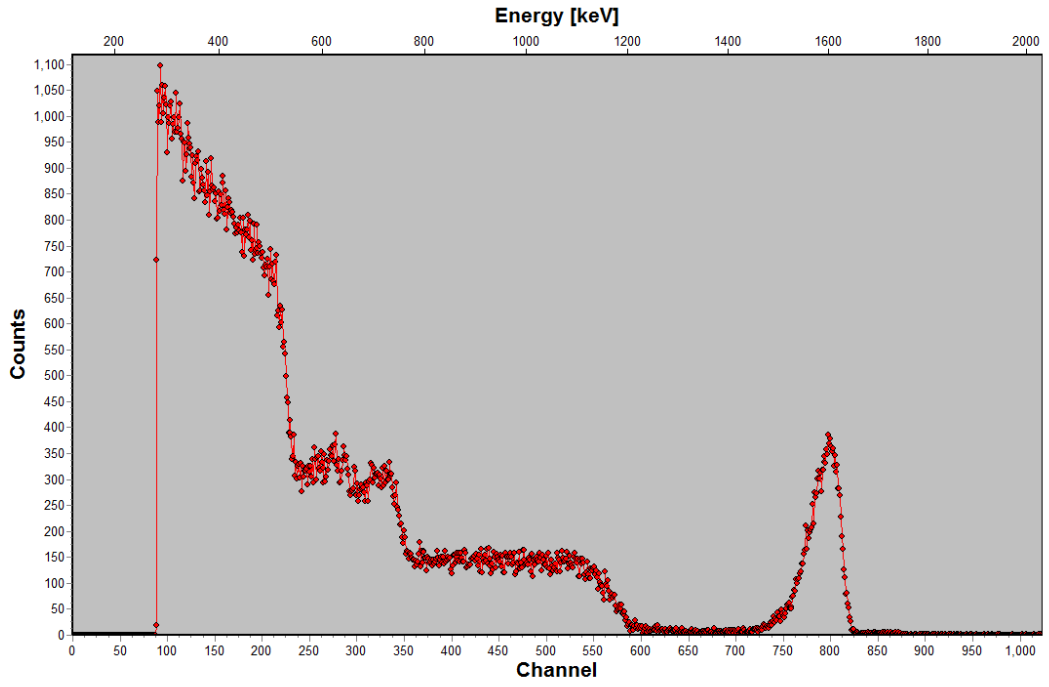

0396

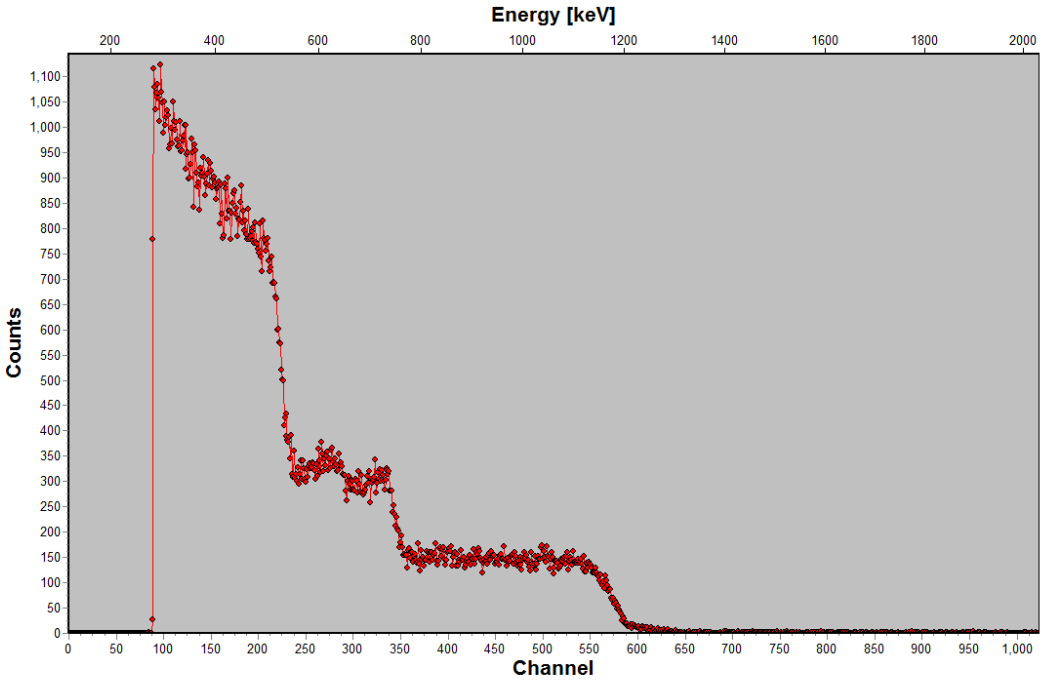

Figure 21:

0352

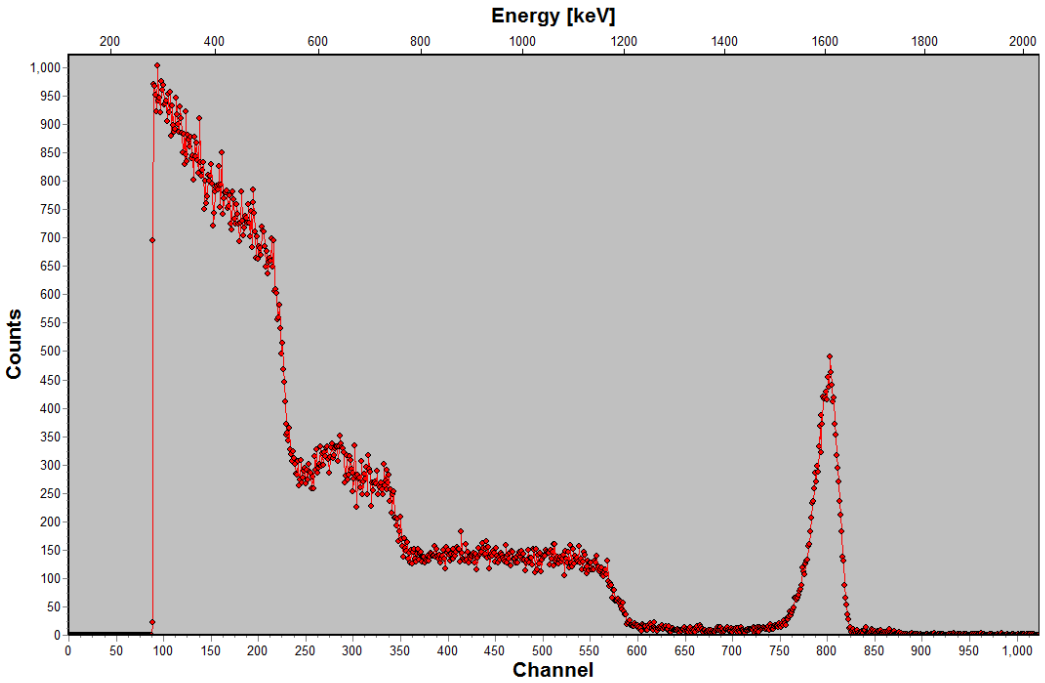

0353

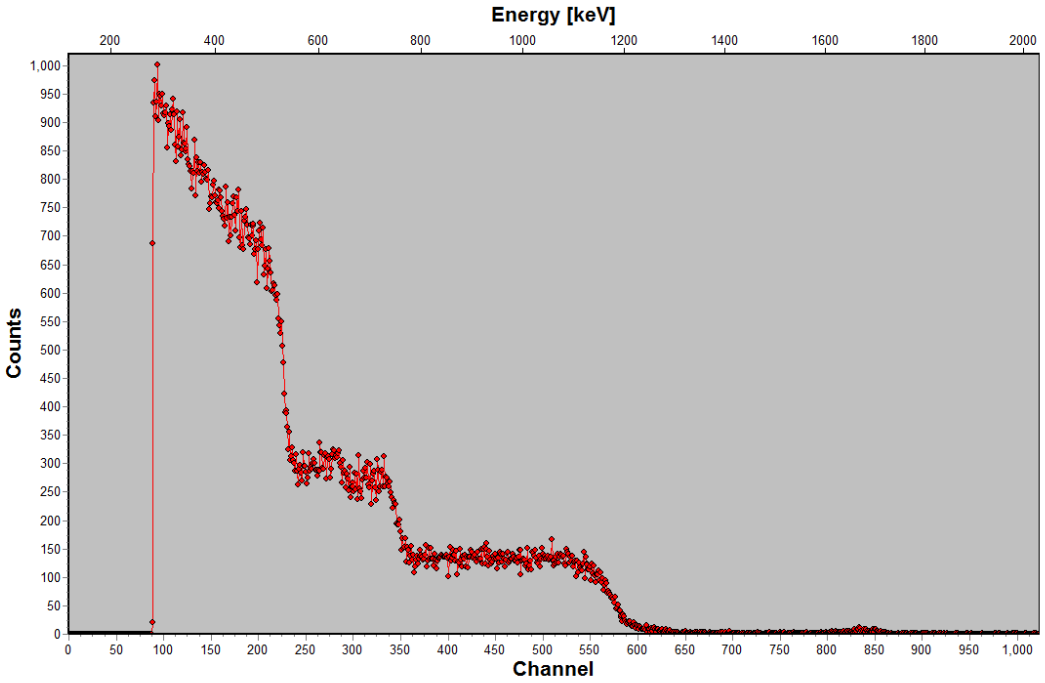

0357

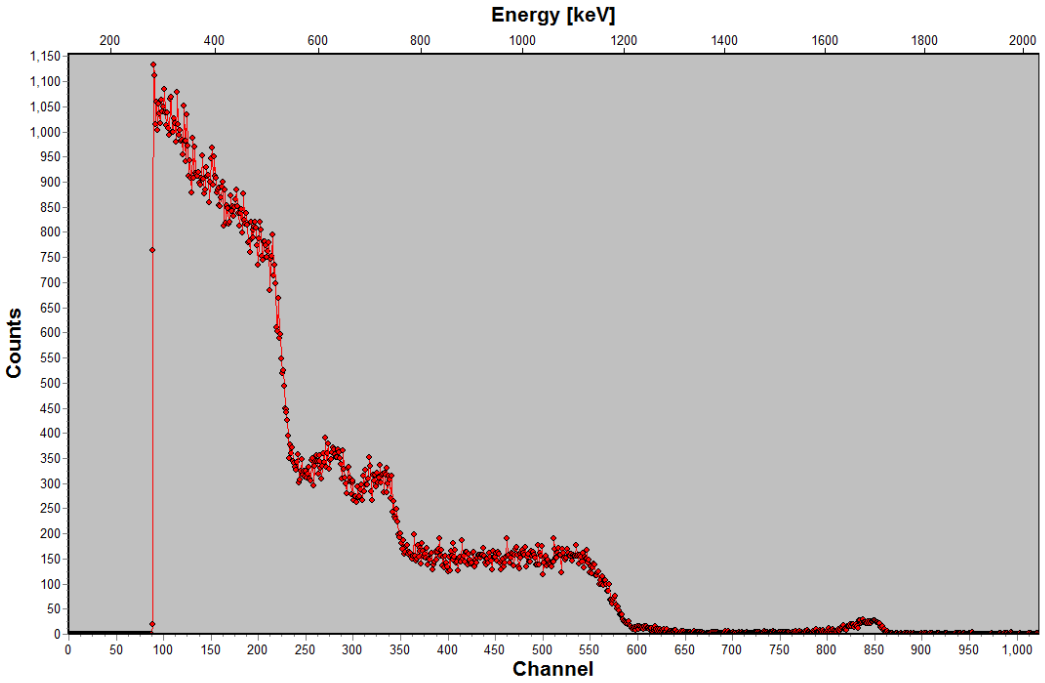

0358

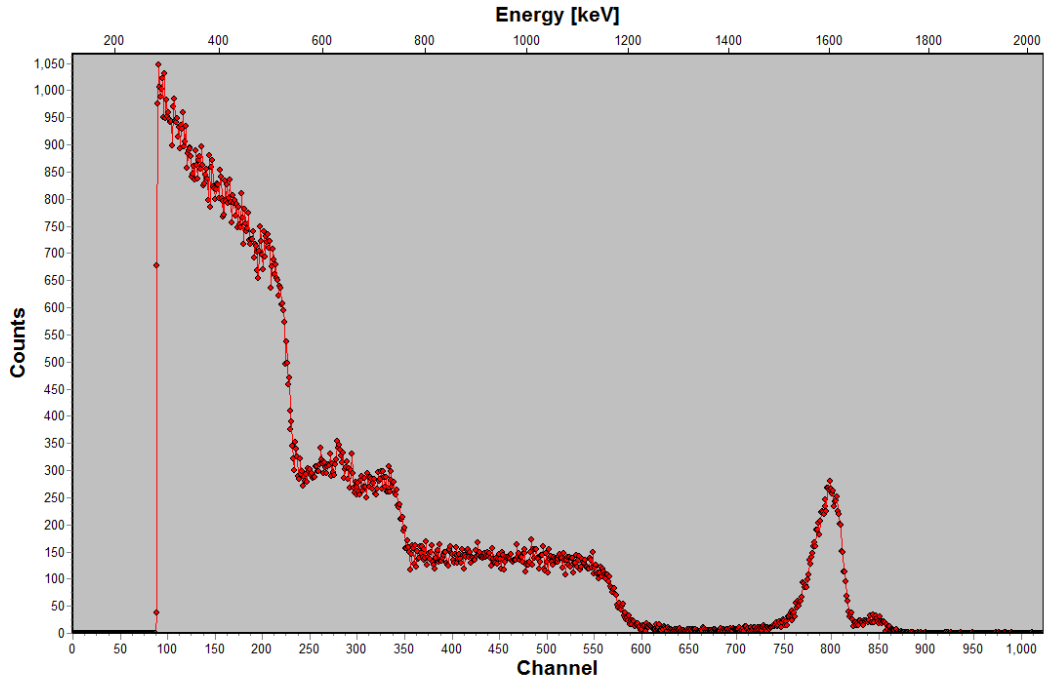

0364

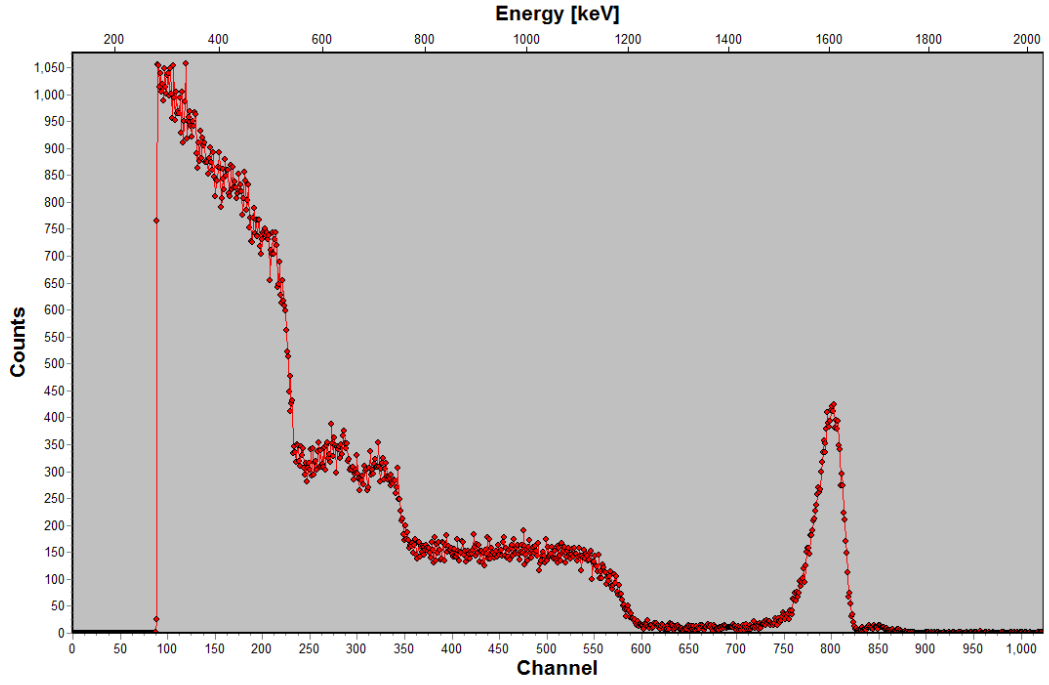

0365

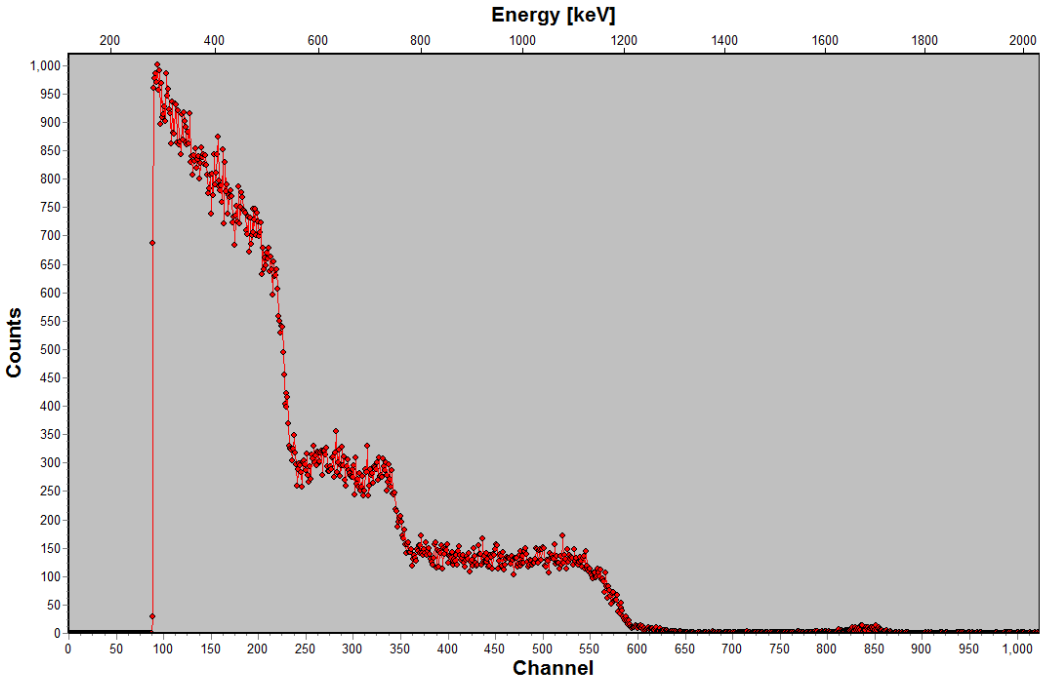

0376

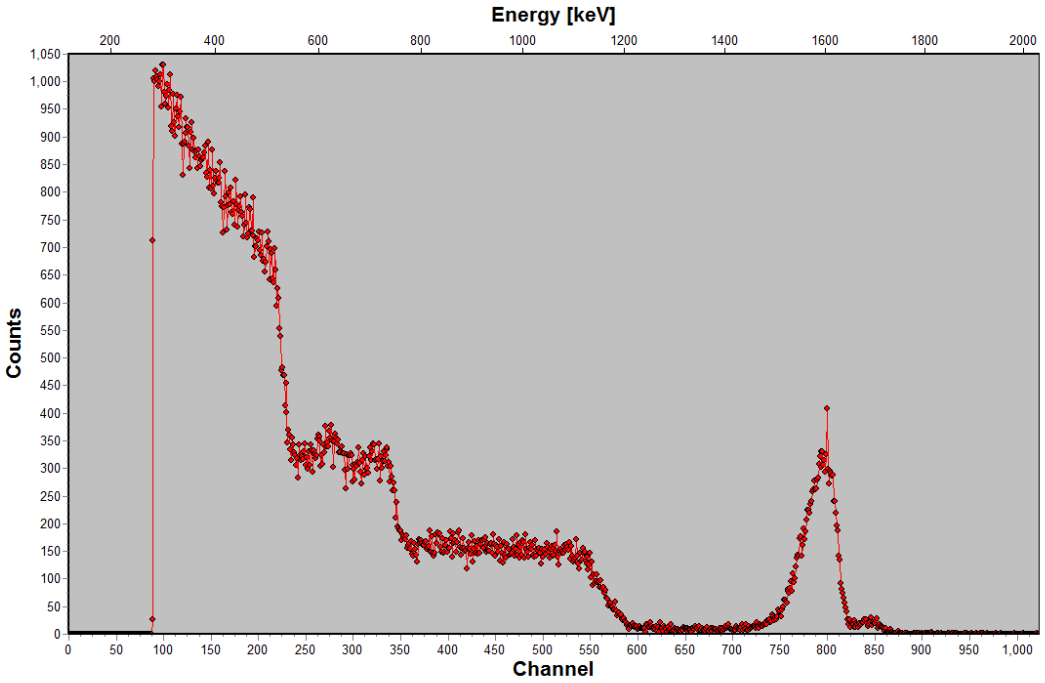

0377

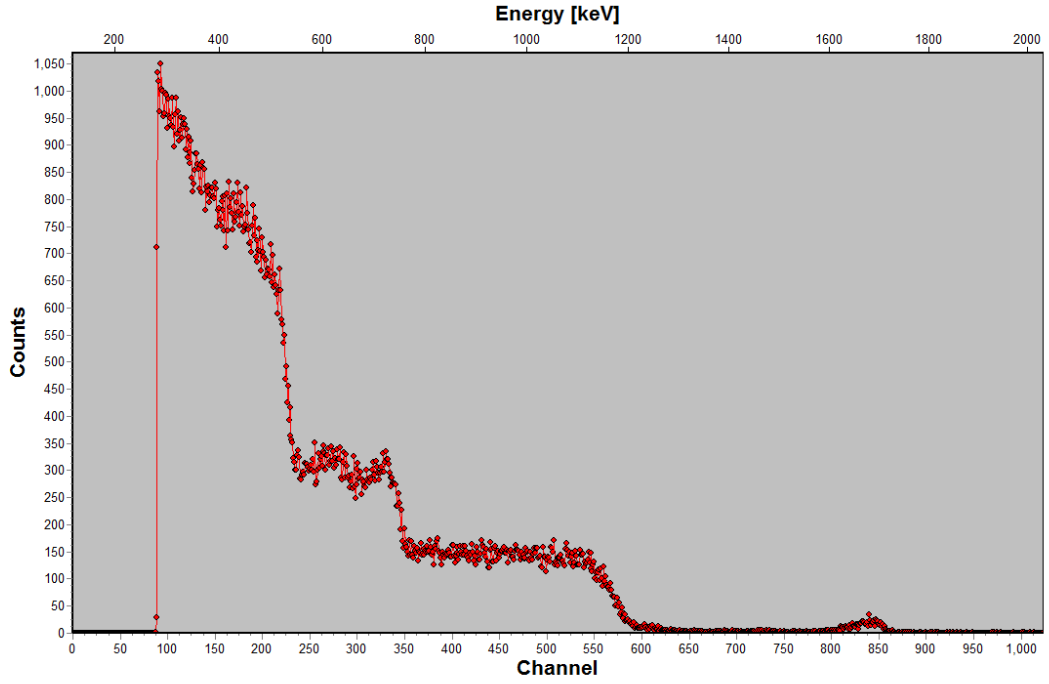

0388

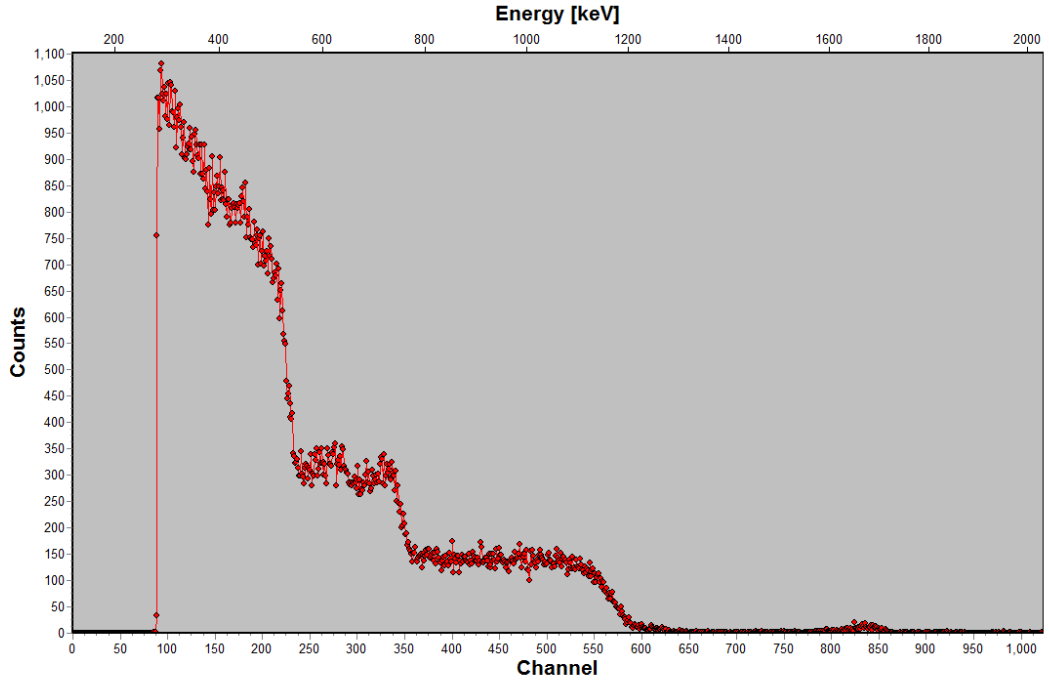

0389

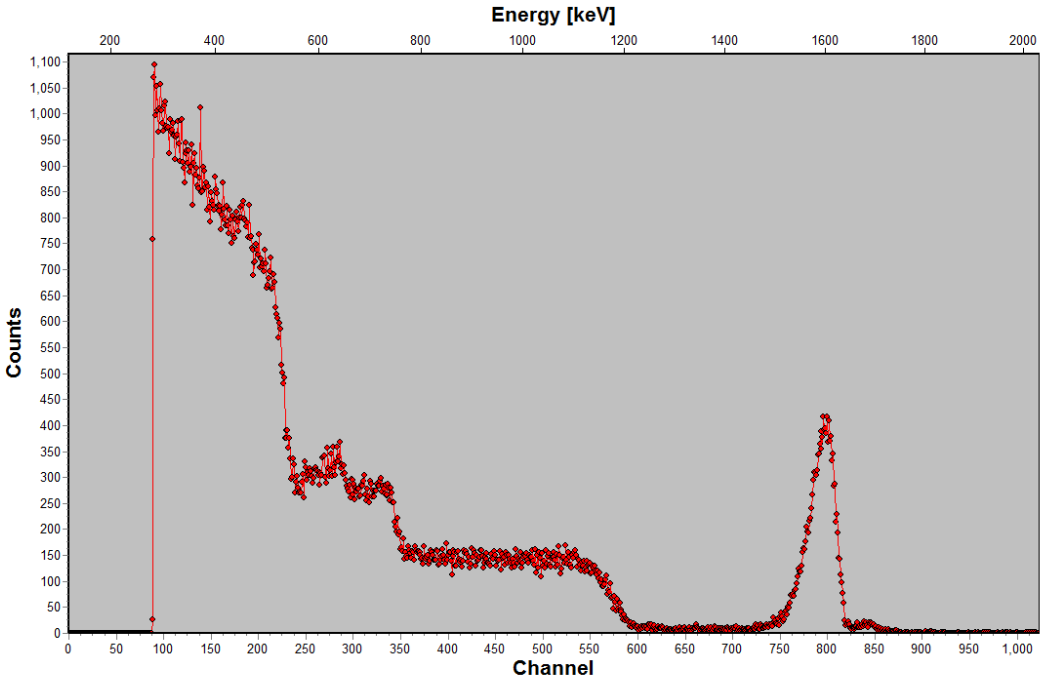

Figure 22:

0361

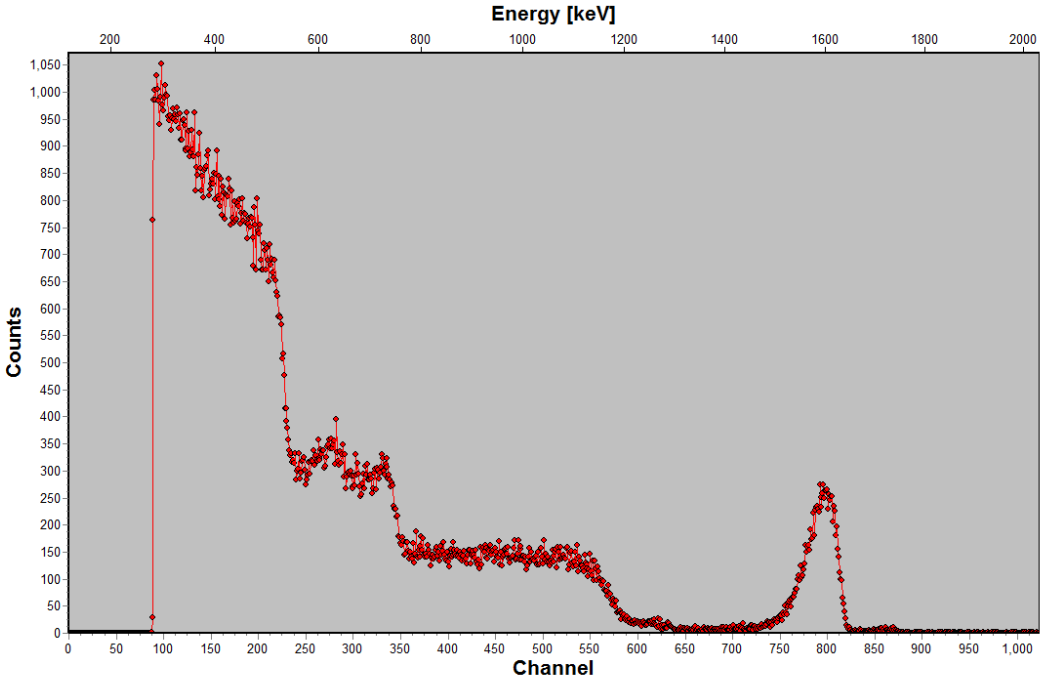

0398

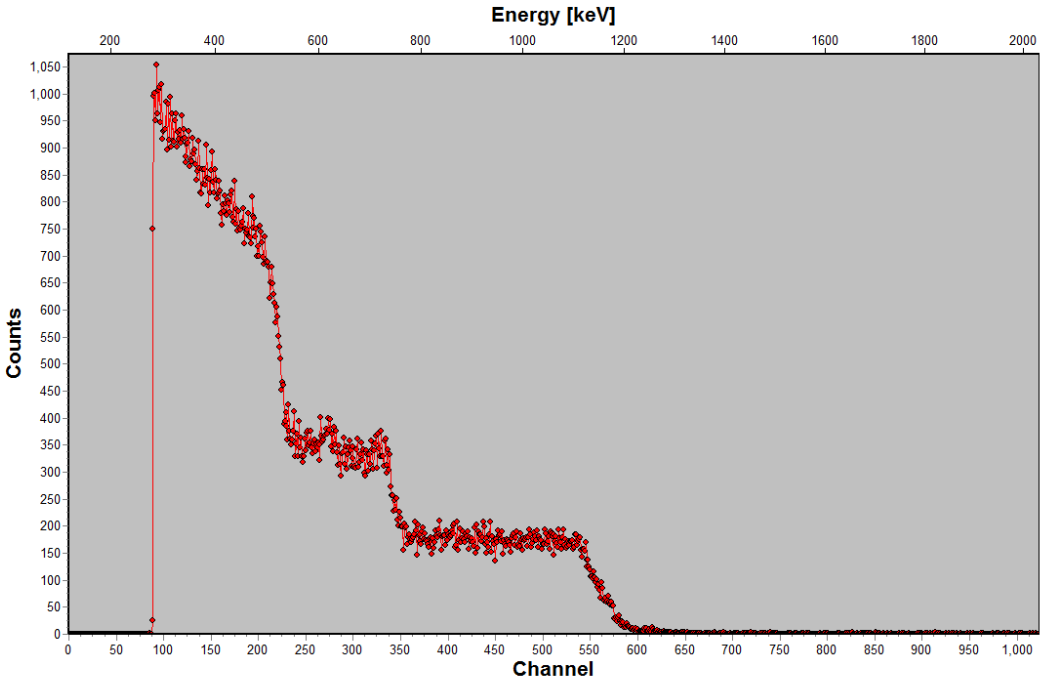

Figure 23:

0359

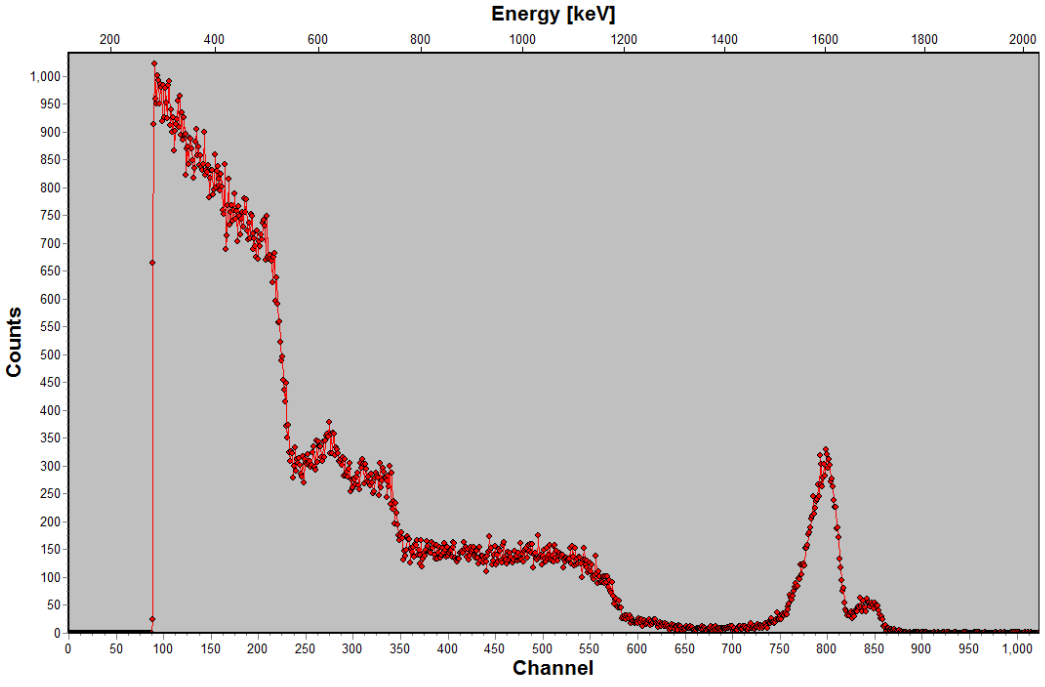

0360

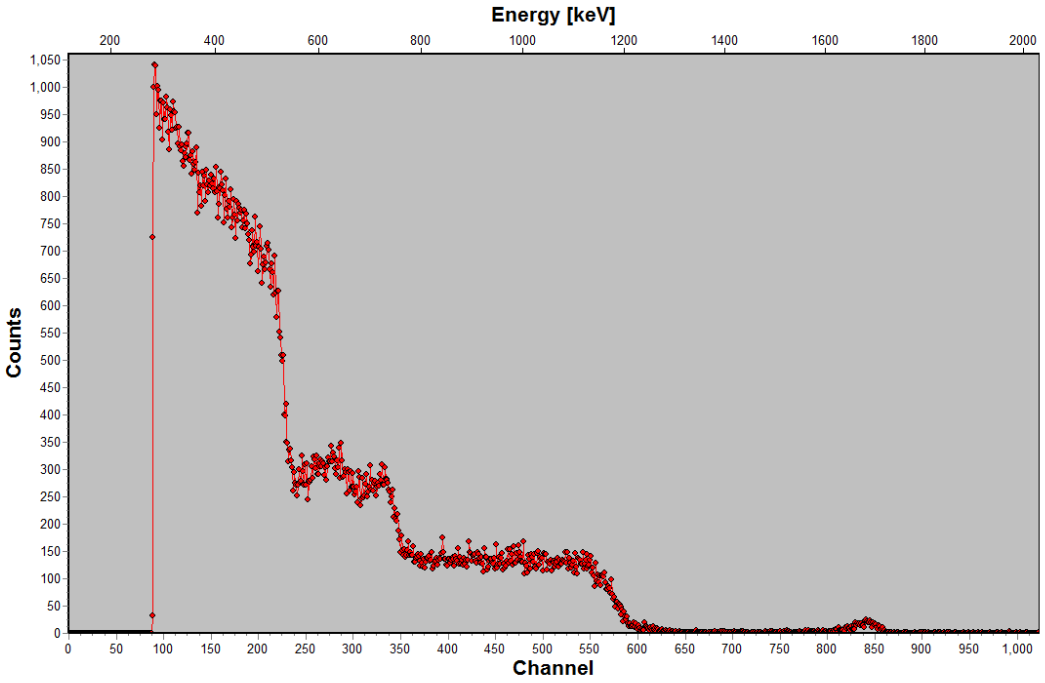

0366

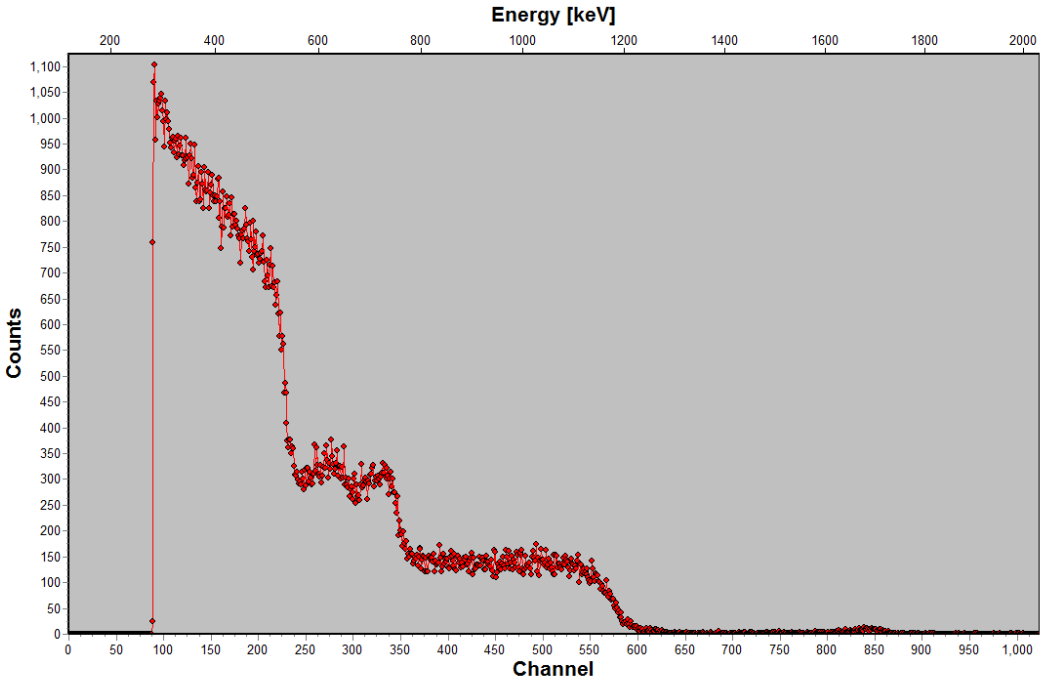

0367

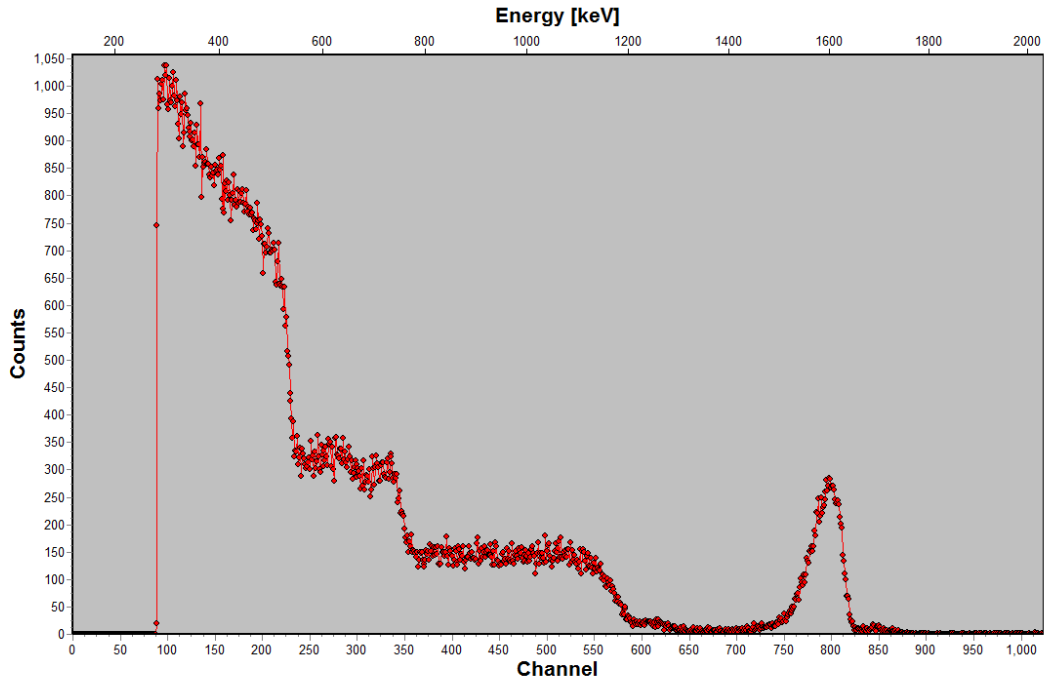

0378

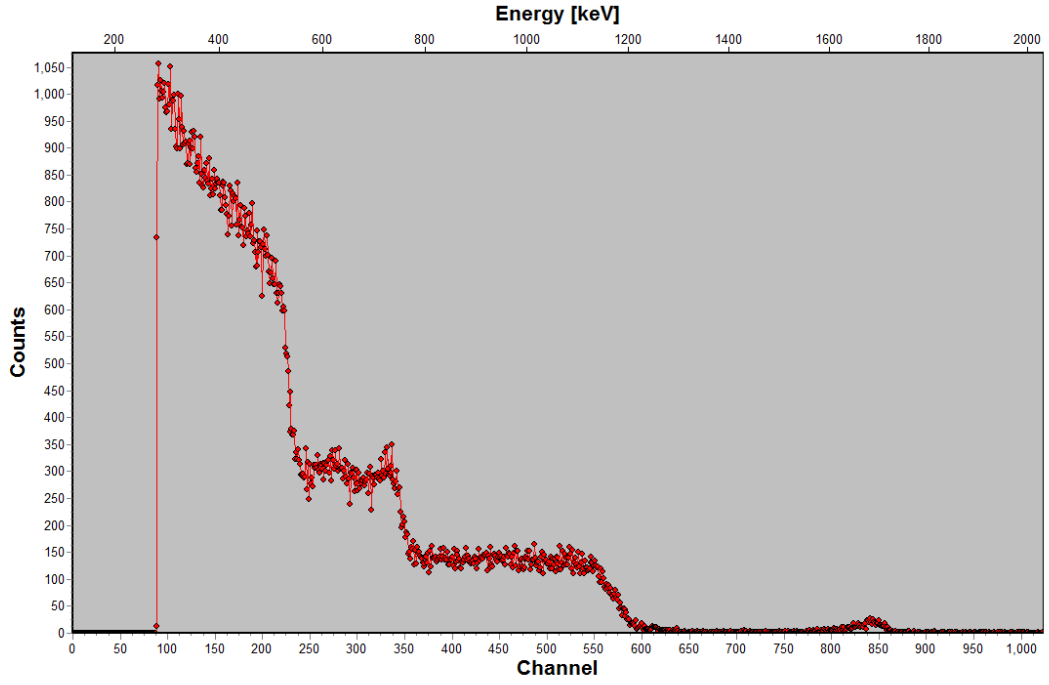

0379

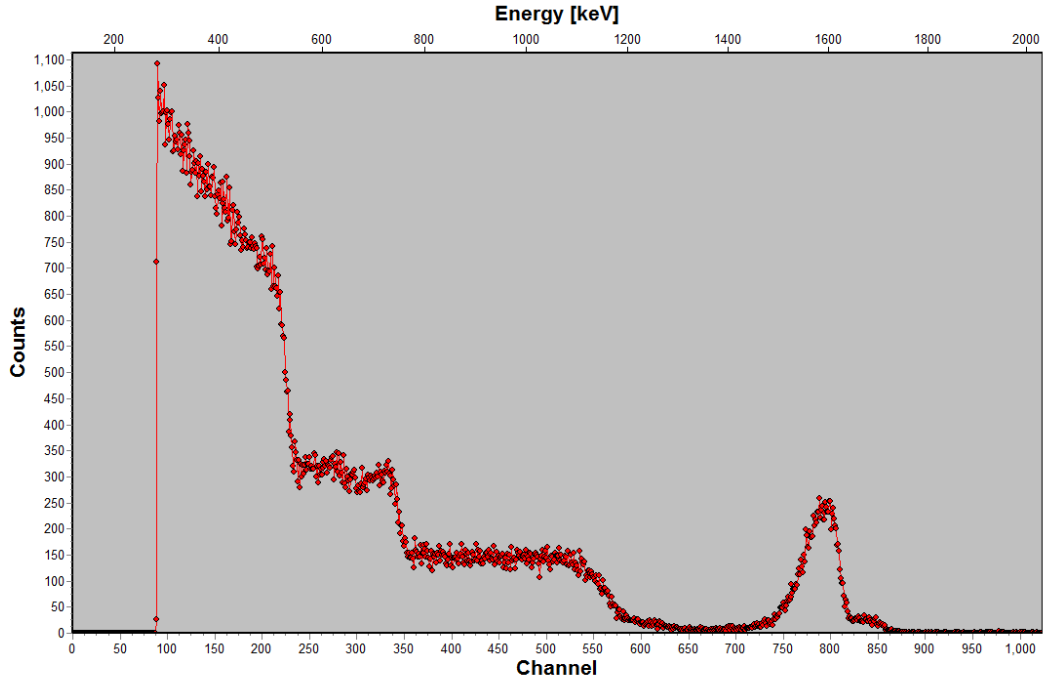

0380

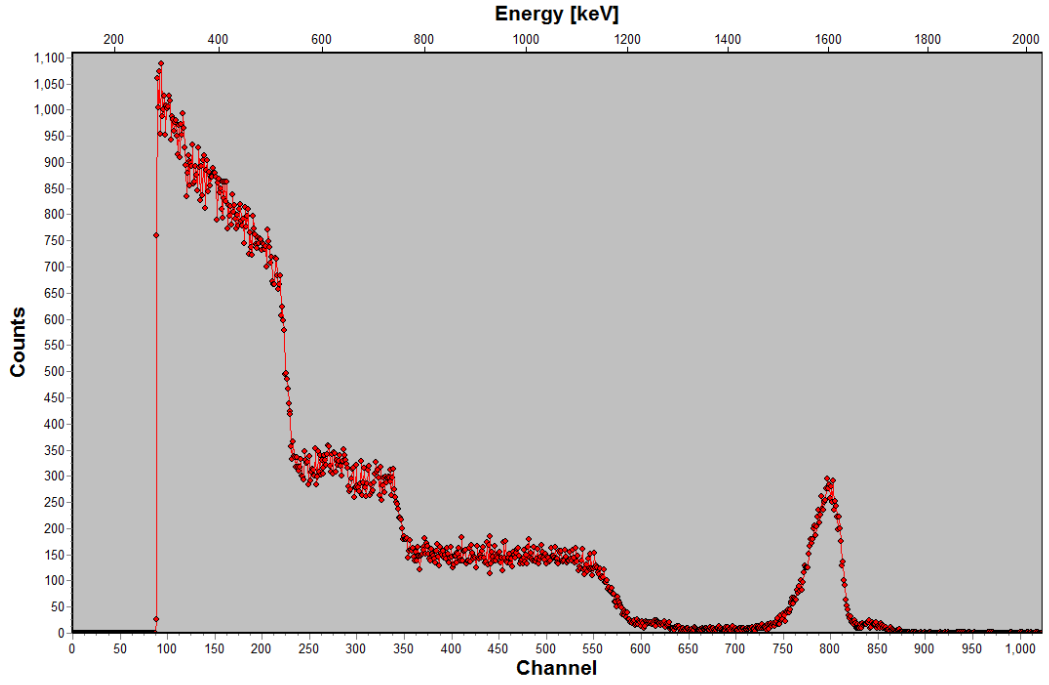

0381

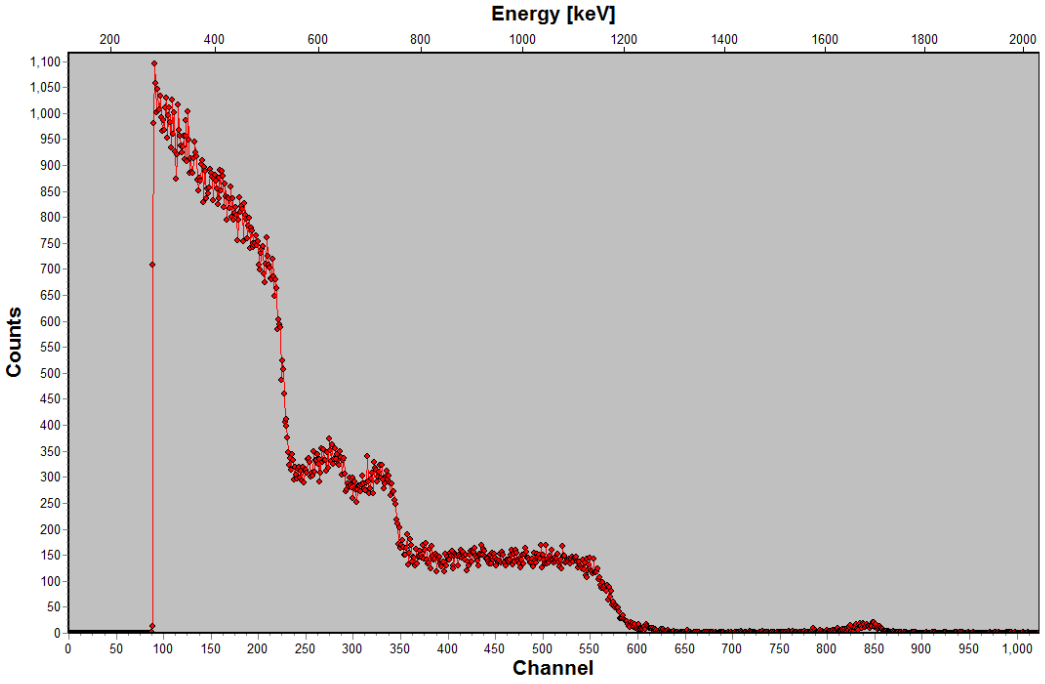

0394

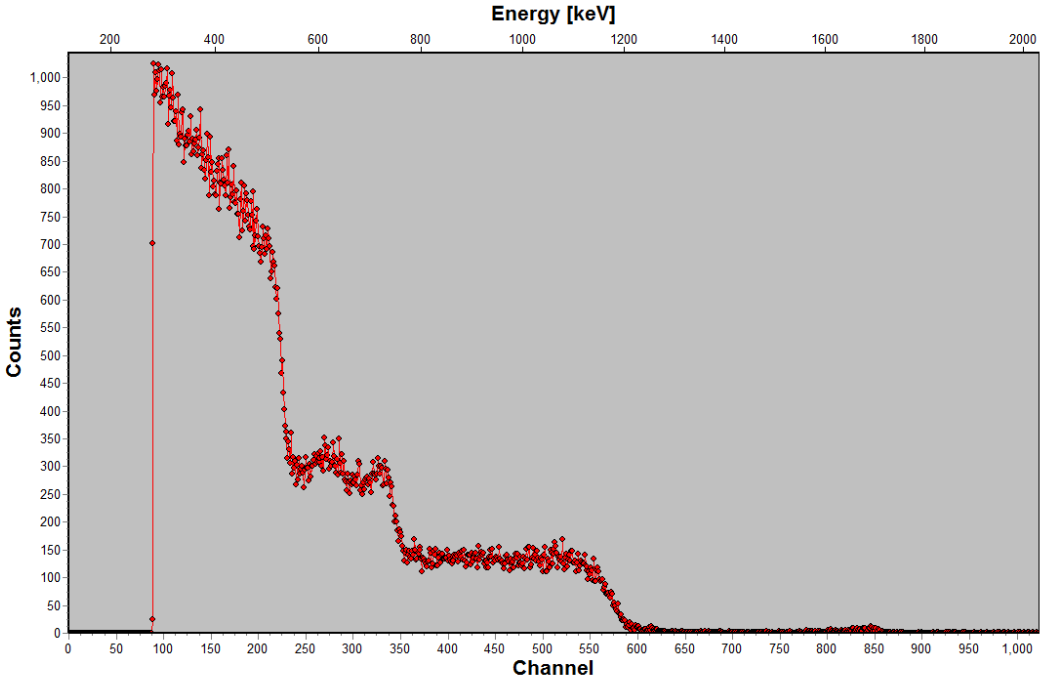

0395

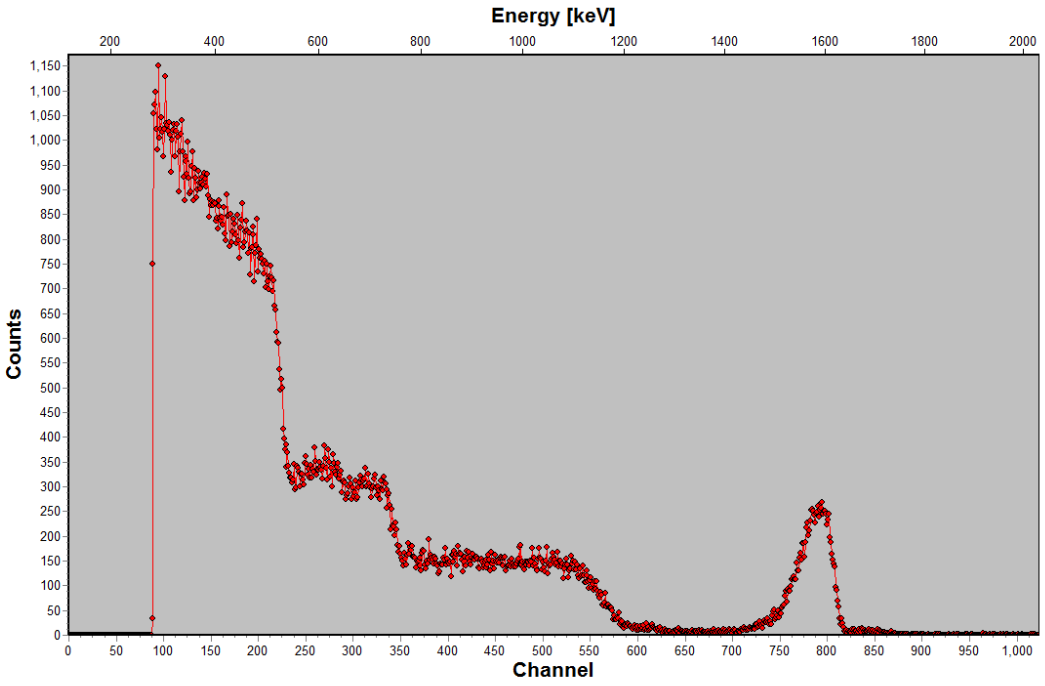

Figure 24:

5 spots average per sample, raw data

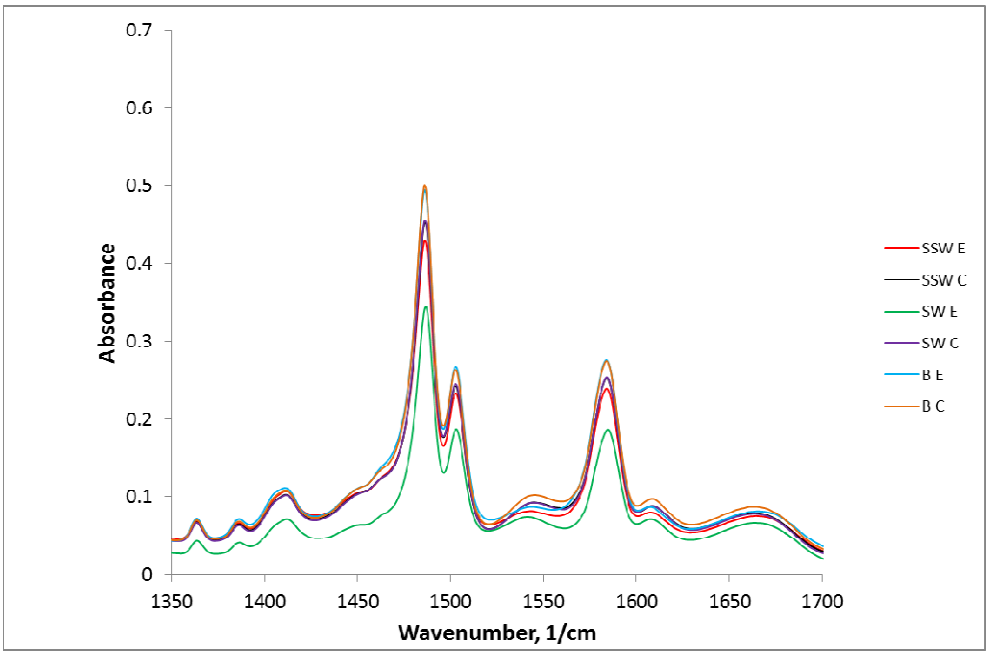

Excel Spreadsheets:

Figure 2, Figure 3, Figure 7, Figure 8

	MCA (ppm)	KI [mg/l]	Exposure time (min)	Hours	CT, MCA
Reactor 1	2	0.06	11520	192	384
Reactor 2	20	0.6	1152	19.2	384
Reactor 3	200	6	115.2	1.92	384
a.)	with synthetic seawater				
b.)	with PBS				
	MCA (ppm)	KBr [mg/l]	Exposure time (min)	Hours	CT, MCA
Reactor 4	2	60	11520	192	384
Reactor 5	20	600	1152	19.2	384
Reactor 6	200	6000	115.2	1.92	384
a.)	with synthetic seawater				
b.)	with PBS				

Figure 5-6, 9-12

Objective: To determine if MCA is reacting with support						Objective: To test larger CTs with KI				
						.@200 ppm NH2Cl	CT	Hours	KI [mg/L]	
.@200 ppm NH2Cl	CT	Hours				Reactor 4	5000	25	6	
Reactor 1	5000	25				Reactor 5	1000	5		
Reactor 2	1000	5				Reactor 6	30000	150		
Reactor 3	30000	150								

Objective: To test larger CTs with KBr						Objective: To test larger CTs with KBr and KI					
.@200 ppm NH2Cl	CT	Hours	KBr [mg/L]			.@200 ppm NH2Cl	CT	Hours	KI [mg/L]	KBr [mg/L]	
Reactor 7	5000	25	6000			Reactor 10	5000	25	6	6000	
Reactor 8	1000	5				Reactor 11	1000	5			
Reactor 9	30000	150				Reactor 12	30000	150			
	*Duplicates of membrane in separate reactors						*Duplicates of membrane in separate reactors				
***a=synthetic seawater; b=PBS											

Calculation of concentration of element X in active layer of SW30HR RO membrane (where X=Br, I, Ag, Ba, Cs etc.)

	PA						
RBS File	Layer thickness [atoms/cm^2]	%C	%O	%N	%H	%Cl	X%
A	1000	0.48	0.09	0.06	0.3672	0.002	0.0008
B	1000	0.48	0.09	0.06	0.367	0.002	0.001
C	1000	0.48	0.09	0.06	0.367	0.002	0.001
RBS File	denominator	%C	%O	%N	%H	%Cl	
A	8.48E+00	6.79E-01	1.70E-01	9.91E-02	4.33E-02	8.37E-03	
B	8.48E+00	6.79E-01	1.70E-01	9.91E-02	4.33E-02	8.37E-03	
C	8.48E+00	6.79E-01	1.70E-01	9.91E-02	4.33E-02	8.37E-03	
RBS File	[mols X /g PA]	density [g Pa/L]	Mols I/L				
A	6.35E-05	1240	7.87E-02				
B	7.94E-05	1240	9.84E-02				
C	7.94E-05	1240	9.84E-02				

Ion probe experiments for blank SW30HR RO membranes:

1.7034 g AgNO3 into 100 mL	1.7034 g / 169.87 g/mol=	0.1003
2.6256 g Ba(NO3)2 into 100 mL	2.6256 g / 261.327 g/mol=	0.1005
2E-4 M then 2E-7 M solutions		

Time (min)	pH, 2E-4 M AgNO3			pH, 2E-7 M AgNO3			pH, 2E-4 M Ba(NO3)2			pH, 2E-7 M Ba(NO3)2		
"pH 6"	T1	T2	T3	T1	T2	T3	T1	T2	T3	T1	T2	T3
3	5.61	5.75	5.76	6.54	5.45	6.13	5.59	6.08	6.23	6.66	6.27	6.05
6	5.66	5.76	5.76	6.41	5.46	6.18	5.75	6.13	6.26	6.49	6.2	6.02
9	5.72	5.76	5.76	6.25	5.47	6.17	5.91	6.16	6.27	6.39	6.14	5.98
Stdev	0.320762979											
Average	5.866666667											
"pH 9.70"												

3	9.57	9.69	9.65	9.69	9.6	9.54	9.63, 9.65, 9.63			9.62, 9.57, 9.54		
6	9.64	9.68	9.66	9.68	9.6	9.54	9.65, 9.65, 9.64			9.63, 9.57, 9.54		
9	9.65	9.69	9.65	9.65	9.6	9.54	9.67, 9.66, 9.64			9.63, 9.57, 9.55		
Stdev	0.052163087											
Average	9.628888889											
"pH 8.82"												
3	8.82	8.85	8.9	8.8	8.86	8.88	8.78, 8.35, 8.79			8.80, 8.75, 8.64		
6	8.84	8.87	8.93	8.78	8.78	8.94	8.78, 8.69, 8.80			8.81, 8.72, 8.67		
9	8.85	8.9	9.2	8.85	8.8	9.2	8.79, 8.68, 8.80			8.80, 8.65, 8.68		
Stdev	0.117957149											
Average	8.891666667											
"pH 7.44"												
3	6.59	6.67	6.68	7.74	7.49	7.31	6.16, 6.57, 6.71			7.15, 6.95, 6.79		
6	6.65	6.68	6.69	7.66	7.41	7.25	6.40, 6.62, 6.72			7.18, 6.80, 6.68		
9	6.67	6.69	6.69	7.5	7.33	7.24	6.52, 6.66, 6.74			6.95, 6.80, 6.67		
Stdev	0.402693095											
Average	7.052222222											
"pH 8.08"												
3	7.18	7.4	7.59	8.29	8.11	8.05	NA			NA		
6	7.24	7.46	7.6	8.21	8.12	8.1	NA			NA		
9	7.27	7.51	7.61	8.19	8.2	8.11	NA			NA		
Stdev	0.381865143											
Average	7.791111111											
"pH 7.89"												

3	7.03	7.75	7.97	8.39	7.98	7.87	NA			NA		
6	7.35	7.92	7.99	8.28	7.92	7.78	NA			NA		
9	7.49	7.96	8.02	8.06	7.87	7.71	NA			NA		
Stdev	0.308176637											
Average	7.852222222											
"pH 9.13"												
3	8.6	8.95					NA			NA		
6	8.62	8.97					NA			NA		
9	8.83	9	9.04	9.23	9.17	9.12	NA			NA		
Stdev	0.203078802											
Average	8.953											

Sample	**%C**	**%O**	**%N**	**%H**	**%Cl**	**%Ag**	**%Ba**
0328	0.48	0.088	0.047	0.38293	0.0018	0.00027	0
0329	0.48	0.088	0.055	0.37493	0.0018	0.00027	0
0330	0.48	0.088	0.055	0.37496	0.0018	0.00022	0.00002
0331	0.48	0.088	0.055	0.37496	0.0018	0.00022	0.00002
0332	0.48	0.095	0.047	0.37655	0.001	0.00045	0
0333	0.48	0.092	0.055	0.3708	0.0018	0.0004	0
0334	0.48	0.092	0.055	0.370873	0.0018	0.0003	0.000027
0335	0.48	0.092	0.055	0.370873	0.0018	0.0003	0.000027
0336	0.48	0.097	0.047	0.3747	0.0012	0.0001	0
0337	0.48	0.098	0.055	0.3658	0.0011	0.0001	0
0338	0.48	0.098	0.055	0.3658	0.0011	0.0001	0
0339	0.48	0.098	0.055	0.3658	0.0011	0.0001	0
0340	0.48	0.098	0.055	0.365815	0.0011	8.5E-05	0
0341	0.48	0.098	0.055	0.365815	0.0011	8.5E-05	0
0342	0.48	0.092	0.055	0.37173	0.0011	0.00017	0
0343	0.48	0.092	0.055	0.37173	0.0011	0.00017	0
0344	0.48	0.092	0.055	0.37173	0.0011	0.00017	0
0345	0.48	0.092	0.055	0.37173	0.0011	0.00017	0
0346	0.48	0.092	0.047	0.37975	0.0011	0.00015	0
0347	0.48	0.092	0.055	0.371755	0.0011	0.00015	0
0348	0.48	0.092	0.047	0.37965	0.0011	0.00025	0
0349	0.48	0.092	0.055	0.37165	0.0011	0.00025	0

weight							
without the ion							
Sample	denominator	%C	%O	%N	%H	%Cl	
0328	8.27E+00	6.96E-01	1.70E-01	7.95E-02	4.63E-02	7.72E-03	
0329	8.38E+00	6.96E-01	1.68E-01	9.19E-02	4.48E-02	7.63E-03	
0330	8.38E+00	6.96E-01	1.68E-01	9.19E-02	4.48E-02	7.63E-03	
0331	8.38E+00	6.96E-01	1.68E-01	9.19E-02	4.48E-02	7.63E-03	
0332	8.35E+00	6.96E-01	1.82E-01	7.88E-02	4.51E-02	4.25E-03	
0333	8.44E+00	6.96E-01	1.74E-01	9.13E-02	4.40E-02	7.57E-03	
0334	8.44E+00	6.96E-01	1.74E-01	9.13E-02	4.40E-02	7.57E-03	
0335	8.44E+00	6.96E-01	1.74E-01	9.13E-02	4.40E-02	7.57E-03	
0336	8.39E+00	6.96E-01	1.85E-01	7.85E-02	4.47E-02	5.08E-03	
0337	8.50E+00	6.96E-01	1.84E-01	9.06E-02	4.30E-02	4.59E-03	
0338	8.50E+00	6.96E-01	1.84E-01	9.06E-02	4.30E-02	4.59E-03	
0339	8.50E+00	6.96E-01	1.84E-01	9.06E-02	4.30E-02	4.59E-03	
0340	8.50E+00	6.96E-01	1.84E-01	9.06E-02	4.30E-02	4.59E-03	
0341	8.50E+00	6.96E-01	1.84E-01	9.06E-02	4.30E-02	4.59E-03	
0342	8.41E+00	6.96E-01	1.75E-01	9.15E-02	4.42E-02	4.64E-03	
0343	8.41E+00	6.96E-01	1.75E-01	9.15E-02	4.42E-02	4.64E-03	
0344	8.41E+00	6.96E-01	1.75E-01	9.15E-02	4.42E-02	4.64E-03	
0345	8.41E+00	6.96E-01	1.75E-01	9.15E-02	4.42E-02	4.64E-03	
0346	8.31E+00	6.96E-01	1.77E-01	7.92E-02	4.57E-02	4.70E-03	
0347	8.41E+00	6.96E-01	1.75E-01	9.15E-02	4.42E-02	4.64E-03	
0348	8.31E+00	6.96E-01	1.77E-01	7.92E-02	4.57E-02	4.70E-03	
0349	8.41E+00	6.96E-01	1.75E-01	9.15E-02	4.42E-02	4.64E-03	

Sample	[mols Ag /g PA]	[mols Ba /g PA]	density [g Pa/L]	Mols Ag/L	Mols Ba/L
0328	2.16E-05	0.00E+00	1240	2.68E-02	0
0329	2.13E-05	0.00E+00	1240	2.65E-02	0
0330	1.74E-05	1.58E-06	1240	2.16E-02	0.0019609 7
0331	1.74E-05	1.58E-06	1240	2.16E-02	0.0019609 7
0332	3.58E-05	0.00E+00	1240	4.44E-02	0
0333	3.14E-05	0.00E+00	1240	3.89E-02	0
0334	2.36E-05	2.12E-06	1240	2.92E-02	0.0026285 2
0335	2.36E-05	2.12E-06	1240	2.92E-02	0.0026285 2
0336	7.91E-06	0.00E+00	1240	9.81E-03	0
0337	7.83E-06	0.00E+00	1240	9.70E-03	0
0338	7.83E-06	0.00E+00	1240	9.70E-03	0
0339	7.83E-06	0.00E+00	1240	9.70E-03	0
0340	6.65E-06	0.00E+00	1240	8.25E-03	0
0341	6.65E-06	0.00E+00	1240	8.25E-03	0
0342	1.34E-05	0.00E+00	1240	1.67E-02	0
0343	1.34E-05	0.00E+00	1240	1.67E-02	0
0344	1.34E-05	0.00E+00	1240	1.67E-02	0
0345	1.34E-05	0.00E+00	1240	1.67E-02	0
0346	1.20E-05	0.00E+00	1240	1.49E-02	0
0347	1.15E-05	0.00E+00	1240	1.42E-02	0
0348	2.00E-05	0.00E+00	1240	2.48E-02	0
0349	1.98E-05	0.00E+00	1240	2.45E-02	0

Ion probe experiments for treated SW30HR RO membranes:

1.7056 g AgNO3 into 100 mL	1.7056 g / 169.87 g/mol=	0.1004		**0 notches=syn sw**		
2.6256 g Ba(NO3)2 into 100 mL	2.6256 g / 261.327 g/mol=	0.1005		**1 notch=buffer**		
2E-4 M then 2E-6 M solutions				**2 notches=sw**		
Time (min)	2E-4 M AgNO3, control+expt			1E-6 M AgNO3, control+expt		
pH #1~5.55- control+expt	T1	T2	T3	T1	T2	T3
3 min	5.37	5.52	5.56	6.34	5.6	5.69
6 min	5.42	5.54	5.6	5.92	5.56	5.66

10 min	5.49	5.55	5.92	5.88	5.55	5.85
Stdev	0.228267766					
Average pH	5.667777778					
pH #2~8.77-control +expt						
3 min	8.6	8.95	9.04	8.54	8.63	8.63
6 min	8.66	9	9.04	8.94	8.75	8.66
10 min	8.81	9	9.04	8.87	8.5	9
Stdev	0.187563981					
Average pH	8.814444444					
pH #3~7.08=control+expt						
3 min	6.83	7.37	7.72	8.06	7.75	7.73
6 min	7.01	7.88	7.61	7.94	7.86	7.71
10 min	7.09	7.29	7.6	7.9	7.76	7.65
Stdev	0.333942037					
Average pH	7.597777778					
pH #5~6.50-control+expt						
3 min	5.94	6.13	6.18	6.97	6.77	6.62
6 min	6.2	6.45	6.45	6.98	6.72	6.57
10 min	6.24	6.39	6.18	6.85	6.65	6.56
Stdev	0.295263536					
Average pH	6.491666667					
*pH #7~10.3						
3 min	10.61	10.59	10.58	10.51	10.51	10.51
6 min	10.61	10.59	10.57	10.51	10.52	10.5
10 min	10.61	10.58	10.57	10.52	10.53	10.51
Stdev	0.040311289					
Average pH	10.55166667					

Sample	**PA**							
atomic	**Layer thickness [atoms/cm^2]**	**%C**	**%O**	**%N**	**%H**	**%Cl**	**%Ag**	**%Br**
0350	1.06E+18	0.48	0.1	0.0501	0.36878	0.001	0.00012	0
0351	1.13E+18	0.48	0.095	0.05	0.36464	0.001	0.00016	0.0092
0352	8.80E+17	0.48	0.075	0.05	0.37985	0.001	0.00015	0.014
0353	9.00E+17	0.48	0.085	0.05	0.3839	0.001	0.0001	0
0354	5.25E+17	0.48	0.085	0.05	0.37838	0.0043	0.00232	0
0355	9.00E+17	0.48	0.085	0.05	0.38365	0.001	0.00035	0

0356	1.01E+18	0.48	0.085	0.05	0.3742	0.001	0.0004	0.0094
0357	9.00E+17	0.48	0.085	0.05	0.38362	0.001	0.00038	0
0358	1.01E+18	0.48	0.085	0.05	0.37607	0.001	0.00043	0.0075
0359	1.03E+18	0.48	0.085	0.05	0.37446	0.0021	0.00044	0.008
0360	8.80E+17	0.48	0.085	0.05	0.38363	0.001	0.00037	0
0361	1.03E+18	0.48	0.095	0.05	0.3658	0.0021	0	0.007
0362	1.03E+18	0.48	0.095	0.05	0.36402	0.0011	0.00018	0.0097
0363	1.00E+18	0.48	0.095	0.05	0.37375	0.0011	0.00015	0
0364	1.00E+18	0.48	0.085	0.05	0.37272	0.0011	0.00018	0.011
0365	1.00E+18	0.48	0.095	0.05	0.37377	0.0011	0.00013	0
0366	1.00E+18	0.48	0.095	0.05	0.37387	0.001	0.00013	0
0367	1.00E+18	0.48	0.095	0.05	0.36509	0.0021	0.00021	0.0075
0374	9.50E+17	0.48	0.105	0.045	0.368699	0.001	0.000301	0
0375	1.05E+18	0.48	0.1	0.043	0.36551	0.0011	0.00039	0.01
0376	1.05E+18	0.48	0.1	0.043	0.36729	0.0011	0.00041	0.0082
0377	9.50E+17	0.48	0.095	0.045	0.378699	0.001	0.000301	0
0378	9.50E+17	0.48	0.1	0.045	0.373699	0.001	0.000301	0
0379	1.05E+18	0.48	0.1	0.043	0.368265	0.0021	0.000435	0.0062
0380	1.00E+18	0.48	0.1	0.043	0.369359	0.0011	0.000341	0.0062
0381	9.75E+17	0.48	0.095	0.045	0.37877	0.001	0.00023	0
0382	1.00E+18	0.48	0.1	0.043	0.3659	0.0011	0	0.01
0383	1.05E+18	0.48	0.1	0.043	0.3675	0.0011	0	0.0084
0388	1.00E+18	0.48	0.1	0.045	0.37382	0.001	0.00018	0
0389	1.00E+18	0.48	0.085	0.043	0.37959	0.0011	0.00031	0.011
0390	1.00E+18	0.48	0.095	0.043	0.37217	0.0011	0.00023	0.0085
0391	1.00E+18	0.48	0.1	0.045	0.37382	0.001	0.00018	0
0394	9.60E+17	0.48	0.095	0.045	0.3789	0.001	0.0001	0

0395	1.05E+18	0.48	0.095	0.043	0.374203	0.0011	0.000197	0.0065
0396	9.40E+17	0.48	0.095	0.045	0.379	0.001	0	0
0397	9.40E+17	0.48	0.1	0.05	0.369	0.001	0	0
0398	1.10E+18	0.48	0.085	0.05	0.384	0.001	0	0
weight								
without the ion								
Sample	**denominator**	**%C**	**%O**	**%N**	**%H**	**%Cl**		
0350	8.47E+00	6.80E-01	1.89E-01	8.29E-02	4.36E-02	4.19E-03		
0351	8.38E+00	6.80E-01	1.81E-01	8.35E-02	4.35E-02	4.24E-03		
0352	8.08E+00	6.80E-01	1.49E-01	8.67E-02	4.70E-02	4.40E-03		
0353	8.24E+00	6.80E-01	1.65E-01	8.50E-02	4.66E-02	4.31E-03		
0354	8.35E+00	6.80E-01	1.63E-01	8.38E-02	4.53E-02	1.83E-02		
0355	8.24E+00	6.80E-01	1.65E-01	8.50E-02	4.66E-02	4.31E-03		
0356	8.23E+00	6.80E-01	1.65E-01	8.51E-02	4.55E-02	4.31E-03		
0357	8.24E+00	6.80E-01	1.65E-01	8.50E-02	4.66E-02	4.31E-03		
0358	8.23E+00	6.80E-01	1.65E-01	8.50E-02	4.57E-02	4.31E-03		
0359	8.27E+00	6.80E-01	1.64E-01	8.47E-02	4.53E-02	9.02E-03		
0360	8.24E+00	6.80E-01	1.65E-01	8.50E-02	4.66E-02	4.31E-03		
0361	8.42E+00	6.80E-01	1.81E-01	8.31E-02	4.34E-02	8.85E-03		
0362	8.38E+00	6.80E-01	1.81E-01	8.35E-02	4.34E-02	4.66E-03		
0363	8.39E+00	6.80E-01	1.81E-01	8.34E-02	4.45E-02	4.65E-03		
0364	8.23E+00	6.80E-01	1.65E-01	8.50E-02	4.53E-02	4.74E-03		
0365	8.39E+00	6.80E-01	1.81E-01	8.34E-02	4.45E-02	4.65E-03		
0366	8.39E+00	6.80E-01	1.81E-01	8.34E-02	4.46E-02	4.23E-03		
0367	8.42E+00	6.80E-01	1.81E-01	8.31E-02	4.34E-02	8.85E-03		
0374	8.47E+00	6.80E-01	1.98E-01	7.43E-02	4.35E-02	4.19E-03		
0375	8.37E+00	6.80E-01	1.91E-01	7.20E-02	4.37E-02	4.67E-03		
0376	8.37E+00	6.80E-01	1.91E-01	7.19E-02	4.39E-02	4.67E-03		

0377	8.32E+00	6.80E-01	1.83E-01	7.57E-02	4.55E-02	4.26E-03		
0378	8.40E+00	6.80E-01	1.90E-01	7.50E-02	4.45E-02	4.23E-03		
0379	8.40E+00	6.80E-01	1.90E-01	7.16E-02	4.38E-02	8.87E-03		
0380	8.37E+00	6.80E-01	1.91E-01	7.19E-02	4.41E-02	4.67E-03		
0381	8.32E+00	6.80E-01	1.83E-01	7.57E-02	4.55E-02	4.26E-03		
0382	8.37E+00	6.80E-01	1.91E-01	7.19E-02	4.37E-02	4.67E-03		
0383	8.37E+00	6.80E-01	1.91E-01	7.19E-02	4.39E-02	4.67E-03		
0388	8.40E+00	6.80E-01	1.90E-01	7.50E-02	4.45E-02	4.23E-03		
0389	8.14E+00	6.80E-01	1.67E-01	7.39E-02	4.66E-02	4.80E-03		
0390	8.29E+00	6.80E-01	1.83E-01	7.26E-02	4.49E-02	4.71E-03		
0391	8.40E+00	6.80E-01	1.90E-01	7.50E-02	4.45E-02	4.23E-03		
0394	8.32E+00	6.80E-01	1.83E-01	7.57E-02	4.55E-02	4.26E-03		
0395	8.30E+00	6.80E-01	1.83E-01	7.26E-02	4.51E-02	4.71E-03		
0396	8.32E+00	6.80E-01	1.83E-01	7.57E-02	4.55E-02	4.26E-03		
0397	8.46E+00	6.80E-01	1.89E-01	8.27E-02	4.36E-02	4.19E-03		
0398	8.24E+00	6.80E-01	1.65E-01	8.50E-02	4.66E-02	4.31E-03		
Sample	**[mols Ag /g PA]**	**[mols Br /g PA]**	**mol I/g PA**	**density [g Pa/L]**	**Mols Ag/L**	**Mols Br/L**	**Mols I/L**	
0350	9.57E-06	0.00E+00	0.00E+00	1240	1.19E-02	0.00E+00	0.00E+00	
0351	1.29E-05	7.40E-04	0.00E+00	1240	1.60E-02	9.18E-01	0.00E+00	
0352	1.25E-05	1.17E-03	0.00E+00	1240	1.56E-02	1.45E+00	0.00E+00	
0353	8.20E-06	0.00E+00	0.00E+00	1240	1.02E-02	0.00E+00	0.00E+00	
0354	1.84E-04	0.00E+00	0.00E+00	1240	2.28E-01	0.00E+00	0.00E+00	
0355	2.87E-05	0.00E+00	0.00E+00	1240	3.56E-02	0.00E+00	0.00E+00	
0356	3.28E-05	7.71E-04	0.00E+00	1240	4.07E-02	9.56E-01	0.00E+00	
0357	3.12E-05	0.00E+00	0.00E+00	1240	3.86E-02	0.00E+00	0.00E+00	
0358	3.53E-05	6.15E-04	0.00E+00	1240	4.37E-02	7.62E-01	0.00E+00	

0359	3.56E-05	6.48E-04	0.00E+00	1240	4.42E-02	8.03E-01	0.00E+00	
0360	3.03E-05	0.00E+00	0.00E+00	1240	3.76E-02	0.00E+00	0.00E+00	
0361	0.00E+00	5.57E-04	1.62E-08	1240	0.00E+00	6.90E-01	2.01E-05	
0362	1.45E-05	7.80E-04	0.00E+00	1240	1.79E-02	9.67E-01	0.00E+00	
0363	1.21E-05	0.00E+00	0.00E+00	1240	1.50E-02	0.00E+00	0.00E+00	
0364	1.47E-05	9.01E-04	0.00E+00	1240	1.83E-02	1.12E+00	0.00E+00	
0365	1.05E-05	0.00E+00	0.00E+00	1240	1.30E-02	0.00E+00	0.00E+00	
0366	1.05E-05	0.00E+00	0.00E+00	1240	1.30E-02	0.00E+00	0.00E+00	
0367	1.67E-05	5.96E-04	1.67E-08	1240	2.07E-02	7.40E-01	2.07E-05	
0374	2.39E-05	0.00E+00	0.00E+00	1240	2.97E-02	0.00E+00	0.00E+00	
0375	3.13E-05	8.04E-04	0.00E+00	1240	3.89E-02	9.97E-01	0.00E+00	
0376	3.30E-05	6.59E-04	0.00E+00	1240	4.09E-02	8.17E-01	0.00E+00	
0377	2.44E-05	0.00E+00	0.00E+00	1240	3.02E-02	0.00E+00	0.00E+00	
0378	2.42E-05	0.00E+00	0.00E+00	1240	3.00E-02	0.00E+00	0.00E+00	
0379	3.46E-05	4.93E-04	0.00E+00	1240	4.29E-02	6.12E-01	0.00E+00	
0380	2.74E-05	4.98E-04	0.00E+00	1240	3.40E-02	6.18E-01	0.00E+00	
0381	1.86E-05	0.00E+00	0.00E+00	1240	2.31E-02	0.00E+00	0.00E+00	
0382	0.00E+00	8.04E-04	0.00E+00	1240	0.00E+00	9.97E-01	0.00E+00	
0383	0.00E+00	6.75E-04	0.00E+00	1240	0.00E+00	8.37E-01	0.00E+00	
0388	1.44E-05	0.00E+00	0.00E+00	1240	1.79E-02	0.00E+00	0.00E+00	
0389	2.56E-05	9.10E-04	0.00E+00	1240	3.18E-02	1.13E+00	0.00E+00	
0390	1.87E-05	6.90E-04	0.00E+00	1240	2.31E-02	8.55E-01	0.00E+00	
0391	1.44E-05	0.00E+00	0.00E+00	1240	1.79E-02	0.00E+00	0.00E+00	
0394	8.10E-06	0.00E+00	0.00E+00	1240	1.00E-02	0.00E+00	0.00E+00	
0395	1.60E-05	5.27E-04	0.00E+00	1240	1.98E-02	6.54E-01	0.00E+00	
0396	0.00E+00	0.00E+00	0.00E+00	1240	0.00E+00	0.00E+00	0.00E+00	
0397	0.00E+00	0.00E+00	0.00E+00	1240	0.00E+00	0.00E+00	0.00E+00	

0398	0.00E+00	0.00E+00	0.00E+00	1240	0.00E+00	0.00E+00	0.00E+00	

Carboxylic curve data:

Seawater control							Seawater experimental				
R-COO, high	0.038						R-COO, high	0.045			
w1	0.52		pKa1	5.1			w1	0.45		pKa1	4.5
w2	=1-B4		pKa2	8.55			w2	=1-I4		pKa2	7.7

pH	[H+]	[R-COO]		pH	[H+]	[R-COO]
0	1	1.57E-07		0	1	6.40835E-07
0.1	0.794328	1.98E-07		0.1	0.794328	8.06757E-07
0.2	0.630957	2.49E-07		0.2	0.630957	1.01564E-06
0.3	0.501187	3.13E-07		0.3	0.501187	1.27859E-06
0.4	0.398107	3.94E-07		0.4	0.398107	1.60963E-06
0.5	0.316228	4.96E-07		0.5	0.316228	2.02636E-06
0.6	0.251189	6.25E-07		0.6	0.251189	2.55097E-06
0.7	0.199526	7.87E-07		0.7	0.199526	3.21138E-06
0.8	0.158489	9.91E-07		0.8	0.158489	4.04272E-06
0.9	0.125893	1.25E-06		0.9	0.125893	5.08922E-06
1	0.1	1.57E-06		1	0.1	6.40653E-06
1.1	0.079433	1.98E-06		1.1	0.079433	8.06468E-06
1.2	0.063096	2.49E-06		1.2	0.063096	1.01518E-05
1.3	0.050119	3.13E-06		1.3	0.050119	1.27787E-05
1.4	0.039811	3.94E-06		1.4	0.039811	1.60848E-05
1.5	0.031623	4.96E-06		1.5	0.031623	2.02454E-05
1.6	0.025119	6.25E-06		1.6	0.025119	2.54808E-05
1.7	0.019953	7.87E-06		1.7	0.019953	3.20681E-05
1.8	0.015849	9.9E-06		1.8	0.015849	4.03548E-05
1.9	0.012589	1.25E-05		1.9	0.012589	5.07775E-05
2	0.01	1.57E-05		2	0.01	6.38836E-05
2.1	0.007943	1.97E-05		2.1	0.007943	8.03592E-05
2.2	0.00631	2.49E-05		2.2	0.00631	0.000101063
2.3	0.005012	3.13E-05		2.3	0.005012	0.000127066
2.4	0.003981	3.94E-05		2.4	0.003981	0.000159708
2.5	0.003162	4.95E-05		2.5	0.003162	0.000200651
2.6	0.002512	6.23E-05		2.6	0.002512	0.000251959
2.7	0.001995	7.84E-05		2.7	0.001995	0.000316181
2.8	0.001585	9.86E-05		2.8	0.001585	0.000396448

2.9	0.001259	0.000124		2.9	0.001259	0.000496585
3	0.001	0.000156		3	0.001	0.000621226
3.1	0.000794	0.000196		3.1	0.000794	0.000775923
3.2	0.000631	0.000246		3.2	0.000631	0.000967249
3.3	0.000501	0.000308		3.3	0.000501	0.001202842
3.4	0.000398	0.000387		3.4	0.000398	0.001491388
3.5	0.000316	0.000484		3.5	0.000316	0.001842471
3.6	0.000251	0.000606		3.6	0.000251	0.002266235
3.7	0.0002	0.000757		3.7	0.0002	0.002772814
3.8	0.000158	0.000943		3.8	0.000158	0.00337145
3.9	0.000126	0.001173		3.9	0.000126	0.004069312
4	1E-04	0.001455		4	1E-04	0.004870062
4.1	7.94E-05	0.001797		4.1	7.94E-05	0.005772347
4.2	6.31E-05	0.00221		4.2	6.31E-05	0.006768501
4.3	5.01E-05	0.002704		4.3	5.01E-05	0.007843829
4.4	3.98E-05	0.003288		4.4	3.98E-05	0.008976838
4.5	3.16E-05	0.003969		4.5	3.16E-05	0.010140606
4.6	2.51E-05	0.004749		4.6	2.51E-05	0.011305205
4.7	2E-05	0.005629		4.7	2E-05	0.012440746
4.8	1.58E-05	0.0066		4.8	1.58E-05	0.013520443
4.9	1.26E-05	0.007648		4.9	1.26E-05	0.014523032
5	0.00001	0.008753		5	0.00001	0.01543416
5.1	7.94E-06	0.009886		5.1	7.94E-06	0.016246623
5.2	6.31E-06	0.011021		5.2	6.31E-06	0.016959685
5.3	5.01E-06	0.012126		5.3	5.01E-06	0.017577801
5.4	3.98E-06	0.013176		5.4	3.98E-06	0.018109156
5.5	3.16E-06	0.01415		5.5	3.16E-06	0.018564274
5.6	2.51E-06	0.015033		5.6	2.51E-06	0.018954899
5.7	2E-06	0.015819		5.7	2E-06	0.019293193
5.8	1.58E-06	0.016506		5.8	1.58E-06	0.019591244
5.9	1.26E-06	0.017097		5.9	1.26E-06	0.019860839
6	1E-06	0.017602		6	1E-06	0.020113435
6.1	7.94E-07	0.018028		6.1	7.94E-07	0.020360265
6.2	6.31E-07	0.018387		6.2	6.31E-07	0.020612536
6.3	5.01E-07	0.018689		6.3	5.01E-07	0.020881657
6.4	3.98E-07	0.018945		6.4	3.98E-07	0.021179473
6.5	3.16E-07	0.019165		6.5	3.16E-07	0.021518441
6.6	2.51E-07	0.019357		6.6	2.51E-07	0.021911708
6.7	2E-07	0.01953		6.7	2E-07	0.022373032
6.8	1.58E-07	0.019692		6.8	1.58E-07	0.022916456
6.9	1.26E-07	0.019851		6.9	1.26E-07	0.023555673

7	1E-07	0.020014		7	1E-07	0.02430302
7.1	7.94E-08	0.020189		7.1	7.94E-08	0.025168072
7.2	6.31E-08	0.020384		7.2	6.31E-08	0.02615594
7.3	5.01E-08	0.020607		7.3	5.01E-08	0.027265451
7.4	3.98E-08	0.020867		7.4	3.98E-08	0.028487588
7.5	3.16E-08	0.021174		7.5	3.16E-08	0.029804634
7.6	2.51E-08	0.021538		7.6	2.51E-08	0.031190465
7.7	2E-08	0.021968		7.7	2E-08	0.032612231
7.8	1.58E-08	0.022475		7.8	1.58E-08	0.034033319
7.9	1.26E-08	0.023065		7.9	1.26E-08	0.035417078
8	1E-08	0.023746		8	1E-08	0.036730549
8.1	7.94E-09	0.024517		8.1	7.94E-09	0.03794742
8.2	6.31E-09	0.025376		8.2	6.31E-09	0.039049697
8.3	5.01E-09	0.026313		8.3	5.01E-09	0.040027981
8.4	3.98E-09	0.027311		8.4	3.98E-09	0.040880597
8.5	3.16E-09	0.028348		8.5	3.16E-09	0.041612005
8.6	2.51E-09	0.029398		8.6	2.51E-09	0.042230951
8.7	2E-09	0.030435		8.7	2E-09	0.042748722
8.8	1.58E-09	0.031431		8.8	1.58E-09	0.043177693
8.9	1.26E-09	0.032365		8.9	1.26E-09	0.043530258
9	1E-09	0.033221		9	1E-09	0.043818123
9.1	7.94E-10	0.033988		9.1	7.94E-10	0.0440519
9.2	6.31E-10	0.034662		9.2	6.31E-10	0.044240924
9.3	5.01E-10	0.035245		9.3	5.01E-10	0.044393221
9.4	3.98E-10	0.035741		9.4	3.98E-10	0.044515578
9.5	3.16E-10	0.036159		9.5	3.16E-10	0.044613656
9.6	2.51E-10	0.036507		9.6	2.51E-10	0.044692129
9.7	2E-10	0.036794		9.7	2E-10	0.044754823
9.8	1.58E-10	0.037029		9.8	1.58E-10	0.044804852
9.9	1.26E-10	0.03722		9.9	1.26E-10	0.044844737
10	1E-10	0.037375		10	1E-10	0.044876511
10.1	7.94E-11	0.0375		10.1	7.94E-11	0.044901808
10.2	6.31E-11	0.0376		10.2	6.31E-11	0.04492194
10.3	5.01E-11	0.037681		10.3	5.01E-11	0.044937954
10.4	3.98E-11	0.037746		10.4	3.98E-11	0.04495069
10.5	3.16E-11	0.037798		10.5	3.16E-11	0.044960816
10.6	2.51E-11	0.037839		10.6	2.51E-11	0.044968865
10.7	2E-11	0.037872		10.7	2E-11	0.044975262
10.8	1.58E-11	0.037898		10.8	1.58E-11	0.044980346
10.9	1.26E-11	0.037919		10.9	1.26E-11	0.044984386
11	1E-11	0.037935		11	1E-11	0.044987595

11.1	7.94E-12	0.037949		11.1	7.94E-12	0.044990146
11.2	6.31E-12	0.037959		11.2	6.31E-12	0.044992172
11.3	5.01E-12	0.037968		11.3	5.01E-12	0.044993781
11.4	3.98E-12	0.037974		11.4	3.98E-12	0.04499506
11.5	3.16E-12	0.03798		11.5	3.16E-12	0.044996076
11.6	2.51E-12	0.037984		11.6	2.51E-12	0.044996883
11.7	2E-12	0.037987		11.7	2E-12	0.044997524
11.8	1.58E-12	0.03799		11.8	1.58E-12	0.044998033
11.9	1.26E-12	0.037992		11.9	1.26E-12	0.044998438
12	1E-12	0.037994		12	1E-12	0.044998759
12.1	7.94E-13	0.037995		12.1	7.94E-13	0.044999014
12.2	6.31E-13	0.037996		12.2	6.31E-13	0.044999217
12.3	5.01E-13	0.037997		12.3	5.01E-13	0.044999378
12.4	3.98E-13	0.037997		12.4	3.98E-13	0.044999506
12.5	3.16E-13	0.037998		12.5	3.16E-13	0.044999608
12.6	2.51E-13	0.037998		12.6	2.51E-13	0.044999688
12.7	2E-13	0.037999		12.7	2E-13	0.044999752
12.8	1.58E-13	0.037999		12.8	1.58E-13	0.044999803
12.9	1.26E-13	0.037999		12.9	1.26E-13	0.044999844
13	1E-13	0.037999		13	1E-13	0.044999876
13.1	7.94E-14	0.037999		13.1	7.94E-14	0.044999901
13.2	6.31E-14	0.038		13.2	6.31E-14	0.044999922
13.3	5.01E-14	0.038		13.3	5.01E-14	0.044999938
13.4	3.98E-14	0.038		13.4	3.98E-14	0.044999951
13.5	3.16E-14	0.038		13.5	3.16E-14	0.044999961
13.6	2.51E-14	0.038		13.6	2.51E-14	0.044999969
13.7	2E-14	0.038		13.7	2E-14	0.044999975
13.8	1.58E-14	0.038		13.8	1.58E-14	0.04499998
13.9	1.26E-14	0.038		13.9	1.26E-14	0.044999984
14	1E-14	0.038		14	1E-14	0.044999988
\						

Syn. seawater control							Syn. seawater experimental				
R-COO, high	0.038						R-COO, high	0.044			
w1	0.36		pKa1	5.2			w1	0.4		pKa1	4.8
w2	0.64		pKa2	8.5			w2	0.6		pKa2	7.6

pH	[H+]	[R-COO]		pH	[H+]	[R-COO]
0	1	8.64E-08		0	1	2.796E-07
0.1	0.794328	1.09E-07		0.1	0.794328	3.51994E-07
0.2	0.630957	1.37E-07		0.2	0.630957	4.43132E-07
0.3	0.501187	1.72E-07		0.3	0.501187	5.57866E-07
0.4	0.398107	2.17E-07		0.4	0.398107	7.02306E-07
0.5	0.316228	2.73E-07		0.5	0.316228	8.84142E-07
0.6	0.251189	3.44E-07		0.6	0.251189	1.11305E-06
0.7	0.199526	4.33E-07		0.7	0.199526	1.40123E-06
0.8	0.158489	5.45E-07		0.8	0.158489	1.76401E-06
0.9	0.125893	6.86E-07		0.9	0.125893	2.2207E-06
1	0.1	8.64E-07		1	0.1	2.7956E-06
1.1	0.079433	1.09E-06		1.1	0.079433	3.51931E-06
1.2	0.063096	1.37E-06		1.2	0.063096	4.43032E-06
1.3	0.050119	1.72E-06		1.3	0.050119	5.57708E-06
1.4	0.039811	2.17E-06		1.4	0.039811	7.02056E-06
1.5	0.031623	2.73E-06		1.5	0.031623	8.83745E-06
1.6	0.025119	3.44E-06		1.6	0.025119	1.11242E-05
1.7	0.019953	4.33E-06		1.7	0.019953	1.40023E-05
1.8	0.015849	5.45E-06		1.8	0.015849	1.76243E-05
1.9	0.012589	6.86E-06		1.9	0.012589	2.21819E-05
2	0.01	8.63E-06		2	0.01	2.79163E-05
2.1	0.007943	1.09E-05		2.1	0.007943	3.51302E-05
2.2	0.00631	1.37E-05		2.2	0.00631	4.42035E-05
2.3	0.005012	1.72E-05		2.3	0.005012	5.5613E-05
2.4	0.003981	2.17E-05		2.4	0.003981	6.99556E-05
2.5	0.003162	2.73E-05		2.5	0.003162	8.79788E-05
2.6	0.002512	3.43E-05		2.6	0.002512	0.000110616
2.7	0.001995	4.32E-05		2.7	0.001995	0.000139032
2.8	0.001585	5.43E-05		2.8	0.001585	0.000174676
2.9	0.001259	6.83E-05		2.9	0.001259	0.000219343
3	0.001	8.59E-05		3	0.001	0.000275252
3.1	0.000794	0.000108		3.1	0.000794	0.000345131
3.2	0.000631	0.000136		3.2	0.000631	0.00043231
3.3	0.000501	0.00017		3.3	0.000501	0.000540823
3.4	0.000398	0.000214		3.4	0.000398	0.000675508
3.5	0.000316	0.000268		3.5	0.000316	0.000842087
3.6	0.000251	0.000336		3.6	0.000251	0.001047216
3.7	0.0002	0.00042		3.7	0.0002	0.001298464
3.8	0.000158	0.000524		3.8	0.000158	0.001604183
3.9	0.000126	0.000654		3.9	0.000126	0.001973224

4	1E-04	0.000813		4	1E-04	0.002414431
4.1	7.94E-05	0.001008		4.1	7.94E-05	0.002935886
4.2	6.31E-05	0.001245		4.2	6.31E-05	0.003543882
4.3	5.01E-05	0.001531		4.3	5.01E-05	0.004241679
4.4	3.98E-05	0.001873		4.4	3.98E-05	0.005028198
4.5	3.16E-05	0.002278		4.5	3.16E-05	0.0058969
4.6	2.51E-05	0.002749		4.6	2.51E-05	0.006835166
4.7	2E-05	0.003291		4.7	2E-05	0.007824509
4.8	1.58E-05	0.0039		4.8	1.58E-05	0.008841775
4.9	1.26E-05	0.004573		4.9	1.26E-05	0.009861255
5	0.00001	0.0053		5	0.00001	0.010857356
5.1	7.94E-06	0.006066		5.1	7.94E-06	0.011807275
5.2	6.31E-06	0.006852		5.2	6.31E-06	0.012693132
5.3	5.01E-06	0.007639		5.3	5.01E-06	0.0135032
5.4	3.98E-06	0.008407		5.4	3.98E-06	0.014232152
5.5	3.16E-06	0.009137		5.5	3.16E-06	0.01488051
5.6	2.51E-06	0.009815		5.6	2.51E-06	0.015453585
5.7	2E-06	0.010432		5.7	2E-06	0.015960267
5.8	1.58E-06	0.010982		5.8	1.58E-06	0.016411884
5.9	1.26E-06	0.011465		5.9	1.26E-06	0.016821304
6	1E-06	0.011885		6	1E-06	0.017202312
6.1	7.94E-07	0.012247		6.1	7.94E-07	0.01756926
6.2	6.31E-07	0.012558		6.2	6.31E-07	0.017936921
6.3	5.01E-07	0.012826		6.3	5.01E-07	0.018320485
6.4	3.98E-07	0.01306		6.4	3.98E-07	0.018735606
6.5	3.16E-07	0.013268		6.5	3.16E-07	0.019198415
6.6	2.51E-07	0.013459		6.6	2.51E-07	0.019725411
6.7	2E-07	0.01364		6.7	2E-07	0.02033312
6.8	1.58E-07	0.013821		6.8	1.58E-07	0.021037444
6.9	1.26E-07	0.014008		6.9	1.26E-07	0.021852611
7	1E-07	0.014212		7	1E-07	0.022789712
7.1	7.94E-08	0.014441		7.1	7.94E-08	0.023854912
7.2	6.31E-08	0.014705		7.2	6.31E-08	0.025047538
7.3	5.01E-08	0.015016		7.3	5.01E-08	0.026358439
7.4	3.98E-08	0.015384		7.4	3.98E-08	0.02776909
7.5	3.16E-08	0.015823		7.5	3.16E-08	0.029251926
7.6	2.51E-08	0.016345		7.6	2.51E-08	0.03077215
7.7	2E-08	0.016964		7.7	2E-08	0.032290898
7.8	1.58E-08	0.017691		7.8	1.58E-08	0.03376923
7.9	1.26E-08	0.018535		7.9	1.26E-08	0.035172112
8	1E-08	0.019501		8	1E-08	0.036471575

8.1	7.94E-09	0.020588		8.1	7.94E-09	0.037648502
8.2	6.31E-09	0.021786		8.2	6.31E-09	0.038692932
8.3	5.01E-09	0.023078		8.3	5.01E-09	0.039603125
8.4	3.98E-09	0.024438		8.4	3.98E-09	0.040383878
8.5	3.16E-09	0.025833		8.5	3.16E-09	0.041044553
8.6	2.51E-09	0.027228		8.6	2.51E-09	0.041597211
8.7	2E-09	0.028587		8.7	2E-09	0.042055073
8.8	1.58E-09	0.029877		8.8	1.58E-09	0.042431375
8.9	1.26E-09	0.031072		8.9	1.26E-09	0.042738617
9	1E-09	0.032155		9	1E-09	0.042988126
9.1	7.94E-10	0.033116		9.1	7.94E-10	0.043189867
9.2	6.31E-10	0.033953		9.2	6.31E-10	0.04335241
9.3	5.01E-10	0.034672		9.3	5.01E-10	0.043482999
9.4	3.98E-10	0.03528		9.4	3.98E-10	0.043587674
9.5	3.16E-10	0.035788		9.5	3.16E-10	0.043671425
9.6	2.51E-10	0.03621		9.6	2.51E-10	0.043738335
9.7	2E-10	0.036556		9.7	2E-10	0.043791728
9.8	1.58E-10	0.036839		9.8	1.58E-10	0.043834296
9.9	1.26E-10	0.037069		9.9	1.26E-10	0.043868207
10	1E-10	0.037254		10	1E-10	0.043895205
10.1	7.94E-11	0.037404		10.1	7.94E-11	0.043916691
10.2	6.31E-11	0.037524		10.2	6.31E-11	0.043933782
10.3	5.01E-11	0.03762		10.3	5.01E-11	0.043947374
10.4	3.98E-11	0.037698		10.4	3.98E-11	0.043958181
10.5	3.16E-11	0.037759		10.5	3.16E-11	0.043966771
10.6	2.51E-11	0.037808		10.6	2.51E-11	0.043973598
10.7	2E-11	0.037847		10.7	2E-11	0.043979024
10.8	1.58E-11	0.037879		10.8	1.58E-11	0.043983336
10.9	1.26E-11	0.037904		10.9	1.26E-11	0.043986761
11	1E-11	0.037923		11	1E-11	0.043989483
11.1	7.94E-12	0.037939		11.1	7.94E-12	0.043991645
11.2	6.31E-12	0.037952		11.2	6.31E-12	0.043993363
11.3	5.01E-12	0.037962		11.3	5.01E-12	0.043994728
11.4	3.98E-12	0.037969		11.4	3.98E-12	0.043995812
11.5	3.16E-12	0.037976		11.5	3.16E-12	0.043996673
11.6	2.51E-12	0.037981		11.6	2.51E-12	0.043997357
11.7	2E-12	0.037985		11.7	2E-12	0.043997901
11.8	1.58E-12	0.037988		11.8	1.58E-12	0.043998333
11.9	1.26E-12	0.03799		11.9	1.26E-12	0.043998676
12	1E-12	0.037992		12	1E-12	0.043998948
12.1	7.94E-13	0.037994		12.1	7.94E-13	0.043999164

12.2	6.31E-13	0.037995		12.2	6.31E-13	0.043999336
12.3	5.01E-13	0.037996		12.3	5.01E-13	0.043999473
12.4	3.98E-13	0.037997		12.4	3.98E-13	0.043999581
12.5	3.16E-13	0.037998		12.5	3.16E-13	0.043999667
12.6	2.51E-13	0.037998		12.6	2.51E-13	0.043999736
12.7	2E-13	0.037998		12.7	2E-13	0.04399979
12.8	1.58E-13	0.037999		12.8	1.58E-13	0.043999833
12.9	1.26E-13	0.037999		12.9	1.26E-13	0.043999868
13	1E-13	0.037999		13	1E-13	0.043999895
13.1	7.94E-14	0.037999		13.1	7.94E-14	0.043999916
13.2	6.31E-14	0.038		13.2	6.31E-14	0.043999934
13.3	5.01E-14	0.038		13.3	5.01E-14	0.043999947
13.4	3.98E-14	0.038		13.4	3.98E-14	0.043999958
13.5	3.16E-14	0.038		13.5	3.16E-14	0.043999967
13.6	2.51E-14	0.038		13.6	2.51E-14	0.043999974
13.7	2E-14	0.038		13.7	2E-14	0.043999979
13.8	1.58E-14	0.038		13.8	1.58E-14	0.043999983
13.9	1.26E-14	0.038		13.9	1.26E-14	0.043999987
14	1E-14	0.038		14	1E-14	0.043999989

Phosphate buffer control							Phosphate buffer experimental				
R-COO, high	0.037						R-COO, high	0.041			
w1	0.42		pKa1	5.3			w1	0.44		pKa1	4.8
w2	0.58		pKa2	8.6			w2	0.56		pKa2	7.8

pH	[H+]	[R-COO]		pH	[H+]	[R-COO]
0	1	7.79E-08		0	1	2.86274E-07
0.1	0.794328	9.81E-08		0.1	0.794328	3.60396E-07
0.2	0.630957	1.24E-07		0.2	0.630957	4.5371E-07
0.3	0.501187	1.56E-07		0.3	0.501187	5.71183E-07
0.4	0.398107	1.96E-07		0.4	0.398107	7.19071E-07
0.5	0.316228	2.46E-07		0.5	0.316228	9.05247E-07
0.6	0.251189	3.1E-07		0.6	0.251189	1.13962E-06
0.7	0.199526	3.91E-07		0.7	0.199526	1.43468E-06
0.8	0.158489	4.92E-07		0.8	0.158489	1.80612E-06
0.9	0.125893	6.19E-07		0.9	0.125893	2.27371E-06
1	0.1	7.79E-07		1	0.1	2.86233E-06
1.1	0.079433	9.81E-07		1.1	0.079433	3.60332E-06
1.2	0.063096	1.24E-06		1.2	0.063096	4.53607E-06

1.3	0.050119	1.55E-06		1.3	0.050119	5.71021E-06
1.4	0.039811	1.96E-06		1.4	0.039811	7.18814E-06
1.5	0.031623	2.46E-06		1.5	0.031623	9.0484E-06
1.6	0.025119	3.1E-06		1.6	0.025119	1.13898E-05
1.7	0.019953	3.91E-06		1.7	0.019953	1.43365E-05
1.8	0.015849	4.92E-06		1.8	0.015849	1.80449E-05
1.9	0.012589	6.19E-06		1.9	0.012589	2.27114E-05
2	0.01	7.79E-06		2	0.01	2.85826E-05
2.1	0.007943	9.81E-06		2.1	0.007943	3.59687E-05
2.2	0.00631	1.23E-05		2.2	0.00631	4.52586E-05
2.3	0.005012	1.55E-05		2.3	0.005012	5.69403E-05
2.4	0.003981	1.96E-05		2.4	0.003981	7.16252E-05
2.5	0.003162	2.46E-05		2.5	0.003162	9.00784E-05
2.6	0.002512	3.1E-05		2.6	0.002512	0.000113256
2.7	0.001995	3.9E-05		2.7	0.001995	0.00014235
2.8	0.001585	4.9E-05		2.8	0.001585	0.000178843
2.9	0.001259	6.17E-05		2.9	0.001259	0.000224576
3	0.001	7.76E-05		3	0.001	0.000281818
3.1	0.000794	9.75E-05		3.1	0.000794	0.000353362
3.2	0.000631	0.000123		3.2	0.000631	0.000442617
3.3	0.000501	0.000154		3.3	0.000501	0.000553714
3.4	0.000398	0.000193		3.4	0.000398	0.000691603
3.5	0.000316	0.000243		3.5	0.000316	0.000862141
3.6	0.000251	0.000304		3.6	0.000251	0.00107214
3.7	0.0002	0.000381		3.7	0.0002	0.001329343
3.8	0.000158	0.000477		3.8	0.000158	0.001642296
3.9	0.000126	0.000595		3.9	0.000126	0.002020047
4	1E-04	0.000742		4	1E-04	0.002471635
4.1	7.94E-05	0.000923		4.1	7.94E-05	0.003005309
4.2	6.31E-05	0.001144		4.2	6.31E-05	0.003627476
4.3	5.01E-05	0.001414		4.3	5.01E-05	0.004341424
4.4	3.98E-05	0.001739		4.4	3.98E-05	0.005145977
4.5	3.16E-05	0.002128		4.5	3.16E-05	0.006034346
4.6	2.51E-05	0.002587		4.6	2.51E-05	0.006993489
4.7	2E-05	0.003123		4.7	2E-05	0.008004321
4.8	1.58E-05	0.003737		4.8	1.58E-05	0.009042937
4.9	1.26E-05	0.004429		4.9	1.26E-05	0.01008277
5	0.00001	0.005194		5	0.00001	0.01109732
5.1	7.94E-06	0.006019		5.1	7.94E-06	0.012062875
5.2	6.31E-06	0.006888		5.2	6.31E-06	0.012960688
5.3	5.01E-06	0.007781		5.3	5.01E-06	0.013778212

5.4	3.98E-06	0.008674		5.4	3.98E-06	0.014509332
5.5	3.16E-06	0.009545		5.5	3.16E-06	0.01515377
5.6	2.51E-06	0.010373		5.6	2.51E-06	0.015715963
5.7	2E-06	0.011142		5.7	2E-06	0.016203784
5.8	1.58E-06	0.01184		5.8	1.58E-06	0.016627327
5.9	1.26E-06	0.012463		5.9	1.26E-06	0.016997936
6	1E-06	0.013009		6	1E-06	0.017327523
6.1	7.94E-07	0.013482		6.1	7.94E-07	0.01762816
6.2	6.31E-07	0.013887		6.2	6.31E-07	0.017911909
6.3	5.01E-07	0.014234		6.3	5.01E-07	0.018190815
6.4	3.98E-07	0.014531		6.4	3.98E-07	0.018477017
6.5	3.16E-07	0.014787		6.5	3.16E-07	0.018782902
6.6	2.51E-07	0.015011		6.6	2.51E-07	0.019121244
6.7	2E-07	0.015212		6.7	2E-07	0.019505284
6.8	1.58E-07	0.015398		6.8	1.58E-07	0.019948659
6.9	1.26E-07	0.015579		6.9	1.26E-07	0.020465123
7	1E-07	0.015762		7	1E-07	0.021067975
7.1	7.94E-08	0.015955		7.1	7.94E-08	0.021769146
7.2	6.31E-08	0.016168		7.2	6.31E-08	0.022577916
7.3	5.01E-08	0.01641		7.3	5.01E-08	0.023499343
7.4	3.98E-08	0.016691		7.4	3.98E-08	0.024532596
7.5	3.16E-08	0.017022		7.5	3.16E-08	0.025669516
7.6	2.51E-08	0.017413		7.6	2.51E-08	0.026893832
7.7	2E-08	0.017878		7.7	2E-08	0.028181442
7.8	1.58E-08	0.018427		7.8	1.58E-08	0.029501978
7.9	1.26E-08	0.019071		7.9	1.26E-08	0.030821557
8	1E-08	0.019817		8	1E-08	0.032106246
8.1	7.94E-09	0.020671		8.1	7.94E-09	0.033325524
8.2	6.31E-09	0.021631		8.2	6.31E-09	0.034455024
8.3	5.01E-09	0.022689		8.3	5.01E-09	0.035478086
8.4	3.98E-09	0.02383		8.4	3.98E-09	0.03638602
8.5	3.16E-09	0.02503		8.5	3.16E-09	0.037177292
8.6	2.51E-09	0.026262		8.6	2.51E-09	0.037856055
8.7	2E-09	0.027494		8.7	2E-09	0.038430439
8.8	1.58E-09	0.028693		8.8	1.58E-09	0.038910923
8.9	1.26E-09	0.029831		8.9	1.26E-09	0.039308997
9	1E-09	0.030886		9	1E-09	0.039636164
9.1	7.94E-10	0.031842		9.1	7.94E-10	0.03990329
9.2	6.31E-10	0.03269		9.2	6.31E-10	0.040120224
9.3	5.01E-10	0.033429		9.3	5.01E-10	0.040295627
9.4	3.98E-10	0.034063		9.4	3.98E-10	0.04043695

9.5	3.16E-10	0.034599		9.5	3.16E-10	0.04055049
9.6	2.51E-10	0.035048		9.6	2.51E-10	0.0406415
9.7	2E-10	0.03542		9.7	2E-10	0.040714317
9.8	1.58E-10	0.035726		9.8	1.58E-10	0.040772493
9.9	1.26E-10	0.035975		9.9	1.26E-10	0.040818916
10	1E-10	0.036178		10	1E-10	0.040855927
10.1	7.94E-11	0.036342		10.1	7.94E-11	0.040885411
10.2	6.31E-11	0.036474		10.2	6.31E-11	0.040908885
10.3	5.01E-11	0.03658		10.3	5.01E-11	0.040927566
10.4	3.98E-11	0.036665		10.4	3.98E-11	0.040942426
10.5	3.16E-11	0.036733		10.5	3.16E-11	0.040954244
10.6	2.51E-11	0.036787		10.6	2.51E-11	0.04096364
10.7	2E-11	0.036831		10.7	2E-11	0.040971109
10.8	1.58E-11	0.036865		10.8	1.58E-11	0.040977045
10.9	1.26E-11	0.036893		10.9	1.26E-11	0.040981762
11	1E-11	0.036915		11	1E-11	0.040985511
11.1	7.94E-12	0.036932		11.1	7.94E-12	0.040988489
11.2	6.31E-12	0.036946		11.2	6.31E-12	0.040990856
11.3	5.01E-12	0.036957		11.3	5.01E-12	0.040992736
11.4	3.98E-12	0.036966		11.4	3.98E-12	0.04099423
11.5	3.16E-12	0.036973		11.5	3.16E-12	0.040995416
11.6	2.51E-12	0.036979		11.6	2.51E-12	0.040996359
11.7	2E-12	0.036983		11.7	2E-12	0.040997108
11.8	1.58E-12	0.036986		11.8	1.58E-12	0.040997702
11.9	1.26E-12	0.036989		11.9	1.26E-12	0.040998175
12	1E-12	0.036991		12	1E-12	0.04099855
12.1	7.94E-13	0.036993		12.1	7.94E-13	0.040998848
12.2	6.31E-13	0.036995		12.2	6.31E-13	0.040999085
12.3	5.01E-13	0.036996		12.3	5.01E-13	0.040999273
12.4	3.98E-13	0.036997		12.4	3.98E-13	0.040999423
12.5	3.16E-13	0.036997		12.5	3.16E-13	0.040999542
12.6	2.51E-13	0.036998		12.6	2.51E-13	0.040999636
12.7	2E-13	0.036998		12.7	2E-13	0.040999711
12.8	1.58E-13	0.036999		12.8	1.58E-13	0.04099977
12.9	1.26E-13	0.036999		12.9	1.26E-13	0.040999817
13	1E-13	0.036999		13	1E-13	0.040999855
13.1	7.94E-14	0.036999		13.1	7.94E-14	0.040999885
13.2	6.31E-14	0.036999		13.2	6.31E-14	0.040999909
13.3	5.01E-14	0.037		13.3	5.01E-14	0.040999927
13.4	3.98E-14	0.037		13.4	3.98E-14	0.040999942
13.5	3.16E-14	0.037		13.5	3.16E-14	0.040999954

13.6	2.51E-14	0.037		13.6	2.51E-14	0.040999964
13.7	2E-14	0.037		13.7	2E-14	0.040999971
13.8	1.58E-14	0.037		13.8	1.58E-14	0.040999977
13.9	1.26E-14	0.037		13.9	1.26E-14	0.040999982
14	1E-14	0.037		14	1E-14	0.040999986